THE UNIVERSITY OF QUEENSLAND

AUSTRALIA

Evaluation of chimeric virus-like particles, capsomeres and bacterial minicells as vaccine delivery platforms

David John Pattinson

A thesis submitted for the degree of Doctor of Philosophy at

The University of Queensland in 2014

School of Medicine / Queensland Institute of Medical Research

Abstract

Malaria is a major public health problem, with an estimated 207 million cases and 627,000 deaths each year as well as associated socio-economic costs. Considerable inroads have been made in the reduction of malaria-related deaths and illness through the widespread use of preventative measures, but an effective vaccine is likely to hold our greatest chance of effectively eliminating the risk of *Plasmodium* infection. However, the most advanced anti-malarial vaccine candidate, RTS,S, has an efficacy rate of approximately 30%, and, alternative novel vaccine delivery platforms are likely to be required.

During my doctoral studies, I have evaluated chimeric virus-like particles (VLPs), chimeric capsomeres and bacterial minicells targeted to dendritic cells as novel vaccine delivery platforms, in a rodent model of malaria.

Chimeric VLPs are formed when recombinant viral structural proteins with foreign antigenic epitopes assemble into a highly repetitive array which resembles the native form of the virus. These VLPs are self-adjuvanting and highly immunogenic with regard to inducing antibody responses. Capsomeres are pentamers of viral capsid proteins which have not formed into VLPs. These are also immunogenic but require co-administration with adjuvants to induce comparable antibody titres to VLPs. Chimeric VLPs and capsomeres with surface exposed *Plasmodium yoelii* circumsporozoite (*Py*CSP) $CD8^+$ and $CD4^+$ T cell and B cell epitopes were constructed using a recently established murine polyomavirus VP1 structural protein scaffold. These constructs were designed so that the platform could be evaluated for their ability to induce cell-mediated immunity as well as antibody responses sufficient to protect against a complex pathogen. Individual and pooled VLPs or pooled capsomere constructs with (pooled VLPs and capsomeres) or without (VLPs only) adjuvant were evaluated in mice for immunogenicity (T cell and antibody responses) and protective capacity in both homologous and heterologous (DNA prime/VLP boost) immunisation regimens. I established that homologous regimens of VLPs and capsomeres induced moderate $CD8^+$ T cell immune responses, and these responses were significantly enhanced by the prime/boost regimen. Both platforms were inefficient at generating a robust $CD4^+$ T cell response, however, capsomere induced responses were superior to those induced by VLPs. Furthermore, I found that both VLPs and to a lesser

extent capsomeres, induced robust antibody responses, and that induced antibodies recognised conformational epitopes on the surface of the sporozoite. Neither VLPs nor capsomeres were able to protect mice from sporozoite challenge, with data suggesting that the magnitude of the response was insufficient.

Bacterial minicells are small anucleate cells which bud off from bacteria during binary fission as a result of premature septum formation. They have shown potential as a drug delivery platform but have not been well studied as a potential vaccine platform. Minicells produced by transformed *E.coli* DS410 bacteria containing recombinant protein and homologous mammalian expression plasmid DNA were purified using a novel purification method. Antigen-loaded minicells were then targeted to dendritic cells (DCs) via endocytic receptors DEC205 or Clec9a using bi-specific antibodies to enhance uptake and antigen presentation by dendritic cells and subsequent enhancement of immunogenicity. This platform was evaluated in an ovalbumin model as well as a murine malaria model to assess immunogenicity and protection capacity. In OTI and OTII ovalbumin models, ovalbumin packaged minicells induced ova-specific antibodies but failed to induce proliferation of adoptively transferred cells or kill ovalbumin $CD8^+$ T cell epitope pulsed lymphocytes in an *in vivo* CTL assay. The amount of target protein in the ovalbumin packaged minicells was only 0.1 µg/dose, and subsequent studies indicated that this antigen load was insufficient for inducing the sought immune responses. In the malaria model, minicells containing *P. yoelii* apical membrane antigen-1 (*Py*AMA-1) protein and plasmid DNA for mammalian expression of *Py*AMA-1, with a protein antigen dose of approximately 1 µg, was evaluated. Blood cytokine and white blood cell activation marker assays, and antibody assays did not indicate any *Plasmodium*-specific responses, and mice were not protected from sporozoite challenge. In each minicell experiment, targeting DCs did not alter the immune responses, however, this was likely dose-related rather than a platform-specific issue.

The potential and limitations of chimeric VLPs, capsomeres and bacterial minicell vaccine delivery platforms were identified which will be useful for future research. Importantly, it was established that chimeric VLPs and capsomeres induce moderate levels of cellular immune responses which complements their capabilities to induce robust antibody responses.

Declaration by author

This thesis is composed of my original work, and contains no material previously published or written by another person except where due reference has been made in the text. I have clearly stated the contribution by others to jointly-authored works that I have included in my thesis.

I have clearly stated the contribution of others to my thesis as a whole, including statistical assistance, survey design, data analysis, significant technical procedures, professional editorial advice, and any other original research work used or reported in my thesis. The content of my thesis is the result of work I have carried out since the commencement of my research higher degree candidature and does not include a substantial part of work that has been submitted to qualify for the award of any other degree or diploma in any university or other tertiary institution. I have clearly stated which parts of my thesis, if any, have been submitted to qualify for another award.

I acknowledge that an electronic copy of my thesis must be lodged with the University Library and, subject to the General Award Rules of The University of Queensland, immediately made available for research and study in accordance with the *Copyright Act 1968*.

I acknowledge that copyright of all material contained in my thesis resides with the copyright holder(s) of that material. Where appropriate I have obtained copyright permission from the copyright holder to reproduce material in this thesis.

David John Pattinson

Publications during candidature

Apte, S., Redmond, A., Groves, P., Schussek, S., Pattinson, D., and Doolan, D. (2013). Subcutaneous cholera toxin exposure induces potent $CD103^+$ dermal dendritic cell activation and migration. Eur. J. Immunol *43*: 2707-2717.

Publications included in this thesis

Nil

Contributions by others to the thesis

Preliminary development of the chimeric murine polyomavirus virus-like particle and capsomere platforms were done previously by various members of the Centre for Biomolecular Engineering at the Australian Institute of Bioengineering & Nanotechnology (AIBN) under the supervision of Professor Anton Middelberg. This did not include the construction of chimeric VP1 proteins used in this work. Transmission electron microscope images were taken by Alice Lei Yu.

Professors Denise Doolan (QIMR) and Anton Middelberg (AIBN), and Doctors Simon Apte and Nani Wibowo have supervised during the course of this doctoral work.

Animal experiment studies were done with assistance from Penny Groves and Joanne Roddick, from the Doolan laboratory.

Statement of parts of the thesis submitted to qualify for the award of another degree

None

Acknowledgements

The culmination of this PhD has been made possible as a result of technical assistance and emotional support from many people. My gratitude goes out to all who have helped guide me through this work.

My primary supervisor Denise Doolan has been an inspiration, and her ongoing support and knowledge has been crucial during both my honours and doctoral studies. To my pseudo-supervisor Simon Apte, I thank you for your mentoring, intellectual contribution in all immunological studies as well as your friendship. To all of the members of the Molecular Vaccines laboratory (QIMR) especially Penny Groves and Jo Roddick, thank you for your valuable support especially with experimental work. The happy lab environment has made it a pleasure to come in, day after day.

Thanks also to Anton Middelberg who became a co-supervisor, accepting me into his laboratory, and assisting with his intellectual input with regards to the VLP and capsomere platforms. Thanks to all members of CBE, especially Yap Chuan and Nani Wibowo provided much support in their supervisory roles, and Tania Rivera-Hernandez for her assistance, emotional support, and on-going friendship.

To my family, Paula, Ethan and Aaron, who have helped me endure the long hours and associated stresses involved in a PhD, thank you for all for your love and support. My wife Paula I also thank for caring for our boys, and running the house whilst I have been heavily engaged in my studies.

My studies were financially supported by an Australian post-graduate award, with top-up scholarships from both QIMR and UQ Advantage, for which I am truly grateful.

Keywords

Vaccine, murine polyomavirus, virus-like particles, capsomeres, bacterial minicells, malaria, circumsporozoite protein, apical membrane antigen-1, ovalbumin, cell-mediated immunity

Australian and New Zealand Standard Research Classifications (ANZSRC)

ANZSRC code: 860801, Human Biological Preventatives (e.g. Vaccines), 80%

ANZSRC code: 110799, Immunology not elsewhere classified, 20%

Fields of Research (FoR) Classification

FoR code: 1107, Immunology, 100%

Table of Contents

List of figures

List of tables

Abbreviations

2YT	2YT broth
aa	amino acid
AF4	asymmetrical flow field-flow fractionation
AMA-1	apical membrane antigen-1
ANOVA	analysis of variance
APC	antigen presenting cell
AUC	area under the curve
BG	bacterial ghost
BHI	brain-heart infusion broth
BMDDC	bone marrow derived dendritic cell
BMDM	bone marrow derived macrophage
BSA	Bovine serum albumin
BsAb	bi-specific antibody
BVP	Bovine polyomavirus
CBA	cytokine bead array
cDNA	complementary DNA
CFSE	carboxyfluorescein succinimidyl ester
CSP	circumsporozoite protein
CT	cholera toxin
CTL	cytotoxic T lymphocyte
DC	dendritic cell
dDCs	dermal dendritic cells
DLN	draining lymph node
DNA	deoxyribonucleic acid
dNTP	deoxyribonucleotide triphosphates
DS410	*E. coli* strain DS410
EDTA	ethylendiaminetetraacetic acid
EGFR	epidermal growth factor receptor
ELISA	enzyme-linked immunosorbant assay
ELISpot	enzyme-linked immunospot
FACS	fluorescence-activated cell sorting
FCAB	flow cytometric assessment of blood
FCS	foetal calf serum
g	relative centrifugal force
G4S	Gly-Gly-Gly-Gly-Ser
GAPDH	glyceraldehyde 3-phosphate dehydrogenase
GFP	green fluorescent protein
GST	glutathione-S-transferase
HaPyV	Hamster polyomavirus
HAT	hypoxanthine-aminopterin-thymidine
HCV	Hepatitis C virus
HEV	Hepatitis E virus
HPV	Human papillomavirus
i.m.	intramuscular
i.p.	intraperitoneal
i.v.	intravenous
ICS	intracellular cytokine staining
IFAT	indirect fluorescence antibody test
IFN-γ	interferon gamma

IL	interleukin
IM	inner membrane
IPTG	isopropyl β- D-1-thiogalactopyranoside
ITNs	insecticide-treated mosquito nets
LAL	limulus amebocyte lysate
LB	Luria-Bertani broth
L buffer	lysis buffer
LCMV	lymphocytic choriomeningitis virus
LPS	lipopolysaccharide
MALS	Multi-angle light scattering
mDCs	migrating dendritic cells
MFI	median fluorescent intensity
MHC	major histocompatibility complex
MPL	monophosphoryl lipid A
MSP-1	merozoite surface protein-1
mRNA	messenger RNA
MuPyV	Murine polyomavirus
nd	nil detected
NHP	non-human primate
NK	natural killer
OD	optical density
OM	outer membrane
OMV	outer membrane vesicle
OVA	chicken ovalbumin
P678-54	*E.coli* strain P678-54
PAMP	pathogen-associated molecular patterns
PBS	phosphate buffer saline
PCR	polymerase chain reaction
PD-L1	programmed death-ligand 1
pDNA	plasmid DNA
PEG	polyethylene glycol
Pi	propidium iodide
polyIC	polyinosinic-polycytidylic acid
pRBC	parasitised red blood cells
qRT-PCR	quantitative real-time PCR
RBC	red blood cells
RFP	red fluorescent protein
RNA	ribonucleic acid
s.c.	subcutaneous
SDS	sodium dodecylsulfate
SDS-PAGE	SDS-polyacrylamide gel electrophoresis
SEM	standard error of the mean
SFM	serum free media
shRNA	short hairpin RNA
siRNA	small interfering RNA
SMP	skim milk powder
TB	terrific broth
TCR	T cell receptor
TEM	transmission electron microscopy
Th	T helper
T_m	melting temperature
TLR	toll-like receptor
TNF	tumor necrosis factor
tRNA	transfer RNA
VIP205	*E.coli* strain VIP205
VLP	virus-like particle
WHO	World Health Organisation

Chapter 1: Introduction

1.1. Malaria

It is estimated that a child under the age of 5 years will die from a malaria-related illness every minute[1], and these figures may be a significant underestimation due to non-diagnosis or the non-reporting of deaths to any formal health system[2]. There now 97 countries with on-going malaria transmission with an estimated 207 million cases and 627 thousand deaths annually[1]. Of these reported deaths, 90% occurred in African countries and 77% occurred in children under 5 years. Since 2004, significant inroads have been made to decrease malaria related morbidity and deaths, which were then estimated at between 350 to 500 million cases and over one million deaths[3]. The impact of the disease extends beyond the human costs of mortality and morbidity to include the associated socio-economic load[4]. This financial burden is distributed primarily to developing countries and would be unsustainable which without international financial support[4]. The most cost-effective and efficient long-term solution to this debilitating disease is likely to come in the form of a vaccine.

The recent reductions in malaria-related deaths and illness can be attributed to preventative measures including the widespread distribution of insecticide-treated mosquito nets (ITNs), residual spraying and preventative therapies, all of which require considerable and on-going financial investment[1]. The distribution of decreased mortality rates from 2000 to 2012 (Figure 1) correlates strongly with the distribution of ITNs or residual spraying. For example, some central African regional populations have less than 50% coverage whereas southern African populations have greater than 80% coverage[1]. This disparity will be reduced with the continued roll-out of ITNs.

The high cost of current preventative measures including ITN distribution, residual spraying and chemoprophylaxis is highlighted by the annual investment of nearly $2 billion (USD) reported by WHO[1]. Despite the apparent success of current efforts, it

will take more money to gain complete global coverage, and to maintain already distributed equipment. Moreover, these benefits will be negated as mosquitoes develop resistance to insecticides or net usage declines due to complacency or net deterioration. Another major issue is the improper use of ITNs with the proportion of children under 5 years sleeping under ITNs being considerably lower than the proportion of households which have ITNs[5].

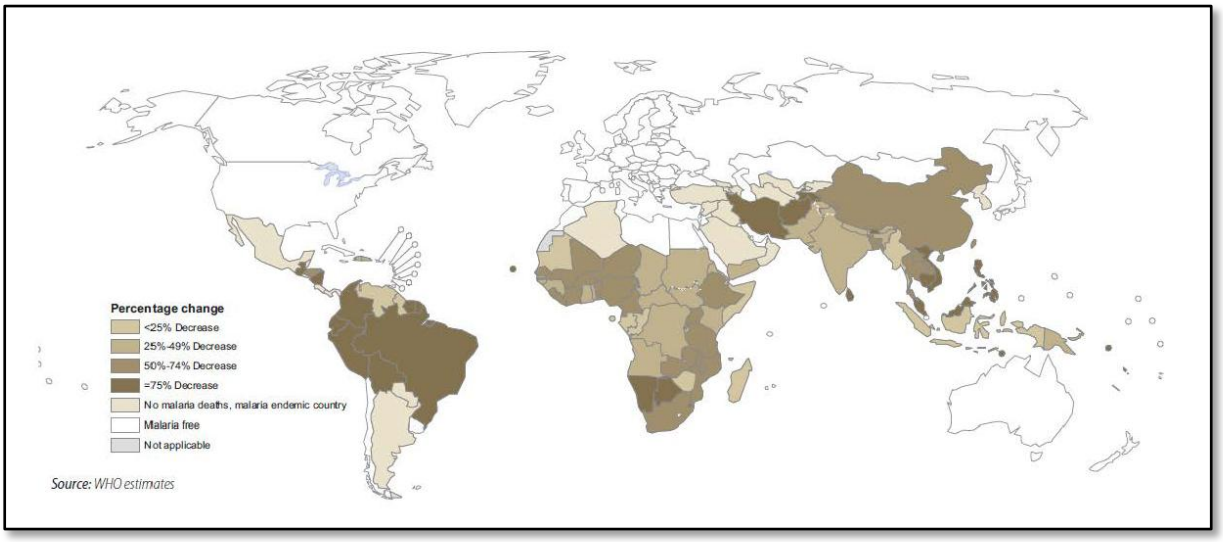

Figure 1: Percentage change in malaria mortality rates from 2000 to 2012[1]

For several decades, the favoured anti-malarial drug was aminoquinoline chloroquine because it was effective and cheap[6]. However, parasite resistance to this drug has evolved and spread rapidly across several continents including Africa, making it obsolete as a first-line treatment in most endemic regions[6,7]. To reduce the potential impact of drug resistance combination therapies are recommended by the WHO with two drugs given in combination[1]. The current recommended treatment for *Plasmodium* infections is an artemisinin-based combination therapy[1], however, there is evidence that parasites are now developing resistance to these drugs[8-11]. Given that artemisinin is the current primary therapeutic, a spread of the resistant parasite could be devastating. As such, new drugs are urgently needed.

Moreover, to reduce the global burden caused by this complex parasite, a combination of strategies in addition to drug based therapeutics is required, including

the development of an effective vaccine. Despite decades of research such a vaccine remains elusive.

1.2. The *Plasmodium* parasite

Malaria is a disease caused by an Apicomplexan parasitic infection of the genus *Plasmodium*. There are five *Plasmodium* species known to be infectious to humans: *P. falciparum*, *P. vivax*, *P. malariae*, *P. ovale* and *P. knowlesi*, a zoonotic parasite which was until recently only reported in old world monkeys[12]. *P. falciparum* has been a primary focus of vaccine and drug intervention research as it is the most life threatening species[1]. However, *P. vivax* has a wider geographical distribution and is responsible for 50% of infections outside of Africa[1]. With mounting drug resistance and increased disease severity, there is growing interest in this species[11]. *P. vivax* also has a hypnozoite dormant liver stage, a feature which it shares with *P. ovale*. These hypnozoites can remain dormant for months to years before undergoing development to merozoites which results in clinical relapses without the need for re-infection[13].

1.2.1. *Plasmodium* lifecycle

The *Plasmodium* parasite has a complex, multi-stage lifecycle requiring both a mosquito vector and human host (Figure 2). Whilst ingesting a blood meal, an infected female *Anopheline* mosquito delivers saliva containing approximately 10 to 100 *Plasmodium* sporozoites[14]. The sporozoites can remain in the skin for between 1 to 6 h before entering the blood or lymphatic systems[15] where they migrate to the liver and invade hepatocytes. Sporozoites differentiate and proliferate by asexual replication for between 5.5 to 10 days (in human infections) depending upon the species[16], producing up to 40,000 merozoites which then rupture the host cell releasing themselves into the blood circulation where they quickly invade erythrocytes[13]. This marks the commencement of the asexual erythrocytic stage, with rapid amplification of the parasite population and clinical manifestations of the disease. After 48 hours of further asexual replication, a single erythrocyte can now contain up to 36 merozoites. Erythrocytes then rupture releasing merozoites which invade uninfected erythrocytes, resulting in a cycle of exponential parasite growth.

Some merozoites can differentiate into male or female gametocytes which circulate in the blood and can be ingested by another mosquito in which sexual reproduction occurs, allowing the infection of another human host and continuation of transmission.

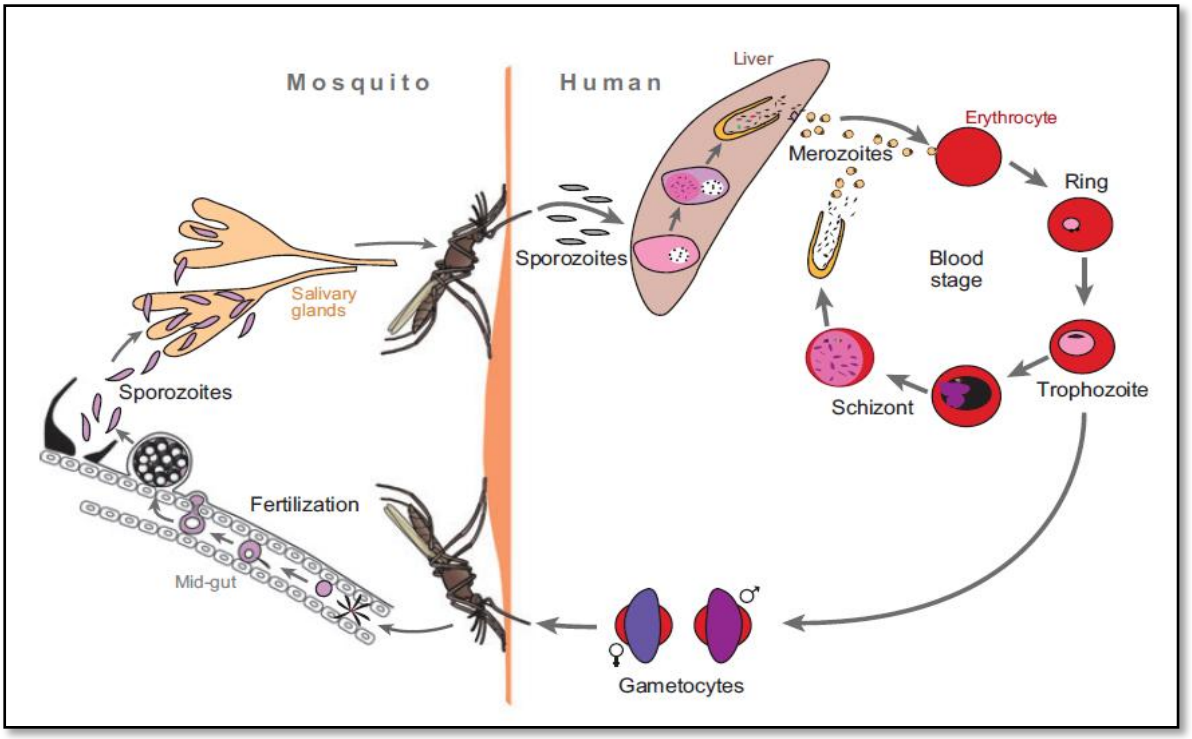

Figure 2: An overview of the *Plasmodium* lifecycle. Sporozoites in the saliva are transmitted from the *Plasmodium* infected female *Anopheline* mosquito, resulting in liver and blood stage infections. Gametocytes are ingested by other mosquitoes and sexual reproduction results in new sporozoites for continuation of the cycle[17].

1.2.2. Pathogenesis

Plasmodium infections may be asymptomatic in people with clinical immunity, but when clinical disease is manifested, cases are categorised as uncomplicated or severe. In uncomplicated malaria, common symptoms include fever, chills, sweats, nausea and vomiting, general malaise, headaches and body aches. These symptoms classically appear every second or third day depending on the infecting species. Severe malaria can be a result of severe anaemia due to erythrocyte destruction and reduced production, cerebral malaria due to microvascular obstructions in the brain, or metabolic acidosis due to reduced tissue perfusion (reviewed in[18]). Further complications can arise as a result of an accumulation of

parasite waste products, and infections during pregnancy can result in low birth weight or foetal loss due to placental infection[18].

1.2.3. Challenges for vaccine development

The *Plasmodium* species parasite has co-evolved with human hosts for a long time, effectively evading innate and adaptive immune responses. With the maturation of the immune system and repeated infections, individuals living in malaria-endemic regions can develop protective responses resulting in clinical immunity to malaria[16,19]. It is reasonable therefore to suggest that a vaccine could offer at least the same degree of protection. Of course, sterile protection would be the ultimate aim of vaccine researchers, preventing severe disease or death in the infected individual, as well as preventing the subsequent transmission of parasites to others. Early research by Freund *et al*[20,21] using non-human primates (NHPs) established that immunisations with killed parasites provided protection from challenge. The ability to protect humans was later shown using irradiated sporozoites delivered by the bite of infected mosquitoes[22]. Evidence of clinical immunity and these foundation studies provide the rationale that a vaccine to eliminate this parasite is achievable.

More than 50 years since the efforts to develop a malaria vaccine began, a feasible and efficient vaccine providing long-lasting protection still eludes researchers. Some are pursuing whole parasite vaccines, whilst others have turned to a sub-unit approach, each with varied successes. The malaria vaccine technology roadmap has set a goal to develop a vaccine with at least 75% protection from clinical malaria by 2030[23]. This goal was modified from the 2006 roadmap where the goal was 80% protection by 2025. This extension further highlights the challenges involved in defeating such a complex foe.

1.3. Vaccines

By exposing an individual to pathogen-specific antigenic material, vaccines stimulate an adaptive immune response which can result in antibody generation and T cell activation and memory which protects an individual from future infections by that or closely related pathogens. Records of vaccination date back to 1000 AD when the

Chinese stored scabs from individuals suffering from mild smallpox infections for one month, then ground up the scabs and inoculated non-infected people intra-nasally[24]. In the following centuries, this practice spread through India, Asia and North Africa before reaching England in the 18th century. This practice was not without serious risk with up to 2% of procedures resulting in the death of the person, and some subjects inadvertently spreading the virus[25]. Edward Jenner in 1796 tested the efficacy of immunisation with cowpox virus to protect from smallpox. The cowpox immunisation resulted in an attenuated infection as that virus was host-specific, but the cowpox virus was similar enough to provide cross-species protection against smallpox. This vaccine approach was widely accepted and nearly 200 years later smallpox was eradicated[25].

With the exception of water sanitisation, vaccines are the most efficient and cost-effective method of protection from disease related morbidity and mortality, improving public health and saving more lives than any other intervention[26]. Recent estimates suggest that current licensed vaccines save in excess of three million lives per year[27]. Through the development of vaccines, we are now protected against various bacterial and viral pathogens which were either debilitating or fatal such as yellow fever, measles, mumps, rubella, typhoid, hepatitis A and B, poliovirus and human papillomavirus[1,27-29]. The traditional "first generation" approach has been to immunise with either inactivated or live attenuated pathogens based on the principles of Louis Pasteur[30]. As our knowledge of pathogens has increased through microscopic imaging, genomic sequencing coupled with proteomic and transcriptomic data, and advances in vaccinology and related technologies; our vaccine delivery platforms have also evolved to a more rational vaccine design[30]. Research into sub-unit vaccines, where selected non-infectious components of a pathogen are given as immunogens, have resulted in vaccines delivering toxoid, pathogen polysaccharide, recombinant protein and virus-like particles[30,31]. These platforms are considered safer than the traditional whole organism approach as there are no infectious agents and therefore the possibility of virulence reversion is removed[31,32]. However, our current vaccine platforms have been either ineffective or inefficient against some pathogens including parasites, viral and bacterial infections such as *Plasmodium*, human immunodeficiency virus and *Mycobacterium*

tuberculosis respectively[27,32]. These three pathogens cause an estimated 4.8 million deaths per year[27].

1.4. Vaccines against malaria

The most cost-efficient and effective measure against *Plasmodium* infections to remove the associated global health problem is likely to be through the development of an effective vaccine. Over time, people living in malaria endemic regions develop clinical immunity to disease, this does not prevent infections, but does limit the clinical symptoms of the disease[19]. A vaccine therefore must provide a better immune response than natural infections.

Vaccines for malaria can be broadly categorised as pre-erythrocytic (sporozoite or liver-stage), erythrocytic (asexual blood-stage), or transmission-blocking (sexual-stage) vaccines, representing key stages of the parasite's life cycle. A pre-erythrocytic vaccine would provide sterile protection by either preventing sporozoite invasion of hepatocytes, or the development of merozoites within infected hepatocytes thereby preventing the development of the blood-stage of the parasite lifecycle and associated clinical symptoms[33,34]. Erythrocytic stage vaccines are designed to reduce the blood-stage parasite burden and decrease associated morbidity and mortality[33]. Sexual stage vaccines are designed to prevent transmission by destroying gametocytes or interfering with their ability to fertilise within the mosquito vector[33]. A multi-gene vaccine targeting each stage of the life-cycle with both antibody and cellular immune responses may be required due to the complexity and immune evasiveness of the *Plasmodium* species[33,35].

The most promising platforms include intravenous (i.v.) immunisations with radiation attenuated sporozoites[36] and the sub-unit VLP RTS,S/AS01 which incorporates the *P. falciparum* circumsporozoite protein (CSP) and is currently in phase 3 clinical trials[37].

1.4.1. Whole organism vaccines

Whole parasite immunisations with either live, attenuated or irradiated sporozoites or parasitised red blood cells have been successful in protecting animals from infection

(reviewed in[38,39]). Four key approaches for whole parasite vaccines include 1) radiation attenuated sporozoites[36,40,41], 2) infectious sporozoites under chloroquine chemoprophylaxis[42,43], 3) genetically attenuated parasites[44,45] and 4) chemically attenuated blood-stage parasites[46].

Immunisations with radiation-attenuated whole organisms are considered the gold standard and have shown to stimulate sterile protection to *P. falciparum* in humans[22,40]. In this platform, viable sporozoites track to the liver and invade hepatocytes, however, their ability to replicate is halted due to the irradiation and they do not develop to the blood stage[47]. Sporozoites can be purified from the salivary glands of infected and irradiated mosquitoes, however, viability retention and limitations of mass production currently limit the feasibility of this platform. These factors are being addressed by Sanaria Inc. (Rockville, MD USA)[41,48]. Using *P. falciparum* sporozoites purified by this facility, Epstein *et al.*[49] in a dose-escalation study using subcutaneous (s.c.) or intradermal (i.d.) administration routes reported sterile protection in two people from an 80 person trial. Subsequently they found that in NHPs that if the sporozoites were administered intravenously, the $CD8^+$ and $CD4^+$ T cell responses in the livers were consistently higher than following s.c. injections. The importance of these cellular responses from sporozoite immunisations has been well established[34,50]. In a follow-up study[36], 100% protection was achieved in six people receiving five i.v. doses of 135,000 sporozoites when challenged 3 weeks after their final immunisation. Protection was dose-dependent as only 60% of people receiving four i.v. doses had sterile protection, and immunogenicity data showed that lower sporozoite doses of 7,500 and 30,000 after 4 or 6 immunisations had markedly reduced antibody and cellular immune responses[36]. Despite this recent success, the distribution of viable irradiated sporozoites requires storage under liquid nitrogen and administration of high doses delivered by at least five i.v. doses. The mean number of sporozoites reportedly in the salivary gland of mosquitoes is between 16,500 and 83,875[51,52], meaning that between 8 and 41 mosquitoes need to be dissected to immunise one individual. The practicality of this platform as a world-wide solution to the problem of malaria is therefore questionable.

1.4.2. Subunit vaccines

Much effort has been invested in the identification of potential vaccine targets for sub-unit vaccines. In *Plasmodium falciparum* the publication of the genome[53], proteome[54] and transcriptome[55,56] has lead to the discovery of many novel vaccine antigen targets[57,58] where antibody and or T cell immune responses are sought.

1.4.2.1. Circumsporozoite protein

The CSP is expressed by sporozoites and liver stage schizonts[59,60]. In sporozoites the protein is secreted at the apex, adhering to the sporozoite surface and is then translocated to the posterior in a manner which drives gliding motility[61]. The CSP also provides key ligands to the heparin sulphate proteoglycans on the plasma membrane of hepatocytes allowing for target cell specificity[62].

The CSP on the surface of sporozoites provides a target for neutralising antibodies only for a short time as they travel from the site of mosquito bite to the liver[63,64]. Following hepatocyte invasion, sporozoites are no longer available for effective antibody targeting. Fortunately, the protein is also expressed by liver schizonts[65,66] and can be displayed by infected hepatocytes in the context of major histocompatibility complex (MHC) class I molecules for antigen-specific $CD8^+$ T cell recognition and responses [67,68]. A vaccine targeting the CSP must provide sterile protection at the liver-stage preventing the parasite's progression to blood-stage where CSP is no longer expressed. A vaccine effective against *Plasmodium* sporozoites is likely to required both cellular and antibody responses.

The CSP is a dominant protective antigen in the whole sporozoite platform[69], and monoclonal antibodies to CSP have been shown to prevent sporozoite infectivity[63]. Due to the limited exposure time of sporozoites from delivery to hepatocyte invasion, it is unlikely that a vaccine totally reliant on anti-CSP antibodies will be successful[70]. Fortunately, the CSP also presents opportunities for $CD8^+$ and $CD4^+$ T cell responses whilst within the host liver[71-75]. Early studies with plasmid DNA incorporating the *Py*CSP conferred sterile protection to mice against *P. yoelii*

sporozoite challenge[76], providing the foundation for subsequent clinical trials of malaria DNA vaccines in humans[77].

The most clinically advanced malaria vaccine candidate is the RTS,S/AS01 subunit vaccine which incorporates a large part of the *P. falciparum* CSP. The RTS,S vaccine comprises a fusion of partial length *P. falciparum* CSP (containing B cell repeats as well as T cell epitopes) (designated RT) combined with the hepatitis B surface protein (designated S) and delivered with GSK proprietary adjuvant AS01[70]. The hepatitis B component enables spontaneous assembly into virus-like particles[78] which RTS,S does following expression in yeast[70]. The AS01 adjuvant comprises a liposome suspension with a lipopolysaccharide (LPS) derivative monophosphoryl lipid A (MPL) and *Quillaja saponaria* 21 (QS21). AS01 has been identified as the most promising of a number of adjuvant systems trialled with this vaccine candidate[79].

In a phase 2 study, adults living in malaria endemic regions immunised with RTS,S in either AS01 or AS02 or combined adjuvants only achieved between 29.5% and 31.7% protection[80]. Nonetheless, this was followed by phase 3 pre-licence trials conducted in seven African countries with over 15,000 participants under 17 months old. With most deaths occurring in children under 5 years[1], this group is perhaps the most important for vaccine protection. In the 14 months following the first immunisation in the 5 to 17 month age group, there was a 50.4% reduction in reported infections and severe malaria incidents were reduced by 45.1%[81]. In the younger group (6 to 12 weeks old), protection from infection and reduced incidents of severe malaria were lower at 30.1% and 26.0% respectively[37]. Despite the inability to provide complete protection, this vaccine would compliment current preventative measures namely chemoprophylaxis and ITNs, resulting in a major reduction in the malaria burden[70].

1.4.2.2. Apical membrane antigen-1

AMA-1 is expressed in multiple stages of the *Plasmodium* life-cycle including sporozoites, liver stages and merozoites and is important for parasite invasion of hepatocytes[82] and erythrocytes[83-85]. This integral membrane protein is located in the

apical rhoptry organelles of the developing and mature merozoite, and relocates to the surface of the merozoite[86]. Consequently it is both a pre-erythrocytic and erythrocytic stage vaccine antigen and a target for which vaccine-induced antibodies and T cell responses are sought. AMA-1 is one of the most studied blood-stage vaccine target antigens, with a large body of animal studies confirming that immune responses against AMA-1 can inhibit the development of the parasite[87]. Antibodies against AMA-1 in persons naturally exposed to *Plasmodium* parasites are higher than any other blood-stage vaccine candidate[88].

Antigen-specific antibodies against AMA-1 are effective at neutralising merozoites and protecting mice from *P. chabaudi* and *P. yoelii* infections[89,90] and non-human primates from *P. falciparum*[91] by preventing merozoite invasion of erythrocytes[92,93]. $CD4^+$ T cell epitopes on *Pc*AMA-1 are reported to be important contributors for antibody and cellular responses[94,95]. Recently sterile protection from a sporozoite challenge in a rodent model was achieved using plasmid DNA and recombinant *Py*AMA-1 protein[96], indicating a role for cellular responses within the infected hepatocyte.

A list of *Pf*AMA-1 clinical trials is presented in the review by Remarque *et al*.[97] Clinical trials with *P. falciparum* AMA-1 recombinant protein with various adjuvants have shown vaccine induced antibody and cellular immune responses with some *in vitro* parasite growth inhibition and a Th1 cell-mediated response[98,99]. Despite these promising results, protection or a reduced parasite burden in human trials has not yet been reported. This may be due to *Pf*AMA1 polymorphisms[100], since protein variability reduces the parasites susceptibility to antibody neutralisation[97].

1.4.3. Pre-erythrocytic and blood-stage protective responses

1.4.3.1. Sporozoite and liver-stage

Antibodies directed to the surface of the sporozoite can neutralise and inhibit sporozoite invasion[63,64,101-103]. However, the number of sporozoites delivered by an infected mosquito bite is very low with a median of only 15[104] and 98% of infected mosquitoes in the field delivering less that 25 sporozoites[105]. This coupled with the

short period of sporozoite exposure to the immune system before invading an hepatocyte[15], which can be as fast as 2 minutes if sporozoites directly enter circulation[106], means that large quantities of circulating antibodies are required for effective neutralisation.

Infected hepatocytes can be cleared by antigen-specific effector cytotoxic $CD8^+$ T cells[67,68] or by immune mediators released by $CD8^+$ and or $CD4^+$ T cells[107], following the recognition the foreign antigens displayed on major histocompatibility complexes. There is a delay of approximately 5.5 to 7 days for *P. falciparum*[108] and much longer in the case of *P. vivax* and *P. ovale* hypnozoites, before merozoites packaged in merosomes bud off from the infected hepatocyte[109] marking the commencement of the erythrocytic stage of infection. This bottle-neck in parasite development makes for an attractive vaccine targeting strategy.

1.4.3.2. Asexual blood-stage

The start of the blood-stage infection is marked by merozoite release from hepatocytes and invasion of erythrocytes. Multiple cycles of replication within successive erythrocytes lead to the clinical manifestations of the disease. In the asexual stage, protective immunity is thought to be antibody mediated with a requirement for high levels of quality antibodies against a breadth of targets[110-112]. The primary mechanism of action of asexual based vaccines is antibody mediated, with surface binding of merozoites resulting in agglutination, blocking erythrocyte invasion, facilitating phagocytosis and through antibody dependent cellular inhibition[113]. A number of antigens have been targeted in clinical trials (reviewed in[113,114]) with most effort focusing on AMA-1 and the merozoites surface protein 1 (MSP-1). MSP-1 antigens are expressed during liver-stage infection[115] and are located on the surface of merozoites, and antibodies against MSP-1 inhibit erythrocyte invasion[116,117]

Most erythrocytic stage sub-unit vaccines have focused on single antigens, and despite effectiveness in animal models, these have not progressed beyond phase II clinical trials[118].

Whole blood-stage parasite strategies have also been investigated with some success in mice[46,119], and in humans[120]. One strategy with either sub-patent low-dose infections of parasitised blood followed by a drug treatment cure[119,120] relies on T cell-mediated immunity, but most other strategies are thought to rely on antibody responses.

1.4.3.3. Multi-stage vaccines

Many researchers anticipate that the ultimate vaccine will comprise of a combination of antigens from various stages of the parasites development[33,97]. Proof of concept for this was demonstrated in a murine vaccine study where the combination of two proteins provided synergistic or additive protection against challenge[121]. Multi-antigen/multi-stage antigens have shown some promise in animal models[121-123] however, clinical trials have been disappointing with poor protective efficacy[118]. For example, NYVAC-Pf7 consisting of seven *P. falciparum* proteins (including CSP, AMA-1 and MSP-1) representing all stages of the parasites life-cycle resulted in poor antibody and moderate cellular responses, with only 1 of 35 individuals protected from challenge, but with a significant delay in the time to reach parasite patency[124].

Generally anti-malarial sub-unit vaccines have shown efficacy in animal models but have failed to be effective in humans[118]. Whilst this may be an antigen selection issue, it is likely to also be influenced by the choice and strength of the co-administered adjuvant. This adjuvant effect was shown in the RTS,S vaccine trials, where the variation of adjuvant systems resulted in different outcomes[37,70,79]. Sub-unit vaccine efficacy may be further enhanced with more potent adjuvants, or through a redesign of the vaccine delivery platforms.

1.5. Virus like particles

Virus–like particles (VLPs) are formed from one or more viral structural proteins which can assemble into a highly repetitive and dense array resembling the native virus structure. VLPs lack all other viral components including DNA or RNA thus they are unable to replicate and non-infectious[125]. The capsid retains natural immune-stimulatory properties[126] and can induce potent cellular and humoral immune

responses without a requirement for adjuvant[127]. The high density and tight antigen spacing on the surface of the VLP is both unique to microbial pathogens[128] and critical for VLP induced antibody production[128,129] thought to be a result from cross-linking B cell receptors[130,131]. The ordered structure constitutes a pathogen-associated molecular pattern (PAMP) recognised by pattern-recognition receptors (PPRs) on host APCs[132,133]. PAMP recognition results in the stimulation of antigen uptake by innate immune cells, and causes the maturation of dendritic cells (DCs) which enhances presentation of antigens to the adaptive immune system[134,135]. The structural importance of VLPs was shown with heat-denatured VLPs resulting in substantially reduced humoral and cellular responses[136]. The intrinsic properties of VLPs provide an effective vaccine delivery platform, and because they are non-infectious, they are safe and readily produced in physical containment 2 (PC2) conditions. Moreover, VLPs are a self-adjuvanting platform as a result of their highly repetitive structure array which mimics the native virus[126,128].

A recent review by Zeltins[31] identifies that at least 110 VLPs have been constructed from 35 viral families including *Hepadnaviridae* (Hepatitis virus), *Papillomaviridae* (Papillomavirus) and *Polyomaviridae* (Polyomavirus). These numbers are markedly increased when examining the number of VLP related publications in a range of technologies including their use as vaccines. Vaccine studies of homologous and chimeric heterologous VLPs have been driven by the success of the hepatitis B virus (HBV) and human papilloma virus (HPV) vaccines[31], and more recently the hepatitis E virus (HEV) VLP based licensed vaccine[137].

1.5.1. Licensed VLP based vaccines

There are three human viral pathogens for which licensed VLP based vaccines are available, each of which is comprised of a single viral protein from their respective target pathogen. The first was developed against HBV, using sera from donors who were negative for HBV virions but positive for the hepatitis B surface antigen (HBsAg), and particles were purified by affinity chromatography and antibody-coated gels, then inactivated with formalin[138,139]. The publication of HBV genome[140,141] was an important step in researchers understanding the viral structure, and the three co-translated structural proteins[139]. Subsequently, advances in recombinant DNA and

protein technologies, bacteria, yeast, insect and mammalian cells have been used to generate effective VLP vaccines against HBV (reviewed in[139]). VLP vaccines are now available for HBV, HPV and most recently the HEV. Details of these vaccines are listed below (Table 1). There are many companies which manufacture HBV vaccines with an extensive list of VLP vaccines both licensed and in clinical development available in a recent review by Kushnir *et al.*[125]

Table 1: Licensed VLP based vaccines

Vaccine	Virus	VLP protein (dose)	Adjuvant (dose)	Dose regimen	Production
Recombivax Merck [142]	HBV	HBsAg (10 µg)	Aluminium hydroxyphosphate (500 µg)	0, 1 and 2 months	Yeast
Engerix-B GSK[143]	HBV	HBsAg (20 µg)	Aluminium hydroxide (250 µg)	0, 1 and 6 months	Yeast
Cervarix GSK[144]	HPV	HPV 16 L1 (20 µg) HPV 18 L1 (20 µg)	AS04 – Aluminium hydroxide (500 µg) and Monophoshoryl lipid A (MPL) (50 µg)	0, 1 and 6 months	Insect cells
Gardasil Merck[145]	HPV	HPV 6 L1 (20 µg) HPV 11 L1 (40 µg) HPV 16 L1 (40 µg) HPV 18 L1 (20 µg)	Aluminium hydroxyphosphate sulphate (225 µg)	0, 2 and 6 months	Yeast
Hecolin Xiamen Innovax[137]	HEV	Hep E antigen (30 µg)	Aluminium hydroxide (800 µg)	0, 1 and 6 months	*E. coli*

All licensed VLP based vaccines are administered by intra-muscular injection and are administered with an aluminium based adjuvant (Table 1). The primary immunological protective mechanism induced by VLPs and responsible for protection against both HBV and HPV infections are neutralising antibodies[139,146] . To prevent acute infection there is a requirement for $CD4^+$ T cell activation to promote memory B cell responses and isotype switching[139]. There is also evidence of $CD8^+$ T cell-mediated protection with established HPV infections[147] as confirmed by genital wart regression[148].

All licensed VLP based vaccines are assembled using a capsid protein of the targeted viral pathogen[125,137]. If the VLP platform was limited to homogenous viral capsids, then the usefulness of the platform would be restricted to only viral pathogens, and further restricted to those from which VLPs could be generated. Fortunately this is not the case with many laboratory and clinical trials showing the VLPs to be efficient carriers of foreign heterologous epitopes, or partial or full length proteins. By incorporating foreign antigens into the non-targeted capsid structural protein, this platform can theoretically target any organism (reviewed in[125,127,149]), greatly increasing the value and versatility of VLPs as a vaccine delivery platform.

1.5.2. Chimeric VLPs

Candidate vaccine target antigens against the *Plasmodium* parasite have been and continue to be identified as our understanding of the parasite and natural or vaccine induced immune responses accumulate[150,151]. These sub-unit antigens may result in an effective vaccine if incorporated into a delivery platform which is highly immunogenic. VLPs are a highly immunogenic vaccine platform for native (homologous) viral antigens, and chimeric VLPs presenting foreign (heterologous) antigens have similar immunological characteristics which have led to their progression to clinical studies[125]. One promising chimeric platform is the RTS,S vaccine incorporating the regions of the *P. falciparum* CSP into the HBsAg viral protein[37] (section 1.4.2.1).

Antigens can be coupled within VLPs by chemical conjugation or genetic fusion. At the genetic level, peptide or protein units are inserted into viral proteins using conventional recombinant DNA techniques. Using this strategy, a viral structural protein is expressed with foreign antigens positioned at internal or surface exposed protein sites[152-154]. The positioning may be important for the type of immune response sought[152,155]. Multiple antigen insertion sites both internal and external can be used in a single construct [79,152] allowing surface exposed antigens to cross-link B cell receptors[130] and potentially better access to proteomic cleavage at terminal regions relevant for T cell epitopes. The disadvantage with genetic antigen insertion is the potential disruption in the expression of the chimeric structural protein as well as the successful formation of VLPs[156,157], with single amino acid variations capable

of platform destabilisation[158]. The current unpredictability both of chimeric VLP formation, and the antigen-specific immunogenicity, means that a single methodology will not be sufficient for all chimeras[127]. To increase the likelihood of VLP stability and to control steric arrangements, flexible linkers are often used to flank antigens[159-161]. Limited studies have evaluated the immunological benefits of flexible linker sequences, with results suggesting minimal differences to non-flanked epitopes[154].

The alternative is chemical conjugation of antigens to pre-formed VLPs. Many conjugation methods have proven successful in VLPs with conjugated antigens ranging from peptides[157,162] to full length proteins[163]. Perhaps the most commercially advanced system is the *E. coli* produced bacteriophage Qβ developed by Cytos Biotechnology in Switzerland. Clinical trials are currently evaluating effectiveness of Qβ VLPs against asthma, Alzheimer's disease, diabetes mellitus and other conditions[125]. This binding system introduces a lysine residue flanked by glycine (x2) linkers on a surface exposed loop which is then coupled to any antigen with a free cysteine group using a heterobifunctional cross linker[156,164]. Qβ VLPs, however, are poorly immunogenic and require the inclusion of adjuvants[127]. Other groups have linked VLPs to antigens using biotinylated VLPs and streptavidin labelled peptides[128] or used peptides with a free sulphydral group to maleimide activated biotinylated VLPs[162]. Electrostatic binding using VLPs with multiple polyanionic sites decorated with polycationic peptides with induced disulfide bode formation has successfully resulted in antigen induced cytotoxic T lymphocyte (CTL) activity[157]. Whilst these conjugation systems are appealing for rapid development and testing of antigenic suitability using the VLP platform, the requirements for carriers and antigens made separately with elaborate binding processes reduce their practicality with inherent increases in manufacturing costs.

1.5.3. Chimeric capsomeres

The viral capsid is comprised of intermediate subunits called capsomeres which can link together using terminal regions of the structural proteins. In the case of the murine polyomavirus, for example, five VP-1 proteins are linked into a pentameric capsomere[165,166]. The flexible C-terminal arms of VP-1 proteins link with

neighbouring capsomeres likened to a rope and clamp system[167]. Researchers have shown that truncating the terminal region of the viral structural protein results in a capsomere unit which is not able to form the capsid unit[168-170]. A vaccine made from this VLP sub-unit removes the need for VLP assembly processing and structural confirmation, making it cheaper and faster to produce. It avoids costly VLP disassembly and reassembly processing to remove contaminants[171]. Furthermore, capsomeres are reported to be more stable than VLPs[172,173] and because there is no requirement for a stable VLP assembly, more and longer-sized antigens can be loaded into the structural protein[170]. Increasing the antigen to carrier ratio can benefit a vaccine platform by both increasing the immune responses to the antigen[174,175] but also decreasing the antibody titres against the carrier[176].

Capsomeres do not possess the ordered array of VLPs and so would be expected to lose the benefits of the VLP platform. Some studies have shown that capsomeres retain some self-adjuvanting immunogenicity[177,178] stimulating humoral and cellular responses which can be further enhanced with the inclusion of adjuvants[170,179]. However, other studies have shown that the inclusion of an adjuvant is essential to enhance capsomere induced immunogenicity, in particular antibody responses[131,173,180]. Few studies have directly compared the immunogenicity of capsomeres and VLPs, but there is a consistent trend indicating VLPs are superior to capsomeres without adjuvants, with respect to antibody titres[173,179]. Induced titres with as high as a 20-fold difference[180], or the requirement to use 40-times higher capsomere dose to achieve equivalent titres have been reported[131]. In most cases, however, this disparity is reduced or eliminated with the inclusion of adjuvants. Differences in capsomere induction of cellular responses was less obvious[131] and these lower responses could be recovered with the inclusion of adjuvants[179]. In one study, IFN-γ ELISpot data comparing various HPV VLP and capsomere constructs indicated that the inclusion of an aluminium hydroxide and MPL based adjuvant did not enhance VLPs but was essential for capsomeres which were otherwise inefficient inducers[179]. In another study, capsomeres were identified as potent inducers of CTL responses without the requirement of adjuvants, where antigen-specific tumour regression was similar to VLPs[169].

1.5.4. Murine polyomavirus

The murine polyomavirus (MuPyV), as the name suggests, is a virus which infects mice and results in the induction of multiple tumours[181]. This virus is a member of the *Polyomaviridae* family and was first isolated by Ludwig Gross in 1953 whilst studying leukaemia development in mice[182]. Since then, polyomaviruses have been identified in a variety of avian and mammalian hosts including humans (JC and BK polyomaviruses), non-human primates (simian virus 40), and hamsters (hamster polyomavirus)[183]. The virus is a non-enveloped, double stranded circular DNA virus with the capsid having icosahedral symmetry[184].

The native structure of MuPyV is formed using three structural proteins including the major capsid protein VP1, and two minor core proteins VP2 and VP3. The capsid comprises of 72 VP1 pentameric capsomeres each linking with other capsomeres and to VP2 and VP3 proteins to form the icosahedral surface with a diameter of approximately 45 nm[185]. *In vitro* experiments have shown that under the correct physiochemical conditions, bacterial produced VP1 proteins can self-assemble into VLPs without the requirement of VP2 or VP3 interactions[166].

After expression of the MuPyV VP1 protein, five monomers self-assemble into a pentameric capsomere which can then assemble into a VLP comprising 72 capsomeres in a T=7*d* icosahedral surface lattice[165]. The formation of VLPs is dependent upon capsomeres binding to each other using amino acids on the C-terminal region of the VP1 protein. This requirement has been confirmed with the removal of 63 amino acids from the C-terminal resulting in capsomeres which are incapable of VLP formation[168,170]. MuPyV VLPs are protective against their native virus in the limitation of induced tumour development[186], however, this platform has a much higher potential in its ability to induce immunological responses against heterologous pathogenic antigens.

In the chimeric MuPyV platform developed by Middelberg and colleagues[173], genomic epitope insertion sites have been created in HI loop (S4) surface exposed region of the VP1 protein (Figure 3). When expressed, the antigen epitopes are flanked by a flexible linker sequence of four glycines and a serine (GGGGS-epitope-

SGGGG). The inclusion of the linker is designed to project the epitope from the VP1 surface and to limit interference in the formation of the VLP. The VP1 chimeric monomers expressed in *E. coli* at gram per litre levels[187] arrange into a pentameric capsomere[166] each containing five antigen epitopes. Capsomeres are harvested from homogenised lysate and chemically induced *in vitro* to self-assemble into VLPs[173,188,189] comprising of 72 capsomeres. Hence a total of 360 epitopes are presented in a structured array resembling the native MuPyV capsid.

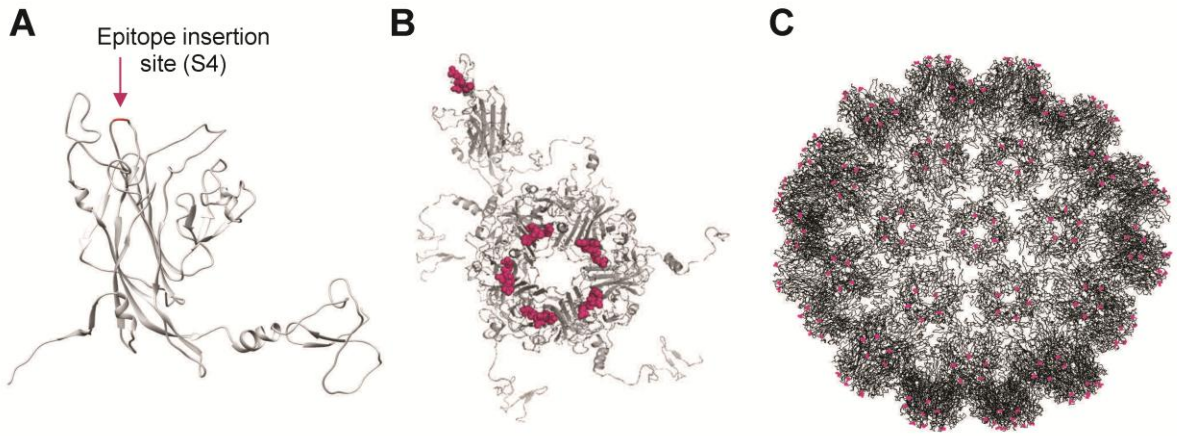

Figure 3: Structure of the chimeric MuPyV VLP. In each image the coloured portions represent the antigen epitope genomically inserted into MuPyV VP1 protein. The chimeric VP1 monomer (A) shows the S4 epitope insertion site on the surface exposed loop. (B) Five monomers combine to form a pentameric capsomere whilst within the *E. coli*. The c-terminal region of each VP1 links with neighbouring capsomeres. (C) The chimeric VLP comprises of 72 capsomeres in a T=7 icosahedral lattice with a total of 360 surface exposed inserted antigens. Images were adapted with permission[190].

VP1 protein production can be achieved using various eukaryotic and prokaryotic organisms and VLP assembly in either *in vivo or in vitro* systems[187,191]. Some systems are more efficient protein producers, are simpler allowing rapid modification, and more cost-effective in large scale manufacturing. To date, the use of VLPs as a vaccine platform has been limited by ineffective scale-up processes and other related manufacturing problems including the removal of contaminants. Studies to optimise bacterial expression of VP1 proteins[189] and the use of fed-batch cultivation in bioreactors[187] have resulted in a feasible bacterial production platform. Recently, the direct use of MuPyV capsomeres as a vaccine platform is also being

investigated[170,173]. Removal of the requirement to form VLPs would reduce production costs by removing dialysis processing and VLP stability requirements.

1.5.5. Dendritic cell activation by VLPs

Dendritic cells are professional antigen presenting cells (APCs) which are potent stimulators of the adaptive immune response. These highly motile cells are present in every organ and tissue throughout the body acting as an interface between the innate and adaptive immune systems[192]. Immature DCs survey their environment by sampling and processing self and foreign proteins and displaying peptide fragments on MHC class I and class II molecules. Without DC maturation stimuli, this presentation can result in tolerance, however, antigens accompanied by danger signals result in the maturation of DCs[193] which can result in immunity. Maturation results in the up-regulation of MHC:peptide complexes, and co-stimulatory CD80 and CD86 receptors, and the production of soluble mediators which can polarise the T cell responses[194]. Importantly, DCs activated in the periphery migrate to lymphoid rich regions to present peptides to naive T cells[195]. Antigens can be processed and displayed on MHC class II molecules for $CD4^+$ T cell presentation, or by the process of cross-presentation displayed on MHC class I molecules for $CD8^+$ T cell recognition[195].

Using ovalbumin-coated polystyrene microspheres with sizes ranging from 20 to 2000 nm, the induction of antibody responses and the stimulation of T cells in mice was clearly shown to be influenced by particular size[196]. The optimal size for DC uptake and activation was shown to be between 40 to 50 nm[196]. An analysis of draining lymph nodes 48 h post i.d. injection determined that the percentage of uptake of the 40 nm beads was significantly higher, and 40 nm bead positive cells populations had the highest proportion of DEC205, CD40 and CD86 surface marker expression[196]. Data indicates that DCs preferentially take up these size particles and become activated, whereas larger particles are cleared by macrophages.

In another size dependant antigen delivery experiment, small particles of between 20 to 200 nm diameters were detected in lymph node resident APCs[197]. These nanoparticles and VLPs (30 nm) entered the lymphatic system and were conveyed

to the lymph nodes, then endocytosed by resident APCs[197]. This feature is important for vaccines seeking $CD8^+$ T cell responses, because studies have shown that it is the $CD8\alpha^+$ lymph node-resident DCs which are central to prime naive $CD8^+$ T cells[198,199]. Both $CD8\alpha^+$ and $CD8\alpha^-$ DCs are efficient at VLP uptake and antigen presentation on MHC class II complexes[200]. The optimal particle size determined by both microsphere experiments[196,197] suggests that VLP platforms with vaccine candidate particles sizing between 22 and 60 nm (HBV: 22 nm, Qβ: 29.4 nm, MuPyV: 51 nm and HPV16: 60 nm)[201] are therefore advantageous at reaching the required innate immune cells.

It is well established that VLPs are capable of inducing DC maturation, and subsequent cellular immunological responses without the requirement for adjuvants[125,127,130]. Several studies have directly evaluated DC maturation by VLPs. *In vitro* cultures of murine bone marrow-derived DCs (BMDDCs) pulsed with MuPyV VLPs showed an up-regulation of DC maturation receptors and interleukin 12p70 (IL-12p70) cytokine production without adjuvant[202]. Bovine papillomavirus (BPV)[157] and hamster polyomavirus (HaPyV)[154] VLPs also up-regulated BMDC activation receptors and IL-12p40 cytokines. Importantly for human vaccine delivery, MuPyV and HaPyV VLPs were efficient at activating human DCs as determined by the up-regulation of activation markers, IL-12 production and a reduction in endocytic capacity[203].

The functional determination of a naive $CD4^+$ T cell is regulated by signal patterns encountered during their initial antigen confrontation[204]. Vaccines targeting intracellular pathogens aim to induce a Th1 responses with key cytokines including IFN-γ and IL-2, with the latter critical for $CD8^+$ T cell memory formation[204,205]. Activated DCs producing large amounts of IL-12 which promotes natural killer (NK) cells to produce IFN-γ which through a number of pathways induces Th1 differentiation[206].

VLPs are not, however, universally immunogenic. In one study, immature human DCs were only marginally activated by JC, BK and SV40 VLPs whereas MuPyV and HaPyV VLPs were potent inducers[203]. Whilst structurally similar, HPV16 and HPV18 VLPs are capable of inducing acute maturation of murine BMDDCs whereas JC and

BK VLPs are efficiently internalised by DCs but fail to stimulate maturation[207]. Others have reported that JC VLPs injected into rabbits only induced immune responses when administered with Freund's complete and incomplete adjuvants[208]. It also appears that the formation of VLPs is a determinant of DC maturation as observed in multiple studies where capsomeres were inefficient at activation of DCs in contrast to the VLPs[157,207].

1.5.6. Cellular immune VLP induced immune responses

As earlier mentioned, VLPs are potent inducers of antibody responses with licensed VLP based vaccines stimulating stable and long-lasting neutralising antibody titres capable of preventing disease[127]. Using the chimeric MuPyV VLP and capsomere platforms, antibodies have been raised against inserted epitopes to target a range of pathogens including influenza and group A streptococcus[170,173,188,209]. However, the cellular responses to VLP vaccines, especially $CD4^+$ T cell responses, are not as well characterised.

Whilst a single $CD8^+$ T cell clone can induce protection from a *Plasmodium* challenge, a high number of these cells are required to achieve sterile protection[210]. A chimeric VLP incorporating a single epitope designed to induce proliferation of a single T cell clone must therefore be a very efficient immune-modulator.

Surprisingly few studies have been done evaluating cellular immunogenicity of VLPs using an ovalbumin transgenic mouse model. In one study, ovalbumin peptide MuPyV VLP chimeras resulted in the *in vitro* proliferation of both OTI and OTII cells, indicating that APCs presented antigen peptides on both MHC class I and class II molecules[202]. Chemically conjugated $OVA_{257-264}$ (OTI) or $OVA_{232-339}$ (OTII) peptides on rabbit haemorrhagic disease virus VLPs have also resulted in the *in vitro* proliferation of transgenic OTI and OTII cells with OTI chimeras inducing target peptide-specific lysis and a delay in B16.OVA tumour development[162,211]. In another study, tumour protection and survival was conferred by immunisations of $OVA_{257-264}$ chimeric MuPyV VLPs and capsomeres with antigen-specific T cell proliferation determined using peptide-specific tetramers[212]. Using chimeric HBV VLPs with either single OTI epitopes or combined OTI and OTII epitopes, T cell receptor-specific

proliferation was observed and cytotoxic lysis of $OVA_{257-264}$ coated cells *in vivo* was detected[213]. It should be noted that in this study, the inclusion of a T helper epitope did not enhance CTL activity in the lysis model[213].

In an early chimeric VLP experiment, Sedlik *et al.* inserted a single $CD8^+$ T cell epitope from lymphocytic choriomeningitis virus (LCMV) into a parvovirus VLP, and following two doses of non-adjuvanted VLPs (10 µg/dose) showed a strong CTL response against peptide-labelled or virus-infected target cells[214]. In those experiments, there was persistent *in vivo* CTL activity for at least 9 months, and mice were completely protected when challenged with a lethal LCMV administered 7 d post-immunisation and were 80% protected when challenged 49 d post-immunisation. By depleting either $CD8^+$ or $CD4^+$ T cells, they showed that protection was $CD8^+$ T cell-mediated[214]. Subsequently, using an LCMV model but a different $CD8^+$ T cell epitope inserted into a HaPyV VLP, antigen-specific $CD8^+$ T cell proliferation and an effective memory response was induced after a single dose of non-adjuvanted VLPs (50 µg), providing 70% protection from infection[215]. The effectiveness of VLPs may be dependent on the carrier with the same epitope inserted into a HBV VLP only capable of inducing weak CTL activity and no protection unless co-administered with adjuvants[216].

To assess the effectiveness of VLPs at achieving clonal CD8+ T cell expansion to reach the proposed the 1% threshold required for protection against *Plasmodium* challenge[210], one has to review studies which have quantified the proportion of epitope-specific $CD8^+$ T cell induced by immunisation. Kawano *et al.* constructed a chimeric SV40 VLP with an influenza A virus CTL epitope and administered a single non-adjuvanted dose (50 µg), then restimulated splenocytes in an ELISpot readout and showed approximately 1.5% of $CD8^+$ T cells produced IFN-γ[161]. Using HPV16 capsomeres in a single dose (5 µg), restimulated splenocytes were less than 0.35% of the $CD8^+$ T cells were positive for IFN-γ[169]. In that study, ELISpot data from splenocytes of VLPs (10 µg) and capsomeres (5 µg) immunised mice had a mean of 580 and 850 IFN-γ spots/10^6 splenocytes respectively and data was highly variable within groups[169]. Combined these studies show the potential of VLPs to achieve

target responses for protection. It would be expected that the inclusion of additional boost immunisations would enhance immunogenicity as reported by others[217,218].

The VLP carrier is itself likely to have $CD4^+$ T cell epitopes which will aid in vaccine-induced antibody responses, but these primed $CD4^+$ T cells will have no effect when encountering the pathogen unless it also has the same epitope[152,219]. An example of carrier-specific $CD4^+$ T cell stimulation was reported using hepatitis C virus (HCV) VLPs with endogenous T helper epitopes[220]. In a malaria vaccine model (ICC-1132), HBV VLPs containing a CSP B cell repeat in an exposed loop and a T cell epitope at the C-terminal were shown to produce CSP-specific $CD4^+$ T cell clones and high antibody titres significantly enhanced by the inclusion of Montanide ISA 720 adjuvants[219]. The inclusion of a pathogen-specific T helper epitope does not, however, guarantee that it will be functional and result in $CD4^+$ T cell priming as shown by Schodel *et al.*[152]. Studies into $CD4^+$ T cell activation by chimeric VLPs with T helper epitopes are very limited. The Th1/Th2 profile has generally been reported only in relation to the skewing of IgG antibody isotypes[221]. It is known that the inclusion of adjuvants can alter the profile with aluminium hydroxide generating a Th2 profile, whilst CpG, MPL and polyIC induce a Th1 skewed result[221].

1.6. Bacterial derived particles as delivery platforms

1.6.1. Bacterial minicells

Bacterial minicells are small anucleate cells which are enzymatically active but are incapable of further cell division because they contain no chromosomal DNA[222-224]. In the 1930's, Gardiner reported a microscopic observation of small spherical non-viable granules resulting from unequal cell division in a strain of *Vibrio cholera*[225]. In 1966, whilst studying the mechanisms of cell division in *E. coli*, Adler and colleagues[226] detected a mutant of the K-12 strain that produced cell-like structures about one-tenth the size of the regular strain and noted that these structures lacked chromosomal DNA. The mutant strain named P678-54 underwent normal binary fission and was therefore able to proliferate, but also produced 'minicells' at the polar regions which were unable to grow or divide[222]. A number of minicell-producing bacteria have now been reported including Gram negative and Gram positive

species[227]. Predominantly *E. coli*, *S. typhimurium* and *Bacillis subtilis* mutants have been investigated[228,229]. Microbiologists studying the replication of bacteria have since confirmed that multiple proteins are responsible for the correct placement and subsequent septum formation during replication (reviewed in [229]). The MinCDE system is an inhibitory system which prevents the formation of the septum at any region other than the mid-cell[229]. Mutations in the *min*B locus containing *min*C, *min*d and *minE* genes disrupting the minCDE system[230], or over-expression of the FtsZ protein[231,232], can result in incorrect septum placement resulting in minicell formation.

Since minicells are enzymatically active[222], can contain plasmid DNA and can produce encoded proteins[223,224,233,234], they are a valuable tool for studying bacterial functions and the effects of recombinant proteins without interference of chromosomal DNA derived factors. Additionally, the use of minicells as a potential medical delivery vehicle has been reported by several groups[227,235-239].

A crude separation process involving centrifugation of minicells on a sucrose gradient removed most of the parent bacteria[222] resulting in a semi-pure yield of minicells was described by Adler *et al*[222] and later by Frazer and Curtiss[225] with the inclusion of a differential centrifugation. This has been the primary purification protocol since that time, however, additional antibiotic incubations[235], and filtration steps[227] have enhanced the removal of viable parent bacteria, so as to be suitable for human use.

1.6.1.1. Bacterial minicells for treatment of cancer

During chemotherapy, patients are administered large systemic doses of toxic drugs which indiscriminately target rapidly dividing cells. To reduce the quantity of drugs and avoid the unwanted side-effects of chemotherapy, bacterial minicells packaged with chemotherapeutic drugs have been successfully targeted to cancer cells using bi-specific antibodies (BsAbs)[227,238]. In the development of this drug-targeting minicell platform, researchers have generated minicell-producing mutants from *S. typhimurium* and *E. coli* by deleting the minCDE gene sequences[227]. Minicell-producing strains were cultured and purified for complete removal of contaminating viable parent bacteria leaving minicells with a diameter of 400 nm ± 20 nm. Using the

RAW 264.7 mouse macrophage cell line, minicells were observed to be internalised in intracellular vacuoles with up to 50 minicells per macrophage[227]. The minicells were then incubated with a range of drugs which were taken up by the minicells either by means of diffusion down a concentration gradient[227], or through charge related interactions through the porin channels[240]. Depending on the drug and concentration, incubation solution and incubation time, each minicell was capable of containing up to 10^7 drug molecules. When mice received an i.v. administration of non-targeted drug-laden minicells, there was no effect on tumour development. However, when minicells were targeted to the epidermal growth factor receptor (EGFR) which is over-expressed on cancer cells[241] using BsAbs, significant inhibition and regression was shown[227]. In those studies, mice received a drug dose which was a 8000-fold dose reduction as compared to a standard systemic treatment. The targeting of the EGFR receptor both delivered the minicell to the correct location, and triggered receptor-mediated endocytosis which was essential for the up-take of minicells by non-phagocytic human breast adenocarcinoma cells[227].

Following this success, the same researchers showed that minicells could be packaged with small interfering RNAs (siRNAs) and plasmid DNA for expression of short hairpin RNAs (shRNA)[227] which down-regulated proteins involved in cancer cell proliferation[242]. In this system, bacteria transformed with plasmid DNA was cultured expressing shRNAs and then purified, whereas siRNA was absorbed into the purified minicells by co-incubation. Analysis showed that each minicell contained approximately 100 copies plasmid DNA, equating to between 3 and 5 µg per 10^{10} minicells, and 12,000 siRNA molecules[238]. Sequential treatment with EGFR targeted delivery of minicells containing siRNA or cytotoxic drugs prevented tumour growth and was also effective against a multidrug-resistant tumour cell line[238]. *In vitro* studies showed that endocytosed minicells were degraded by endosome/lysosome fusion[238] and the plasmid DNA translocated to the nucleus where shRNA expression occurred[239].

In both studies[227,238], the targeting of tumour cells with BsAbs was essential for delivery to cancer-specific cells and receptor mediated endocytosis which ultimately resulted in tumour growth inhibition or regression. BsAbs were made by protein A/G

coupling of the Fc region of two monoclonal antibodies specific for the O-antigen on the surface of the minicell or against EGFR over-expressed on some tumour cells.

1.6.1.2. Bacterial minicells as a potential vaccine platform

Whilst bacterial minicells are devoid of chromosomal DNA, they can contain plasmid DNA and, because they are still enzymatically active, they can express encoded proteins post-separation from the parent bacteria [225,233,243,244]. This feature has recently been exploited by two research groups for vaccine-related studies, where either plasmid DNA or recombinant proteins from heterologous pathogens were packaged within minicells[235-237,245]. The biotech company Vaxiion Inc (San Diego) explored the potential of minicell up-take and the subsequent transfer of plasmid DNA using the eukaryotic Cos-7 cell line. They showed expression of a GFP reporter protein in 25% of cultured cells co-incubated with minicells, but only when minicells expressed and displayed the *Yersinia pseudotubeculosis* invasin protein[235]. This invasin protein interacts with α1β5 integrins on the surface of otherwise non-phagocytic cells resulting in receptor-mediated endocytosis of bacteria[246,247].

In a subsequent study, mice were immunised with minicells containing GFP protein or GFP encoded plasmid DNA for mammalian expression, or both. Following a three dose i.m. regimen, minicells containing either GFP or plasmid DNA elicited an anti-GFP IgG antibody response and a synergistic effect was observed when minicells contained both protein and plasmid DNA[236]. Oral, intranasal and i.m. routes each induced significant IgG titres as compared to the naive control, however, i.m. immunisations induced a 4-fold higher response[236]. The mean titre, however, was less than 1250, and the ability of such low titre antibodies to protect from challenge would need to be assessed. *In vitro* experiments showed minicells could be taken up by phagocytic cell lines including J774A.1, RAW264.7 and bone marrow-derived macrophages (BMDMs) and BMDDCs[236]. Whilst the reported transfection efficiency was only between 0.02 and 0.2%, those studies did demonstrate that APCs could uptake and express plasmid DNA delivered in minicells[236].

Only one study has evaluated the capacity of minicells to induce $CD8^+$ T cell responses and confer T cell-mediated protection. In that study, the effectiveness of

protein and plasmid DNA loaded minicells was assessed using a LCMV model with the LCMV nucleoprotein antigen[237]. The minicells were able to induce peptide-specific $CD8^+$ T cell IFN-γ^+ responses and protection from LCMV challenge. Following a 3 dose i.m. regimen, almost 5% of $CD8^+$ T cells produced IFN-γ in response to antigen-specific peptide restimulation, and this response was similar to a 50 µg/dose regimen of naked plasmid DNA. To evaluate the dose requirements for efficient protection, mice received doses ranging from 10^7 to 10^{10} minicells in log increments. Protection was most effective in mice (8/9) at the highest dose and efficiency was lost as doses decreased (2/5, 1/5 and 0/5) [237]. The effective antigen load in a 10^{10} minicell dose was 1.2 ± 0.2 µg of protein and 3.0 ± 0.7 µg of plasmid DNA.

The priming of protective $CD8^+$ T cell responses has also been reported in minicells produced by *S. typhimurium* using an ovalbumin model[245]. That study reported that heterologous antigen protein delivery to the cytosol of APCs required the up-regulation of the type III secretion system (T3SS) coupled with chimeric proteins which include pathway specific homing signals[248] to increase antigen presentation and transgenic OT I $CD8^+$ T cell proliferation[245]. These secretion systems are also present in some species of *E. coli*[249], however, the data from the LCMV study indicates either the absence of T3SS or at least the up-regulation requirements[237].

1.6.2. Outer membrane vesicles

There are three components to the envelope of Gram negative bacteria, specifically the outer membrane (OM) composed mostly of LPS, the inner membrane (IM) composed of phospholipids, and the viscous fluid in the periplasmic space[250]. OMVs form when the OM bulges away from the IM and pinches off forming spherical vesicles of between 20 to 250 nm in diameter which are surrounded by the OM and contain proteins from within the periplasm[250]. OMVs are a naturally secreted product from a wide variety of Gram negative bacteria which reportedly serve multiple purposes including the mediation of the exchange of DNA, protein and signalling molecules[250-252].

Bexsero® is a multi-component Meningococcal B vaccine produced by Novartis, which in 2013 achieved licensure for human use[253]. The vaccine consists of three recombinant *Neisseria meningitidis* serogroup B proteins, and an outer membrane vesicle (OMV) from the New Zealand NZ98/254 strain each adsorbed on aluminium hydroxide. This is the first vaccine licensed using a bacterium-like particle. Other *N. meningitidis* OMV based clinical trials conducted between 1987 and 2008 have reported a vaccine effectiveness of between 47 to 83%[254-259].

Various methods have been used to purify OMVs from bacterial cultures. The technique used for recent clinical trials[254,255,259] involves sodium deoxycholate detergent extraction and differential centrifugation. Due to the small size of the OMVs other researchers have used a slow speed centrifugation to remove the bulk of parent bacteria followed by sequential 0.45 µm and 0.22 µm filtration then high speed centrifugation[260,261] some using ammonium sulphate precipitation after filtration to enrich OMVs[262,263].

Predictably, there are a range of proteins in both the OM as well as the lumen, and because the vesicles form only from the periplasm[250] it would be unexpected to find cytoplasmic proteins. Analysis of Bexsero® showed that whilst 90% of the total protein amounts were OM proteins, 5% were periplasmic proteins and 5% were proteins from within the cytosol[264]. The unexpected high amounts of cytoplasmic proteins are likely an effect of the detergent extraction process, with OMVs harvested with filtration contained only two cytoplasmic proteins and the amount of OM proteins was increased[265]. Using a mutated *N. meningitidis* which constitutively produces higher amounts of OMVs with increased OM and reduced cytosolic proteins, the capacity of OMVs to induce protective efficacy across a wider panel of MenB strains was increased[265].

The small spherical nature of OMVs result in a high surface area to volume ratio which explains the high ratio of OM proteins in OMV proteomic analysis[264]. With limited periplasm or cytoplasm proteins, it would be difficult for OMVs to deliver high amounts of heterologous antigens unless they were concentrated in the OM. In an evaluation of foreign antigens delivered to the periplasm, GFP fused with the twin arginine transporter (Tat) signal sequence was expressed in *E. coli* resulting in the

isolation of GFP to the periplasm and detectable but very low quantities of GFP in the OMVs[266]. Predictably, antigens directed to the OM showed greater success[266,267]. Chen and colleagues[267] fused GFP to the bacterial hemolysin ClyA which localised to the OM and was comprised 5% of the total protein content of OMVs. Following two immunisations with OMVs with an effective dose of 2.5 µg GFP, significant anti-GFP IgG responses were detected, however, these were similar to GFP adsorbed to aluminium hydroxide and the Cly-GFP purified protein administered with blank OMVs[267]. Whilst some have detected the presence of DNA encoding virulence genes in OMVs[261] delivery of plasmids to the periplasm and low lumen volumes make this platform seem unlikely to succeed.

1.6.3. Bacterial ghosts

Bacterial ghosts (BGs) are produced following the expression of gene E from bacteriophage ΦX174, which results in the formation of a transmembrane tunnel through the IM and OM of Gram negative bacteria (reviewed in [268,269]). Due to osmotic pressure differences between the cytoplasm and the medium, the cytoplasm is forced out of the bacteria leaving an intact IM and OM structure[270]. The size of the BG is dependent on the bacteria from which it has been derived, with the larger size increasing their antigen load capacity as compared to the minicell or OMV platforms. The larger size of ghosts and the non-requirement of particle size isolation as per minicells and OMVs simplifies the purification process to require only centrifugation[271]. The large size of BGs may, however, be detrimental when delivering antigens targeted to DCs which preferentially take up much smaller particles[196].

In a recent review, Muhammad *et al.*[269] presented an overview of BG vaccine trials for both human and veterinary medicine. Trials included those using the empty cell envelope as homologous immunogens, as well as proteins and plasmid DNA for heterologous pathogens. The majority of studies reported antigen-specific antibody response, some Th-1 type responses, and others with significant cellular immune responses[269]. The stimulation of the immune system is likely enhanced by the retention of LPS and PAMPs on the BGs.

Chemotherapeutic drugs have been loaded by a simple 5 min co-incubation with BGs, and shown to stay within the lumen and not adhere to the membranes[272]. Despite the transmembrane tunnel remaining after loading the drugs, approximately 80% of the free drugs in the lumen, were retained following dialysis for 10 h and at least 50% retention was maintained after 5 days[272]. Importantly, there was efficient uptake of the BGs by Caco-2 cancer cells, and subsequent drug release had a potent anti-proliferation effect[272]. To prevent leakage of drugs from BGs, a system was devised which seals the tunnels using lipid vesicles with a biotin-streptavidin coupling method[273]. BGs were efficiently taken up by macrophages and cancer cells and the carried drugs were released within the cell[273].

Genetically fused protein anchor sequences to antigen proteins enables transformed bacteria to express vaccine targets which are transported to the IM or OM prior to controlled tunnel lysis[274]. These proteins are retained as part of the BG and are capable of inducing moderate antibody responses.

Concentrated plasmid DNA can be loaded into BGs by co-incubation[271,275,276], with the negatively charged DNA binding by electrostatic interactions with the positively charged moieties of the IM[275] with up to 6000 plasmid copies per BG[275]. Efficient uptake and protein expression was observed using a variety of BGs, by RAW 264.7 murine macrophages[275], murine BMDDCs[271] and human monocyte-derived DCs[276].

This platform is still in early stages of development and its ability to induce robust antibody and cellular responses is yet to be established. The ability of BGs to result in the maturation of APCs also requires further attention. Whilst there are reports of increased inflammatory cytokines and IL-12 in porcine DCs and RAW264.7 cells[277] human monocyte-derived DCs showed no up-regulation of CD11c, CD40 or CD86 receptors, and a down-regulation of CD80 and CD83 receptors despite high uptake and expression[276].

1.7. Thesis outline, aims and hypothesis

My thesis was designed to comprehensively evaluate novel vaccine delivery platforms for their ability to induce antibody and cellular immune responses, as well as their ability to provide protection from *P. yoelii* 17XNL sporozoite challenge. The

platforms included chimeric VLPs and chimeric capsomeres to deliver defined foreign epitope immunogens, and bacterial minicells targeted to DCs which harbour recombinant protein and plasmid DNA.

Aim 1: Evaluate the immunogenicity and protective efficacy of chimeric MuPyV VLPs with exposed *Py*CSP $CD8^+$ T cell, $CD4^+$ T cell and B cell epitopes.

Hypothesis: VLPs presenting defined *Plasmodium* epitopes will be highly immunogenic stimulating B and T cell responses to levels sufficient to confer protection against parasite challenge.

Project summary: The VLP platform of choice uses bacterial produced recombinant MuPyV VP1 structural protein with a *P. yoelii* CSP epitope genetically inserted into the S4 surface exposed loop with flanking G4S linker sequences. VLPs are inducible *in vitro* under physiochemical conditions to self-assemble into structures which resemble the native virus, retaining viral self-adjuvanting properties. This platform developed by the Middelberg group has been shown to induce robust antigen-specific antibody responses[173,188], but the platform has not been previously assessed for its ability to induce cellular responses. Chimeric VLPs were constructed to include *Py*CSP epitopes: $CD8^+_{280\text{-}288}$ T cell[73]; $CD8^+_{59\text{-}67}$ T cell[75]; $CD4^+_{281\text{-}296}$ T cell[72]; $CD4^+_{57\text{-}70}$ T cell[74]; $CD4^+_{59\text{-}79}$ T cell[71]; or a dimer of the B cell central repeat $(QGPGAP)_2$[63]. Constructs which were efficiently produced by bacteria and formed VLPs were used in a series of immunisation experiments. Immunogenicity and protection was evaluated using individual or pooled constructs, pooled constructs with and without polyIC adjuvant, and used also in conjunction with *Py*CSP plasmid DNA in a heterologous prime-boost regimen. For protective efficacy analysis, mice immunised with VLPs or capsomeres were challenged with *P. yoelii* 17XNL sporozoites.

Aim 2: Evaluate the immunogenicity and protective efficacy of chimeric MuPyV capsomeres with exposed *Py*CSP $CD8^+$ T cell, $CD4^+$ T cell and B cell epitopes.

Hypothesis: Capsomeres presenting defined *Plasmodium* epitopes will be highly immunogenic stimulating B and T cell responses to levels sufficient to confer protection against parasite challenge.

Project summary: The same epitopes were inserted into the chimeric capsomere platform also developed by the Middelberg group but in this platform each epitope was inserted into three locations within the truncated MuPyV VP1 protein[170]. In a VLP comparative study, pooled capsomeres co-administered with polyIC were used to immunise mice in a homologous regimen, or with *Py*CSP plasmid DNA in a prime boost regimen. For protective efficacy analysis, mice immunised with VLPs or capsomeres were challenged with *P. yoelii* 17XNL sporozoites.

Aim 3: Evaluate vaccine efficacy of *E. coli* minicells containing ovalbumin or *PyAMA-1* plasmid DNA and recombinant protein, and targeted to DCs using BsAbs against the minicell surface and DC receptors DEC205 or Clec9A.

Hypothesis: Targeting DCs with bacterial minicells containing plasmid DNA and recombinant proteins will induce effective antigen-specific T cell and antibody responses and confer protection from parasite challenge.

Project summary: The bacterial minicell platform was selected over the OMV and BG platforms because they are able to package cytoplasmic proteins and plasmid DNA, and minicells are smaller than BGs making them more open to DC uptake[196]. Only two studies have evaluated minicell potential as a vaccine platform to deliver both recombinant protein and plasmid DNA[236,237]. Those studies showed minicells could induce antibody[236] and cellular[237] immune responses, but the transfection efficacy in APCs was low (0.2-0.002%)[236]. Bacterial minicells have not previously been targeted to APCs as a vaccine delivery platform. In an effort to enhance DC uptake of minicells, my studies have coupled minicells to BsAbs to target DEC205 or Clec9a DC surface receptors. Minicell producing *E. coli* DS410 was transformed with plasmid DNA for both bacterial and mammalian expression of antigens including chicken ovalbumin or *P. yoelii* AMA-1. Bacterial cultures were induced to express the antigen and then minicells were purified using a novel purification process removing all viable parent bacteria, whilst retaining a high minicell yield. Minicells with or without BsAbs were used to immunise mice to assess their antigen-specific immunogenicity and protective efficacy using a *P. yoelii* 17XNL sporozoite challenge.

Chapter 2: Materials and Methods

2.1. Bacteria

Table 2: *E. coli* strains

Strain	**Antibiotic resistance**	**Use**	**Source**
P678-54	Streptomycin	Minicell producing [222]	Dr Judya Praszkier (University of Melbourne)
DS410	Streptomycin	Minicell producing [278]	Dr Miguel Vicente (Spanish National Biotechnology Centre)
VIP205	Kanamycin	Minicell producing[232]	Dr Miguel Vicente (Spanish National Biotechnology Centre)
Top 10	Streptomycin	Cloning	Invitrogen, CA, USA
DH5α	Nil	Cloning	Invitrogen, CA, USA
Omnimax 2T1	Nil	Cloning	Invitrogen, CA, USA
Rosetta (DE3) pLysS	Chloramphenicol	VP1 protein production	Novagen, CA, USA

2.2. Vectors

Table 3: Expression and cloning vectors

Name	**Expression**	**Antibiotic selection**	**Tag**	**Comments and source**
pVR1020	Mammalian	Kanamycin	Nil	Empty vector Vical Inc.
pVR2516	Mammalian	Kanamycin	Nil	*Py*CSP gene in pVR1020, Vical Inc.
modVR1020	Mammalian	Kanamycin	Nil	Empty vector pVR1020 with additional restriction sites in MCS, Vical Inc. With modifications by Dr. Don Gardiner
pIASO	Mammalian	Chloramphenicol	V5	Mod VR1020 modified to be chloramphenicol resistant and includes a V5 epitope (section 4.2.9.1)
pVRV5	Mammalian	Kanamycin	V5	ModVR1020 modified to include a V5 epitope (section 4.2.9.2)

pBAD/Myc-His A	Bacterial	Ampicillin	c-Myc + His	Protein expression induced by addition of L-arabinose, Invitrogen
pTrcHis2A	Bacterial	Ampicillin	c-Myc + His	Protein expression induced by addition of IPTG, Invitrogen
pDual GC	Bacterial and mammalian	Kanamycin	c-myc + His	Dual expression vector, bacterial expression induced by IPTG, Stratagene, La Jolla, CA, USA
pIVEX-His/Ha	Bacterial	Ampicillin	HA + His	Empty vector pIVEX 2.4d modified to include an N-terminal HIS tag and C-terminal HA tag [279]
pGEM-T	Cloning	Ampicillin	Nil	Cloning vector, Promega Corporation, WI, USA

2.3. Mice

All mice were female, aged between 5 and 10 weeks and were purchased and/or maintained under specific pathogen-free conditions at the QIMR Berghofer animal facility. All studies were approved by the QIMR Animal Ethics Committee and were conducted in accordance with the Australian Code of Practice for the Care and Use of Animals for Scientific Purposes (2004). Mice were euthanised using either CO_2 asphyxiation or cervical dislocation.

Table 4: Experimental mouse species and source

Strain	**Strain features**	**Source**
BALB/c	$H2K^d$ haplotype, inbred	ARC
C57BL/6	$H2K^b$ haplotype, inbred, expresses *b* allele of the CD45 molecule (CD45.2)	ARC
CS-TCR	BALB/c background, $H2K^d$ haplotype, transgenic for restricted T cell receptor specific for P. *yoelii* circumsporozoite protein 280-288 (SYVPSAEQI)	Bred at QIMR Berghofer animal facility
OT-I	C57BL/6 background, $H2K^b$ haplotype, transgenic for restricted T cell receptor (Vα2/Vβ5) specific for chicken ovalbumin 257-264 (SIINFEKL)	Bred at QIMR Berghofer animal facility
OT-II	C57BL/6 background, $H2K^b$ haplotype, transgenic for the mouse αβ-T cell receptor that pairs with the CD4 co-receptor and is specific for chicken ovalbumin 323-339 (ISQAVHAAHAEINEAGR)	Bred at QIMR Berghofer animal facility
B6.SJL-$Ptprc^a$ (PTP)	C57BL/6 background, $H2K^b$ haplotype, genetically modified inbred, expresses *a* allele of the CD45 molecule (CD45.1)	ARC

2.4. Sporozoites

Experimental challenges utilised *Plasmodium yoelii* 17XNL cryopreserved sporozoites obtained from Dr. Stephen Hoffman (Sanaria Inc., Rockville, MD, USA). Vials were thawed in a 37°C water bath then diluted to 5 x 10^3 sporozoites / ml in PBS with 2 % naive mouse serum and maintained at room temperature (RT) until administered in a 200 µl i.v. dose.

2.5. Immunisations

Intra-muscular injections (i.m.): mice were injected i.m. with 50 µg of plasmid DNA diluted to 50 µl in PBS into each tibialis anterior muscle using an insulin syringe with a 29 gauge needle (BD Biosciences) fitted with a plastic collar to limit needle penetration.

Subcutaneous (s.c.) and Intraperitoneal injections (i.p.): Mice were injected with VLP's, capsomeres, peptides or recombinant proteins in adjuvant or minicells delivered s.c. at the base of the tail, or i.p. in a dose not exceeding 100 µl using an insulin syringe with a 27 gauge needle (Terumo, Somerset, NJ, USA) delivered as a single bolus.

Intravenous injections (i.v.): Mice were pre-warmed under a heat lamp then injections given into lateral tail veins in a dose of 200 µl using an insulin syringe with a 27 gauge needle (Terumo, USA).

Specific details of experimental immunisations are mentioned in the experimental design at the beginning of each research chapter.

2.6. Molecular biology

2.6.1. Competent bacteria

Glycerol stocks of various *E. coli* strains were streaked onto LB agar plates with appropriate antibiotics and incubated overnight at 37°C. A single colony was selected and transferred into 10 ml tubes with 3 ml LB and appropriate antibiotics

then incubated overnight at 37°C and 225 RPM. A 100 ml culture was then inoculated with 100 µl of the starter culture and incubated at 37°C and 225 RPM until the OD_{600} was 0.5. Cultures were then cooled on ice for 10 min then centrifuged (3000 x *g*, 10 min, 4°C). The bacterial pellet was then resuspended in 100 ml of cold $CaCl_2$ [0.1 M] and incubated on ice for 1 h. Bacteria were again centrifuged (3000 x *g*, 10 min, 4°C) then the pellet resuspended in 7 ml of cold $CaCl_2$ [0.1 M] with 10% glycerol. Aliquots of 100 µl were transferred to 1.5 ml eppendorf tubes and snap frozen in an ethanol bath on dry ice and then stored at -70°C. Transformation efficiency was assessed by transforming bacteria with plasmid and incubating spread plates overnight.

2.6.2. Target gene amplification

2.6.2.1. PCR amplification of genes

All gene amplification was done by polymerase chain reactions (PCR) using either Pfu turbo DNA polymerase (Agilent Technologies, CA, USA) or KOD Hot Start DNA polymerase (Novagen, CA, USA) each with proof-reading activity. PCR reagent concentrations and DNA polymerase, as well as reaction conditions including annealing and extension times and temperatures, were optimised for each gene. All PCR reactions were in 50 µl reaction volumes each with 0.2 mM dNTPs, 0.3 mM of forward and reverse primers, 1U of polymerase, between 5 to 50 ng of template DNA and either MgCl and $MgSO_4$ with concentrations varied between 1.5 to 4.0 mM and 1.5 to 2.5 mM respectively.

A standard PCR protocol used a denaturation of 95°C for 2 min; 5 cycles of 95°C for 20 s, 50°C for 20 s and 68°C for 1 min/kb of DNA; 30 cycles of 92°C for 20 s, 55°C for 15 s and 68°C for 1 min/kb of DNA; and a final extension at 68°C for 5 min. For non-*Plasmodium* genes, extension temperatures were increased to 72°C. Amplification was assessed visualising band intensity after agarose gel electrophoresis (section 2.6.3.1).

*Py*CSP and *Py*AMA-1 genes were PCR amplified from the pVR2516 plasmid (Table 3), or genomic DNA recovered from Plasmodium yoelii 17XNL sporozoites (section

2.4) respectively. Primers used for PCR amplification are detailed in (Appendix D) and protein sequences are listed in (Appendix E).

The plasmids pBlueRIP/Ova and pBlueRIP/Tfr-ova were a gift from Professor Francis Carbone (University of Melbourne, Victoria, Australia). These plasmids include cDNA for chicken ovalbumin (OVA) and a fusion protein with a region from the human transferrin receptor and chicken ovalbumin[280] (Tfr-Ova) respectively. These plasmids were used to PCR amplify both Ova and Tfr-Ova genes. Primers used for PCR amplification are detailed in (Appendix D).

Plasmids containing a green fluorescent protein (GFP) and red fluorescent protein (RFP) were obtained from Dr. Don Gardiner (QIMR Berghofer, Herston, Qld, Australia). These were used to PCR amplify fluorescent genes. Primers used for PCR amplification are detailed in (Appendix D).

2.6.3. Digestion, ligation and clonal selection

2.6.3.1. Electrophoresis and gel extraction

For electrophoresis, 0.8% agarose gels were made with either ethidium bromide or SYBR safe DNA gel stain (Invitrogen, CA, USA). Gels were run using a tris-borate buffer (TBE) (Appendix A) in a Mini-Sub cell GT tank (Bio-Rad Laboratories, CA, USA) with a Power-Pac 300 (Bio-Rad) power supply. Samples were pre-mixed with a New England Biolabs (NEB) gel loading dye (New England Biolabs Inc., MA, USA) then gels were run for 90 min with power set at 90 V and 400 mA. For size determination, a 1 Kb DNA ladder (NEB) was run in parallel.

Agarose gels were viewed under UV light and where necessarily bands were excised. DNA was extracted from gel slices using a QIAquick gel extraction kit (Qiagen Pty Ltd, Hilden, Germany) according to the manufacturer's protocol with all elution steps done with water.

2.6.3.2. Restriction enzyme digestion

All restriction enzymes were purchased from NEB (New England Biolabs Inc., MA, USA) and reaction reagent buffers and volumes were in accordance to the manufacturer's protocol. Reagents mixed in PCR tubes were incubated at either 25°C (*Apa*I digestions only) or 37°C for between 1 h to 6 h depending on the efficiency of the enzyme. Products were separated by gel electrophoresis and appropriate size bands were excised and DNA extracted (section 2.6.3.1).

2.6.3.3. Ligation

All DNA ligations used T_4 ligase (NEB) using recommended reaction conditions. Ligation reactions used 50 ng of vector in a vector:insert ratio of between 1:3 and 1:50. The amount of insert was calculated using the following formula.

$$\frac{\text{ng of vector x kilobase pairs of insert}}{\text{kilobase pairs of vector}} \text{ x ratio} = \text{ng of insert}$$

Ligation reactions were incubated overnight at 16°C followed by heat inactivation using a 10 min incubation at 65°C.

2.6.3.4. Transformations

Tubes of competent bacteria were thawed on ice then 10 µl ligation mix or approximately 500 ng of purified plasmid was added, flicked to mix, then incubated on ice for 30 min. Tubes were then immersed in a 42°C water bath for 1 min then recovered on ice for 5 min. Then 800 µl of SOC media (Appendix A) was added to tubes which were then shaken in an incubator at 225 RPM and 37°C for 1 h. A spread plate was made using 100 µl of the mixture onto LB agar with appropriate selective antibiotics. Once the plate had dried, they were inverted and incubated at 37°C overnight.

2.6.3.5. Colony PCR

Following the overnight incubation of transformation plates, colony isolates were selected and mixed into 20 µl of sterile water in PCR tubes, and then 5 µl was removed and stored. The remaining 15 µl was heated to 94°C for 4 min then vortexed and centrifuged for 1 min to pellet bacteria, and then 5 µl of the supernatant was used as the PCR template.

Each 20 µl PCR reaction comprised of 2 µl PCR buffer (10x), 1.2 µl $MgCl_2$ [50 mM], 0.4 µl dNTP [20 mM], 0.4 µl of forward and reverse primers [10 nM], 0.1 µl of platinum taq DNA polymerase (Invitrogen), 10.5 µl of water and 5 µl of PCR template. The PCR protocol was: 94°C for 3 min; then 30 cycles of 92°C for 15 s, 45°C for 20 sec and 72°C for 1 min per kilobase of product; followed by 72°C for 5 min. Electrophoresis was then conducted with the PCR product using 0.8% agarose gels with band size estimated using a 1 kb DNA ladder (NEB, MA, USA). Positive colonies were streaked onto transfer plates with appropriate selection antibiotics and incubated overnight at 37°C

2.6.3.6. Plasmid purification and bacteria storage

Bacterial colonies were selected from transfer plates and incubated overnight in a 50 ml falcon tube with 7 ml LB with appropriate selection antibiotics. For colony storage, 300 µl of the culture was combined with 300 µl of sterile glycerol which was vortexed and frozen in ethanol and dry ice then stored at -70°C. The remaining culture was used for plasmid extraction using a Qiagen miniprep kit (Qiagen Pty Ltd, Germany) following the manufacturer's protocol. Plasmid elution was done using 50 µl of water and quantified on a nanodrop 2000 (Thermo Fisher Scientific, MA, USA).

2.6.3.7. Sequencing

Sequencing was done using the BigDye Terminator v3.1 (Invitrogen) using ¼ reactions following the manufacturer's protocol. Analysis was conducted by QIMR Berghofer core facilities. Sequence confirmation was checked using either the National Centre for Biotechnology Information (NCBI) nucleotide Basic Local

Alignment Search Tool (Blastn) or Vector NTI (Invitrogen) sequence alignment software.

All sequencing for the VLP and capsomere platforms (section 3.2.1) was done by the Australian Genome Research Facility (AGRF, Brisbane, Australia).

2.7. Molecular biology for minicell platform

2.7.1. Vector construction pIASO and pVRV5

The pIASO vector was constructed from modVR1020 (Table 3) by replacing the kanamycin resistance gene with the chloramphenicol resistance gene, and inserting a V5 epitope tag at the C-terminal region of the multiple cloning site.

The pVRV5 vector was also constructed from modVR1020 by inserting a V5 epitope tag at the C-terminal region of the multiple cloning site.

Details of each vector construction are provided in (section 4.2.9).

2.8. SDS-PAGE and Western Blot

Proteins were analysed by sodium dodecyl sulphate polyacrylamide gel electrophoresis (SDS-PAGE) coupled with either coomassie blue staining or western blot. Samples were diluted in a mix of lysis buffer (Appendix A) load dye and NuPage reducing agent (Novex, CA, USA) to a maximum volume of 15 µl in 1.5 ml Eppendorf tubes. Tubes were heated at 95°C for 12 min, vortexed and allowed to cool, then spun momentarily. Samples were loaded onto self poured 10% acrylamide/bis-acrylamide (Biorad, CA, USA) SDS-PAGE gels and run at 150 V for 60 min in running buffer (Appendix A). Each gel contained a lane with a Novex Sharp pre-stained protein standard (Novex, USA). To determine protein quantity, a protein with a known concentration was run on the gel in a serial dilution.

For western blot analysis, an Immobilon membrane (Millipore, MA, USA) was pre-wet with methanol, then equilibrated in transfer buffer (Appendix A), and then sandwiched beside the SDS-PAGE gel. Transfer was done in a mini trans-blot cell (Biorad, CA, USA) transfer tank at 100 V for 2 h in transfer buffer. The membrane

was then blocked overnight at 4°C in Odyssey blocking buffer (Li-cor, Nebraska, USA), washed and stained using α-His peroxidase antibodies (Roche Diagnostics, Germany) diluted to 1:5000 in PBS + 0.1% Tween20. Following 2 h at RT on a rocker, the membrane was washed and developed using Amersham ECL Prime western blot detection reagent (GE Healthcare, UK) then imaged on an ImageQuant LAS 5000 (GE healthcare Biosciences, Uppsala, Sweden).

When gels were analysed using the Li-cor Odyssey Classic (Li-cor, USA), after the overnight blocking, membranes were stained with rabbit α-c-Myc epitope (Thermo Pierce, IL, USA) diluted to 1:2500 and incubated for 1 h at RT, then donkey α-rabbit IR dye 800 (Li-cor, USA) diluted 1:15000 and incubated for 1h at RT, both dilutions were done in blocking buffer + 0.1% Tween20. The membrane was then washed in PBS + 0.1% Tween20 and rinsed with PBS then milliQ water before being imaged.

2.9. Experimental cell preparation and restimulation

2.9.1. Harvesting lymphocytes

Single cell suspensions were made by physical disruption of spleen or lymph nodes passing them through a 100 µm nylon mesh (Biologix Plastics Co.Ltd, Jiangsu, China) with 5 ml Dulbecco's media with 2% FCS (Dulbecco's 2%)(Appendix A). Cells were centrifuged (600 x *g*, 4 min, 4°C) and supernatant removed. Removal of red blood cells (RBCs) was achieved by either buffer disruption or density gradient cell centrifugation.

In the buffer disruption method, cells were incubated for 5 min at 37°C in 5 ml of pre-warmed red cell removal buffer (Appendix A) then washed in Dulbecco's 2% and resuspended in KD-MEM with 10% FCS (Appendix A). Alternatively, single cell suspensions in 10 ml of Dulbecco's 2% were under laid with 5 ml of Ficoll-Paque Plus (GE Healthcare Biosciences, Uppsala, Sweden) and centrifuged (800 x *g*, 10 min, 4°C) with a slow brake. Lymphocytes were harvested from the interface and washed in Dulbecco's 2% then resuspended in KD-MEM with 10% FCS. All wash steps used the same centrifuge conditions (600 x *g*, 4 min, 4°C).

Cells were counted microscopically using trypan blue (HyClone Laboratories Inc., UT, USA) staining and a haemocytometer then diluted as required prior to distribution for assays.

2.9.2. $CD8^+$ and $CD4^+$ T cell purification and CFSE labelling

Single cell suspensions were prepared (section 2.9.1) from both spleens and lymph nodes from naive OTI, OTII or CS-TCR mice (Table 4). $CD8^+$ and $CD4^+$ T cells were enriched by positive selection using mouse CD8a (Ly-2) or CD4 (L3T4) microbeads (Miltenyi Biotec GmbH, Bergisch Gladbach, Germany) according to the manufacturer's protocol using a magnetic column.

For *in vitro* proliferation assays, cells were then washed in Dulbecco's with 0.1% FCS then resuspended at 10^7 cells/ml in pre-warmed (37°C) Dulbecco's 0.1% with 5 µM carboxyfluorescein diacetate succinimidyl ester (CFSE; Molecular Probes, Victoria, Australia). The cells were incubated at 37°C for 10 min then washed three times in Dulbecco's 2% and then resuspended in KD-MEM with 10% FCS.

Selective cell purification and CFSE staining was assessed by flow cytometry. Cells were surface stained for CD8 or CD4 markers as well as Vα2 (OTI and OTII cells) or Thy1.1 (CS-TCR) markers (Appendix C) with analysis performed on a BD LSRFortessa (BD Biosciences, CA, USA).

2.9.3. Restimulation for cellular immunogenicity assays

2.9.3.1. A20 cell line

The A20 cell line (mouse B cell lymphoma, ATCC # TIB208) was used for antigen presentation during *in vitro* immunogenicity assays. This suspension cell was cultured in KD-MEM media with 5% FCS (Appendix A) at 37°C and 5% CO_2. Following peptide stimulation or transfection (below) cells were irradiated with approximately 16666 cGy in a Cs 137 irradiator.

2.9.3.2. Positive controls

For ELISpot and cytometric bead arrays (sections 2.10.1.8 and 2.10.1.9) positive control wells concanavalin A (ConA; Sigma Aldrich, NSW, Australia) was added post-irradiation at 5 µg/ml of total well volume. For intracellular cytokine staining (section 2.10.1.10) cells were incubated with phobol 12-myristate 13-acetate (PMA) and ionomycin (both from Sigma Aldrich) at 5 ng/ml and 500 ng/ml respectively of total well volume. This stimulant was added post-irradiation and at the same time that GolgiPlug (BD Biosciences, CA, USA) was added giving a total of 6 h stimulation.

2.9.3.3. Peptide stimulation

All peptides were synthesised by Mimotopes Pty Ltd (Victoria, Australia) and resuspended in 100% dimethyl sulfoxide (DMSO; Sigma Aldrich, MO, USA) and stored at -70°C. Prior to irradiation, A20 cells were pulsed with either *Py*CSP $CD8_{280-288}$ (SYVPSAEQI) or $CD4_{59-79}$ (YNRNIVNRLLGDALNGKPEEK) individual peptides or pooled *Py*CSP $CD8_{280-288}$, $CD4_{59-79}$ and B cell (QGPGAPQGPGAP) peptides. Each peptide was added so that the final post-distribution well concentration was 10 µg/ml.

2.9.3.4. Transfections

A20 cells were maintained in culture between 1-2 x 10^6 cells/ml prior to transfections. Transfections were done using an AMAXA Nucleofactor system kit V (Lonza Group, Basel, Switzerland) following the manufacturer's protocol. Each reaction used 5 x 10^6 A20 cells and 5 µg of pVR2516 (*Py*CSP) or pVR1020 (transfection control) both from Vical Inc., using Program L-13 or C-25 on an AMAXA Nucleofector I device (Lonza Group).

2.9.3.5. Culture conditions

All cell cultures were done in humidified incubations at 37°C and 5% CO_2.

2.10. Immunology assays

2.10.1. Cellular assays

2.10.1.1. Dendritic cell migration to draining lymph nodes following minicell injections

To assess the migration profile of dendritic cells ($MHCII^{high}$ $CD11c^{high}$), C57BL/6 mice (n=1/condition) received s.c. injections of either 10^{10} ovalbumin loaded minicells with and without BsAbs to target DEC205 (section 4.2.12), empty minicells or ovalbumin protein (100 µg) with cholera toxin (CT; 1 µg). Injections were given at 6 h intervals from 48 to 24 h before draining lymph nodes were harvested. Single cell suspension from DLNs of each mouse were transferred into 96-well V-bottom plates and centrifuged (600 x *g*, 4 min, 4°C) then resuspended in 2.4G hybridoma supernatant (to block Fc receptors) for 10 min. Cells were washed and stained for MHCII and CD11c cell surface markers (Appendix C) for 20 min, then washed and resuspended in MACS buffer with propidium iodide (Pi). Cells were analysed on an LSR Fortessa (BD Biosciences, NSW, Australia). Post-acquisition analysis was done using FlowJo software version 9.4 (Treestar, Ashland, OR, USA) to determine the frequency of MHCII and CD11c high cells.

2.10.1.2. Ovalbumin minicell induced proliferation of OTI and OTII cells by migrating dendritic cells

C57BL/6 mice (n=5/group) received s.c. injections of ovalbumin loaded or empty minicells (10^{10} minicells/dose) with and without BsAbs to target DEC205 or a non-specific receptor LTF_2 (section 4.2.12). Control groups received either PBS or ovalbumin (100 µg) both with 1 µg of CT. Draining lymph nodes were harvested after 24 h, pooled within groups and made into single cell suspensions (section 2.9.1). Fc receptors were blocked for 10 min in 2.4G hybridoma supernatant, and then stained with antibodies against MHCII, CD11c and CD103 (Appendix C) for 20 min on ice. Cells were then washed and resuspended in MACS buffer with Pi then sorted on a

FACSAria (BD Biosciences, USA) into dual MHCII^{high} and CD11c^{high} populations, with these cells further sorted into CD103^{high} or CD103^{low} populations.

The sorted cells were then washed and resuspended in KD-MEM media (Appendix A) with 10% FCS then transferred into 96-well U-bottom plates at 10^4 cells per well in triplicates. Wells then received 5 x 10^4 of either OTI or OTII purified and CFSE stained cells (section 2.9.2). Cells were incubated at 37°C and 5% CO_2 for 3 d then transferred to a 96-well V-bottom plate and centrifuged (600 x *g*, 4 min, 4°C). Cells were resuspended in 2.4G hybridoma supernatant to block Fc receptors for 10 min, and then washed and stained for Vα2, CD8 and CD4 cell markers (Appendix C). Cells were washed and resuspended in MACS buffer with Pi then analysed on an LSR Fortessa (BD Biosciences). Post-acquisition analysis was done using FlowJo software version 9.4 (Treestar, USA) to determine the median fluorescence intensity (MFI) of CFSE in both OTI and OTII cells.

In a separate experiment, C57BL/6 mice (n=1/condition) were injected s.c. in the flank with ovalbumin packaged minicells (10^{10}) with and without BsAbs to DEC205, empty minicells (10^{10}), PBS or ovalbumin protein (100 µg) with CT (1 µg). Injections were given at 6 h intervals from 48 to 24 h before draining lymph nodes were harvested and single cell suspensions made in KD-MEM with 10% FCS (section 2.9.1). These cells were then irradiated for 30 min, and then 5 x 10^5 cells were transferred into 96-well U-bottomed plates. Each well then received 5 x 10^4 of either OTI or OTII purified and CFSE stained cells (section 2.9.2) and cultures incubated for 3 to 5 days. After incubation, cells were washed, stained and analysed as described above. Cells were analysed on an LSR Fortessa (BD Biosciences) with CFSE detected with the 530/30 detector on the 488 nm laser. Post-acquisition analysis was done using FlowJo software version 9.4 (Treestar, USA) to determine the MFI of CFSE in both OTI and OTII cells.

2.10.1.3. In vitro stimulation of CS-TCR transgenic cells

Purified and CFSE stained CS-TCR CD8$^+$ T cells (section 2.9.2) resuspended at 1 x 10^6 cells/ml in KD-MEM + 10% FCS were distributed adding 100 µl/well into 96-well U-bottom plates. Cells were then combined with 5 x 10^6 lymphocytes isolated

(section 2.9.1) from five naive BALB/c mice. Each well then received either *Py*CSP$_{280\text{-}288}$ peptide, CD8 VLPs, CD8 capsomeres, wild type VLPs or wild-type capsomeres all at a final concentration of 10 µg/ml. Cells were cultured at 37°C and 5% CO_2 and analysed after 2, 3, 4 and 5 days by flow cytometry.

Cells were transferred to 96-well V-bottom plates and centrifuged (600 x *g*, 4 min, 4°C) then resuspended in 20 µl of 2.4G hybridoma supernatant for 10 min to block Fc receptors. Cells were washed and stained for Thy1.1 and CD8 cell surface markers (Appendix C) for 20 min, then washed and resuspended in MACS buffer with Pi. Cells were analysed on an LSR Fortessa (BD Biosciences) with CFSE detected with the 530/30 detector on the 488 nm laser. The median CFSE fluorescence intensity of Thy1.1$^+$ CD8$^+$ T cells was calculated using FlowJo software version 9.4 (Treestar, USA).

2.10.1.4. Adoptive transfer proliferation

CD8$^+$ and CD4$^+$ T cells were purified from OTI and OTII mice respectively using previously described methods (section 2.9.2). Cells were adoptively transferred by i.v. injection (section 2.5) into PTP mice (Table 4). After each immunisation, blood was analysed to determine the frequency of transferred cells. Ten microlitres of blood was centrifuged (600 x *g*, 4 min, 4°C) then resuspended in antibodies directed against CD45.2, Vα2, CD8 and CD4 receptors (Appendix C) with an incubation at 4°C for 20 min. Cells were washed then resuspended immediately in FCAB fix/lyse buffer (Appendix A) and incubated at 37°C for 10 min. Cells were washed and resuspended in MACS buffer then analysed on an LSR Fortessa (BD Biosciences).

Following the final immunisation mice received a further i.v. cell transfer for CTL assay (section 2.10.1.5) then were sacrificed after 16 h. Single cell suspensions of spleen and draining lymph nodes (section 2.9.1) were obtained using the red cell removal buffer protocol, and blood was also collected. Cells were stained (as above) however, the spleen and lymph node samples were not lysed, and were instead resuspended in MACS buffer with Pi for analysis.

For all samples, post-acquisition analysis was done using FlowJo software version 9.4 (Treestar, USA). The frequency of double positive CD45.2 and CD8 or CD4 cells as to the lymphocyte population gated on FSC and SSC plots was calculated.

2.10.1.5. In vivo cytolytic assay

Single cell suspensions were made using spleen and lymph nodes from naive PTP mice (Table 4) and lymphocytes purified using a ficol density centrifugation (section 2.9.1). The cells were incubated with or without ovalbumin$_{257-264}$ (SIINFEKL) peptide at 10 µg/ml for 1 h at 37°C, then washed in Dulbecco's + 0.1% FCS. SIINFEKL coated and uncoated cells were then stained with 2.5 µM and 0.5 µM BD Horizon violet cell proliferation dye 450 (VPD450; BD Biosciences, USA) respectively at 37°C for 10 min with frequent mixing. Cells were washed three times in Dulbecco's + 2% FCS then resuspended in PBS. Differential staining was confirmed by flow cytometry. Cells were counted and combined in a 1:1 ratio.

Following the final immunisation in the ovalbumin model experiments mice received an i.v. transfer of 9 x 10^6 of the combined VPD450 stained cells. Sixteen hours later mice were euthanised and single cell suspensions of spleen and draining lymph nodes (section 2.9.1) were obtained using the red cell removal buffer protocol, and blood was also collected. Cells were stained with antibodies against CD45.1 (PTP mice) and CD45.2 (OTI and OTII mice) receptors (Appendix C) with an incubation at 4°C for 20 min. Blood samples were resuspended in FCAB fix/lyse buffer (Appendix A) and incubated at 37°C for 10 min, then washed and resuspended in MACS buffer. Spleen and lymph node samples were resuspended in MACS with Pi. All samples were analysed on an LSR Fortessa (BD Biosciences, Australia) with post-acquisition analysis using FlowJo software version 7.6 (Treestar, USA).

In the spleen and lymph node samples, viable lymphocytes were gated on forward and side scatter then Pi. Blood samples which had been fixed, were gated only on forward and side scatter parameters. Then CD45.1 cells were gated and VPD450 high and low populations were quantified. The specific lysis was calculated using the following formula-

$$\frac{(Count\ of\ VPD450\ low) - (count\ of\ VPD450\ high)}{(count\ of\ VPD450\ low)} * 100 = Specific\ lysis\ (\%)$$

2.10.1.6. WBC staining for activation markers

In the *Py*AMA-1 minicell experiment, following their final immunisation mice were challenged 1000 *P. yoelii* 17XNL sporozoites. Blood samples were collected pre-challenge then daily from days 2 to 10 and then every second or third day until day 22 post-challenge. Samples were obtained by a tail snip with 12 µl of blood collected and diluted in 12 µl of FCAB buffer containing double the amount of EDTA [4 mM] (to prevent clotting) in a 96-well V-bottom plate. Approximately 1.7 µl of blood was used for the analysis of white blood cells (WBCs). Cells were resuspended in a pool of antibodies against CD4, CD8, CD11a, CD19, CD49d, CD69, CD86, PD-L1 (CD274), PD-1(CD279) and Gr-1 (Ly-6G/C) (Appendix C) and incubated at 4°C for 20 min. Cells were washed and resuspended in FCAB fix/lyse buffer (Appendix A) and incubated at 37°C for 10 min, then washed and resuspended in MACS buffer. Pooled samples from each immunisation group were stained with isotype controls. All samples were analysed on an LSR Fortessa (BD Biosciences, Australia) with post-acquisition analysis using FlowJo software version 9.4 (Treestar, USA).

The medium florescence intensity (MFI) of activation markers, and cell counts were compared during the time-course of infection. Comparisons were made between groups and within groups where groups contained protected mice.

2.10.1.7. Assessment of serum cytokines

In the *Py*AMA-1 minicell experiment, blood was collected immediately before challenge and daily from day 2 to day 10. Here 12 µl of blood collected from the tail tip was diluted in 12 µl of FCAB buffer containing double the amount of EDTA [4 mM] in a 96-well V-bottom plate. The plate was centrifuged (600 x *g*, 4 min, RT), then 6 µl of supernatant was transferred to a new V-bottomed plate and snap frozen (-80°C) for later analysis. A pool of supernatant each group was also collected (6 µl total volume) and similarly stored for analysis.

Samples were processed according to the manufacturer's protocol using the cytometric bead array (CBA) kit with selected mouse cytokines using flex sets (BD Biosciences). For pooled samples, bead and detector flex sets for interleukins IL-1b, IL-2, IL-4, IL-5, IL-6, IL-10, IL-12p70 and IL-13, as well as IFN-γ and TNF. Individual samples were analysed only for IL-6, IFN-γ and TNF cytokines with samples taken from days 7 and 8 post-challenge. Analysis was performed on an LSR Fortessa (BD Biosciences, NSW, Australia) using a high-throughput sampler (HTS). Post-acquisition data analysis was performed using FCAP Array 3.0 software (Soft Flow Inc., Pecs, Hungary).

2.10.1.8. IFN-γ ELISpot

Following the final immunisation in the VLP and capsomere experiments, splenocytes were harvested as previously described (section 2.9.1) using red cell removal buffer, and then cells were counted. MSIPS4510 multiscreen ELISpot plates (Merck Millipore, Darmstadt, Germany) were pre-coated overnight at RT with 100 µl of sterile PBS containing 100 µg/ml anti-mouse IFN-γ (BD Biosciences, San Jose, CA, USA). Wells were then blocked with KD-MEM + 10% FCS for 3 h at 37°C, before adding combined splenocyte (5×10^5)/A20 (1.5×10^5) treated cultures (section 2.9.3) in quadruplicates. Treatments included transfected A20 cells, peptides individually or pooled, or A20 cells with ConA or without stimuli.

Plates were incubated at 37°C and 5% CO2 for 40 h then washed with PBS with 0.05% Tween20 (PBST). Then 75 µl of PBS containing 0.5% BSA (PBS-BSA) and 2 µg/ml biotinylated anti-mouse IFN-γ (BD Biosciences, USA) was added to each well and incubated at 37°C for 3 h before being washed in PBST. Then 75 µl of PBS-BSA with 1 µg/ml streptavidin-horseradish peroxidase (BD Biosciences, USA) was added to each well and incubated for 1 h at RT, before being washed with PBST and finally PBS. Plates were developed using 50 µl/well of AEC substrate (BD Biosciences, USA) for 5 min before being flooded with water and dried. Spots were counted using the AID ELISpot reader system (Autoimmun Diagnostika GmbH, Strassberg, Germany). For analysis, background responses detected in A20 only wells were

subtracted from spots detected in A20 plus peptide wells. Likewise, pVR1020 transfected A20 spots were subtracted from pVR2516 stimulated wells.

2.10.1.9. Cytometric bead array

Following the final immunisation in the VLP and capsomere experiments, splenocytes were harvested as previously described (section 2.9.1). Using 96-well round-bottom plates, 5 x 10^5 splenocytes and 1.5 x 10^5 irradiated A20 cells were combined and mixed with *Py*CSP peptides alone or pooled or with A20 cells with conA or without stimuli as described above (section 2.9.3). Cultures were incubated at 37°C and 5% CO_2 for 72 h, and then culture supernatant was collected and stored at -70°C for subsequent analysis. Pooled supernatant was analysed for interleukins IL-1b, IL-2, IL-4, IL-5, IL-6, IL-10, IL-12p70 and IL-13, as well as IFN-γ and TNF using the mouse cytometric bead array flex kit (BD Biosciences, USA) following the manufacturer's protocol. Individual samples were analysed only for selected cytokines which was determined after running pooled samples. Samples were analysed using a FACSArray instrument (BD Biosciences, USA) and analysed using the FCAP array software (BD Biosciences, USA).

2.10.1.10. Intracellular cytokine staining

Following the final immunisation in the VLP and capsomere experiments, splenocytes were harvested as previously described (section 2.9.1). Using 96-well U-bottom plates, 5 x 10^5 splenocytes and 1.5 x 10^5 irradiated A20 cells were combined and mixed with *Py*CSP peptides alone or pooled or with A20 cells with PMA/Ionomycin or without stimuli as described above (section 2.9.3). GolgiPlug (BD Biosciences, CA, USA) was added to each well to 0.1%, then cultures were incubated for 4 h at 37°C and 5% CO_2. Cells were then centrifuged (600 x *g,* 4 min) then washed in MACS buffer. CD8 and CD4 surface-markers were stained with fluorochrome-conjugated antibodies (Appendix C) for 30 min at 4°C. Cells were washed in MACS buffer then fixed with 1% paraformaldehyde for 15 min at RT, then washed and stained for intracellular cytokines IFN-γ, IL-2 and TNF with antibodies (Appendix C) diluted in Cytofix/Cytoperm (BD Biosciences) and incubated overnight

at 4°C. The cells were then washed and resuspended in MACS buffer, and then flow cytometric analysis was performed on a Fortessa LSR flow cytometer (BD Biosciences, CA, USA). Post-acquisition data analysis was performed using FlowJo software version 9.4 (Treestar, Ashland, OR, USA). Pooled samples from each immunisation group, under each restimulation condition, were stained with antibody isotype controls and analysed as described above.

2.10.2. Antibody assays

2.10.2.1. ELISA

Various capture antigens were used in different experiments each specific for the antigen immunisation component. For the VLP experiments the capture antigen was either 5 µg/ml of *Py*CSP B cell repeat epitope peptide (QGPGAPx3) with an incorporated polystyrene binding tag with glycine linker (RIIIRRIRGGGG)[281,282] (Mimotopes, Vic, Australia) or 1 µg/ml of *Py*CSP protein (Naval Medical Research Center, US Navy, MD, USA). Ovalbumin minicell experiments use chicken ovalbumin protein (Sigma-Aldrich) diluted to 5 µg/ml. *Py*AMA-1 minicell experiments used *Py*AMA-1 purified protein diluted to 1.5 µg/ml, which had been generated using RTS reactions and purified using Talon beads (section 4.2.6).

Nunc maxisorp 96-well flat bottom plates (Thermo Fisher Scientific, MA, USA) were coated with 100 µl of capture antigen diluted in a carbonate buffer (Appendix A), and incubated overnight at 4°C. Plates were washed twice with PBS then blocked with 230 µl of PBS with either 2% bovine serum antigen (BSA, Sigma Aldrich, MO, USA) or 5% skim milk powder (SMP) at 37°C for 2 h. Plates were washed twice with PBS then 100 µl of sera diluted in PBS with 0.1% BSA or SMP was added to triplicate wells. When assessing end-point antibody titres, the serum was then diluted 2-fold down the plate. In some cases sera was added at a fixed dilution only. Plates were incubated at 37°C for 2 h then washed three times in PBS with 0.02% tween20 (PBST). For IgG responses, plates were then incubated in biotinylated donkey α-mouse IgG (Jackson ImmunoResearch Laboratories Inc. PA, USA) diluted 1:20000 in PBS-BSA or SMP 0.1% at 37°C for 1 h, washed , then further incubated in streptavidin-HRP (BD Biosciences, USA) diluted 1:1000 in PBS-BSA or SMP 0.1%

and 0.2% tween20 at 37°C for 1 h. For IgG isotype responses, plates were incubated in HRP conjugated goat α-mouse IgG1, rabbit α-mouse IgG2a, goat α-mouse IgG2b, or goat α-mouse IgG3 (Invitrogen, CA, USA) all diluted 1:3000 in PBS-BSA or SMP (0.1%) and tween20 (0.2%) and incubated at 37°C for 1 h. Plates were washed 5 times in PBST (0.05%) then twice in PBS. Plates were developed by adding 50 µl/well of tetramethylbenzidine liquid substrate (TMB T4444, Sigma Aldrich, MO, USA) and left for 10 min at RT in the dark before stopping the reaction with 50 µl/well of TMB stop reagent (S5814, Sigma Aldrich, USA). Plates were then read on a VersaMax micro plate reader (Molecular Devices, CA, USA) at 450 nm.

For analysis, the OD_{450} mean plus three standard deviations of triplicate blank wells (no sera) was subtracted from the OD_{450} of each well, and then the mean of sample triplicates were determined. Samples were deemed antibody positive when post-subtraction values were positive. When a single sera dilution was used, blank-subtracted OD_{450} triplicate means were reported. When reporting antibody titrations equal to 1, a logarithmic equal based on four serial dilutions was determined using Microsoft Office Excel 2007 (Microsoft Corporation, WA, USA), which was used to calculate the titre where at OD_{450}=1.0.

2.10.2.2. Flow cytometry based IFAT

Anti-parasite antibody levels prior to, and during the course of infection were assessed using a flow cytometric procedure as previously described[283]. Briefly, blood samples collected for the serum cytokine (section 2.10.1.7) or FCAB (section 2.10.3.1) assays were centrifuged (600 x g, 4 min) then supernatant was removed either 6 µl or 1 µl respectively. The 1 µl samples were diluted in 167 µl of FCAB buffer then 6 µl was added to 6 µl of *P. yoelii* 17XNL blood-stage parasite extract in a 96-well V-bottom plate and incubated for 30 min at RT. Samples were washed and resuspended in anti-mouse IgG-FITC (Biolegend, USA) for 30 min at 4°C. Samples were washed and resuspended in 35 µl of FCAB buffer (Appendix A), then analysed on an LSR Fortessa (BD Biosciences, NSW, Australia) using a high-throughput sampler (HTS). Post-acquisition data analysis was performed with FlowJo software version 9.4 (Treestar Inc., Ashland, OR, USA). The parasite extract was gated on

forward and side scatter then the median fluorescence intensity of FITC was determined and reported for individual mice.

2.10.2.3. IFAT slides

Antibody affinity to the surface of *P. yoelii* 17NXL sporozoites was assessed using a previously described protocol[284] with some modifications. Sporozoites were centrifuged (10000 x *g,* 5 min) then resuspended to 10^3 sporozoites per 10 µl of Medium 199 (Life Technologies, NY, USA). Then 10 µl was added to pre-drawn (Barrier Pap pen) wells on a microscope slide and air dried at RT before being stored at -70°C. Prior to use, slides were returned to RT in a desiccation cabinet. Pooled sera from each immunisation group, collected 7 days after the final immunisation, was diluted 1:400 in filtered PBS with 2% BSA, then 10 µl was added to each well and incubated at 37°C in a humid box. Wells were gently washed with PBS then stained with 10 µl of FITC conjugated anti-mouse IgG (BD Biosciences, USA), diluted 1:30 in filtered PBS containing 0.005% Evans blue. Slides were incubated for 30 min in a humid chamber then washed gently with PBS. A cover slide was mounted over PBS with 10% glycerol and slides viewed on an EVOS fluorescence microscope (x400) (Advanced Microscopy Group, Washington, USA). Samples were treated as positive when fluorescence was detected on the sporozoite surface.

2.10.3. Protection efficacy assays

2.10.3.1. Flow cytometry assessment of blood (FCAB)

Parasitemia quantification was done using a flow cytometric assessment of blood (FCAB) assay as previously described[285]. Blood samples were collected immediately before challenge then daily from day 2 to day 10, and then every 2nd or 3rd day until the infection was resolved. Briefly, 2 µl of blood was collected from the tail tip of mice and immediately diluted into 200 µl of FCAB buffer (Appendix A). Six microlitres of diluted blood was transferred into a 96-well V-bottomed plate and stained with 15 µl of anti-CD71-PE (Biolegend, San Diego, USA). Cells were washed and resuspended in 30 µl of FCAB fixation and lysis buffer (Appendix A) and incubated for 10 min at 37°C. The cells were then washed and resuspended in FCAB buffer containing

bisbenzimide Hoechst 33342 (Sigma-Aldrich, USA) at 0.5 µg/ml and incubated for 20 min at 4°C. Flow cytometric analysis was performed on an LSR Fortessa (BD Biosciences, NSW, Australia) using a high-throughput sampler (HTS). Post-acquisition data analysis was performed with FlowJo software version 9.4 (Treestar Inc., Ashland, OR, USA). The gating strategy as previously described[285] removed lymphocytes and platelets, with parasitised RBCs quantified by nucleic acid content stained with hoechst. A naive/non-infected control group was included in the analysis with detected background responses subtracted from infection groups. The area under the curve (AUC) of blood-stage parasitemia over time was calculated using GraphPad Prism software version 6.0 (Graph-Pad, CA, USA).

2.10.3.2. Quantitative reverse transcription PCR

Parasite burden in livers of challenged mice was assessed by qRT-PCR as previously described[286,287] with some modifications. Livers were harvested from mice 42 h post challenge and homogenised in 5 ml of RLT lysis buffer (Qiagen Pty Ltd, Vic, Australia) with 1% β-2-mercaptoethanol (Sigma-Aldrich) using a TissueRuptor hand-held homogeniser (Qiagen, Hilden, Germany) with disposable tips. Using a medium speed setting to avoid frothing, livers were homogenised for 1 min. A 200 µl sample was then used for RNA extraction using an RNeasy mini kit (Qiagen) following the manufacturer's protocol. RNA was eluted in 60 µl of water then quantified using a Nanodrop Spectrophotometer (Thermo Fischer Scientific). Using 2.5 µg of RNA per reaction, cDNA was synthesised using a SuperScript VILO cDNA synthesis kit (Invitrogen) in 10 µl reaction volumes following the manufacturer's protocol. Reactions were incubated for 10 min at RT, then for 2 h at 37°C, and then the reactions were terminated by heating to 85°C for 5 min.

The cDNA was then diluted to 50 µl in water and used as a template for qRT-PCR reactions. For *Py*18S cDNA quantification, a Taqman Fast Advanced master mix (Applied Biosystems, Australia) with a custom made Taqman probe [250 nm] (6FAM-CTGGCCCTTTGAGAGCCCACTGATT-BHQ-1) and primers [1 um] (5'-CTTGGCTCCGCCTCGATAT and 3'- TCAAAGTAACGAGAGCCCAATG) (Applied Biosystems) were mixed with 2 µl of cDNA in 15 µl reactions. Samples were loaded into 0.1 ml strip tubes (Qiagen) and run on a Rotor-gene 3000 or 6000 PCR machine

(Corbett Research, Mortlake, NSW). The running protocol was hold at 50°C for 2 min, hold at 95°C for 2 min then 50 cycles of 95°C for 5 s and 60°C for 30 s. Between cycles acquisition was taken from the FAM channel. cDNA samples were also used to quantify the glyceraldehyde 3-phosphate dehydrogenase (GAPDH) housekeeping gene. Here a GAPDH kit (Applied Biosystems) combined with platinum Taq polymerase, PCR buffers and $MgCl_2$ (Invitrogen), dNTPs (Promega) and 2 µl of cDNA were combined in a 15 µl reaction volume. The running protocol was hold at 95°C for 2 min then 45 cycles of 95°C for 5 s and 60°C for 30 s with acquisition on the FAM channel.

In each reaction a standard curve was generated by running a 10-fold titration of either *Py*18S or GAPDH cloned cDNA. Data was analysed using Rotor-gene 6000 series software version 1.7 (Corbett Research) and presented as a ratio of copies of *Py*18S per 10^5 copies of GAPDH.

2.11. Statistical analysis

All statistical analysis was done using GraphPad Prism Version 6.00 (GraphPad Software Inc., CA, USA). Unless otherwise stated, where multiple comparisons were made, data was first log transformed, and then analysed using one-way ANOVA followed by Bonferroni's post-hoc test. Results were considered statistically significant when $p<0.05$. Statistical significance is graphically represented as $p< 0.05$ *, $p<0.01$**, $p<0.001$*** and $p<0.0001$****.

Chapter 3: Evaluation of the capacity of chimeric VLPs and capsomeres to induce antigen-specific immune responses and protective efficacy

3.1. Introduction

VLPs are formed when recombinant viral structural proteins assemble into a highly repetitive array which resembles the native form of the virus. Foreign antigen sequences can be incorporated within the VLP protein sequences, allowing for the development of chimeric VLPs capable of targeting pathogens with antigens of interest[125,127,149]. These units do not contain genomic material, so are incapable of replication, yet they highly immunogenic and very good inducers of antibody responses[125,127,130].

The MuPyV VLP platform has been developed by the Middelberg laboratory[173], such that foreign epitopes flanked by flexible linker sequences can be displayed on surface exposed regions of VLPs[173]. The modified MuPyV VP1-S4-G4S[173] has an epitope insertion site flanked by a flexible linker amino acid sequence (GGGGS-epitope-SGGGG) on the S4 surface exposed loop of the VP1 structural protein. Bacterial expression of the MuPyV VP1 protein results in the formation of pentameric capsomere units which can be subsequently be harvested[166,288]. Expression and purification processes have been developed and optimised such that high yields of chimeric proteins can be obtained[173,187,189,289]. These purified capsomeres can then be chemically induced *in vitro* to self-assemble into VLPs[166,288,289].

In order to reduce production costs and time involved in VLP formation, direct use of chimeric MuPyV VP1 capsomeres as a vaccine platform has also been investigated by the Middelberg laboratory[170,173]. By removing the first 28 and last 63 amino acids from the VP1 protein, the capsomeres are unable to form VLPs because those residues are essential for forming links with surrounding capsomeres[170]. Without the requirement for stable VLP formation, a greater number of epitopes can be

incorporated into the capsomeres[170]. Furthermore, increasing the antigen to vector ratio can result in increased target-specific immune responses[174,175], and decrease anti-carrier antibody titres[170,176]. The capsomeres are produced and purified in the same manner as the VLPs, however, the chemical VLP induction step is not required, hence the reduced production costs and time[170].

Whilst antibody responses generated by immunisation with chimeric VLPs are well documented (reviewed in[125]), little research has been done to evaluate their efficacy at generating cellular responses, or conferring protection from complex pathogens. *In vitro* studies have shown that chimeric polyomavirus VLPs with $CD8^+$ T cell epitopes can activate epitope-specific $CD8^+$ T cells[154,161]. Furthermore, VLP immunisations reportedly induce *in vivo* clonal proliferation of adoptively transferred epitope-specific $CD8^+$ T cells, tumour growth inhibition, and protection from lymphocytic choriomeningitis virus has been described[215]. In comparison to VLPs, capsomeres are reportedly less efficient at generating IgG antibody responses and require co-administration with adjuvants[131,173]. In contrast, in two HPV16 L1 model studies, capsomeres reportedly induced cellular responses which were similar to VLP induced responses[131,169], and induced tumour regression in the absence of adjuvants[169].

Whilst VLPs are self-adjuvanting[127,290], capsomeres require the inclusion of adjuvants to initiate antibody responses[170,173], and adjuvants also enhance cell-mediated IFN-γ responses[131,179]. In the Middelberg laboratory, with the aim of increasing antibody responses alone, the adjuvant of choice has been aluminium hydroxide[170,173]. In this study, however, an adjuvant efficient at inducing cellular immune responses was required. The selected adjuvant was polyIC which is a synthetic analogue of double stranded RNA acting on TLR3[291]. This adjuvant is effective at inducing a IL-12 and type I interferon response and DC maturation with increased MHC II expression and antigen cross-presentation (reviewed in[292,293]). As a result polyIC stimulates antibody and $CD4^+$ T cell responses[294,295] and enhances $CD8^+$ T cell primary and memory responses[293,296,297]. PolyIC administered with HIV-1 VLPs has been shown to improve antigen immunogenicity, eliciting higher IgG titres and eliciting a Th1 biased IgG subclass (IgG_{2a} and IgG_3) response[221]. In another study it was reported that influenza VLPs co-administered with polyIC enhanced DC

maturation, increased endpoint antibody titres and induced $CD8^+$ T cell clonal proliferation[298].

The *Plasmodium* species circumsporozoite protein is the most studied antigen for anti- malaria sub-unit vaccines in mice and humans. It is the antigenic component in the virus-like particle RTS,S which is the most advanced human vaccine against *Plasmodium falciparum*[37]. It is therefore logical to include this protein in the evaluation of novel vaccine delivery platforms. Liver-stage protection from sporozoite challenge can be achieved by either $CD8^+$ T cell[72,73,299] or antibody responses[63,300] thus we evaluated both cellular and antibody responses using chimeric VLPs and capsomeres as a vaccine delivery platform. An effective pre-erythrocytic vaccine is likely to require high amplitude immune responses[73,210,301].

The selected CD8, CD4 and B cell epitopes for insertion into the chimeras are all from the *P. yoelii* CSP and have each been identified as relevant for vaccine development. The *Py*CSP $CD8^+_{280\text{-}288}$ dominant epitope was identified on a $CD8^+$ T cell following immunisations with *P. yoelii* sporozoites[73]. A clone of this cell adoptively transferred into naive mice was able to protect against subsequent challenge with both *P. yoelii* and *P. berghei* sporozoites[73]. The *Py*CSP subdominant $CD8^+_{58\text{-}67}$ T cell epitope has been reported to eliminate infected hepatocytes *in vitro* and induce $CD8^+$ T cell proliferation and peptide-specific CTL responses[75]. Whilst protection can be afforded by CD8 T cells alone, the inclusion of $CD4^+$ T helper epitopes have been shown to enhance $CD8^+$ T cell responses[302]. Also, the passive transfer of an IgG_3 monoclonal antibody against the *PyCSP* central repeat region (QGPGAP) can provide complete protection from sporozoite challenge[63]. A separate chimera was constructed incorporating either the CD8 dominant, CD8 subdominant, or a dimer of QGPGAP for VLPs and capsomeres. To examine whether the inclusion of T helper epitopes would enhance responses in the VLP or capsomere platforms, the *Py*CSP dominant $CD4^+_{280\text{-}295}$ T cell epitope[72] , or $CD4^+_{57\text{-}70}$ T cell epitope[74], or subdominant $CD4^+_{59\text{-}79}$ T cell epitope[71] hereafter referred to as CD4 dominant 1 or 2 or subdominant respectively, were individually used to construct chimeric VLP and capsomere constructs.

This study involved a comprehensive comparison of antibody and $CD8^+$ and $CD4^+$ T cell responses as well as protection from *Plasmodium yoelii* 17XNL sporozoite challenge. Chimeric MuPyV capsomere and VLP constructs incorporating defined *Py*CSP $CD8^+_{280-288}$ T cell epitope [73], or $CD4^+_{59-79}$ T cell epitope [71],or B cell repeat epitopes $(QGPGAP)_2$[63] were evaluated as these constructs has high expression of soluble protein and formed VLPs. Capsomeres and in some cases VLPs were co-administered with polyIC as an adjuvant, and a heterologous DNA prime-boost regimen was included.

3.2. Methods

3.2.1. Genomic construction of chimeric proteins

3.2.1.1. Target selection and E. coli optimisation

Complementary oligonucleotides for the *Py*CSP dominant $CD8^+_{280-288}$T cell (SYVPSAEQI)[73], sub-dominant $CD8^+_{58-67}$T cell (IYNRNIVNRL)[75], dominant $CD4^+_{280-295}$ T cell (SYVPSAEQILEFVKQI)[72], dominant $CD4^+_{57-70}$T cell (KIYNRNIVNRLLGD)[74], sub-dominant $CD4^+_{59-79}$T cell (YNRNIVNRLLGDALNGKPEEK)[71], and B cell repeat (QGPGAPQGPGAP)[63] epitopes were codon-optimised for *E. coli* expression (Appendix B) and then synthesized and HPLC purified by GeneWorks (Adelaide, Australia).

3.2.1.2. Genomic construction of chimeric VP1 proteins for VLPs

The plasmid pGEX-VP1 comprising the pGEX-4T-1 (GE Healthcare Biosciences, Chalfont St.Giles, UK) expression vector and the murine polyomavirus VP1 genomic sequence (M34958) inserted between the *Bam*HI and *Xho*I restriction enzyme sites was a gift from Professor Robert Garcea (University of Colorado, Colorado, USA). This plasmid was further modified inserting an AfeI restriction enzyme site at position 293, then flanking the site with GGGGS (G4S) linker sequences to generate pGEX-VP1-S4-G4S[173]. The protein sequence is listed in (Appendix E).

The pGEX-VP1-S4-G4S (1 µg) was linearised by AfeI restriction enzyme (NEB, MA, USA) digestion in a 50 µl reaction at 37°C for 4 h. To limit self-ligation, 5' phosphate groups were removed by adding 1 µl of alkaline phosphatase (10 units, NEB, MA, USA) and continuing 37°C incubation for 1 h. The mixture was then loaded into a 0.8% agarose gel and separated by electrophoresis. Bands at the expected size (6145 bp) were excised and purified using a PureLink quick gel extraction kit (Invitrogen, CA, USA) following the manufacturer's protocol with DNA eluted in water.

Epitope-specific complimentary oligonucleotides (100 µM stock) were annealed by mixing 8 µl of each complementary oligonucleotide with 84 µl of annealing buffer (Appendix A). In a thermocycler, tubes were heated to 95°C for 5 min then the temperature was reduced to match the oligonucleotide melting temperature (Tm; Appendix B) for 30 min, followed by a further temperature decrease of 0.1°C/s until reaching 25°C. Annealed oligonucleotides (2 µl) were then phosphorylated by adding 0.5 µl of T4 ligation buffer, 1 µl of T4 polynucleotide kinase (10 units, NEB, MA, USA) and 1.5 µl water and heating to 37°C for 1 h, then heat inactivating at 70°C for 20 min to inactivate the kinase, then diluting with 95 µl of water.

The digested vector and phosphorylated annealed oligonucleotides were ligated in a 1:50 ratio using T4 DNA ligase (NEB) in a 20 µl reaction for 3 h at RT. Then chemically competent *E. coli* Omnimax 2 T1 or DH5α (Invitrogen, CA, USA) were transformed (section 2.6.3.4) using 5 µl of the ligation mix, and cultured overnight on LB agar plates with 100 µg/ml ampicillin. Colony isolates were screened by colony PCR (section 2.6.3.5), then cultured in LB media with 100 µg/ml ampicillin and used for plasmid purification using PureLink quick plasmid miniprep kit (Invitrogen, CA, USA) following the manufacturer's protocol and eluting in water.

Chimeric plasmids were designated CD8 dominant, CD8 sub-dominant, CD4 dominant 1, CD4 dominant 2, CD4 sub-dominant and B Cell and all were confirmed by DNA sequencing (AGRF, Brisbane, Australia).

3.2.1.3. Genomic construction of chimeric VP1 proteins for capsomeres

The pGEX-VP1 plasmid DNA was previously modified to truncate the VP1 gene removing the first 28 N-terminal and the last 63 C-terminal amino acids. Then restriction enzyme sites *Pml*I, *Nae*I, *Afe*I and *Sna*BI were inserted into positions 28, 85, 293, and 380 respectively according to the original VP1 position. This vector was designated VP1ΔNΔC^{170} and was used as the starting plasmid for all capsomere constructs. The protein sequence is listed in (Appendix E).

Oligonucleotides as described in VLP construction (section 3.2.1.1), were cloned into the VP1ΔNΔC^{170} by staff at the Protein Expression Facility (University of Queensland, St. Lucia, Australia). Each oligonucleotide was inserted into positions 28, 293 and 380 and confirmed by genomic sequencing (AGRF, Brisbane, Australia).

3.2.2. Protein expression

VP1 protein expression was done according to previously described methods[189]. Briefly, chemically competent *E. coli* Rosetta (DE3) pLysS bacteria (Novagen, CA, USA) were transformed with either pGEX-VP1 (wild-type VP1) or each of the chimeric plasmids and grown overnight on LB agar. Colony isolates were transferred into 5 ml TB media (Appendix A) and incubated overnight at 30°C and 180 RPM. This starter culture was used to inoculate either 400 or 800 ml of TB media in baffled flasks with 400 or 800 µl respectively. Cultures were incubated at 37°C and 180 RPM until the OD_{600} reached 0.4 – 0.5. The culture was then cooled under slightly chilled tap water for 10 or 20 min (for 400 or 800 ml cultures respectively) with frequent mixing to distribute heat, before inducing protein expression with 0.2 mM Isopropyl β-D-1-thiogalactopyranoside (IPTG). Cultures were then incubated at 26°C and 180 RPM overnight, and then harvested by centrifugation (6000 x *g*, 4°C, 20 min). The pellet was then stored at -80°C. Protein expression and solubility was assessed by coomassie stained SDS-PAGE gels. The molecular weights of constructs are listed in (Appendix F). All media was supplemented with ampicillin (50 µg/ml) and chloramphenicol (34 µg/ml).

3.2.3. Protein purification process

3.2.3.1. VLP and capsomere purification process

The MuPyV VP1 proteins were expressed with a glutathionine-s-transferase (GST) tag on the N-terminus for purification using affinity purification as previously described[189]. Bacterial pellets were thawed and resuspended in 30 ml lysis buffer[303] (Appendix A) per 800 ml of culture generated pellet then sonicated (Branson Ultrasonics Corporation, Connecticut, USA) at output 30 for 4 cycles of 40 s each. Samples were rested on ice for 10 min between cycles. The lysate was centrifuged (18 000 RPM, 4°C, 20 min) then the supernatant was filtered through a 0.45 um syringe driven filter.

The filtered lysate was passed through a 5 ml GSTrap HP affinity column (GE Healthcare, UK) pre-equilibrated with of L buffer. Unbound protein was washed out with L buffer, and then the GST-tagged VP1 proteins were eluted using an elution buffer (Appendix A).

The GST tag was cleaved using 40 units of thrombin (GE Healthcare, UK) per ml of protein with a 2 h incubation at RT. Insoluble aggregates were isolated by centrifugation (15000 x *g*, 4°C, 5 min). The supernatant was collected and passed through a Superdex 200 10/300 GL column (GE Healthcare, UK) pre-equilibrated with L buffer, which separated capsomeres separated from aggregates and GST by size exclusion chromatography.

3.2.3.2. Endotoxin removal

Endotoxin was removed from the capsomere fractions using Vivapure Q maxi H ion exchange columns (Sartorius Stedim, Gottingen, Germany). Columns were equilibrated with 4 ml of L buffer (with NaCl increased to 300 mM), and centrifuged (500 x *g*, 4°C, 5 min). Capsomere fractions were combined and NaCl concentration increased to 300 mM by adding 20 µl of 5 M NaCl per 250 µl of capsomeres. These were loaded onto columns and centrifuged (500 x *g*, 4°C, 5 min) then the flow through was returned to column and the process was repeated three times.

Samples were then analysed by an LAL-based assay using an Endosafe PTS reader (Charles River Laboratory, MA, USA) following the manufacturer's protocol and considered suitable for use if results were less than 5 EU/ml.

3.2.3.3. VLP assembly

To cause the assembly of VLPs, purified VP1 capsomeres were dialysed in slide-a-lyzer dialysis cassettes (10K MWCO, Thermo Scientific, Illinois, USA) against assembly buffer 1 (Appendix A) at 50 ml of buffer per 100 µl of capsomeres, for 15 h at RT with stirring. The cassettes were then transferred into the same volume of PBS and dialysed for 24 h at 4°C as previously described[189,304].

For the capsomere platform, protein expression and purification was done using the same protocols as the VLPs, however, because capsomeres were unable to form VLPs, they were dialysed only against PBS for 24 h at 4°C with stirring.

3.2.3.4. Protein quantification

The theoretical molecular weight and extinction co-efficient for each construct was estimated using ProtParam[305]. Protein concentration was calculated using Beer-Lambert's Law: $A = \varepsilon \times b \times C$, where A is the UV absorbance at 280 nm, ε is the extinction coefficient, b is the path length of the sample (1 cm using cuvette), and C is the concentration of the sample (M).

3.2.4. Confirmation of VLP formation

3.2.4.1. AF4-MALS

VLP formation was analysed using Asymmetrical Flow Field-Flow Fractionation with multi-angle light scattering (AFFFF-MALS) using an Eclipse 2 AFFFF system coupled with a Dawn EOS MALS system (Wyatt Technology Corporation, Santa Barbara, USA) as previous described[13]. Approximately 18 µg of each construct was injected into the system in a total volume of 30 µl with VLPs diluted in PBS.

3.2.4.2. TEM

Wild-type and chimeric VLPs were applied to 200-mesh copper grids coated with Formvar film (Proscitech, QLD, Australia) for 2 min then washed with water. Grids were then stained with 1% (w/v) uranyl acetate for 1 min, dried and visualized with a JEOL 1010 (JEOL Ltd., Tokyo, Japan) microscope at 100 kV. Electron micrographs were recorded digitally using a side-mounted Morada camera (Olympus-Soft Imaging System GmbH, Muenster, Germany) with iTEM Software version 3.2 (Soft Imaging System GmbH). All images were obtained by Alice Lei Yu (AIBN, University of Queensland).

3.3. Experimental design

In initial studies to confirm that chimeric $CD8_{280-288}$ VLPs and capsomeres could induce antigen-specific recognition of the *Py*CSP $CD8_{280-288}$ epitope, an *in vitro* model was established using purified $CD8^+$ T cells from transgenic CS-TCR mice (Table 4) stained with CFSE (section 2.10.1.3). In CS-TCR mice, all $CD8^+$ T cell receptors are specific for the *Py*$CSP_{280-288}$ epitope. These $CD8^+$ T cell epitope-specific cells were co-cultured with splenocytes from naive BALB/c mice and stimulated with either wild-type or CD8 chimeric VLPs or capsomeres, or a synthetic peptide representing the defined *Py*CSP $CD8^+_{280-288}$ T cell epitope. The cells were analysed on days 2, 3 and 4, to assess epitope recognition by proliferation of CS-TCR cells as identified by the decrease in CFSE intensity within cells following division.

In the subsequent series of VLP and capsomere studies, BALB/c mice were immunised three times at 3 week intervals by with VLPs, capsomeres, peptides or PyCSP plasmid DNA in either homologous or heterologous prime/boost regimen. Immunisations were administered s.c. at the base of the tail in a 100 µl dose. Plasmid DNA immunisations were given by i.m. injection into the tibialis anterior muscle in 2 x 50 µl injections. Details of immunisations are presented below (Table 5 and Table 6). Each series of experiments followed the same experimental design (Figure 4), with duplicate experimental groups in each experiment used for either immunogenicity or protection evaluations.

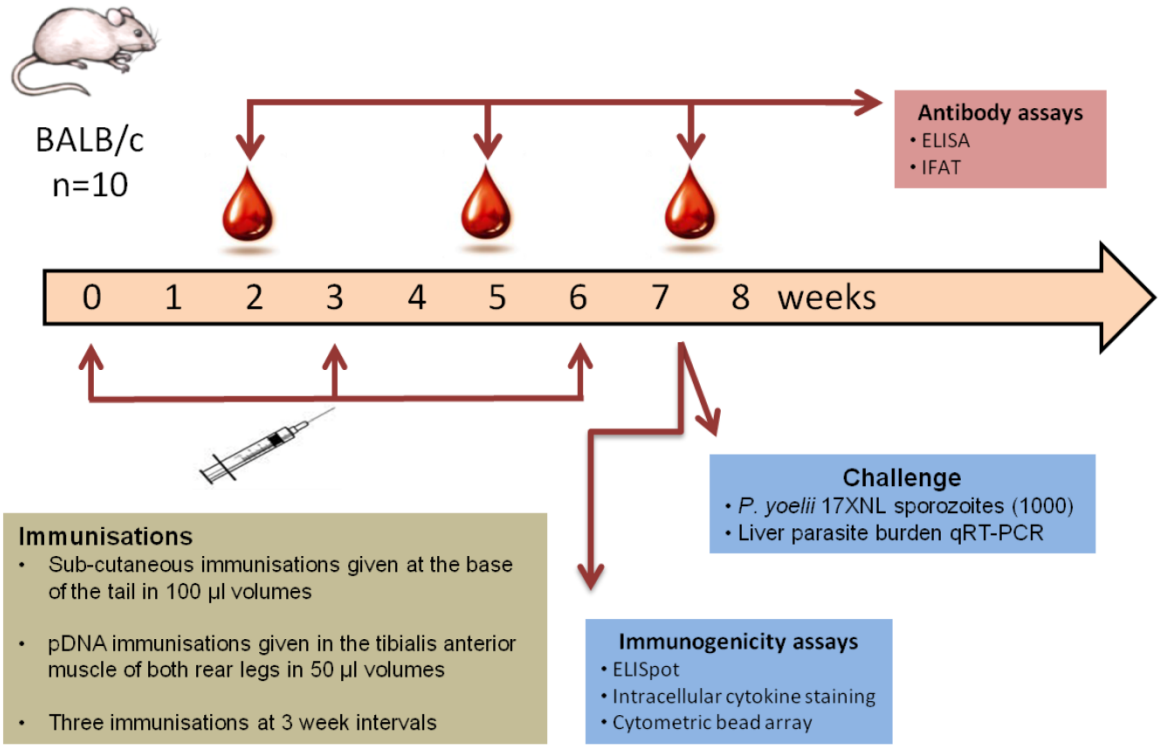

Figure 4: Experimental design for all in vivo VLP and capsomere experiments. BALB/c mice (n=10/group) were immunised three times at three week intervals with either VLPs, capsomeres, peptides by s.c. injection at the base of the tail in a 100 µl volume in a homologous regimen. Other groups received two primes with *Py*CSP plasmid DNA in the tibialis anterior muscle with 50 µg administered i.m. to each hind leg. Sera were collected 14 d post-immunisation for doses 1 and 2, and 5 days after dose 3. The sera were subsequently used for antibody analysis by ELISA and IFAT. T cell responses were assessed by ELISpot, cytometric bead arrays and intracellular cytokine staining, using splenocytes harvested 7 days after the final immunisation (n=5 mice/group). For the analysis of protective efficacy, 8 d after the final immunisation, mice (n=5 mice/group) were challenged with an i.v. injection of 1000 cryopreserved *P. yoelii* 17XNL sporozoites. Protective efficacy was determined by harvesting livers 42 h post-challenge and quantifying parasite RNA using qRT-PCR.

Antibody responses were assessed by ELISA and IFAT using sera collected post-immunisation. ELISA capture antigens included PST-tagged *Py*CSP B cell repeat peptide and *Py*CSP recombinant protein (section 2.10.2.1). IFAT was used to assess the capacity of induced antibodies to recognise the surface of *P. yoelii* sporozoites (section 2.10.2.3).

T cell responses were assessed by ELISpot, cytometric bead arrays (CBA) and intracellular cytokine staining (ICS), using splenocytes harvested 7 days after the final immunisation (n=5 mice/group) as previously described (section 2.10.1).

For the analysis of protective efficacy, 8 d after the final immunisation, mice (n=5 mice/group) were challenged with an i.v. injection of 1000 cryopreserved *P. yoelii* 17XNL sporozoites. Protective efficacy was determined by harvesting livers 42 h post-challenge and quantifying parasite RNA using qRT-PCR (section 2.10.3.2).

The first series of experiments was designed to evaluate the immunogenicity and protective capacity of individual and pooled VLPs using peptides corresponding to the epitope insert in the VLP chimeras as comparators (Table 5). Additionally the relative capacity of homologous versus heterologous DNA prime/VLP boost regimen was evaluated.

Table 5: Immunisations for first series of VLP experiments

Group	**Immunisations**
CD8 VLP	30 µg of $CD8_{280-288}$ VLP
CD4 VLP	30 µg of $CD4_{59-79}$ VLP
B cell VLP	30 µg of B cell VLP
Pooled VLP	10 µg of each $CD8_{280-288}$, $CD4_{59-79}$ and B cell VLPs
CD8 peptide	30 µg of $CD8_{280-288}$ peptide with 50 µg polyIC
CD4 peptide	30 µg of $CD4_{59-79}$ peptide with 50 µg polyIC
B cell peptide	30 µg of B cell peptide with 50 µg polyIC
Pooled peptide	30 µg of each $CD8_{280-288}$, $CD4_{59-79}$ and B cell peptides with 50 µg polyIC
DNA+pooled VLP	2 x primes with 100 µg PyCSP pDNA (pVR2516) + boost with pooled VLPs
DNA+pooled peptide	2 x primes with 100 µg PyCSP pDNA (pVR2516) + boost with pooled peptides
Wild VLP	30 µg of wild-type VLP
Ovalbumin	30 µg of each $CD8_{257-264}$ and $CD4_{323-339}$ ovalbumin peptides with 50 µg polyIC
PBS	100 µl PBS

In the second series of experiments, the immunisations were consistent with the first series (Table 5); however, the dose of chimeric VLPs in the pooled VLP groups was increased to 30 µg of each construct for a better comparison to individual VLP immunisations. An additional group received three doses of *Py*CSP plasmid DNA

only (100 µg) to further distinguish the immunological benefits of the pooled VLP or peptide boost.

A third series of experiments, was designed to compare the immunogenicity and protective capacity of chimeric VLPs and capsomeres. Due to constraints imposed by the large number of groups, mice were immunised only with pooled VLPs, capsomeres or corresponding peptides. Specifically, BALB/c mice (n=10/group) were immunised with three doses at 3 week intervals with constructs as described below (Table 6). In the heterologous DNA prime-boost regimen, mice received 100 µg of *Py*CSP plasmid DNA for the first two immunisations, followed by a final dose of pooled capsomeres, VLPs or peptide as for the homologous regimen.

Table 6: Immunisations for third series of VLP experiments

Group	**Immunisations**
VLP	10 µg of each $CD8_{280-288}$, $CD4_{59-79}$ and B cell VLPs
VLP+pIC	10 µg of each $CD8_{280-288}$, $CD4_{59-79}$ and B cell VLPs with 50 µg polyIC
Caps+pIC	10 µg of each $CD8_{280-288}$, $CD4_{59-79}$ and B cell capsomeres with 50 µg polyIC
Pep+pIC	30 µg of each $CD8_{280-288}$, $CD4_{59-79}$ and B cell peptides with 50 µg polyIC
DNA+VLP	2 x primes with 100 µg PyCSP pDNA (pVR2516) + boost with VLP
DNA+VLP+pIC	2 x primes with 100 µg PyCSP pDNA (pVR2516) + boost with VLPs+pIC
DNA+Caps+pIC	2 x primes with 100 µg PyCSP pDNA (pVR2516) + boost with Caps+pIC
DNA+Pep+pIC	2 x primes with 100 µg PyCSP pDNA (pVR2516) + boost with Pep+pIC
DNA	3 x doses of 100 µg PyCSP pDNA (pVR2516)
Wild VLP+pIC	30 µg of wild-type VLP with 50 µg polyIC
Wild Caps+pIC	30 µg of wild-type capsomeres with 50 µg polyIC
PBS	100 µl PBS

3.4. Results

3.4.1. Construction of chimeric VLPs

Six chimeric MuPyV VP1-S4-G4S proteins were constructed each confirmed by sequencing. Following bacterial expression, total and soluble fractions were separated by electrophoresis to evaluate expression and solubility of chimeric

proteins. Each chimeric construct was expressed by the bacteria, however, the CD8 subdominant and CD4 dominant 1 and 2 chimeric proteins were predominantly insoluble (Figure 5). Repeated transformations and cultures failed to increase the yield of soluble protein with these chimeras.

The molecular weight of each chimera was: Wild-type, 69.6 kDa; CD8 dominant, 70.5 kDa; CD8 subdominant, 70.8 kDa; CD4 dominant 1, 71.4 kDa; CD4 dominant 2, 71.3 kDa; CD4 subdominant, 72.0 kDa; and B cell, 70.6 kDa (Appendix F).

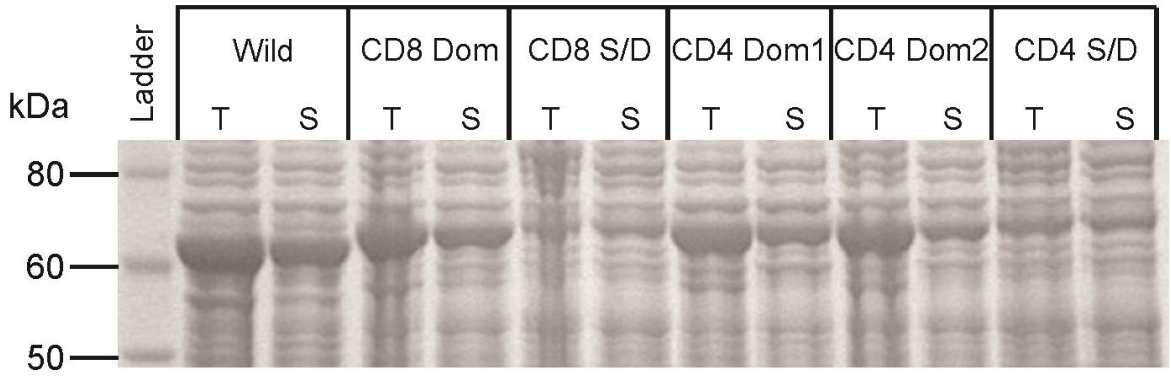

Figure 5: Protein expression and solubility of chimeric MuPyV VP1-S4-G4S constructs. Rosetta DE3 pLysS *E. coli* were transformed with plasmid DNA from each chimeric VP1 construct. Colony isolates were selected for overnight starter cultures which were subsequently used to inoculate 400 ml of TB media with ampicillin [50 µg/ml] and chloramphenicol [24 µg/ml] in 2 L baffled flasks. At OD_{450} ~ 0.5, cultures were induced with IPTG [0.2 mM]. Cultures were incubated overnight at 26°C with shaking at 180 RPM, then bacteria were harvested by centrifugation and pellets lysed by sonication. A total (T) fraction was taken directly from lysed bacteria, whilst the soluble (S) fraction was taken from the supernatant of lysed and centrifuged bacteria. Fractions were run on a 10% SDS-PAGE gel then stained with coomassie. A molecular weight ladder (Novex sharp pre-stained) was run (left lane) in parallel with other samples.

The CD8 dominant, CD4 sub-dominant and B cell constructs each progressed through the purification process with good yields after GST purification and thrombin digestion followed by s200 column size-exclusion chromatography (Figure 6). However, the yields for the CD8 subdominant and CD4 dominant 1 and 2 constructs were very low as compared with the other constructs. An SDS-PAGE analysis showed that for these constructs, most of the protein was passing through the column and not being captured by the column matrix. Nonetheless, whilst the yields

were low for these constructs, sufficient protein was available for thrombin digestion. Following thrombin digestion to separate the GST-tag, protein instability was observed in the CD8 sub-dominant, and CD4 dominant 1 and 2 constructs, as determined by protein aggregation. The quantity of protein in eluted fractions from the s200 column were too low for both of the CD4 dominant constructs and so no further work could be done with them. The CD8 sub-dominant yield was also low but was sufficient to determine if VLPs would form.

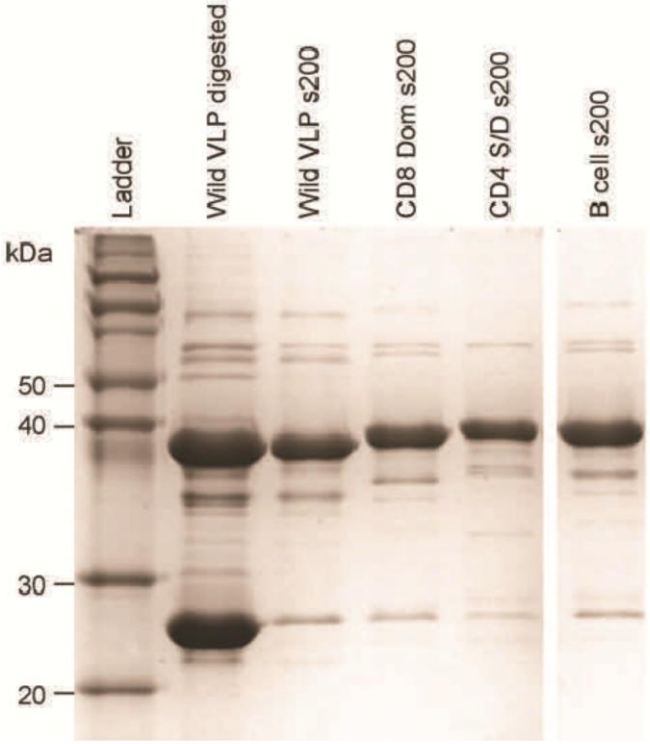

Figure 6: Thrombin digested chimeric proteins following size exclusion chromatography. Chimeric proteins isolated using a GST column were digested with thrombin and isolated using a Sephadex s200 chromatography column. Isolated proteins were run on an 10% SDS-PAGE gel and then stained with coomassie. Successive lanes from left to right lanes contained a molecular weight ladder (Novex sharp pre-stained) followed by post-thrombin digested wild VLP pre- and post-s200 purification, and s200 purified protein fractions from CD8 dominant, CD4 sub-dominant and B cell chimeric MuPyV VP1-S4-G4S proteins.

Hereafter the chimeric $CD8_{280-288}$ dominant VLP, $CD4_{59-79}$sub-dominant VLP and B cell VLP are named CD8 VLP, CD4 VLP and B cell VLP respectively. Following dialysis in assembly buffer and then PBS, VLPs were quantified using $UV_{280\ nm}$ absorbance (section 3.2.3.4) and characterised by transmission electron microscopy and AF4-MALS (section 3.2.4). VLP formation was observed in wild-type, CD8280-288 dominant, CD459-79 subdominant and B cell chimeras (Figure 7). The chimeras had a similar morphology to wild-type VLPs. The mean radius of VLPs: Wild type, 19.99 nm; CD8 VLPs, 20.75 nm; CD4 VLPs, 21.16 nm; B cell VLPs, 20.99 nm, were slightly larger than wild type VLPs as expected with the addition of exogenous amino acids.

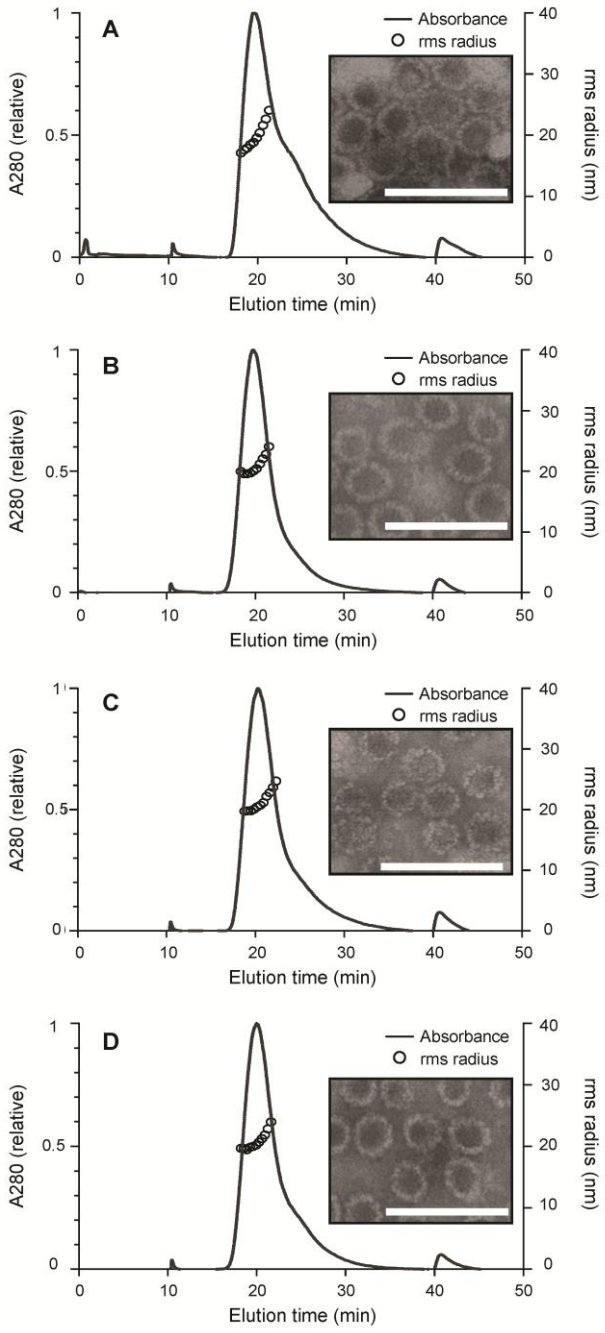

Figure 7: Structural analysis of *in vitro* assembled chimeric murine polyomavirus virus-like particles. Wild and chimeric MuPyV VP1-S4-G4S proteins were expressed in *E. coli* and purified by liquid chromatography. Proteins were dialysed against an assembly buffer to form VLPs, then against PBS. Post-assembly solutions were analysed to detect the formation of (A) wild-type VLPs, and (B) $CD8_{280\text{-}288}$, (C) $CD4_{59\text{-}79}$, and (D) B cell VLP chimeras using asymmetrical flow field-flow fractionation coupled with multi-angled lights scattering (AF4-MALS) and transmission electron microscopy. UV_{280} absorbance is presented relative to peak absorbance (solid line) for each sample, and particle size is presented as root-square-radius (open circles). TEM scale bar represents 100 nm.

The CD8 sub-dominant chimera also formed VLPs, however, the protein yield was approximately one-sixth of the other constructs, despite having double the original culture volume. Despite repeated attempts, the yield of VLPs for this construct was insufficient to proceed to animal experiments. Of the six chimeric VLPs originally intended for this project, only three were sufficient to proceed in animal experiments as a result of the mentioned protein instability and yield issues.

3.4.2. Proliferative capacity of CD8 chimeric VLPs and capsomeres

To determine if the *Py*CSP $CD8_{280-288}$ T cell epitope included in chimeric VLPs and capsomeres would be processed, presented and recognised by host cells with transgenic CS-TCR cells, an *in vitro* CFSE stained CS-TCR proliferation assay was used. Peptides, VLPs and capsomeres were studied at 10 µg/ml with proliferation indicated by the dilution of CFSE in cells resulting in lower MFI values. Proliferation was detected in all groups presenting the respective CD8+280-288 T cell epitope (Figure 8). The highest rate of proliferation was seen in the peptide and capsomere groups both of which induced rapid proliferation, significantly higher than respective controls and to the $CD8_{280-288}$ VLPs as seen after 2 days in culture ($p<0.0001$). The $CD8_{280-288}$ VLPs induced a less efficient proliferation response and was not significantly different to wild-type VLPs until after 3 days of incubation. Furthermore, after 2 and 3 days of incubation proliferation induced by $CD8_{280-288}$ VLPs was significantly less than both $CD8_{280-288}$ peptide and $CD8_{280-288}$ capsomeres ($p<0.0001$). However, significance between the $CD8_{280-288}$ constructs was lost by day 4, following rapid $VLP_{280-288}$ induced proliferation (Figure 8).

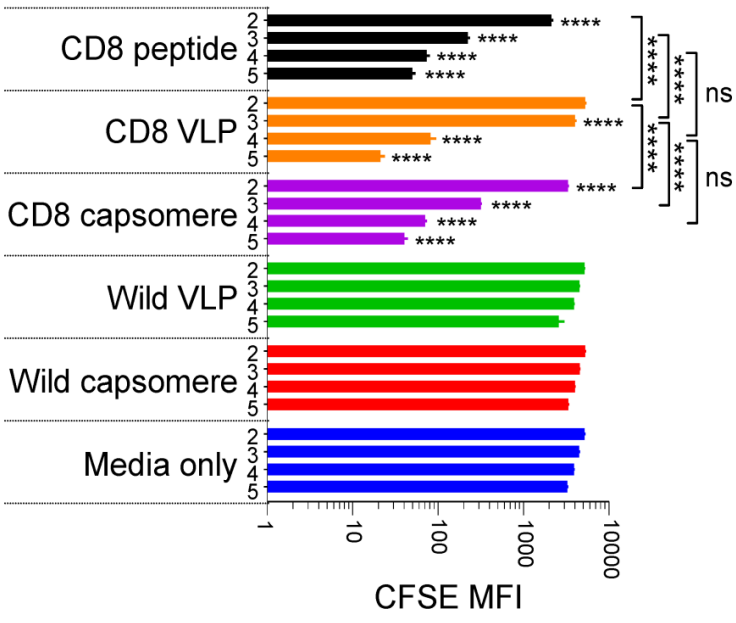

Figure 8: Proliferation of CS-TCR $CD8^+$ T cells following *in vitro* stimulation with VLPs, capsomeres and peptide. $CD8^+$ T cells from naive CS-TCR transgenic mice were purified by positive selection, stained with CFSE, and combined with splenocytes from naive BALB/c mice (n=5). Cells were incubated in media supplemented with either *Py*CSP $CD8_{280-288}$ peptide, $CD8_{280-288}$ chimeric VLPs, $CD8_{280-288}$ chimeric capsomeres, wild-type VLPs or wild-type capsomeres, all at 10 µg/ml, or in media alone. Cultures were analysed by flow cytometry after 2, 3, 4, and 5 days to determine the median fluorescence intensity (MFI) of CFSE in $Thy1.1^+CD8^+$ CS-TCR viable cells.

3.4.3. Chimeric VLPs with 10 µg/construct in pooled immunisations

Having established that the *Py*CSP $CD8^{+}_{280\text{-}288}$ T cell epitope presented in the context of chimeric VLPs or capsomeres was capable of inducing epitope-specific proliferation of TCR-specific $CD8^{+}_{280\text{-}288}$ T cells, immunogenicity and protective efficacy were evaluated in subsequent experiments.

3.4.3.1. Cellular immunogenicity

To assess the ability of chimeric VLPs to induce cellular immune responses, splenocytes from immunised mice were harvested and single cell suspensions were restimulated for ELISpot, CBA and ICS assays. Comparisons were made between single and pooled construct immunisations to look for evidence of any synergistic or inhibitory effects.

CD8 T cell chimeric VLP induced responses

ELISpot results (Figure 9) showed that the $CD8_{280\text{-}288}$ VLP induced significant IFN-γ spot forming cells (SFCs) when stimulated with pooled peptide or transfected A20 cells as compared with the PBS control ($p<0.001$). The peptide-specific IFN-γ response induced by the $CD8_{280\text{-}288}$ VLP was similar to that induced by immunisations with $CD8_{280\text{-}288}$ peptide formulated in polyIC. When restimulated with *Py*CSP transfected A20 cells immunisations with $CD8_{280\text{-}288}$ VLPs resulted in significant IFN-γ responses ($p<0.01$), which were absent in the peptide immunised mice. CBA analysis of IFN-γ production following pooled peptide restimulation (Figure 10) corroborated the ELISpot results with significant $CD8_{280\text{-}288}$ VLP induced responses relative to the PBS control ($p<0.0001$). An IFN-γ response could also be detected by ICS but this was not significant (Figure 11).

CD4 T cell chimeric VLP induced responses

Despite the demonstrated immunogenicity of $CD8_{280\text{-}288}$ chimeric VLPs, the $CD4_{59\text{-}79}$ chimeric VLP immunisations failed to generate any significant cytokine responses as assessed by IFN-γ ELISpot, CBA or ICS assays. Significant IFN-γ and TNF responses could be detected from the positive control comparator $CD4_{59\text{-}79}$ peptide +

polyIC immunised mice when their splenocytes were restimulated with either pooled peptide (p<0.0001) or transfected A20 cells (p<0.01) in ELISpot assays (Figure 9). This group also had significant IFN-γ (p<0.0001) and TNF (p<0.01) responses in CBA analysis (Figure 10) as well as $CD4^+$ T cells expressing IFN-γ (p<0.0001) or IL-2 (p<0.001) in ICS assays (Figure 11), when restimulated with pooled peptides as compared to PBS controls.

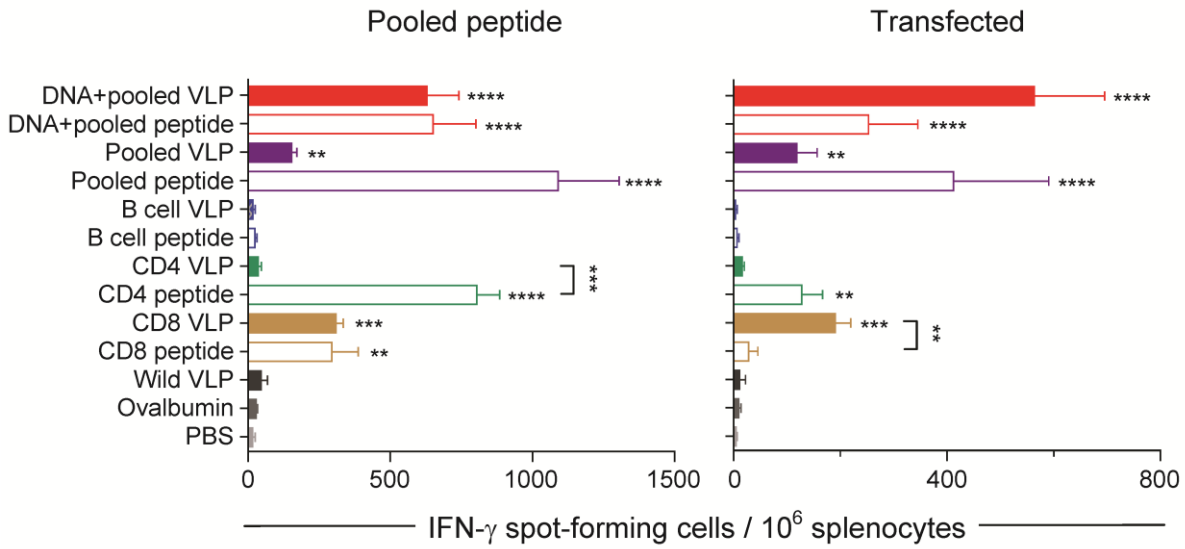

Figure 9: IFN-γ ELISpot responses induced by individual (30 µg) or pooled (10 µg each) chimeric VLP immunisations. BALB/c mice (n=5/group) received three s.c. immunisations at 2 week intervals of wild type VLPs (30 µg), individual VLP constructs (30 µg,) or pooled VLPs (10 µg each), individual (30 µg) or pooled peptides (30 µg each) with polyIC (50 µg), or a prime boost regimen using two i.m. *Py*CSP plasmid DNA (100 µg) primes then an s.c. boost using either pooled VLPs or peptides with polyIC. Splenocytes (5 x 10^5/well) were cultured and restimulated with irradiated A20 cells (1.5 x 10^5/well) either with pooled *Py*CSP $CD8_{280\text{-}288}$, $CD4_{59\text{-}79}$ and B cell peptides, or with pVR2516 *Py*CSP plasmid DNA transfected and irradiated A20 cells (5 x 10^4/well) for 40 h. IFN-γ spot forming cells/million splenocytes are presented as group means + SEM. Statistical comparisons are made to the PBS control group, and between homologous VLP and peptide groups using log-transformed data with significance determined using one-way ANOVA followed by Bonferroni's post-hoc test. p<0.05 *, p<0.01 **, p<0.001 *** and p<0.0001 ****.

B cell chimeric VLP induced responses

The B cell chimeric VLP was designed to induce antibody but not cellular immune responses. As expected, no cytokine responses could be detected in ELISpot (Figure 9) or ICS assays (Figure 11).

Pooled VLP induced responses

In this experiment, mice in the pooled VLP immunisation group received 10 µg of each chimeric construct per dose. Significant IFN-γ responses were detected when restimulated with pooled peptides (p<0.01) or *Py*CSP transfected A20 cells (p<0.01) in an ELISpot assay (Figure 9), as well as pooled peptides (p<0.001) in the CBA analysis (Figure 10).To determine whether pooling VLPs had an influence (positive or negative) on immunogenicity, statistical comparisons were made to single construct VLP immunisations. No significant effect of pooling chimeric VLPs was evident in any of the cellular assays (Figure 9, Figure 10, Figure 11).

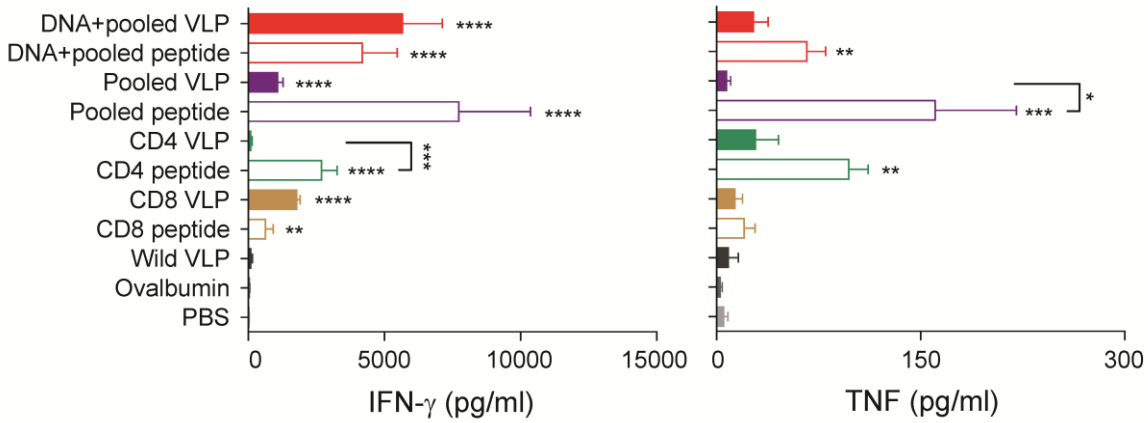

Figure 10: IFN-γ or TNF expression induced by individual (30 µg) or pooled (10 µg each) chimeric VLP immunisations. Mice (n=5/group) were immunised as previously described (Figure 9). Splenocytes (5 x 10^5/well) were cultured with irradiated A20 cells (1.5 x 10^5) and restimulated with pooled *Py*CSP $CD8_{280\text{-}288}$, $CD4_{59\text{-}79}$ and B cell peptides for 72 h. Data are presented as mean + SEM for IFN-γ and TNF cytokines (pg/ml) detected in culture supernatant by CBA analysis. Statistical comparisons are made to the PBS control group, and between homologous VLP and peptide groups using log-transformed data with significance determined using one-way ANOVA followed by Bonferroni's post-hoc test. p<0.05 *, p<0.01 **, p<0.001 *** and p<0.0001 ****.

Heterologous DNA prime/boost regimen

To evaluate if the immunogenicity induced by a homologous VLP regimen could be enhanced using a prime/boost regimen, mice received two *Py*CSP plasmid DNA primes followed by a single boost with either pooled VLPs or pooled peptides formulated in polyIC. The heterologous DNA/pooled VLP group had a moderate, but non-significant increase in IFN-γ responses as compared to mice immunised with homologous pooled VLPs (Figure 11). Moreover, this only group to achieve a $CD8^+$

T cell IFN-γ positive population that was significant relative to the controls (Figure 11). However, due to constraints in the size of the study a plasmid DNA only immunised group could not be included in this study. It is possible that the significant IFN-γ responses induced could be due to the DNA prime alone.

TNF and other cytokine responses

The primary readout for cellular immunogenicity assays was IFN-γ since this is the cytokine implicated in *Py*CSP protection. Other than IFN-γ, the only notable cytokine response was TNF as assessed by CBA (Figure 10) and ICS (Figure 11). However, although TNF responses could be detected following VLP immunisations, the levels of TNF were low in both the CBA (Figure 10) and ICS (Figure 11) assays and were not significantly different from controls. In contrast, immunisations with pooled peptides with and without plasmid DNA priming induced significant TNF responses in the CBA assay ($p<0.01$ and $p<0.001$ respectively), as well as $CD4^+$ T cell IL-2 responses in the ICS ($p<0.05$ and $p<0.0001$ respectively). These responses appear to be modulated by the CD4 peptide.

However, other cytokines were also analysed, specifically: IL-1β, IL-2, IL-4, IL-5, IL-6, IL-10, IL-12p70 and IL-13 in pooled culture supernatants were assessed by CBA. Most of these cytokines were very low, at or near the limit of detection for this assay (data not presented). The $CD4_{59\text{-}79}$ peptide, pooled peptide and DNA/peptide immunised groups had a spike in IL-6 (159,172 and 98 pg/ml respectively) and IL-13 (1394, 1892 and 673 pg/ml respectively) when stimulated with pooled peptides, but no robust cytokine response could be detected in all other groups including VLP immunised mice.

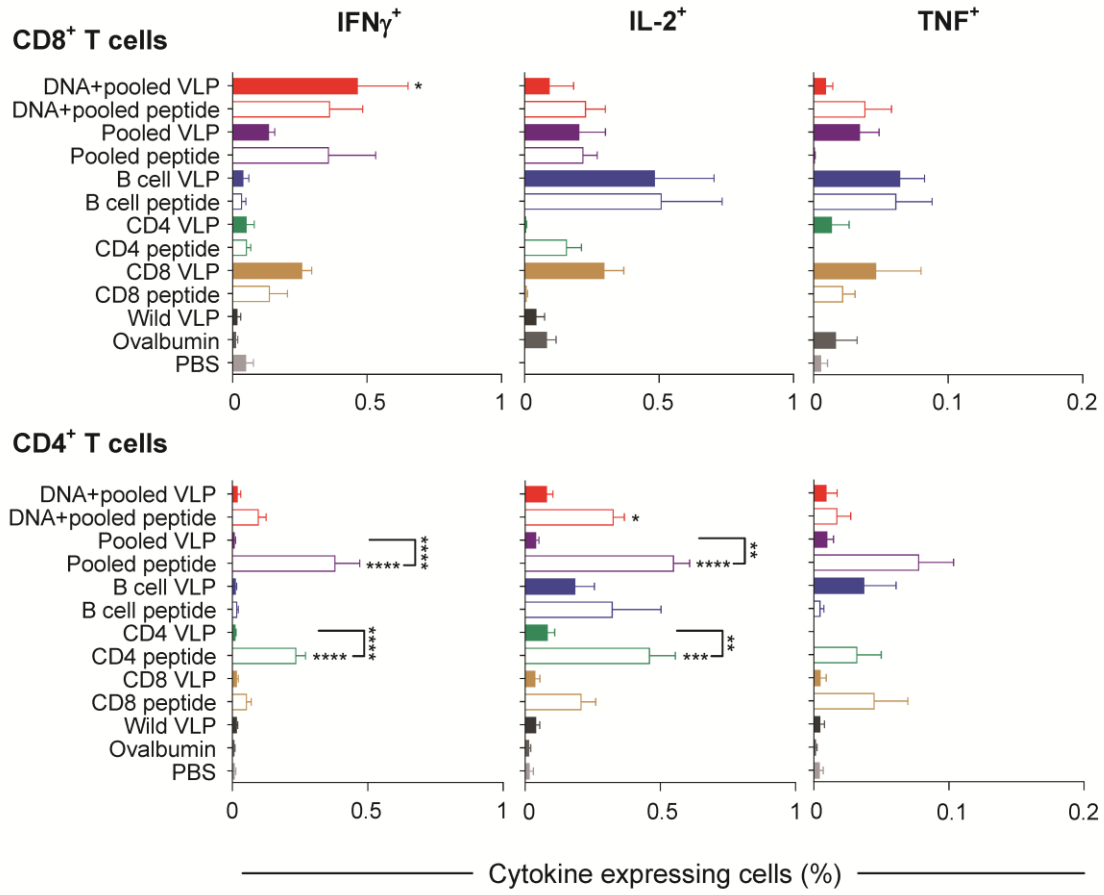

Figure 11: IFN-γ, IL-2 and TNF expressing T cells induced by individual (30 µg) or pooled (10 µg each) chimeric VLPs. Mice (n=5/group) were immunised as previously described (Figure 9). Splenocytes (5 x 10^5/well) were cultured with irradiated A20 cells (1.5 x 10^5/well) and restimulated with pooled *Py*CSP $CD8_{280-288,}$ $CD4_{59-79}$ and B cell peptides for 18 h. For the final 6 h, wells were supplemented with GolgiPlug (0.1%). Cells were stained for $CD8^+$ and $CD4^+$ T cell receptors then intracellular stained for IFN-γ, IL-2 and TNF cytokines. Cells were analysed by flow cytometry. Statistical comparisons are made to the PBS control group, and between homologous VLP and peptide groups using log-transformed data with significance determined using one-way ANOVA followed by Bonferroni's post-hoc test. $p<0.05$ *, $p<0.01$ **, $p<0.001$ *** and $p<0.0001$ ****.

3.4.3.2. Antibody responses

To assess antigen-specific antibody responses induced by the chimeric VLP immunisations, ELISA assays were conducted using the polystyrene-tagged *Py*CSP B cell repeat peptide as a capture antigen. Results show that immunisations with B cell VLPs administered individually or as pooled VLPs induce robust antibody responses (Figure 12 and Figure 13). However, the data show that a single VLP dose is insufficient to induce robust antibody responses with two to three doses

required (Figure 12). Following the final immunisation the endpoint titre of B cell VLP immunised mice was 4-fold higher than the pooled VLP immunised mice (Figure 12B). Titres increased 2-fold between the second and third immunisation of B cell VLPs in contrast to the pooled VLPs which had stabilised after the second immunisation. Endpoint titres were determined in individual mice following the final immunisation in the pooled VLP groups with and without DNA priming and B Cell VLP mice (Figure 13) with no significant differences detected between these groups. After the second VLP dose, a dominant IgG1 response was evident, with a class switch to IgG3 occurring after the third immunisation (Figure 12A).

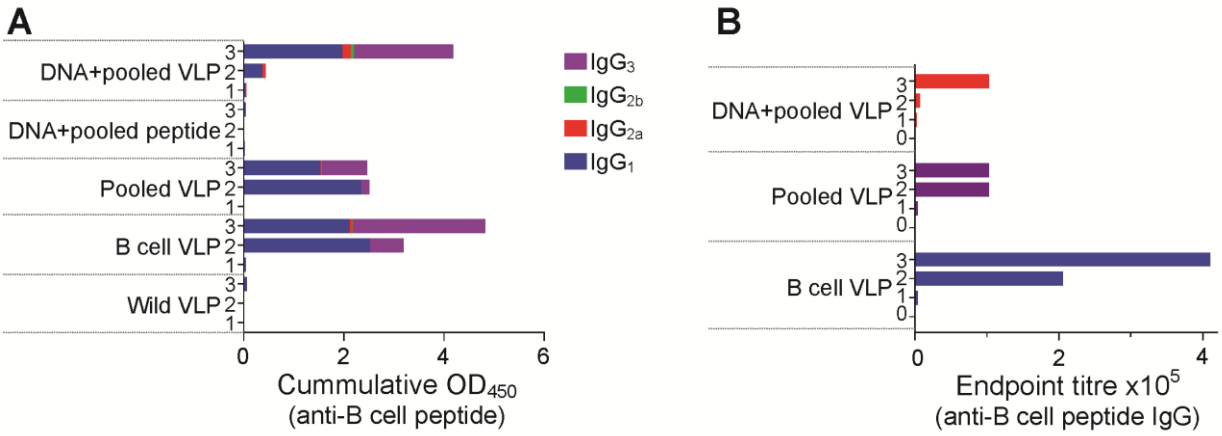

Figure 12: Anti-B cell peptide antibody responses following immunisations. Mice (n=5/group) were immunised as previously described (Figure 9). Sera collected pre-immunisation (0) and following successive doses (1,2 and 3) was assayed by ELISA to detect antibody responses against the *Py*CSP B cell peptide. (A) Pooled sera collected after each immunisation was diluted 1:800 to determine IgG isotype responses displayed as cumulative OD_{450} values. (B) Pooled sera were used to determine the total IgG endpoint titres following each dose.

An ELISA was conducted using individual sera against the PST-tagged *Py*CSP B cell repeat peptide to determine endpoint IgG titres (Figure 13). Sera used in this assay were obtained following immunisations for this experiment, as well as from a subsequent experiment in which pooled VLPs were given at 30 µg per construct (section 3.4.4). The endpoint titre of each group was significantly higher than the PBS group ($p<0.0001$). In homologous VLP immunisations, there were minor and non-significant variations between groups, and each group was significantly better than homologous DNA immunisations ($p<0.0001$). In the prime/boost regimen, the

lower 10 µg/construct boost resulted in significant higher endpoint titres as compared to the 30 µg/construct boost (p<0.01).

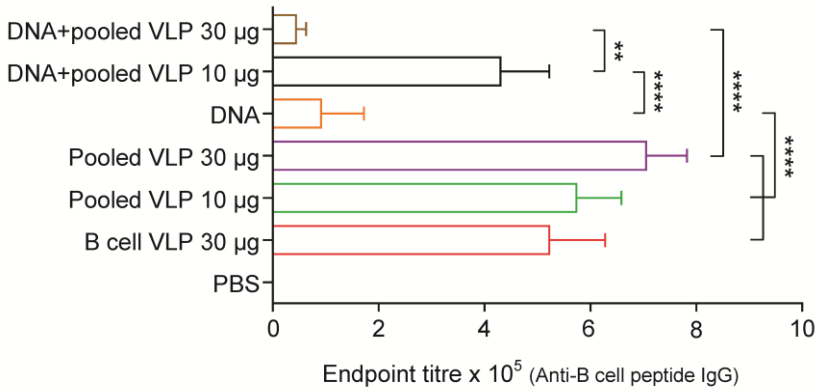

Figure 13: IgG comparisons between VLP experiments using 10 or 30 µg per construct in pooled VLP immunisations. In two series of experiments mice (n=10/group) immunisations as previously described with 10 µg/construct (Figure 9) or 30 µg/construct (section 3.4.4) in pooled VLPs. Sera collected following the final immunisations were simultaneously analysed by ELISA to determine the anti-B cell peptide-specific IgG endpoint titre. Data is presented as mean endpoint titre + SEM. Statistical comparisons are made between immunisation groups using log-transformed data with significance determined using one-way ANOVA followed by Bonferroni's post-hoc test. p<0.01 **, p<0.0001 ****.

3.4.3.3. Protection

To evaluate the protective efficacy of chimeric VLPs, immunised mice (n=5/group) were challenged with 1000 *P. yoelii* 17XNL sporozoites. Parasite RNA in homogenised livers was quantified by q-RT-PCR[286] and reported as a ratio to mouse GAPDH housekeeping gene (Figure 14). There were no significant differences detected between any of the immunisation groups. However, mice immunised with a DNA prime and pooled VLP boost had a 38% reduction in liver-stage parasite burden relative to the PBS control group, and two mice in that group had no parasite RNA detected in their liver.

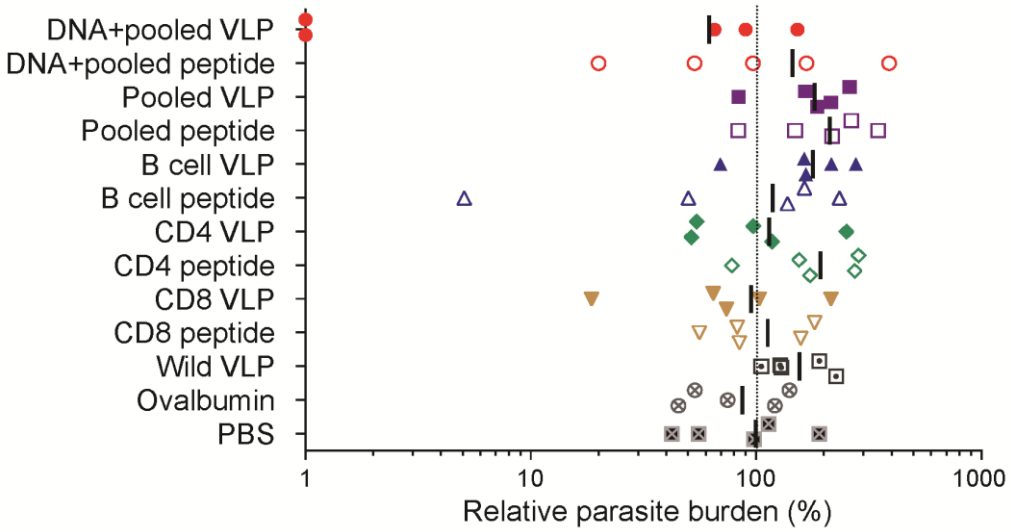

Figure 14: Protective capacity induced by individual (30 µg) or pooled (10 µg each) chimeric VLPs using homologous or heterologous immunisation regimens. Mice (n=5/group) were immunised as previously described (Figure 9). Mice were challenged 8 days after the final immunisation by i.v. injection of 1000 *P. yoelii* 17XNL cryopreserved sporozoites. Parasite burden was assessed by qRT-PCR analysis of *Py*18s RNA extracted from livers harvested 42 h post-challenge and calculated as a ratio to the GAPDH housekeeping-gene RNA. Data was normalised to the PBS control and presented as a relative parasite burden. Individual results are shown with bars representing the group mean. Log-transformed ratio data was analysed using one-way ANOVA followed by Bonferroni's post-hoc test. No significant differences were detected between groups.

3.4.4. Chimeric VLPs with 30 µg/construct in pooled immunisations

In the next series of experiments, the pooled VLP immunisations were modified to include 30 µg of each chimeric VLP per dose. By doing so, equivalent dose comparisons could be made between individual and pooled constructs in the cellular immunogenicity assays. To identify the cell phenotype responses in assays for these experiments, *Py*CSP $CD8^{+}_{280\text{-}288}$ or $CD4^{+}_{59\text{-}79}$ T cell peptides were used individually and pooled to restimulate splenocytes.

3.4.4.1. Cellular immunogenicity

CD8 chimeric VLP induced IFN-γ responses

Consistent with data from the previous experiment (section 3.4.3.1), $CD8_{280\text{-}288}$ chimeric VLPs induced significant IFN-γ responses when restimulated with either the

$CD8_{280-288}$ peptide (p<0.0001) or *Py*CSP transfected A20 cells (p<0.0001) in the ELISpot assay (Figure 15). Consistent with this ELISpot detected response, the CBA assay detected significant levels of IFN-γ in culture supernatant with splenocytes from $CD8_{280-288}$ VLP immunised mice (p<0.0001) (Figure 16). No significant responses were detected with the $CD8_{280-288}$ VLP immunised mice in the ICS analysis (Figure 17). In each assay, there were only minor but not significant differences between the $CD8_{280-288}$ VLP and $CD8_{280-288}$ peptide immunisations. This confirmed the capacity of $CD8_{280-288}$ chimeric VLPs to induce robust $CD8^+$ T cell responses.

CD4 chimeric VLP induced IFN-γ responses

Also consistent with data from the previous experiment (section 3.4.3.1), no significant IFN-γ responses following immunisations with the $CD4_{59-79}$ VLP could be detected by ELISpot, or ICS assays (Figure 15, Figure 17). There was a significant (p<0.01) albeit a very small IFN-γ response detected in the CBA (Figure 16). In contrast, robust IFN-γ responses were detected with experimental groups immunised with the positive control comparator $CD4_{59-79}$ T cell peptide in polyIC in each assay (p<0.0001).

Pooled VLP induced IFN-γ responses

Immunisations with pooled ($CD8_{280-288}$, CD4 and B cell) VLP construct induced significant IFN-γ responses (p<0.0001) when restimulated with $CD8_{280-288}$ peptide, pooled peptides or transfected A20 cells in the ELISpot analysis (Figure 15). Responses to the individual peptides showed that the response was dominated by the $CD8_{280-288}$ peptide with very low CD4 peptide-induced activation, consistent with the lack of responses detected following immunisations with the chimeric $CD4_{59-79}$ VLP construct. Consistent with the ELISpot data, the CBA results (Figure 16) showed robust IFN-γ responses with significant responses detected when restimulated with pooled peptide (p<0.0001) or $CD8_{280-288}$ peptide (p<0.0001) at a similar magnitude. In the CBA assay, very low (87 pg/ml) but nonetheless significant response was detected in the pooled VLP immunised mice following $CD4_{59-79}$ peptide restimulation (p<0.01). Pooled VLP immunisations induced significant $CD8^+$ T cells

producing IFN-γ (p<0.01) detected in ICS analysis (Figure 17). Overall, there was no evidence to indicate any synergistic or inhibitory antigen-specific immune effects from pooling VLPs.

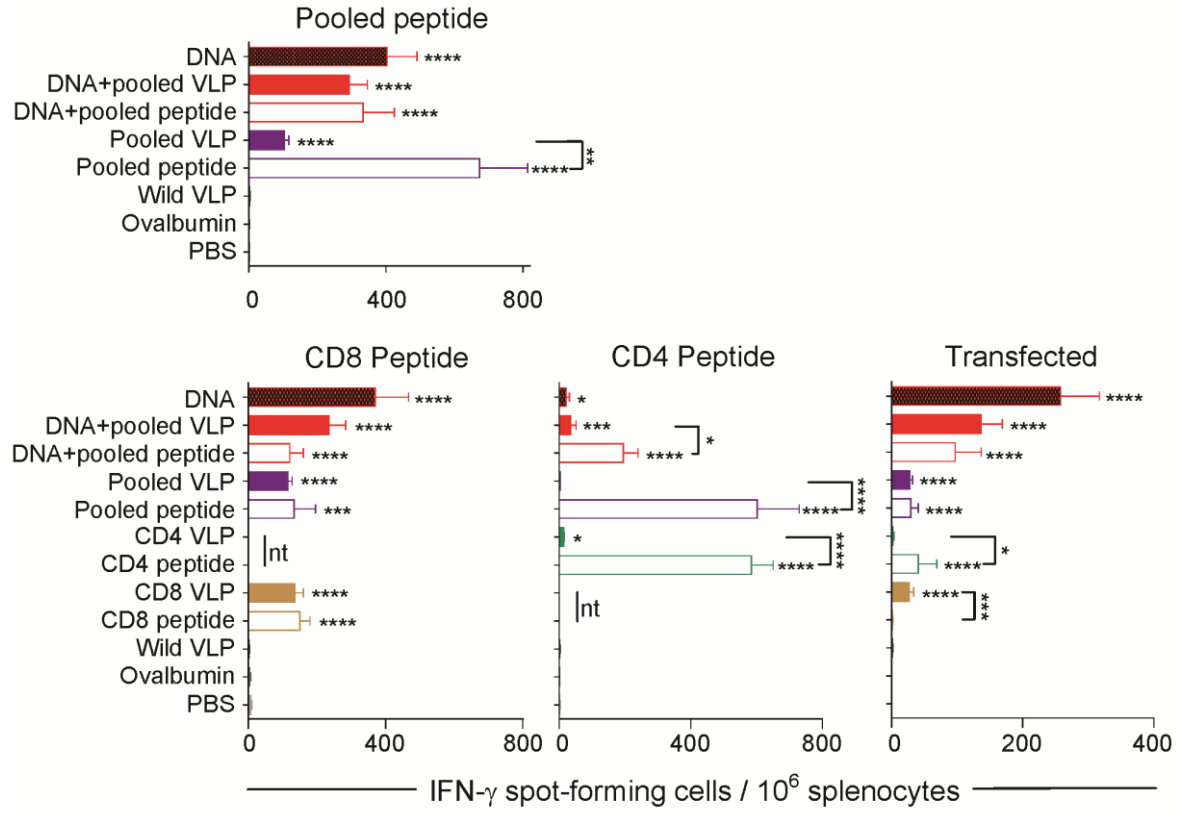

Figure 15: IFN-γ ELISpot responses induced by individual (30 µg) or pooled (30 µg each) chimeric VLP immunisations. BALB/c mice (n=5/group) received three s.c. immunisations at 2 week intervals of wild type VLPs (30 µg), individual VLP constructs (30 µg,) or pooled VLPs (30 µg each), individual (30 µg) or pooled peptides (30 µg each) with polyIC (50 µg), with three i.m. *Py*CSP plasmid DNA (100 µg) or a prime boost regimen using two i.m. *Py*CSP plasmid DNA (100 µg) primes then an s.c. boost using either pooled VLPs or peptides with polyIC. Splenocytes (5 x 10^5/well) were cultured and restimulated with irradiated A20 cells (1.5 x 10^5/well) either with individual or pooled *Py*CSP $CD8_{280-288}$,$CD4_{58-79}$ and B cell peptides, or with irradiated and pVR2516 *Py*CSP plasmid DNA transfected A20 cells (5 x 10^4/well) for 40 h. IFN-γ spot forming cells/million splenocytes are presented as group means + SEM. Statistical comparisons are made to the PBS control group, and between homologous VLP and peptide groups using log-transformed data with significance determined using one-way ANOVA followed by Bonferroni's post-hoc test. p<0.05 *, p<0.001 *** and p<0.0001 ****. (nt, not tested).

Heterologous DNA prime/boost regimen induced IFN-γ responses

The relative effectiveness of heterologous DNA prime/VLP boost versus homologous pooled VLP regimens was investigated. Significant IFN-γ responses were detected in heterologous as well as homologous regimens when splenocytes were restimulated with pooled peptide (p<0.0001) or *Py*CSP transfected A20 cells (p<0.0001) in the ELISpot assay (Figure 15). Consistent with earlier experiments, the response was primarily attributed to the $CD8_{280\text{-}288}$ peptide epitope (p<0.0001), with a small but never the less significant response to the $CD4_{59\text{-}79}$ peptide (p<0.001). The magnitude of the detected responses was not significantly higher in the heterologous versus homologous regimens, despite a 2-fold increase in the mean SFCs. A similar result was noted by CBA of IFN-γ in culture supernatants (Figure 16) with significant responses detected with pooled (p<0.0001), $CD8_{280\text{-}288}$ (p<0.0001) and $CD4_{59\text{-}79}$ (p<0.001) peptide restimulation, with a skew towards the $CD8_{280\text{-}288}$ peptide. In the ICS analysis (Figure 17), significant $CD8^+$ T cells producing IFN-γ were detected with pooled peptide restimulation when compared to the PBS control (p<0.01).

In this experiment, the inclusion of a *Py*CSP plasmid DNA group allowed for some determination as to the capacity of each component in the prime/boost regimen to stimulate immune responses. Immunisations with DNA only was clearly effective at inducing IFN-γ responses when restimulated with the $CD8_{280\text{-}288}$ peptide alone or pooled peptides, and to a lesser extent with the CD4 peptide, as shown in each cellular immune assay (Figure 15, Figure 16, Figure 17).

TNF and other cytokine responses

As with the earlier series of experiments (section 3.4.3.1), IFN-γ was the primary readout for cellular responses. Other cytokines, specifically: IL-1β, IL-2, IL-4, IL-5, IL-6, IL-10, IL-12p70, IL-13, TNF and IFN-γ in culture supernatants were detected by CBA analysis. Data was consistent with earlier experiments with predominant IFN-γ and TNF responses (Figure 16, Figure 17), whilst other detected cytokines were at or near the levels of detection for the assay.

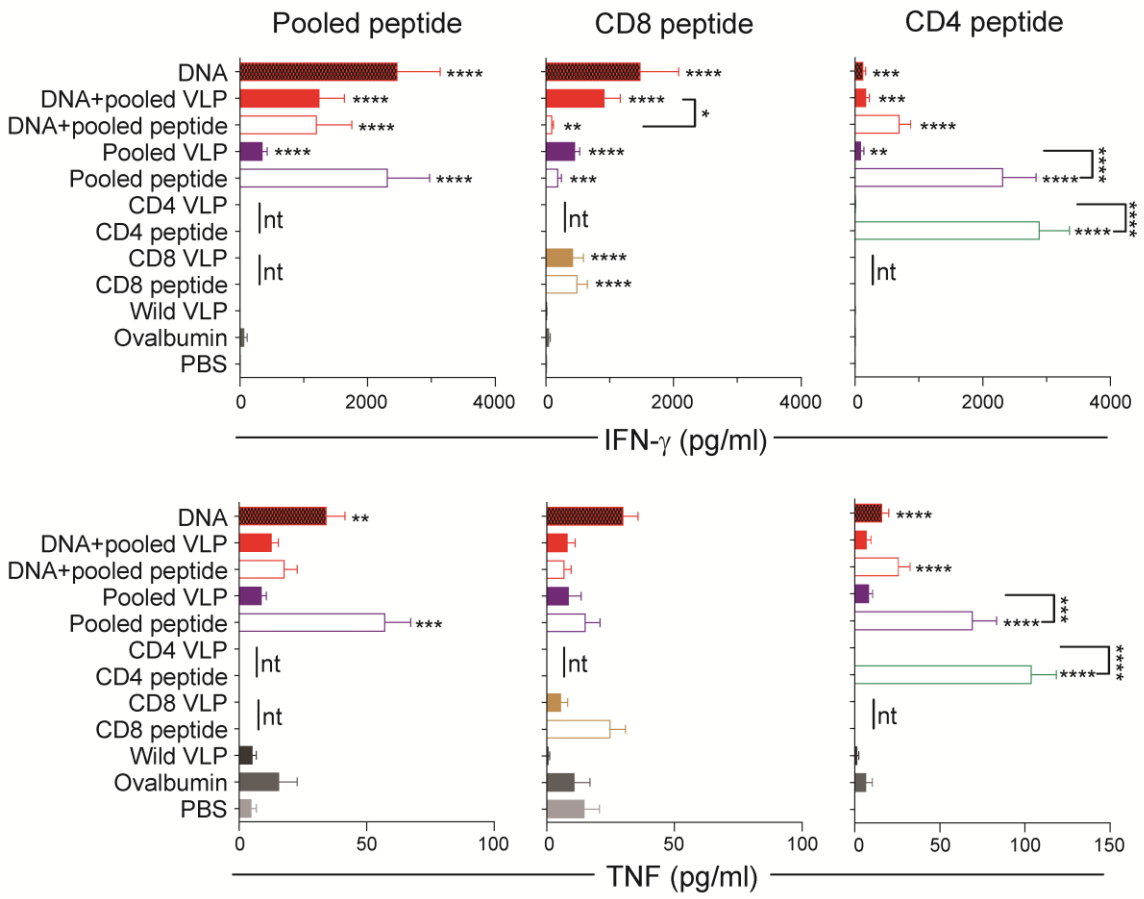

Figure 16: IFN-γ or TNF expression induced by individual (30 µg) or pooled (30 µg each) chimeric VLP immunisations. Mice (n=5/group) were immunised as previously described (Figure 15). Splenocytes (5 x 10^5/well) were cultured with irradiated A20 cells (1.5 x 10^5/well) and restimulated with individual or pooled *Py*CSP $CD8_{280-288}$, $CD4_{58-79}$ and B cell peptides for 72 h. Data are presented as mean + SEM for IFN-γ and TNF cytokines in pg/ml detected in culture supernatant by CBA analysis. Statistical comparisons are made to the PBS control group, and between homologous VLP and peptide groups using log-transformed data with significance determined using one-way ANOVA followed by Bonferroni's post-hoc test. $p<0.05$ *, $p<0.01$ **, $p<0.001$ *** and $p<0.0001$ ****. (nt, not tested).

The peptide immunisation groups had increased IL-6 and IL-13 levels which appeared to be driven by the CD4 peptide and were absent in VLP immunised groups. Splenocytes from pooled peptide immunised mice which were restimulated with pooled peptides, $CD8_{280-288}$ or $CD4_{59-79}$ peptides had increased IL-6 (110, 9 and 117 pg/ml respectively) and IL-13 (834, 64 and 904 pg/ml respectively) responses detected in the CBA assay.

The CBA data showed VLP-induced TNF responses were low (Figure 16), consistent with the earlier VLP experiment (Figure 10). In the ICS analysis, VLPs did not induce significant $CD8^+$ or $CD4^+$ T cells expressing either IL-2 or TNF. The peptide immunised groups did not achieve significant IL-2 responses in any restimulation, and TNF responses were only evident in $CD4^+$ T cells following pooled peptide or $CD4_{59\text{-}79}$ peptide restimulation.

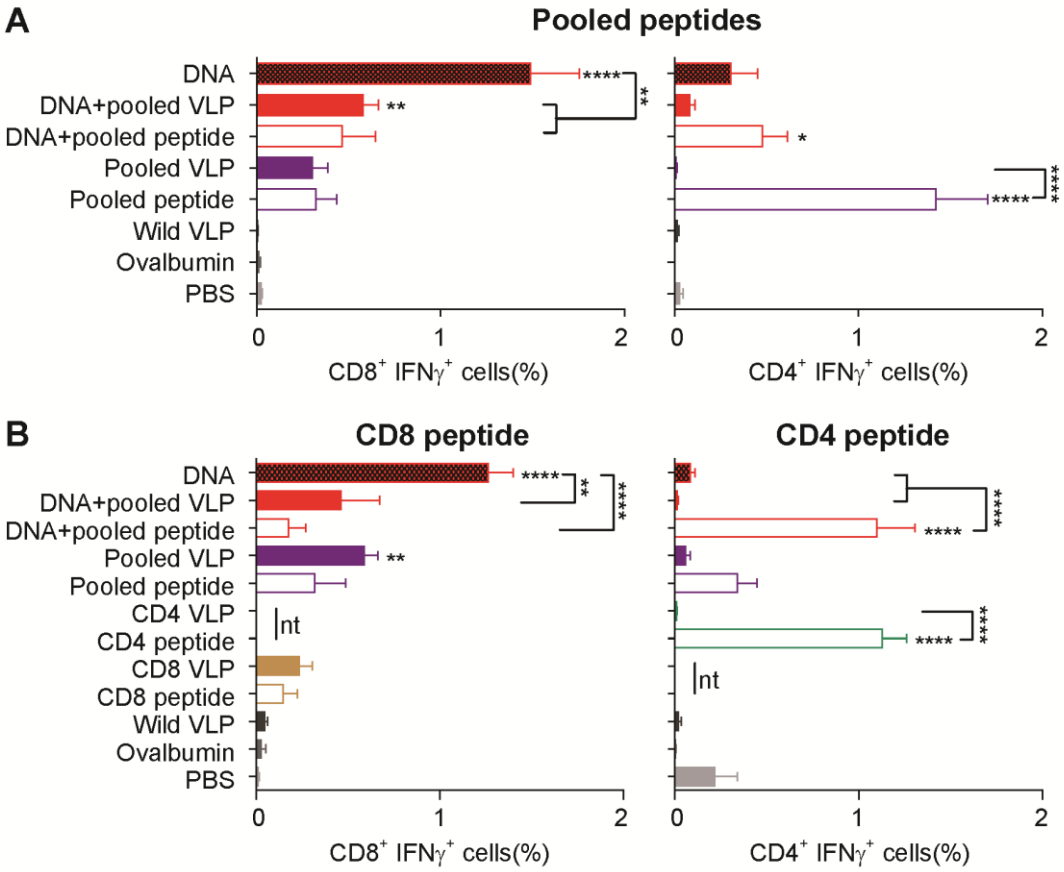

Figure 17: IFN-γ expressing T cells following immunisation and *Py*CSP peptide restimulation. Mice (n=5/group) were immunised as previously described (Figure 15). Splenocytes (5 x 10^5/well) were cultured with irradiated A20 cells (1.5 x 10^5/well) and restimulated with (A) pooled *Py*CSP $CD8_{280\text{-}288}$, $CD4_{58\text{-}79}$ and B cell repeat peptides or (B) with individual peptides; for 18 h with wells supplemented with GolgiPlug (0.1%) for the final 6h. Cells were stained for $CD8^+$ and $CD4^+$ T cell receptors then intracellular stained for IFN-γ. Statistical comparisons are made to the PBS control group, and between homologous VLP and peptide groups using log-transformed data with significance determined using one-way ANOVA followed by Bonferroni's post-hoc test. $p<0.05$ *, $p<0.01$ **, $p<0.001$ *** and $p<0.0001$ ****. (nt, not tested).

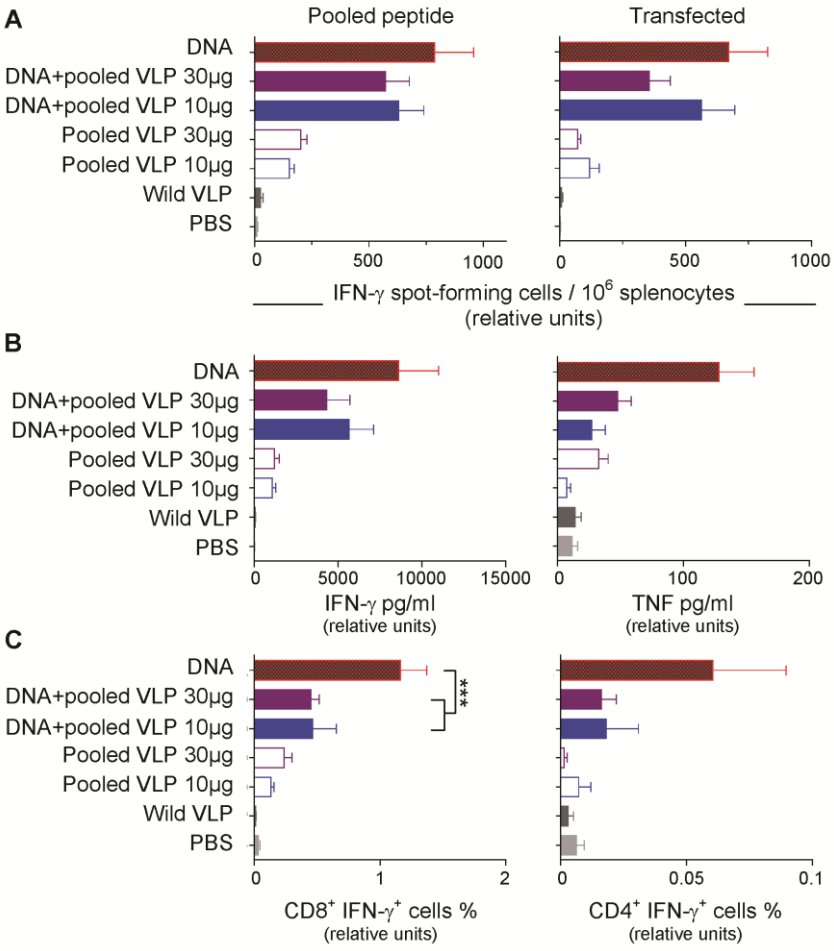

Figure 18: Cellular immune response comparisons between VLP experiments. In two series of experiments mice (n=5/group) received three s.c. immunisations at 2 week intervals of either wild type VLPs (30 µg), pooled VLPs at either 10 or 30 µg of each construct, three i.m. *Py*CSP plasmid DNA (100 µg), or a prime boost regimen using two i.m. *Py*CSP plasmid DNA (100 µg) primes then a boost using either pooled VLPs at either 10 or 30 µg of each construct. Data from (A) ELISpot (B) cytometric bead array and (C) intracellular cytokine staining have been normalised to data from mice immunised with a DNA prime/pooled peptide boost regimen. Data is presented as mean + SEM in relative units for each assay. Statistical comparisons are made between groups with VLP doses at 10 or 30 µg per construct per dose or between mice receiving DNA in a homologous or heterologous regimen, using log-transformed data with significance determined using one-way ANOVA followed by Bonferroni's post-hoc test. $p<0.001$ ***.

To determine whether pooled VLPs were more immunogenic at either 10 µg/construct or 30 µg/construct in either homologous or heterologous DNA prime/boost regimens, data between the two sets of VLP experiments were normalised based on the DNA/pooled peptide immunised mice. Data from ELISpot, CBA and ICS immunogenicity assays (Figure 18) show no significant effect of VLP dose. DNA only immunisations were consistently higher than any other regimen in

each of the data sets (Figure 18). Significant differences between DNA only or prime/boost immunisations were only detected in ICS data with $CD8^+$ T cells expressing IFN-γ (p<0.001) (Figure 18C). The data also shows trend of higher cellular responses in the prime/boost immunisations as compared to the homologous regimen but the differences were not significant (p>0.05).

3.4.4.2. Antibody responses

To assess the capacity of VLPs to induce antigen-specific antibody titres, an ELISA was conducted using pooled sera collected after each immunisation, and the PST-tagged PyCSP B cell repeat peptide as the capture antigen (Figure 19A). Consistent with the previous study (section 3.4.3.2), this data indicated that a second VLP immunisation was required for VLP induced robust antibody responses. The DNA/VLP regimen with only a single dose of VLPs had an endpoint titre of only 12.5% of that of the pooled VLP homologous regimen. DNA immunisations are poor at inducing antibody responses, and consistent with earlier results (Figure 12), peptides with and without DNA priming were also ineffective.

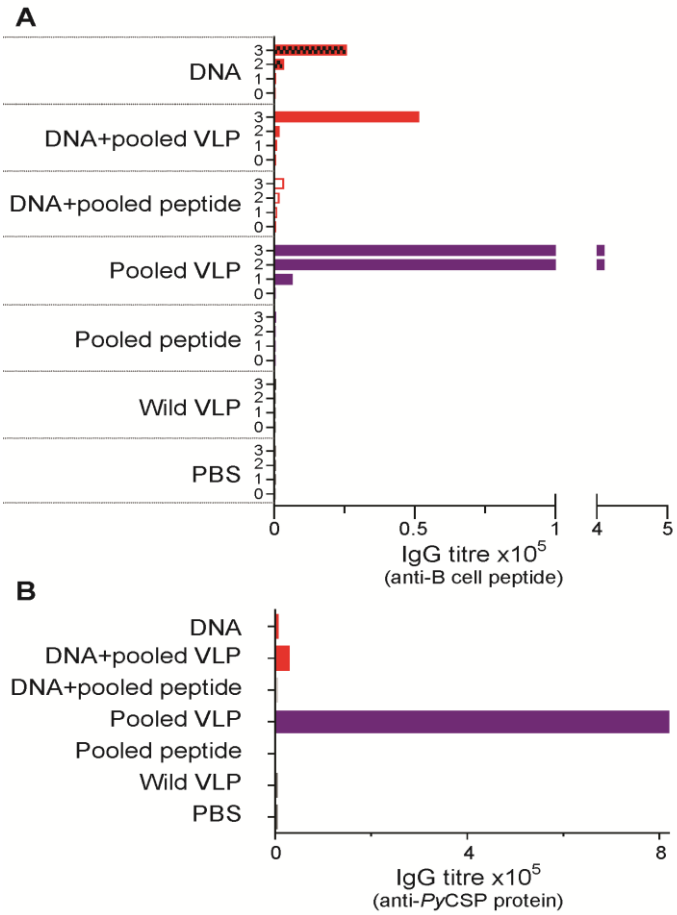

Figure 19: Immunisation induced anti-B cell peptide and *Py*CSP antibody responses. Mice (n=5/group) were immunised as previously described (Figure 15). (A) Sera collected pre-immunisation (0) and following successive doses (1,2 and 3) was pooled then used with ELISA to detect *Py*CSP B cell peptide-specific total IgG endpoint titres. (B) *Py*CSP recombinant protein-specific IgG endpoint titres were determined by ELISA using pooled sera collected following the final immunisation.

To confirm that the chimeric VLP induced antibodies were able to recognise *Py*CSP protein in addition to peptide epitope, an ELISA was conducted using *PyCSP* recombinant protein as the capture antigen (Figure 19B). Using pooled sera collected after the final immunisation, a high anti-*Py*CSP antibody titre was present in mice immunised with three doses of pooled VLPs. A low endpoint titre was detected in the DNA/VLP immunised mice receiving only a single VLP immunisation. Using individual sera against the PST-tagged *Py*CSP B cell repeat peptide (Figure 13), the pooled VLP endpoint titre was significantly higher than DNA alone or the DNA/VLP regimen (p<0.0001).

3.4.4.3. Protection

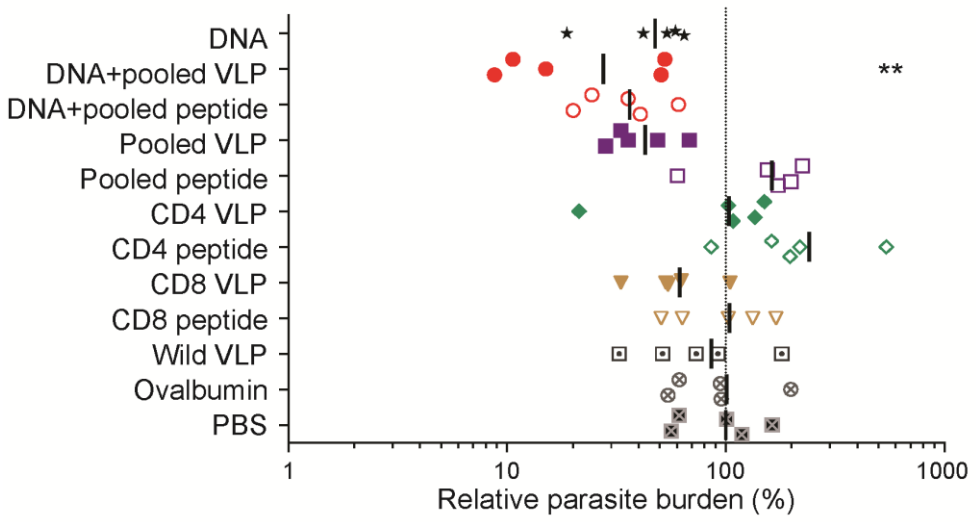

Figure 20: Protective capacity induced by individual (30 µg) or pooled (30 µg each) chimeric VLPs using homologous or heterologous immunisation regimens. Mice (n=5/group) were immunised as previously described (Figure 15). Mice were challenged 16 days after the final immunisation with i.v. injection of 1000 *P. yoelii* 17XNL cryopreserved sporozoites. Parasite burden was assessed by qRT-PCR analysis of *Py*18s RNA extracted from livers harvested 42 h post-challenge and calculated as a ratio to the GAPDH housekeeping-gene RNA. Data was normalised to the PBS control and presented as a relative parasite burden. Individual results are shown with bars representing the group mean. Log-transformed ratio data was analysed using one-way ANOVA followed by Bonferroni's post-hoc test. p<0.01 **

To evaluate the protective efficacy of chimeric VLPs with the higher dose of pooled VLP constructs (30 µg each), immunised mice (n=5/group) from each group were challenged with 1000 sporozoites, then parasite RNA was quantified from

homogenised livers using qRT-PCR[286]. A significant reduction in the ratio of parasite *Py*18S RNA to mouse GAPDH RNA was noted in mice immunised with the heterologous DNA prime and pooled VLP boost ($p<0.01$) (Figure 20). This equates to a mean 72% reduction in the liver parasite burden relative to the PBS immunised group. Whilst protection in the pooled VLP immunised mice did not reach significance, there was a mean 57% reduction in liver-stage parasite burden relative to the PBS control.

3.4.5. Chimeric capsomeres

Next, the immunogenicity and protective capacity of chimeric capsomeres was evaluated, in comparison to chimeric VLPs. Due to constraints in the size of this study, capsomere immunisations were administered in pools and not individual constructs. Capsomeres were co-administered with polyIC as an adjuvant to enhance immune responses with a bias towards a Th1 response. Chimeric VLPs used in this series of experiments were the same as previously described (section 3.4.1) and characterised (Figure 7)

3.4.5.1. Construction of chimeric capsomeres

Chimeric capsomere constructs were made using the VP1ΔNΔC[170] backbone with either *Py*CSP CD8, CD4 or B cell epitope sequences (consistent with VLPs) genetically inserted into the N-terminus, the S4 loop, and the C-terminus. Chimeric capsomeres were expressed in *E. coli* then purified using a GST-affinity column followed by size exclusion chromatography. Endotoxin was removed using ion-exchange columns, and then capsomeres were dialysed against PBS. Capsomeres lacked the ability to form VLPs and therefore were not analysed by TEM or AF4-MALS. The predicted molecular weight of each chimera was: CD8 dominant, 61.9 kDa; CD8 subdominant, 62.8 kDa; CD4 dominant 1, 64.5 kDa; CD4 dominant 2, 64.0 kDa; CD4 subdominant, 66.2 kDa; and B cell, 62.0 kDa (Appendix F). The yield and solubility were similar to the results described for the chimeric VLP constructs with low solubility in the CD8 subdominant, CD4 dominant 1 and CD4 dominant 2 constructs. Due to the low solubility and to maintain consistency with the VLP

constructs, only the chimeric *Py*CSP $CD8_{280-288}$ dominant, $CD4_{59-79}$ subdominant and B cell capsomeres were used in subsequent pooled immunisations.

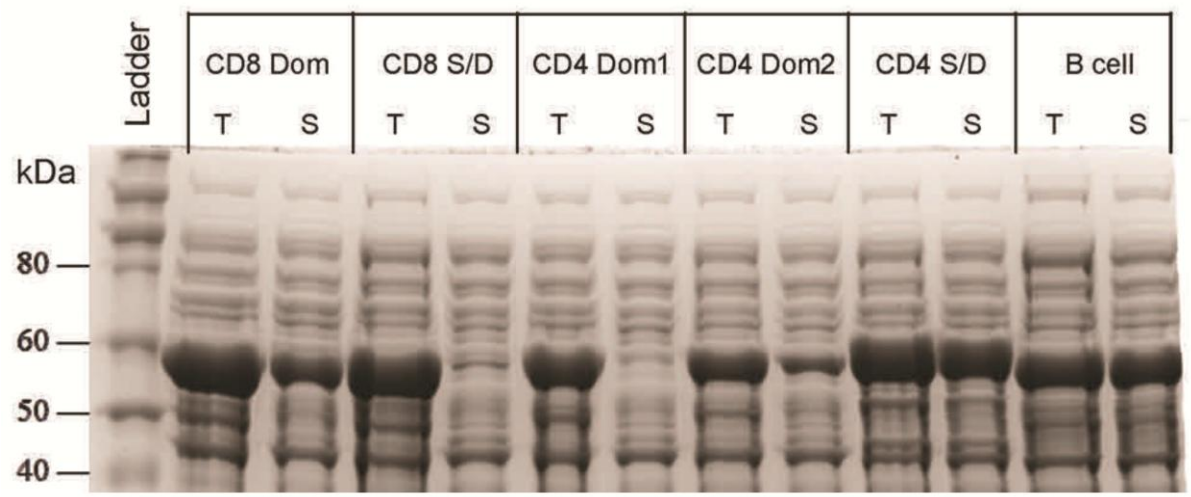

Figure 21: Protein expression and solubility of chimeric capsomere constructs. Rosetta DE3 pLysS *E. coli* were transformed with plasmid DNA from each chimeric VP1ΔNΔC construct. Colony isolates were selected for overnight starter cultures which were subsequently used to inoculate 400 ml of TB media with ampicillin [50 µg/ml] and chloramphenicol [24 µg/ml] in 2 L baffled flasks. At OD_{450} ~ 0.5, cultures were cooled in tap water for 10 min, and then induced with IPTG [0.2 mM]. Cultures were incubated overnight at 26°C with shaking at 180 RPM, then bacteria were harvested by centrifugation and pellets lysed by sonication. A total (T) fraction was taken directly from lysed bacteria, whilst the soluble (S) fraction was taken from the supernatant of lysed and centrifuged bacteria. Fractions were run on a 10% SDS-PAGE gel then stained with coomassie. A molecular weight ladder (Novex sharp pre-stained) was run (left lane) in parallel with other samples.

3.4.5.2. Cellular immunogenicity

To determine if immunisations with chimeric capsomeres could induce antigen-specific cellular immune responses, splenocytes from immunised mice were harvested and single cell suspensions restimulated for ELISpot, CBA and ICS assays. In parallel, chimeric VLPs were evaluated to determine if capsomeres were more or less efficacious than VLPs. Additionally, VLPs co-administered with polyIC were evaluated to determine if VLP immune responses could be enhance with adjuvants.

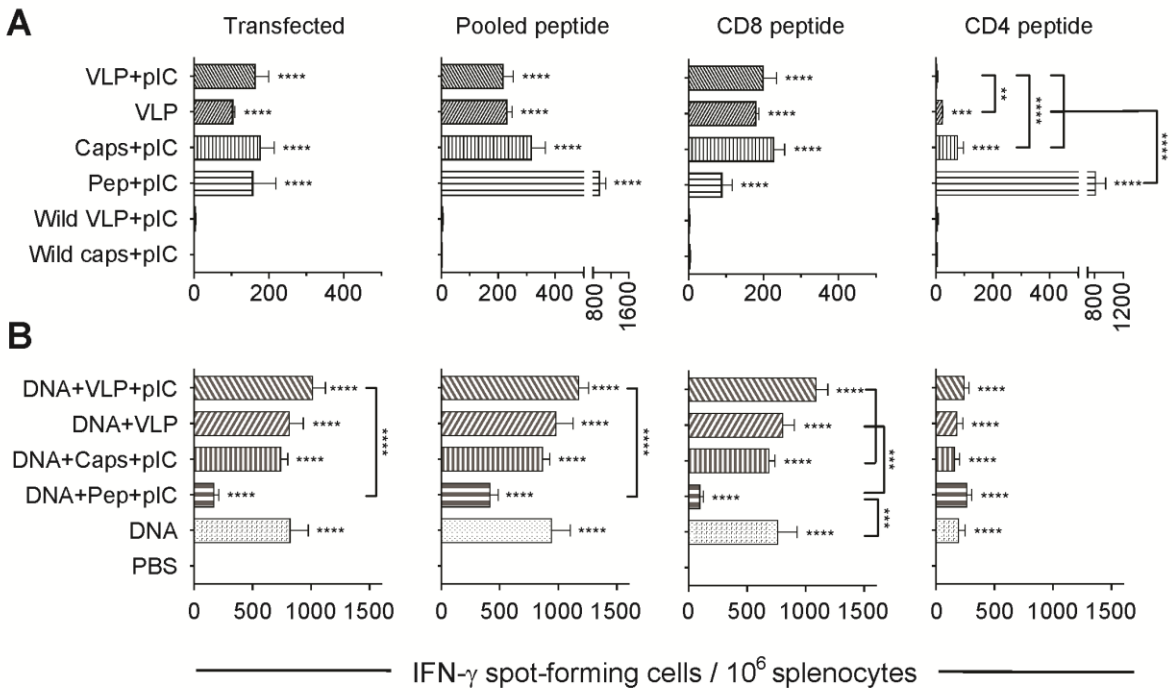

Figure 22: IFN-γ ELISpot analysis of responses induced by capsomere or VLP immunisations. BALB/c mice (n=5/group) received three immunisations at 2 week intervals with; (A) wild-type VLPs or wild-type capsomeres (30 µg), pooled chimeric VLPs or capsomeres (CD8, CD4 and B cell: 10 µg/construct), or pooled *Py*CSP peptides (30 µg/peptide), all co-administered with polyIC (50 µg) by s.c. injections. One group received pooled VLPs without adjuvant: or (B) three i.m. doses of *Py*CSP plasmid DNA (100 µg), or a heterologous DNA prime-boost regimen with two i.m. *Py*CSP plasmid DNA primes followed by a single s.c. boost with VLPs or capsomeres as described above, with a PBS injected control. Splenocytes (5 x 10^5/well) were cultured and restimulated with pVR2516 *Py*CSP plasmid DNA transfected and irradiated A20 cells (5 x 10^4/well) or with irradiated A20 cells (1.5 x 10^5/well) with individual or pooled *Py*CSP CD8 $_{(280-288)}$ CD4 $_{(58-79)}$ and B cell peptides, or for 40 h. IFN-γ spot forming cells (SFCs) were quantified with data displayed as mean SFCs per 10^6 splenocytes + SEM. Statistical comparisons made to the PBS injected control group, and between immunisation groups with significance determined using one-way ANOVA followed by Bonferroni's post-test. p<0.05 *, p<0.01 **, p<0.001 *** and p<0.0001 ****.

Like VLPs, capsomeres induced significant IFN-γ responses following restimulation with either *Py*CSP transfected A20 cells, *Py*CSP $CD8_{280-288}$ peptide or pooled ($CD8_{280-288}$, $CD4_{59-79}$ and B cell) peptides (p<0.0001) as compared to the PBS control group (Figure 22). There were no significant differences between responses induced by immunisations with capsomeres versus VLPs. There were only minor and non-significant differences with any of the vaccine groups immunised with the homologous (Figure 22A) or heterologous DNA prime-boost regimen (Figure 22B).

However, significant increases were detected in the heterologous groups boosted as compared to respective homologous immunisations with capsomeres (p<0.001), VLPs and VLPs with polyIC (p<0.0001) following *Py*CSP transfected A20 restimulation, or capsomeres (p<0.01), VLPs and VLPs with polyIC (p<0.0001) following peptide restimulation.

When splenocytes were stimulated with either *Py*CSP $CD8_{280-288}$ or $CD4_{59-79}$ peptides, it was apparent that most of the capsomere and VLP immunisation responses were directed to the $CD8^{+}_{280-288}$ T cell epitope (Figure 22). The peptide-specific response induced by capsomeres was similar to that induced by peptide formulated in adjuvant for the $CD8_{280-288}$ peptide, but was significantly lower for the $CD4_{59-79}$ peptide. Notably, the capsomeres did induce a significant IFN-γ response to the $CD4_{59-79}$ peptide, relative to the PBS control (p<0.0001). The highest IFN-γ responses were induced by the heterologous DNA primed/VLP and polyIC boost regimen. However, these responses weren't significantly higher than the groups immunised with heterologous DNA/capsomeres or DNA/VLPs, or with three doses of *Py*CSP plasmid DNA alone, each of which had a similar magnitude of response.

A broad array of cytokines including IL-1β, IL-2, IL-4, IL-5, IL-6, IL-10, IL-12p70, IL-13, TNF and IFN-γ were assayed by CBA using pooled culture supernatant. Most cytokine levels at or near the level of detection for this assay (data not presented). Robust IFN-γ and TNF responses were detected in individual culture supernatants (Figure 23). The IFN-γ profile was similar to that detected by ELISPOT (Figure 22). Significant levels of IFN-γ detected as compared to the naive control group (p<0.001) for all capsomere and VLP groups. Capsomeres did not induce a TNF response against either peptide, whereas VLP immunisations did induce a response against both peptides.

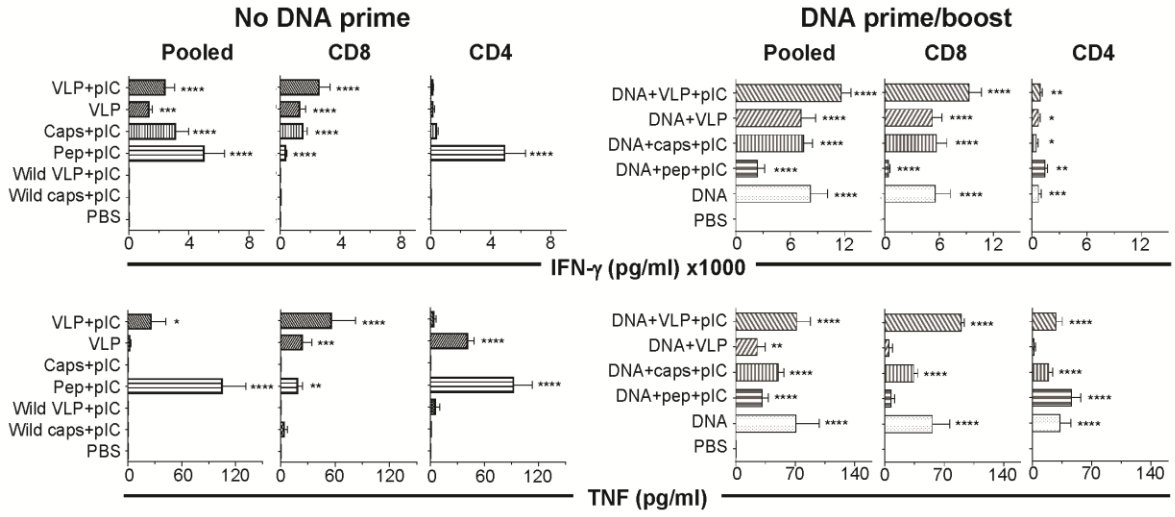

Figure 23: IFN-γ or TNF expression induced by chimeric capsomere or VLP immunisations. BALB/c mice (n=5/group) were immunised as previously described (Figure 22). Splenocytes (5 x 10^5/well) were cultured with irradiated A20 cells (1.5 x 10^5) and restimulated with either individual or pooled *Py*CSP $CD8_{280-288}$, $CD4_{58-79}$, and B cell peptides and incubated for 72 h. Culture supernatant was assayed using a cytometric bead array to quantify IFN-γ and TNF cytokine levels. Data is separated into mice receiving no plasmid DNA primes (left) or those receiving the prime/boost regimen (right) and displayed as mean pg/ml + SEM. Statistical comparisons were made to the PBS injected control group. Significance was determined using one-way ANOVA followed by Bonferroni's post-test. $p<0.05$ *, $p<0.01$ **, $p<0.001$ *** and $p<0.0001$ ****.

Consistent with the ELISpot and CBA data, ICS data showed that capsomere immunisations induce IFN-γ but not TNF responses with the IFN-γ predominantly being generated by $CD8^+$ T cells (Figure 24). Significant responses were detected in DNA prime/capsomere boost regimens, but increases appear to be a result of the DNA priming as opposed to the capsomere boost.

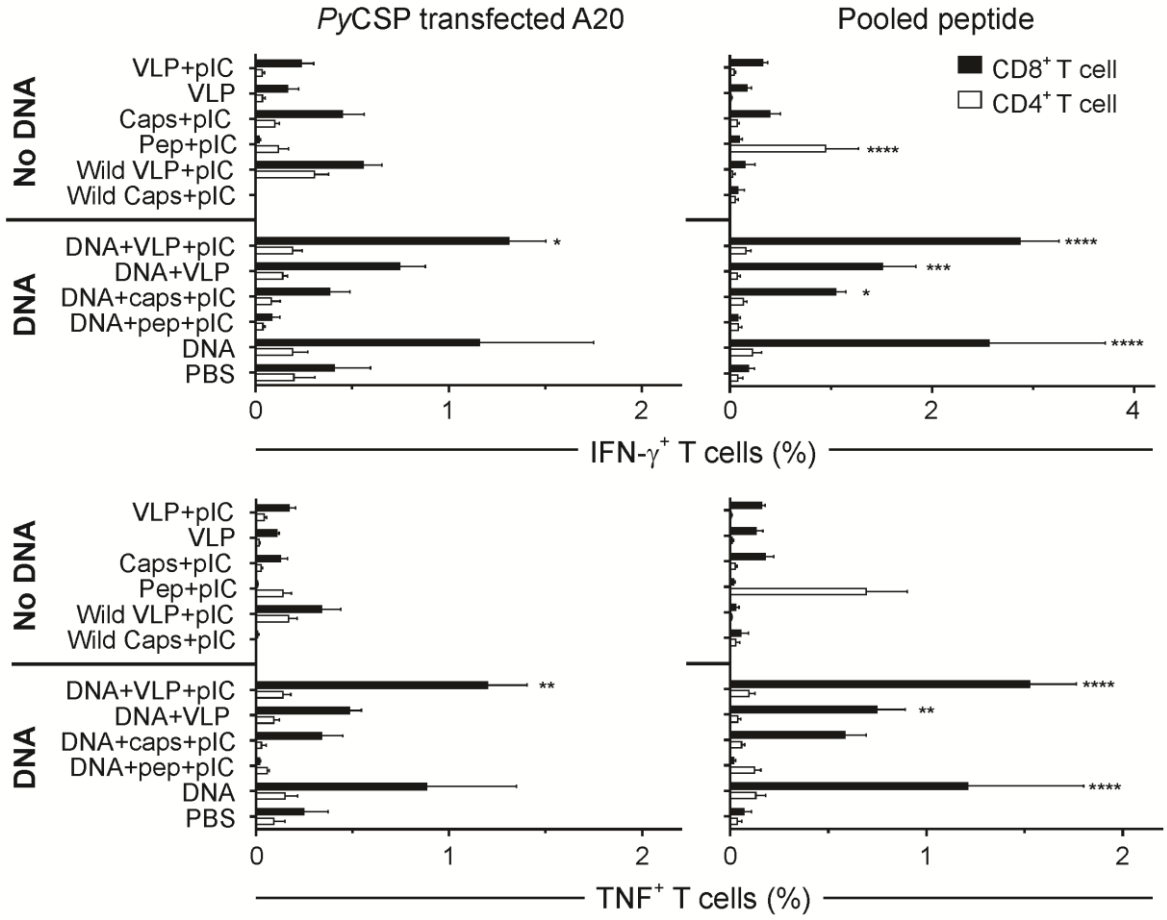

Figure 24: IFN-γ and TNF expressing T cells induced by chimeric capsomere or VLP immunisations. BALB/c mice (n=5/group) were immunised as previously described (Figure 22). Splenocytes (5 x 10^5/well) were cultured with irradiated A20 cells which had been either transfected with *Py*CSP plasmid DNA, or incubated with pooled *Py*CSP $CD8_{280-288}$, $CD4_{58-79}$ and B cell peptides for 6 h with 0.1% Golgi Plug supplemented media. Cells were stained for CD8 and CD4 receptors, then permeabilized and stained for IFN-γ and TNF cytokines then analysed by flow cytometry. The frequency of CD8 or CD4 positive cytokine expressing cells are shown as the group mean + SEM (n=5 mice/group) with $CD8^+$ and $CD4^+$ T cells represented by solid black bars or empty bars respectively. Statistical comparisons are made to the PBS injected control group with significance determined using one-way ANOVA with Bonferroni's post-test. $p<0.05$ *, $p<0.01$ **, $p<0.001$ *** and $p<0.0001$ ****.

3.4.5.3. Antibody responses

ELISA assays against the PST- *Py*CSP B cell repeat peptide were performed using individual mouse sera collected 10 days following the final immunisation (Figure 25A). Capsomere or VLP ± polyIC immunisations all induced significant antibody titres when compared to the PBS control group ($p<0.0001$), but capsomeres were significantly less effective than VLPs ($p<0.05$) or VLPs with polyIC ($p<0.01$). In

contrast to cellular immune responses, antibody responses were reduced by heterologous immunisations with VLP relative to the homologous regimen (p<0.01). However, antibody responses were increased by heterologous immunisation with a capsomere boost, relative to the homologous regimen. VLPs co-administered with polyIC induced the highest IgG antibody titres, however, these were not significantly increased relative to VLPs without polyIC.

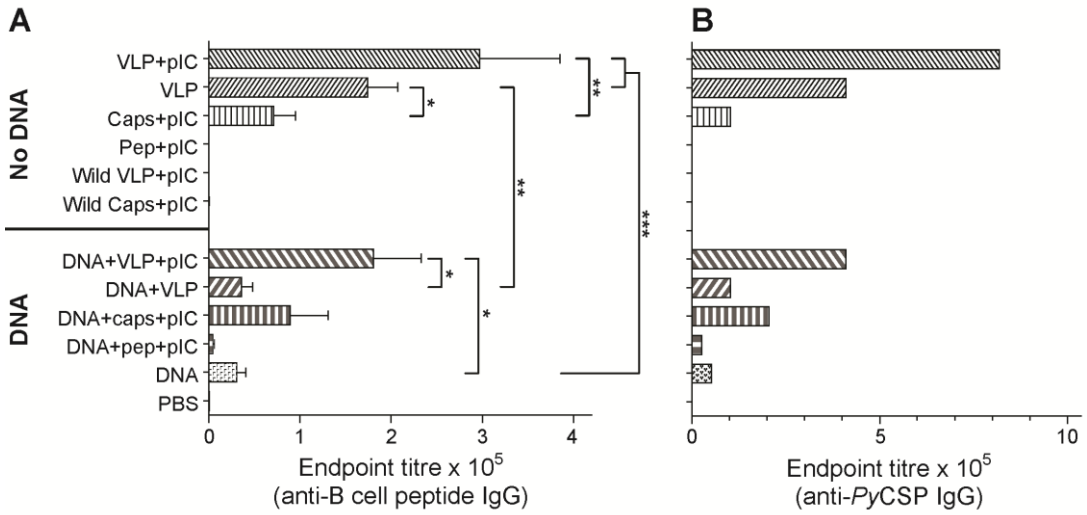

Figure 25: IgG antibody responses against the *Py*CSP B cell peptide and *Py*CSP protein following capsomere or VLP immunisations. Mice (n=10/group) were immunised as previously described (Figure 22). Sera collected from mice five days after final immunisation was analysed by ELISA. (A) Using a *Py*CSP B cell repeat epitope linked to a polystyrene binding tag as a capture antigen, individual IgG endpoint titres were determined. (B) Using *Py*CSP protein as the capture antigen, IgG endpoint titres were detected with pooled sera. Data is displayed as mean endpoint titre + SEM. Inter-group significance was determined using log-transformed data analysed using one-way ANOVA followed by Bonferroni's post-test. p<0.05 *, p<0.01 **, and p<0.001 ***.

To confirm that the antibodies induced by capsomeres and VLPs could recognise the native *Py*CSP protein, pooled sera collected after the final immunisation was assayed using ELISA with the recombinant protein as the capture antigen (Figure 25B). Higher endpoint titres were detected with a profile similar to those obtained against the B cell peptide (Figure 25A).

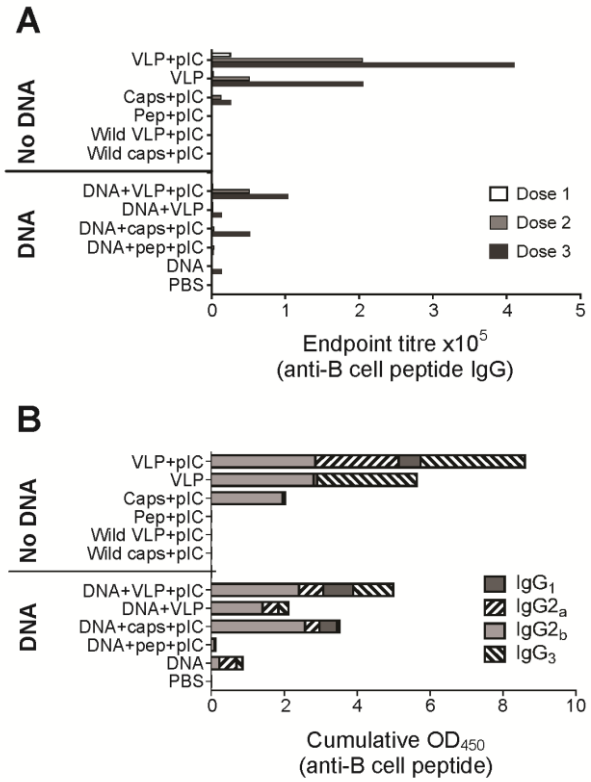

Figure 26: Dose-related antibody responses and isotype differentiation induced by capsomere or VLP immunisations. Sera was collected from BALB/c mice (n=5/group) following each immunisation of VLP, capsomeres or peptides in a three dose homologous or a heterologous *Py*CSP DNA prime boost regimen. Pooled sera was analysed by ELISA using the *Py*CSP B cell repeat epitope linked to a polystyrene binding tag as the capture antigen. (A) Immunisation related peptide-specific total IgG titres were assessed using sera collected following each immunisation. (B) Sera collected 5 days after the final immunisation was used to assess peptide-specific IgG_1, IgG_{2a}, IgG_{2b} and IgG_3 antibody isotypes.

The kinetics of the antibody responses were investigated using pooled sera collected after each immunisation, IgG responses to the *Py*CSP B cell repeat peptide (Figure 26A). Antibody titres increased in each of the homologous capsomere and VLP immunisation groups after successive immunisations. In groups receiving the heterologous regimen, DNA primes induced low antibody responses which were increased by boosting with capsomeres or VLPs but only with the co-administration of polyIC.

Antibody isotype responses against the *Py*CSP B cell repeat peptide were also determined (Figure 26B). Capsomeres, VLPs and VLPs with polyIC induce similar IgG_1 responses; however, it was only the VLP groups where IgG_3 responses were detected. The homologous VLP immunisation groups had higher levels of IgG_3 but

similar levels of IgG_1 indicating that doses 2 and 3 shift responses towards an IgG_3 bias. IgG_{2a} responses are increased with the inclusion of polyIC in the VLP but not with the capsomere mice. Moderate IgG_{2a} responses were also present in the DNA group and the heterologous DNA prime groups.

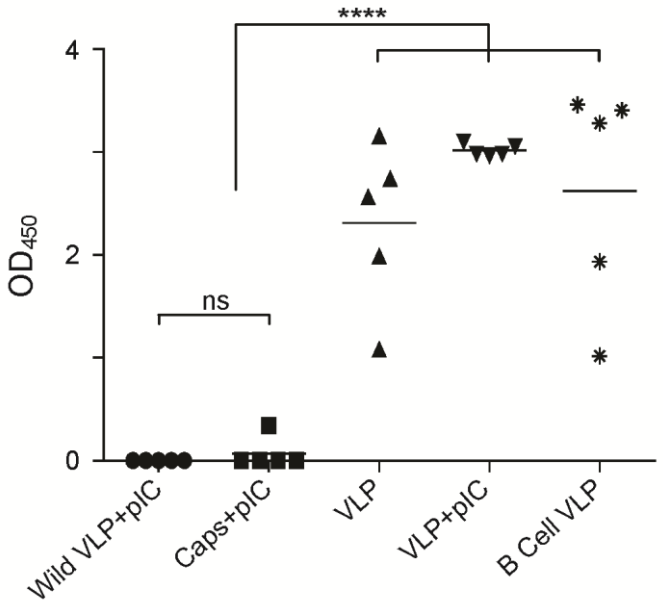

Figure 27: IgG_3 responses following capsomere or VLP immunisations. BALB/c mice (n=5/group) were immunised three times with capsomeres with polyIC, VLPs ± polyIC, or B cell VLPs. Five days after the final boost sera from individual mice was collected, diluted 1:400 and analysed for IgG_3 antibodies specific for the *Py*CSP B cell repeat epitope linked to a polystyrene binding tag. Plates were developed and OD_{450} values are displayed for individual mice with bars representing the group mean. Inter-group significance was determined using one-way ANOVA followed by Bonferroni's post-test $p<0.0001$ ****.

To confirm that the IgG_3 response was consistent within groups, an ELISA against the *Py*CSP B cell repeat peptide was conducted with individual sera obtained after the final immunisation (Figure 27). In this assay, individual sera from mice immunised with B cell VLPs (only) in the first series of experiments were also included. Mice immunised with B cell VLPs or pooled VLPs ± polyIC had significant increases in IgG_3 when compared to the capsomere immunised sera ($p<0.0001$). The capsomere induced IgG_3 titre was not significantly different to the wild type VLP control ($p>0.05$).

To confirm that induced antibodies recognised native sporozoites, an IFAT was conducted using *P. yoelii* 17XNL sporozoites, with pooled sera from mice immunised with capsomeres, VLPs ± polyIC both in the homologous and heterologous immunisation regimens (Figure 28). Each of the displayed immunisation groups were

considered positive for sporozoite recognition. *Py*CSP plasmid DNA alone and with pooled peptides was also positive, however, the intensity of the staining was lower, consistent with the lower titres detected by ELISA (Figure 25). All negative control groups and the pooled peptide with polyIC group were negative for surface staining.

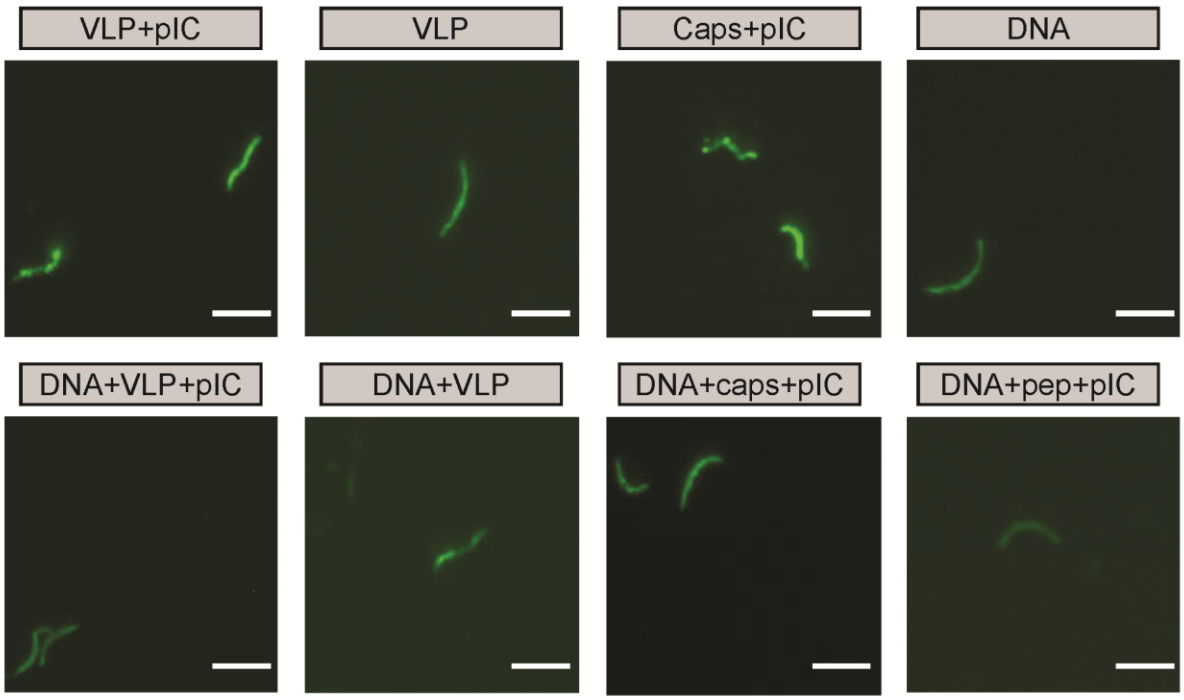

Figure 28: IFAT detection of capsomere or VLP immunisation induced anti-sporozoite antibodies. Mice (n=10/group) were immunised using a three dose regimen with either homologous VLPs, capsomeres or *Py*CSP plasmid DNA, or a heterologous *Py*CSP plasmid DNA (x2) prime followed by a single VLP or capsomere boost as previously described (Figure 22). Sera collected from mice five days after final immunisation was pooled, diluted to 1:400 and then used against *P. yoelii* 17XNL sporozoite coated slides. Slides were then stained using FITC conjugated anti-mouse IgG antibodies and viewed on an EVOS fluorescence microscope. Scale bars are 10 µm.

3.4.5.4. Protection

To evaluate protection, immunised mice were challenged with 1000 *P. yoelii* 17XNL cryopreserved sporozoites. Parasite RNA in homogenised livers detected by qRT-PCR[286] reactions are calculated as a ratio to the mouse GAPDH housekeeping gene then normalised to the PBS control (Figure 29). No protection was apparent in any of the groups. This lack of protection is consistent with earlier experiments (Figure 14 and Figure 20), with the exception of the DNA prime/VLP boost regimen which

showed protective capacity when the VLP boost included 30 µg of each construct (Figure 20).

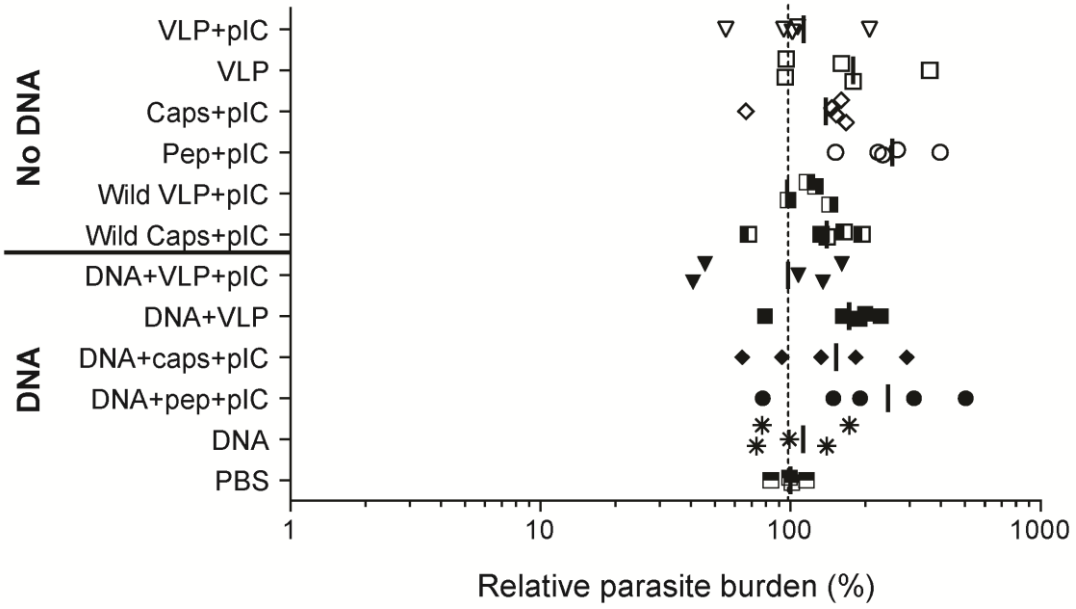

Figure 29: Protective capacity of chimeric VLPs or capsomeres against sporozoite challenge. BALB/c mice (n=5/group) received three immunisations with either homologous pooled VLPs or capsomeres, or a heterologous DNA prime-boost regimens. Mice were challenged 12 days after the final immunisation with 1000 *P. yoelii* 17XNL cryopreserved sporozoites. Parasite burden was assessed by qRT-PCR analysis of *Py*18s RNA extracted from livers harvested 42 h post-challenge and calculated as a ratio GAPDH housekeeping-gene RNA. Data was normalised to the PBS control and presented as a relative parasite burden. Individual results are shown with bars representing the group mean. No significant differences were detected between groups.

3.5. Discussion

3.5.1. Chimeric MuPyV VP1-S4-G4S and VP1ΔNΔC expression and assembly

Six chimeric MuPyV VP1-S4-G4S and VP1ΔNΔC constructs were successfully generated, each incorporating a single $CD8^{+}_{280\text{-}288}$ T cell[73,75], $CD4^{+}_{59\text{-}79}$ T cell[71,72,74] or B cell repeat[63] epitope derived from *Py*CSP. Each chimera was able to produce recombinant protein in transformed *E. coli* as detected on an SDS-PAGE gel. There was, however, some variation with regards to the level of protein being expressed and importantly for purification, the solubility of the protein (Figure 5). GST-purification of lysate was performed using only the soluble fraction, and as a result of

the low protein solubility associated with the CD8 subdominant, and CD4 dominant 1 and 2 chimeras, the recovered protein fractions were very low. For the constructs under study, each epitope was inserted into the S4 surface-exposed loop on MuPyV VP1 flanked by G4S linker sequences[173].

It was anticipated that the insertion of epitopes into this region would be less likely to interfere with the VLP formation and surface exposure would optimise the generation of target-specific antibodies[152,175]. However, following the insertion of any epitopes, the retention of the protein characteristics and the ability to form VLPs is currently unpredictable[156,157]. This insert disruption effect was clearly displayed by Rueda *et al.*[158] when various ovalbumin chimeras with different flanking arrangements resulted in highly variable expression. In fact, the variation of a single amino resulted in a highly efficient protein expression being reduced to barely detectable levels[158]. There are four surface loops on the MuPyV VP1 protein[306] and the insertion site is likely to influence the stability of the protein. In one study, epitopes of various sizes were inserted into four sites of the HaPyV but only two of the four sites efficiently expressed recombinant protein and formed VLPs whereas the other two sites had drastically reduced expression[176]. A similar result was reported using a bovine papillomavirus L1 protein where only one of four chimeras formed using loop regions resulted in proper formation of VLPs[157]. In my study four of the six epitopes inserted into the S4 surface loop successful formed VLPs, however, only three of these had sufficient yields to continue to animal experiments (Figure 7). It is possible that alternative insertion sites may have resulted in better expression of the remaining constructs. Given that the majority of the epitopes used in this study were targeting cellular and not antibody responses, there was no requirement to insert them into surface exposed regions, and they could have been inserted in non-exposed terminal regions of the VP1 protein. It may be that T cell epitopes bound to terminal regions could result in increased T cell immune responses as shown by Crisci *et al.* where ovalbumin CD8 epitopes inserted into N-terminal of rabbit hemorrhagic disease virus VLPs resulted in higher IFN-γ, significantly higher target-specific lysis and protection from vaccinia virus expressing OVA protein[155].

The chimeric capsomere constructs had a similar profile to VLPs with regards to the level of expression of soluble proteins (Figure 21). It would appear that the reduction

in soluble protein expression was directly related to the inserted epitopes. However, because the capsomere constructs also had each epitope inserted into the S4 surface loop, no determination can be made as to the effect of the position of the epitope on solubility of the protein.

3.5.2. Cellular responses

Whilst the antibody inducing capacity of chimeric MuPyV VLPs and capsomeres has been well established[170,173,188], their ability to induce epitope-specific T cell responses has been as poorly studied.

In vitro proliferation of $CD8^+$ T cells

To evaluate the recognition and subsequent proliferation of epitope-specific $CD8^+$ T cells, CFSE-stained CS-TCR cells were incubated *in vitro* with $CD8_{280-288}$ chimeric VLPs and capsomeres. Both constructs induced robust proliferation, confirming that the inserted epitope was able to be processed using the MHC class I pathway and properly presented to the transgenic T cells. Whilst the processing pathway was not determined, it is likely that immature DCs from the naive mouse spleen, have taken up the VLPs as a result of their size[193], become activated as a result of their self-adjuvanting highly ordered repetitive array[127,130], and by cross-presentation[195] have displayed the epitope recognised by CS-TCR cells. Capsomeres do not possess the same size and structural characteristics as VLPs[165,166] and have been shown to require the inclusion of adjuvants to enhance antibody generation[170,173] and to enhance cellular responses[179] to levels equivalent to that induced by VLPs. However, this adjuvant requirement is not universal with one study showing non-adjuvanted HPV L1 capsomeres to be potent CTL inducers[169]. The results with MuPyV VLPs and capsomeres (Figure 8) indicate that whilst both platforms resulted in CS-TCR proliferation at similar levels, the capsomere induced response commenced earlier. This may be a result of the fact that capsomeres have triple the amount of the $CD8_{280-288}$ epitope within the VP1 protein, or due to the location of the epitopes at both terminal regions as well as S4 loop in capsomeres, as opposed to the VLPs with a single insertion at the S4 loop. These insertion sites have been standard for the MuPyV VLP and capsomere constructs used in other

models[170,173,188]. There is no *Py*CSP $CD4^+$ T cell equivalent model to assess the $CD4_{59\text{-}79}$ VLP or capsomere constructs.

Cellular immune responses induced by immunisations with chimeric VLPs or capsomeres

The data presented in this chapter obtained from independent experiments have established that immunisations with either $CD8_{280\text{-}288}$ VLP constructs alone, or as pooled VLPs were able to induce moderate levels of IFN-γ production by $CD8^+$ T cells. This antigen-specific recognition confirms that the CD8 chimeric VLP had been presented post-immunisation to naive $CD8^+$ T cells, and that this presentation was via MHC class I molecules[195]. These results are consistent with previous studies reporting chimeric VLPs with a single CD8 epitope induced CTL activity mediated by $CD8^+$ T cells[155,214]. Data from intracellular cytokine staining assays have shown a maximum mean frequency of $CD8^+$ T cells expressing IFN-γ to be 0.59% when mice were immunised with pooled VLPs using 30 µg of each construct (Figure 17) which may have been insufficient for protection[210]. There was no evidence to support any additive or synergistic effects on $CD8^+$ T cell antigen-specific stimulation when VLPs were administered as a pool with the $CD4_{59\text{-}79}$ VLP.

In the studies reported in this chapter, both chimeric capsomeres and VLPs were able to induce antigen-specific IFN-γ responses upon restimulation with the $CD8^+_{280\text{-}288}$ T cell peptide and *Py*CSP transfected cells as evaluated by ELISpot. Capsomeres tended to result in higher magnitude responses which may be a result of higher antigen load per construct, or a result of the positioning of epitopes[155], or due to a reduced anti-carrier effect[176]. Furthermore, the ICS assay confirmed that the bulk of these responses were produced by $CD8^+$ T cells (Figure 24) with a mean $CD8^+$ T cell IFN-γ expressing frequency of only 0.4% with the homologous pooled capsomere regimen. The activation of this population confirms that *in vivo* both platforms are capable of inducing $CD8^+$ T cell responses and the $CD8_{280\text{-}288}$ epitopes must therefore have been processed and displayed on MHC class I molecules.

The *Py*CSP $CD4^+_{59\text{-}79}$ T cell epitope has reportedly been able to induce functional $CD4^+$ T cell populations of either T_H1 or T_H2 phenotype capable of inducing T cell

proliferation responses and helping antibody responses[71]. Experimental data obtained in the studies reported here show that the chimeric *Py*CSP $CD4_{59-79}$ VLPs could induce only very weak epitope-specific cellular responses. However, immunisations with capsomeres presenting the same epitope induced stronger CD4 peptide-specific cellular response detected in the ELISpot assay (Figure 22). In contrast, the response of mice immunised with pooled peptides adjuvanted with polyIC were robust. This may be a dose related effect with peptide immunisations including 30 µg of the $CD4_{59-79}$ peptide, whilst the epitope component in chimeric VLPs and capsomeres was only 0.52 µg and 1.77 µg respectively per dose. It is not feasible to increase the VLP dose to nearly 600 µg which would be required to give a 30 µg epitope equivalent dose. There was little immunological benefit obtained by inclusion of the $CD4_{59-79}$ chimeric capsomere or VLP with the pooled immunisations. It may have been beneficial to immunise mice with $CD8_{280-288}$ VLPs combined with the $CD4_{59-79}$ peptide in adjuvant which induced epitope-specific robust responses.

The carrier MuPyV VP1 protein is likely to contain $CD4^+$ T helper epitopes similar to those in the HBV core protein[152,202], however, those would provide no immunological assistance when challenged by the *Plasmodium* parasite. For this reason, mice were immunised with pooled VLPs including the $CD4_{59-79}$ VLP, aiming to induce a synergistic $CD8^+$ T cell response by providing $CD4^+$ T cell help for optimal $CD8^+$ T cell effector activity. Data from immunogenicity assays did not show any synergistic or additive responses provided by the CD4 helper epitope after restimulation with the $CD8_{280-288}$ peptide or transfected cells. This is likely to be due to the poor induction of $CD4^+$ T cell responses by VLPs and capsomeres. Further, increasing the dose from 10 µg to 30 µg per construct in the pooled VLP groups had minimal effect on antigen-specific cellular responses.

Determination of the appropriate dose for the VLP and capsomere experiments relied on earlier experimental data (sections 3.4.3 and 3.4.4) as well as the fact that current licensed VLP vaccines contain between 10 to 40 µg of each construct per dose[137,142-145]. Various doses have been utilised in mice experiments. In one study, high doses of 100 µg did not significantly improve vaccine effectiveness over a 20 µg dose[307], but in another 40 µg was significantly better than 8 µg[155], although each of these used different carrier VLPs. In a study using MuPyV VLPs with intranasal

administration, the optimal dose was for IFN-γ responses was 16.6 µg with only a slight decrease with a 5.55 µg dose, whereas an increased dose of 50 µg resulted in a greater than 10-fold decrease[217]

3.5.3. Antibody responses

It is well established that VLPs are very effective at inducing antigen-specific antibody responses (reviewed in[130]) perhaps due to their ability cross-link B cell surface receptors[308] acting in a T cell independent manner[309,310]. Previous studies using chimeric capsomeres with adjuvants, have shown that platform to also be strong inducers of antibodies directed against inserted antigens[170,173,188]. Herein it was shown that VLPs induced high IgG titres against the *Py*CSP B cell epitope. These antibody titres increased following successive doses indicative of the generation of both memory and plasma B cell responses which in turn suggests the involvement of T helper cells[311]. These T helper epitopes may be carrier related, as titres in pooled VLPs were similar to B cell VLP only immunisations. Importantly, at least two doses were required for each platform to achieve high IgG titres, with a third also beneficial. A single dose was ineffective. This is consistent with other studies[170,175,217,219] as well as the requirement for three immunisations with licensed VLP vaccines[125].

Capsomere immunisations resulted in IgG titres which were significantly less than VLPs with and without polyIC (Figure 25). The reduced efficacy of capsomeres relative to VLPs is inconsistent with other studies[170,173], and is likely a result of the adjuvant choice with previous studies using alhydrogel known to be a strong inducer of antibodies[170,173]. PolyIC, however, is known to be an effective adjuvant skewing towards a Th1 response, enhancing T cell responses[221,312,313]. Isotype analysis showed that capsomeres generated an IgG_1 response but not an IgG_3 response which was induced with VLPs with and without adjuvant, or an IgG2a and $IgG2_b$ response induced by VLPs with polyIC (Figure 26). The inclusion of polyIC increased titres consistent with previous studies with VLPs with a skewed T_H1 isotype profile[221].

The IgG_3 antibody isotype reported here with VLP immunisations contrasts with results observed using Group A Streptococcus J8 peptide antigen chimeric VLPs

and capsomeres where IgG_1 was the dominant IgG isotype and no IgG_3 was detected[173]. It would appear therefore, that the development of IgG_3 is related to the chimeric epitope presented in the VLP structure rather than to the platform itself. In the first series of experiments (section 3.4.3), mice immunised with three doses of homologous chimeric B cell VLPs had a similar IgG_3 responses to those receiving pooled VLPs. This established that it wasn't the inclusion of the $CD8^+_{280-288}$ or $CD4^+_{59-79}$ T cell epitopes in pooled chimeric VLP immunisations that were responsible for the IgG_3 subclass. We speculate that the IgG_3 response present in mice immunised with VLPs but not capsomeres, may be related to APC uptake and induced activation status. IgG_3 antibodies have previously been identified as important for protection against various pathogens[314,315] including *Plasmodium* parasites[300] and IgG_3 monoclonal antibodies raised against the *Py*CSP repeat (QGPGAP) have previously protected BALB/c mice from a *P. yoelii* 17XNL sporozoite challenge[63].

Antibodies generated by each platform were capable of recognising the B cell repeat epitope, as well as recombinant *Py*CSP protein as shown by ELISA, and the native parasite as shown by IFAT against sporozoites. This shows that the confirmation of the epitope was on the VLP was similar to that presented in the context of the native protein.

3.5.4. Impact of adjuvant

All licensed human VLP based vaccines are administered with aluminium containing adjuvants[125]. The effect of formulating VLPs with adjuvant has been contradictory with reports that adjuvants are beneficial[316,317] essential[216] or not necessary[161,188,215]. In the case of capsomeres, adjuvant inclusion appears to be essential, at least for antibody induction[170,173,308]. To assess adjuvant enhancement of VLPs in this study, one group was immunised with VLPs which were co-administered with polyIC. PolyIC is a synthetic double-stranded RNA adjuvant which targets TLR3 and has previously been used to enhance antibody responses but particularly T_H1 T cell immune responses in other vaccine platforms[294,295,297,312]. In our studies, we saw a general increase in cellular immune responses when VLPs were co-administered with polyIC, however, these were not statistically significant. However, polyIC

inclusion resulted in higher antibody titres and included both IgG_{2a} and IgG_{2b} isotypes which were not detected in VLP without adjuvant or capsomere regimens.

3.5.5. Impact of a heterologous prime/boost regimen

Plasmid DNA encoding *Py*CSP is immunogenic in mice and is capable of inducing sterile protection in BALB/c mice from a low dose sporozoite challenge[76]. However, several studies have shown that plasmid DNA as a homologous delivery platform, does not provide complete protection against sporozoite challenge in the murine model[76,318,319]. However, when incorporated in a heterologous prime/boost regimen, there are many examples of enhanced immunogenicity and protection with DNA prime-boost regimens using various antigen delivery systems encoding the same antigen or epitope[93,320-324] including VLPs[325] as a boost immunogen. Our data show that a heterologous prime-boost regimen with either a VLP or a capsomere boost was better at inducing cellular responses than the homologous counterpart, achieving levels similar to that induced by plasmid DNA alone. The DNA prime/VLP with polyIC boost consistently induced the highest cellular immune responses, however, these responses were not significantly better than those induced using the homologous DNA regimen. The prime-boost gain in induced cellular responses was, however, countered by a decrease in antibody titres. In the homologous VLP regimen, antibody titres were low after the first dose but were increased with subsequent boosts. Therefore a heterologous regimen involving a DNA prime followed by multiple VLP boosts would likely result in higher antibody responses and maintain robust T cell activity. A second VLP boost may also result in significant enhancement of IFN-γ responses as seen in a previous study[217].

3.5.6. VLP and capsomere induced protective efficacy

Following sporozoite inoculation from an infected mosquito, or by i.v. challenge, the sporozoite tracks to the liver where it invades hepatocytes. During a murine infection with *P. yoelii*, the parasite replicates within the hepatocyte and merozoites are subsequently released into the circulation after a minimum of 46 hours[326]. Livers were harvested from mice 42 hours post challenge (section 2.10.3.2) to enable maximal opportunity for protective immune responses to clear infected cells, whilst

ensuring that the parasites had not left the liver. This published protocol produces a reliable quantitative measure of the degree of infection, and hence the degree of protection afforded by immunisations[286]. Infections were not allowed to progress to the blood stage as the *Py*CSP antigens incorporated with the VLP and capsomere constructs would not be effective due to the non-expression of CSP during that phase of the *Plasmodium* life-cycle[59,60].

Despite the levels of cellular and antibody responses generated by mice within the various VLP and capsomere immunisation groups, both platforms had a poor capacity to confer protection against sporozoite challenge. Liver-stage protection has previously been achieved by adoptively transferring a $CD8^{+}_{280\text{-}288}$ T cell clone[299], or by passive transfer of monoclonal antibodies specific to the *Py*CSP central repeat[63]. These protective antigenic epitopes were incorporated within capsomere and VLP chimeras, and did generate epitope-specific cellular and antibody responses. In studies reported herein, the immunological data supports the potential of VLPs to protect, the failure to protect suggests the magnitude of VLP or capsomere induced responses were insufficient to reach a protective threshold[301]. This is consistent with other studies where protection correlated with the number of adoptively transferred clonal $CD8^{+}_{280\text{-}288}$ T cells where sterile protection was achieved with 20×10^{6} cells[73], or with the number of memory $CD8^{+}$ T cells stimulated by immunisations[210,301], or with the amount of passive transferred monoclonal antibodies[63].

3.6. Conclusion

Studies reported in this chapter confirmed that the MuPyV chimeric VLP and capsomere platforms were capable of inducing antigen-specific antibody responses, and established for the first time in this model, their capacity to induce cellular immune responses. IFN-γ readouts showed that both capsomeres and VLPs induced a similar and moderate level of $CD8^{+}$ T cell responses, although these responses were not as robust as those induced by plasmid DNA. In contrast, $CD4^{+}$ T cell responses induced by VLP immunisations were very low, whereas capsomere immunisations were modest perhaps as a result of increased epitope concentrations or positional changes within the capsomere. High levels of antibody responses were generated by immunisations with VLPs with a lower antibody response induced by

capsomeres; these responses were markedly better than those induced by plasmid DNA alone. The prime/boost regimen incorporating the benefits of each platform, produced a broad cellular and antibody; data suggest that this would be further enhanced with the inclusion of a second VLP or capsomere boost to raise antibody titres. These data support expanding evaluation of VLP and capsomere platforms into a wider range of liver-stage *Plasmodium* antigens targeted by a T cell response. In this study only a narrow range of antigenic targets were assessed against a complex pathogen with a multi-staged lifecycle an over 5300 putative proteins[53]. Previous studies have suggested that multiple antigen targets may be required for protection from *Plasmodium* challenge[111,121,327]. With approximately 2000 active genes, and 816 identified proteins present during *Plasmodium* liver-stage of infection[328] there are an extensive range of targets which could be assessed. However, it would be appropriate to first evaluate alternative epitope insertion sites within the MuPyV VP1 protein in order to determine if other sites allow for increased protein stability and enable high expression of soluble proteins, and further to evaluate site-specific immune responses. In the studies reported herein, VLP and capsomeres were administered by s.c. injections. Different routes of administration of VLPs[329] and other platforms has been shown to alter immunological[329,330] and protective outcomes[330] and should also be considered in future studies.

Chapter 4: Development of the minicell platform

4.1. Introduction

Although bacterial minicells were first reported in the 1930s, it was not until 1966 when minicells were purified from a mutated strain of *E. coli* that their research potential was realised[225,226]. Minicells are spherical cell-like structures and are comprised of the bacterial cell wall and cytoplasm components of the bacteria[222,225]. They are enzymatically active, but contain no chromosomal DNA so they are unable to replicate[222,226]. Minicells can however, contain plasmid DNA, and have the required machinery to produce plasmid-encoded proteins[223,224,233,234]. Minicells form as a result of the incorrect placement of the bacterial septum during cell division caused by either disruptions to the minCDE genes or over-expression of the FtsZ gene[230-232].

In my studies, the proposed use for minicells as a vaccine delivery platform was to deliver recombinant protein antigens and plasmid DNA for mammalian expression of the target antigen, and target the minicells to DCs using BsAbs. The *E. coli* mutant minicell producing strains P678-54[222], DS410[278] and VIP205[232], each derived from the K12 strain, were obtained for the purpose of this study (section 2.1). P678-54 was the original mutant strain produced by Adler and colleagues[222], and the DS410 strain was derived from P678-54 after mating it with the Hfr donor CSH74[278]. Both strains constitutively produce minicells. The VIP205 strain was derived by uncoupling the FtsZ gene from the natural promoter and placing it under the control of a *tac* promoter in order to control FtsZ protein expression with IPTG[232]. In this case IPTG supplementation was required for normal cell division but increasing IPTG resulted in over-expression of FtsZ protein and minicell formation[232].

The originally published minicell purification protocol overlayed a concentrated culture on a continuous sucrose gradient resulting in one normal-sized bacteria per 10^3 to 10^4 minicells[222]. Whilst numerous methods have since been utilised[225,227,236,331-334], most use a combination of differential low and high force

centrifugation, followed by density gradient centrifugation using a linear sucrose gradient, as described by Frazer and Curtiss[225]. This method does not remove all contaminating bacteria with approximately 1 bacteria per 10^5 to 10^6 minicells reported[335,336]. Whilst this may be satisfactory for genetic or functional analyses, it is not acceptable for parenteral administration to animals. Giacalone *et al.*[236,237] modified the standard purification procedure to include treatment with ciprofloxacin which reduced contamination to between 1.5 and 2.0 parent bacteria per 10^8 minicells. Subsequently MacDiarmid *et al.*[227] described a minicell purification method incorporating differential and density gradient centrifugation with various filtration steps, salt induced elongation and antibiotic treatments, removing all viable bacteria.

Some *in vitro* studies have shown that phagocytic cells (but not non-phagocytic cells) including macrophages and DCs are capable of internalising minicells[227,236], however, the efficiency of uptake by those cells as determined by expression of plasmid-encoded proteins was only between 0.02 and 0.2%[236]. Efficient receptor mediated endocytosis in non-phagocytic cells was, however, observed when minicells were targeted to cell receptors including integrins on Cos-7 cells[235] and the epidermal growth factor receptor (EGFR) on human cancer cells[227]. In the latter study, targeting was achieved using Fc receptor cross-linked monoclonal antibodies to EGFR and the O-antigen on the minicell surface[227].

The advantage of targeting delivery of antigens to particular cells is to increase up-take and reduce dose requirements. There have been many studies showing that antigens targeted to various DC receptors can enhance cellular and antibody immune responses (reviewed in[337,338]). Most studies have focused on the DEC205 endocytic receptor, however, there has been recent interest in targeting the C-type lectin Clec9a receptor with studies showing potent induction of $CD4^+$ T cell responses[339], and high antibody titres without the requirement of DC stimulants[340]. Antigens targeted to either DEC205 or Clec9a can induce $CD8^+$ T cell responses and CTL activity if administered with adjuvants for DC activation including LPS and polyIC[339].

The minicell OM contains a large amount of LPS which in itself acts as a TLR4 agonist[341] likely to activate DCs. However, LPS causes endotoxic shock when sepsis

occurs, and as such it is important that no viable bacteria are administered in minicell immunisations. To address safety concerns over the administration of minicells, safety studies have been conducted on pigs and showed only minor inflammatory responses and fever which were diminished by 4 h and 2 h respectively[227]. Furthermore, studies on mice and dogs have not reported any signs of illness following doses of up to 10^{10} minicells with multiple immunisations[227,236-238]. Importantly, EnGeneIC Ltd (Sydney, Australia) reports that a first-in-man phase I clinical trial has recently been completed showing an excellent safety profile for minicells (http://www.engeneic.com/profile.html accessed 8 July 2014).

4.2. Materials and Methods

4.2.1. Mice

All animal work for the minicell platform used specific pathogen-free female BALB/c mice aged 6-8 weeks, purchased from the Animal Resource Centre (Perth, Australia).

4.2.2. Minicell producing *E. coli* strains

Minicell producing *E. coli* strains VIP205[222] and DS410[278] were a gift from Dr Miguel Vicente, Spanish National Biotechnology Centre, Spain. The *E. coli* P678-54 strain[232] was a gift from Dr Judya Praszkier, University of Melbourne.

4.2.3. Vectors

Table 7: Vectors used in the minicell platform

Name	Expression	Antibiotic selection	Protein tag	Comments and source
pVR1020	Mammalian	Kanamycin	Nil	Empty vector, Vical Inc.
modVR1020	Mammalian	Kanamycin	Nil	Empty vector pVR1020 with additional restriction sites in MCS, introduced by Dr. Don Gardiner, QIMR (unpublished)

pIASO	Mammalian	Chloramphenicol	V5	Mod VR1020 modified to be chloramphenicol resistant and includes a V5 epitope (section 4.2.9.1)
pVRV5	Mammalian	Kanamycin	V5	ModVR1020 modified to include a V5 epitope (section 4.2.9.2)
pBAD/Myc-His A	Bacterial	Ampicillin	c-Myc + His	Protein expression induced by addition of L-arabinose, Invitrogen
pTrcHis2A	Bacterial	Ampicillin	c-Myc + His	Protein expression induced by addition of IPTG, Invitrogen
pDual GC	Bacterial and mammalian	Kanamycin	c-myc + His	Dual expression vector, bacterial expression induced by IPTG, Stratagene, La Jolla, CA, USA

4.2.4. Plasmid construction for minicell platform

All plasmid constructs were made using standard molecular cloning techniques as described above (section 2.6). Each insert was confirmed by sequencing.

4.2.5. Molecular cloning of constructs

Plasmid DNA constructs were generated using standard molecular cloning techniques as described in (section 2.6). The *Py*CSP and *Py*AMA-1 genes were PCR amplified from pVR2516 or *P. yoelii* 17XNL genomic DNA respectively (section 2.6.2) and cloned into the pBAD/Myc-His A, pTrcHis2A, pIASO and pVRV5 vectors. Chicken ovalbumin cDNA and a fusion gene Tfr-Ova^{280} were PCR amplified from plasmid DNA (section 2.6.2) and cloned into the pDual GC vector. GFP was amplified from plasmid DNA and cloned into pBAD/Myc-His A, pTrcHis2A, and pDual GC vectors. Finally, RFP was PCR amplified from plasmid DNA and cloned into pIASO and pVRV5 vectors.

4.2.5.1. Bacterial expression plasmids

For the minicell platform, genes encoding *PyCSP*, *Py*AMA-1, and green fluorescent protein (GFP) were separately inserted into the vectors pBAD/Myc His 2A and pTrc

His 2a both from Invitrogen (Table 7) For recombinant protein expression using the Rapid Translation System (RTS; 5 Prime GmbH, Hamburg, Germany) (section 4.2.6) both *Py*CSP and *Py*AMA-1 genes were separately inserted into pIVEX-HIS/HA[279].

4.2.5.2. Mammalian expression plasmids

The genes encoding *Py*CSP, *Py*AMA-1 and a red fluorescent protein (RFP) were separately inserted into the pIASO and pVRV5 vectors (section 4.2.9.2).

4.2.5.3. Dual expression plasmids

The pDual GC vector (Table 3) has a single insertion site using restriction enzyme *Eam*1 104, also recognised by the *Ear*I restriction enzyme. This restriction site was also present in the ovalbumin and tfr-ovalbumin genes. Following the manufacturer's guidelines, in gene PCR reactions, dCTP was replaced by 5-methyl-dCTP (NEB). All other cloning techniques were as earlier described (section 2.6). Cloning was done in Omnimax 2T1 bacteria which are suitable to highly methylated DNA transformations. GFP, which did not have any internal *Eam*1 1011 restriction sites, was inserted into pDual GC using standard techniques.

4.2.6. *Py*AMA-1 protein expression and purification

The vector pIVEX-HIS 3.2 vector (Roche Applied Science, Castle Hill, NSW) was previously modified so that the expressed protein would include a C-terminal HA tag (pIVEX HIS/HA[279]). The *Py*AMA-1 gene was ligated into the pIVEX-HIS/HA vector then recombinant protein expression utilised the RTS 100 *E. coli* HY kit (5 Prime GmbH, Hamburg, Germany) which is a cell-free protein system using *E. coli* lysate. Following the manufacturer's protocol, 50 µl reactions were incubated for 6 h at 25°C and 500 RPM in an Eppendorf thermomixer (Eppendorf, NSW, Australia).

The recombinant *Py*AMA-1 was purified using 1 ml of cobalt Talon resin (Clontech Laboratories Inc., Mountain View, CA). The Talon resin was equilibrated in Talon wash buffer (Appendix A) with 8 M urea. The RTS products were pooled and diluted in the wash buffer with 8 M urea which was then added to the resin and incubated for

20 min at 4°C. The resin was then transferred into an Econo-Pac chromatography column (BioRad, CA, USA) and washed twice in wash buffer. To remove endotoxin, the column was washed using 10 column volumes of wash buffer including 0.1% Triton X-114 at 4°C, then washed with 20 column volumes of wash buffer. The protein was then eluted using Talon wash buffer with imidizole increased to 150 mM. The elution buffer was then exchanged with PBS by doing three washes using a 4 ml 10K Amicon ultra filtration tube (Merck Millipore, Billerica, MA). The tubes were centrifuged (4000 x *g*, 15 min) with 4 ml of PBS added after each spin. Finally the concentrated protein was diluted in 420 µl of PBS. Protein concentration was then measured using a nanodrop spectrometer (Thermo Fischer Scientific) and further characterised by western blot using antibodies against the histidine tag.

4.2.7. Optimisation of minicell culturing conditions

4.2.7.1. General incubation conditions

Unless otherwise stated, all incubations were performed at 37°C with shaking of liquid cultures at 220 RPM. All media was supplemented with either ampicillin (60 µg/ml), kanamycin (50 µg/ml), or chloramphenicol (34 µg/ml) alone or in combination, as appropriate for selection of transformants.

4.2.7.2. Incubation conditions for E. coli VIP205

E. coli VIP205 contains the FtsZ gene in the bacterial genome which is under the control of the bacterial P*tac lacI*^{q} expression system[232]. As a result, IPTG is required for FtsZ gene expression required for binary fission, and excessive IPTG results in over-expression of the FtsZ gene resulting in the formation of minicells. For regular growth conditions, the media was supplemented with kanamycin (50 µg/ml) and IPTG (10 µM). For the formation of minicells, the concentration of IPTG was increased to 30 µM. This strain is resistant to kanamycin.

4.2.7.3. Single and dual transformations

Each minicell producing *E. coli* strain was made competent using protocols standard for traditional cloning as previously described (Section 2.6.1). Competent bacteria were transformed with bacterial expression plasmids or dual transformed with bacterial and mammalian expression plasmids (section 4.2.3). In some cases, a two-step procedure was adopted where bacteria were transformed with a single plasmid, returned to a competent state, and then transformed with the second plasmid.

Green fluorescent protein (GFP) was used as a model for protein production. GFP plasmids in pBAD, pTRCHis2A and pDUAL GC (Table 7) were used as single transformants, or coupled with pIASO or pVRV5 plasmids with red fluorescent protein (RFP) as double transformants. Transformed colonies isolated on agar plates with appropriate antibiotic selection were used to inoculate starter cultures which were incubated overnight in LB media with selection antibiotics. These were subsequently used to inoculate LB media and the bacterial culture grown until the OD_{600} was approximately 0.5. Cultures were then induced to express GFP using either L-arabinose (Sigma-Aldrich, MO, USA) or IPTG (Promega, WI, USA) at various concentrations and incubated at either 26°C or 37°C and 220 RPM to investigate optimal culture conditions for protein expression. Culture samples were taken before and at various time-points after induction and snap frozen on dry ice. These samples were centrifuged (4000 x *g*, 5 min) and resuspended in PBS then analysed by flow cytometry to assess the percentage of GFP expressing bacteria as well as the GFP median fluorescence intensity.

4.2.7.4. Growth media

To assess the influence of culture media on protein and minicell yield, pDual GC-GFP transformed minicell producing *E. coli* were grown in LB, TB, 2YT or BHI media. A transformed colony isolate was vortexed in LB and then used to inoculate each type of media to generate a starter culture. This starter culture was incubated overnight then used to inoculate media (the same media as the starter culture) and the bacterial culture grown until the OD_{600} was approximately 0.5. Cultures were then induced with a titration of IPTG at 0, 0.2, 0.5 and 1 mM, and incubated overnight.

OD_{600} was determined and the median fluorescence intensity of GFP measured using flow cytometry with minicells gated on forward and side scatter. Minicells were purified by differential centrifugation followed by an OptiPrep density gradient centrifugation (section 4.2.8) then visualised using the EVOS microscope (Advanced Microscopy Group, USA) using the x 40 objective and either bright-field or GFP fluorescence settings. Minicells were quantified based on the OD_{600} (section 4.2.8).

4.2.7.5. Temperature conditions

The effect of incubation temperature on protein yield was assessed using five colonies from DS410 and P678-54 strains either single or dual transformed with pTrcHis2A-GFP and pVRV5-RFP. Starter cultures were grown until reaching an OD_{600} ~ 0.5. Cultures were then induced with 0.5 mM IPTG and incubated overnight at 26 or 37°C. The percentage of bacteria expressing GFP and the median fluorescence intensity (MFI) of GFP was determined by flow cytometry as described above.

In a separate experiment, a colony of DS410 transformed with pDUAL GC-OVA was used to inoculate 4 L of LB broth which was incubated until OD_{600} ~ 0.5. Half of the culture was then cooled in tap water for 10 min with mixing and then induced with 0.5 mM IPTG and incubated overnight at 26°C and 200 RPM. The other half was maintained at 37°C and induced with 0.5 mM IPTG and incubated overnight at 200 RPM. Minicells were then purified as described in section 4.2.8, and the amount of minicells was quantified for each condition. Purified minicells were used for a western blot (section 2.8) using anti-His peroxidase (Roche Diagnostics, Germany) and developed using Amersham ECL Prime western blot detection reagent (GE Healthcare, PA, USA). A serial dilution of maltose binding protein (MBP, 42.5 kDa) with a histidine tag was run in adjoining lanes to quantify the expressed OVA protein in minicells.

4.2.8. Minicell purification

For large-scale cultivation prior to purification, transformed *E. coli* DS410 were used to make starter cultures which were in-turn used to inoculate 400 ml of LB in 1 L

bottles. Cultures were incubated at 37°C and 200 RPM until an OD_{600}~0.5 was reached, at which time IPTG [0.5 mM] was added, and the incubations continued overnight.

Cultures were cooled to 4°C and then centrifuged (1500 x *g*, 15 min, 4°C) in 1L centrifuge bottles using a JLA 8-1000 rotor (Beckman Coulter, CA, USA). The supernatant was harvested and then re-centrifuged (15000 x *g*, 45 min, 4°C). The pellets were resuspended in working media (150 mM NaCl + 30 mM Tris-HCl + 3 mM EDTA in milliQ water) at 10 ml per L of culture. A discontinuous 5-25% OptiPrep™ gradient was prepared in 50 ml polycarbonate screw cap centrifuge bottles, using the OptiPrep™ density gradient medium (Axis-Shield, Oslo, Norway) in diluent media (150 mM NaCl + 10 mM Tris-HCl + 1 mM EDTA in milliQ water). Six ml of the resuspended pellet was then layered on top of the discontinuous OptiPrep™ gradient and centrifuged (1500 x *g*, 45 min, 4°C) in a JS-13.1 swinging bucket rotor (Beckman Coulter) with slow acceleration and no brake. Minicells were detected by microscopic examination in the 5% to 10% OptiPrep™ bands. These layers were harvested, diluted in working media and then centrifuged (15000 x *g*, 15 min, 4°C) in the JS-13.1 rotor to pellet. Media used during centrifugation was kept chilled.

Pellets were resuspended in 10 ml of LB broth with selection antibiotics and 0.5 mM IPTG, and then incubated for 1 h at 37°C and 200 RPM. The NaCl concentration was then increased to 0.8 M and cultures incubated for a further 3 h. To kill remaining parent bacteria, the cultures were treated with gentamycin (200 µg/ml) and chloramphenicol (34 µg/ml), followed by a further 3 h incubation.

The cultures were then diluted in working media and centrifuged (15000 x *g*, 15 min, 4°C). Pellets were resuspended in working media at 6 ml per L of original culture and then layered on top of a density gradient and centrifuged as described above. The minicell layers were harvested then diluted in working media and centrifuged (15000 x *g*, 15 min, 4°C). The pellet was resuspended in saline with 100 mM D-trehalose (Sigma-Aldrich, USA) as a lyoprotectant at 5 ml per L of culture.

The quantification of minicells was calculated using the formula [235]

$$Number\ of\ minicells\ per\ ml = OD_{600}\ x\ 5.0\ x\ 10^{10}$$

To confirm the absence of viable parent bacteria, 10^{10} minicells were spread onto an antibiotic free agar plate and incubated overnight at 37°C. Minicells were frozen at -70°C then freeze-dried and stored at -70°C.

4.2.9. Vector construction

4.2.9.1. Construction of pIASO

The designed minicell platform required bacteria to transformed with a mammalian expression vector. It was intended to use the modVR1020 (D. Gardiner, unpublished) which is a modified version of the pVR1020 (Vical Inc., CA, USA) vector which has kanamycin as a selection marker (Table 3). However, the minicell producing *E. coli* VIP205 is resistant to kanamycin, making the strain incompatible with the vector. It was therefore necessary to modify the vector by changing the antibiotic resistance gene. The kanamycin resistance gene was not flanked with restriction sites so the antibiotic resistance genes could not be simply digested and ligated. Instead a multi-staged reconstruction was required, as depicted (Figure 30).

For the purpose of adding restriction sites which flank the antibiotic resistance gene, primers were designed to PCR amplify regions A and C from modVR1020 with each primer including either vector-specific *Spe*I or *Bgl*II restriction sites or new restriction sites *Apa*I or *Mfe*I (Appendix D). Also primers including *Apa*I or *Mfe*I (Appendix D) were used to PCR amplify the region $B_{(2)}$ chloramphenicol resistance gene from a Gateway entry vector (Invitrogen).

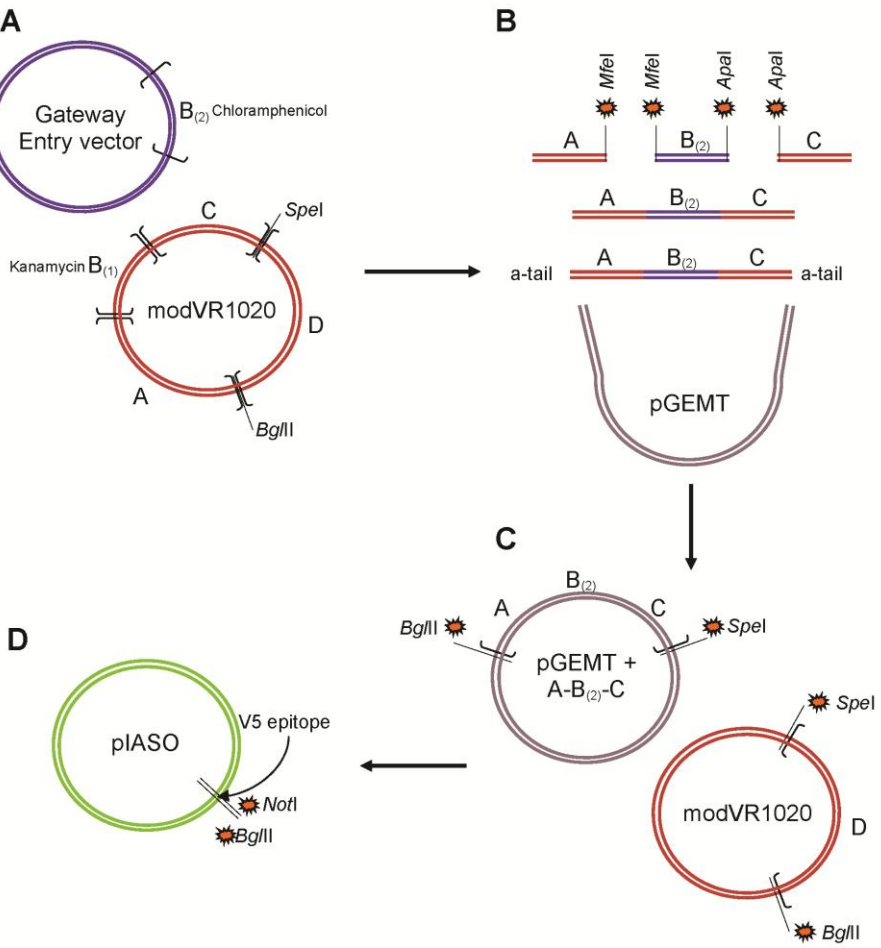

Figure 30: Schematic following the construction of the pIASO vector. (A) Regions A, $B_{(2)}$ and C were PCR amplified using primers designed to introduce restriction sites *Mfe*I and *Apa*I. (B) The purified PCR products were digested with *Mfe*I and *Apa*I restriction enzymes and ligated with T4 DNA ligase. The ligation mix was used as a PCR template for amplification of the ligated product. The purified PCR was then A-tailed and ligated into the pGEMT vector. (C) The pGEMT A+$B_{(2)}$+C was purified following clonal expansion, then this vector and modVR1020 was digested with *Spe*I and *Bgl*II restriction enzymes. The combined A, $B_{(2)}$ and C was ligated to region D using T4 DNA ligase. (D) The vector was digested using *Bgl*II and *Not*I restriction enzymes and the annealed V5 oligonucleotides were ligated into the vector using T4 DNA ligase. The resulting vector was chloramphenicol resistant and has the V5 epitope at the c-terminal of the multiple cloning site.

Each region was PCR amplified, using a standard 50 µl PCR mix (section 2.6.2) using 1 µl of 10 µM forward and reverse primers corresponding to region (Appendix D). PCR reactions followed the standard protocol (section 2.6.2) using 30 cycles with a 50°C annealing temperature and a 2 min extension. PCR products were loaded into a 0.8% agarose gel and separated by electrophoresis. Bands of the appropriate size (region A 1880 bases, region $B_{(2)}$ 680 bases, region C 654 bases) were excised

and purified using the QIAquick gel extraction kit (Qiagen, Valencia, CA, USA) following the manufacturer's protocol with DNA eluted in water. PCR products from each region (Figure 30) were then digested using restriction enzymes specific to both primer-encoded palindromes using 10 µl reactions, incubated for 4 h at 37°C. Products were separated by electrophoresis and DNA bands extracted as previously described. Regions A, $B_{(2)}$ and C were then combined in a 25 µl ligation mix (section 2.6.3.3) with 400 ng of each digested product and incubated overnight at 16°C. This ligation mix was then used as a template for a PCR reaction combining all three regions from *Spe*I to *Bgl*II into a single length of DNA at 2850 bases. This PCR product was excised from an agarose gel as described above.

The A, $B_{(2)}$ and C combined product was then A-tailed and ligated into the intermediate pGEMT vector (Promega Corporation, USA), following the manufacturer's protocol. Ligated product was then transformed into chemically competent *E. coli* DH5α by heat shock (section 2.6.3.4) and incubated overnight on LB agar plates with 60 µg/ml of ampicillin with IPTG and x-gal for blue/white insert screening. White colonies were screened by colony PCR (section 2.6.3.5) to confirm the presence of inserts. A selected PCR positive colony was incubated overnight in LB broth with ampicillin then plasmid DNA extracted (section 2.6.3.6).

The pGEMT-$AB_{(2)}$C and modVR1020 vectors were then digested with both *Spe*I and *Bgl*II restriction enzymes (section 2.6.3.2) then excised from an agarose gel as described above. A ligation reaction (section 2.6.3.3) in a 6:1 ratio (modVR1020 region D:$AB_{(2)}$C) was transformed into *E. coli* DH5α (section 2.6.3.4) then incubated overnight on LB agar plates with 25 µg/ml chloramphenicol. Colony PCR on isolates was used to confirmed the presence of the $B_{(2)}$ chloramphenicol resistance gene.

Complimentary primers were designed to encode the V5 epitope and to have overhanging *Not*I (5') and *Bgl*II (3') regions complimentary to *Bgl*II and *Not*I digested DNA for direct ligation. These primers were annealed by combining 1 µl of each at 10 mM, with18 µl of water in a PCR tube. Samples were heated to 94°C and then cooled by 1°C/min to 20°C. Purified chloramphenicol resistant modVR1020 was digested with *Bgl*II and *Not*I restriction enzymes and gel extracted. The insert was ligated into the vector (section 2.6.3.3) in a 6:1 ratio (V5 insert:vector) and then

transformed into *E. coli* DH5α (section 2.6.3.4) then incubated overnight on LB agar plates with 25 µg/ml chloramphenicol. Colony PCR (section 2.6.3.5) confirmed V5 insertion.

To confirm that the vector contained all modifications, the vector was digested using pre-existing *Spe*I and *Bgl*II and newly inserted *Apa*I or *Mfe*I. Fragment lengths were then determined by gel electrophoresis. The MCS region was sequenced to confirm restriction sites were intact, and that a single V5 epitope was inserted. This vector was named pIASO.

4.2.9.2. Construction of pVRV5

When using the minicell producing *E. coli* DS410 and P678-54 strains the antibiotic resistance incompatibility as described above with VIP205 was no longer present. It was decided to use the original modVR1020 vector and modify it by inserting the V5 epitope into the C-terminal of the MCS so that host cell produced protein could be identified using anti-V5 antibodies. The V5 epitope was inserted into modVR1020 as described above for the construction of the pIASO vector. The annealed V5 primers were ligated into modVR1020 digested with *Spe*I and *Bgl*II restriction enzymes. All incubations were done in media supplemented with kanamycin and the MCS was sequenced, confirming a single V5 insert. The vector was named pVRV5.

4.2.10. Hybridoma generation

The minicell platform in this study was targeted to DCs using BsAbs. A monoclonal antibody against the surface of the minicells was required for inclusion into the BsAbs, however, a commercial antibody could not be sourced, so a hybridoma was generated. The protocol for hybridoma development was derived from a well established protocol described by Harlow and Lane[342]. Bacterial minicells isolated from cultures of *E. coli* DS410 and *E. coli* P678-54 were injected i.p. into BALB/c mice at a dose of 10^{10} minicells in saline, with three doses at 3 week intervals. The mouse with the highest anti-parent bacterial titre then received 10^{10} minicells diluted in saline, with 100 µl i.v. and 400 µl i.p. injections. Three days later the spleen was aseptically extracted and fused with a cultured mouse myeloma cell line SP2/0.

A single cell suspension was prepared by passing the spleen through a 100 µm cell strainer (BD Falcon) and suspended in 5 ml of serum-free media (SFM) (Invitrogen), then centrifuged (100 x *g*, 5 min, 15°C) and washed 3 times in 5 ml SFM. The fusion protocol required that 1/10th of the cells be myeloma cells. Cultured myeloma cells were counted, pelleted, and resuspended in 10 ml of SFM and washed three times (100 x *g*, 5 min, 15°C), then resuspended in 20 ml SFM. The splenocytes and myeloma cells were combined in a 50 ml tube at a 1:10 ratio and incubated for 5 min in a 37°C water bath, and then centrifuged (100 x *g*, 5 min, 15°C). After removing all supernatant, the tube was gently tapped to loosen the pelleted cells. To achieve cell fusion, 1 ml of pre-warmed (37°C) hybrimax 50% polyethylene glycol (PEG) 1500 MW (Sigma-Aldrich, MO, USA) was slowly added and stirred for 1 min, then stirred for a further minute. SFM was added at 1 ml/min for 2 min with stirring, and then a further 8 ml added over 3 min. SFM was added to a total volume of 45 ml. The cells were centrifuged (90 x *g*, 3 min, 15°C) and resuspended in 40 ml of SFM supplemented with 15% FCS and 1:1000 IL-6 supernatant. The cells were then transferred into four 96-well flat bottom plates at 100 µl per well, and incubated overnight at 37°C and 5% CO_2. For hybridoma selection, cells were cultured with hypoxanthine-aminopterin-thymidine (HAT; Invitrogen) supplemented hybridoma media from the second day. Every three days, 100 µl of well supernatant was replaced with fresh HAT supplemented hybridoma media.

When wells were approximately at 50% confluence, the supernatant was screened to assess the presence of antibodies with affinity to parent bacteria. Cultures of both bacterial strains were incubated with supernatant, washed and resuspended in anti-mouse IgG secondary antibody, and then analysed by flow cytometry. Bacteria were gated on forward and side scatter, and then wells were assayed for the MFI of the secondary antibody fluorochrome. Wells with a high MFI (high affinity) with both strains of bacteria, and good cell growth were then sub-cultured in progressively larger wells and further screened.

Selected wells were then single cell sorted using the FACS Aria (BD Biosciences, USA) into 96-well plates each with HAT supplemented hybridoma media. Following cell growth, supernatant was screened to identify clones producing antibodies to the surface of the bacteria. The optimal wells were screened antibody isotypes using a

mouse immunoglobulin isotyping kit (BD Biosciences, USA) following the manufacturer's protocol. Clones were frozen and stored under liquid nitrogen or cultured for antibody purification (section 4.2.11).

4.2.11. Antibody purification

Hybridomas producing antibodies against the LPS endotoxin core (HB-8298, ATCC, USA), minicells (section 4.2.10) and DEC-205 (NLDC-145 clone) were cultured in tissue culture flasks increasing from 25 cm^2 to 175 cm^2 in hybridoma culture media (Appendix A). Once cells were established in the larger flasks, they were diluted in 1 L of culture media with FCS decreased to 2%. Cell cultures were continued for 3 weeks by which time cells were predominantly dead.

To remove cells and debris, flask contents were centrifuged (300 x *g*, 10 min, 4°C) then the supernatant was filtered using a 0.22 µm bottle-top filter. The filtrate was then stirred at 4°C whilst ammonium sulphate was slowly added adding 350 g per litre of filtrate (55% saturation). Stirring continued for a further 3 h at 4°C allowing time for proteins to precipitate.

After the mixture was centrifuged (10000 x *g*, 20 min, 4°C), the supernatant was discarded and the pellets combined and resuspended in 200 ml of saturate ammonium sulphate diluted to 50% saturation in PBS. This was again centrifuged (10000 x *g*, 20 min, 4°C), and the pellet resuspended in 48 ml of PBS and then dialysed using 12,000 to 14,000 MWCO dialysis tubing (Thermo Fisher Scientific, MA, USA). The tubing was inserted into 2 L of binding buffer (Appendix A) and stirred at 4°C overnight, then for two 4 h periods each in fresh binding buffer. The dialysed protein was removed from the dialysis tubing and diluted with 48 ml of binding buffer then antibodies were purified using a protein G gamma sepharose column (GE Healthcare, PA, USA) and a UV detector (BioRad, CA, USA). All fluids were run at 1 ml per min. The column was pre-equilibrated in binding buffer before loading the dialysed protein. The column was then washed with binding buffer then antibodies were eluted using 0.5 M acetic acid in MilliQ water. Peak fractions were collected and pH neutralised to pH 7.0 by adding Tris-HCl pH 9.0, and then filtered through a 0.22 µm syringe filter. Antibody quantification was done using a nanodrop

2000 (Thermo Fisher Scientific, MA, USA) detecting UV_{280nm} absorbance. Aliquots were stored at 4°C.

4.2.12. Bi-specific antibodies

4.2.12.1. Formation of bi-specific antibodies

The formation of bi-specific antibodies (BsAbs) using protein A/G has been previously described[227], however, the protocol was modified as follows. BsAbs were formed by coupling the Fc regions of antibodies using Pierce recombinant protein A/G (Thermo Scientific, IL, USA) in a 9:9:1 ratio. Into a 1.5 ml Eppendorf tube, 27 µg of α-minicell and 27 µg of either anti-DEC205 or anti-Clec9a antibody was added and mixed, followed by 3 µg of protein A/G. The mix was diluted by adding 200 µl of saline, and then incubated overnight at 4°C on a rocker.

4.2.12.2. Coupling bi-specific antibodies to minicells

Lyophilised minicells (5×10^{10}) were resuspended in 250 µl of saline and 50 µl of BsAbs, and then incubated for 1 h at RT on a rocker. To remove excess unbound antibodies, minicells were centrifuged (13000 x *g*, 15 min) and the pellet was resuspended in 500 µl of saline ready for immunisations.

4.2.12.3. Confirmation of formation

Antibodies against minicells and DEC205 were biotinylated using the lightning-link biotin conjugation kit (Innova Biosciences, Cambridge, UK) following the manufacturer's protocol. BsAb conjugates were formed using α-minicells and α-DEC205 either alone (mono-specific) or combined (bi-specific) with antibodies with and without biotinylation. GFP packaged DS410 strain minicells (2×10^9) were incubated with 20 µl of 1:100 diluted biotinylated α-minicells and α-DEC205 or with 20 µl of 1:20 diluted mono-specific or bi-specific antibody conjugates for 1 h at RT on a rocker, and then centrifuged (13000 x *g*, 15 min). Pellets were resuspended in 20 µl of 1:800 diluted streptavidin-DyLight 649 (Biolegend, USA) and incubated for 20 min at RT. Controls included unstained minicells and minicells incubated with

streptavidin-DyLight 649 only. Minicells were then washed and resuspended in PBS, and then analysed on a BD LSR Fortessa (BD Biosciences, CA, USA). Post-acquisition analysis was done using FlowJo software version 9.4 (Treestar, OR, USA). Analysis gates were set using empty minicells and GFP minicells to distinguish minicells from debris.

4.2.13. Confirmation of the presence of plasmid DNA in minicells

To confirm the presence of plasmid DNA in minicells, a PCR reaction similar to a colony PCR (section 2.6.3.5) was performed. DS410 minicells (5 x 10^9) containing pDual-OVA or pDual-Empty (no insert) single transformants, or pTrc-AMA1 and pVRV5-AMA1 or pTrc-Empty and pVRV5 empty dual transformants were used in each reaction. Minicells were resuspended in 20 µl of water in PCR tubes and heated to 94°C for 4 min then vortexed and centrifuged for 30 s. Five microlitres was then used in each PCR reaction. Reactions included the T7 forward and pDual GC SV40 reverse vector-specific primers for pDual minicells, and the *Py*AMA1-pVRV5 forward and reverse primers for dual transformed minicells. Remaining reagents and run protocols were as previously described. Samples were separated by electrophoresis in 0.8% agarose gels.

4.2.14. Minicell safety assessment

4.2.14.1. Immunisation protocols

Female BALB/c mice (n= 4/group) were immunised with three s.c. or i.p. injections at 3 week intervals with either DS410 strain empty minicells at 10^{10}, 10^8 (s.c) or 10^6 (s.c.) per dose, or P678-54 strain empty minicells at 10^{10} (s.c.) per dose, or LPS with 100 mM trehalose at a dose equivalent to 10^{10} minicells, or saline with 100 mM trehalose. The total volume of each injection was 100 µl.

4.2.14.2. Weight variation

Prior to each injection mice were weighed using digital scales, then weighed again daily for the next 5 days. To assess weight variance, the daily weight was subtracted

from the pre-injection weight and the differential area under the curve (AUC) was calculated using GraphPad Prism software version 6.0 (Graph-Pad, CA, USA). Statistical comparisons were made between the differential AUC of each group and the saline using the same administration route using one-way ANOVA with Bonferroni's multiple comparisons test. Between groups and between doses comparisons were done using two-way ANOVA with Bonferroni's multiple comparisons test.

4.2.14.3. Assessment of serum cytokines

Prior to each injection and 1, 4, 6 and 24 h post-injection, 10 µl of blood was collected from the tail tip of each mouse and diluted in 10 µl of MACS buffer in 96-well V-bottomed plates. Plates were centrifuged (600 x *g*, 4 min, 4°C) then 5 µl of individual and group pooled supernatant was collected and stored at -70°C. Pooled supernatant from each group at each time-point was analysed by CBA as previously described (section 2.10.1.9).

4.3. Results

4.3.1. Purification of minicells

In the development of the minicell vaccine delivery platform, it was necessary to purify minicells from bacterial cultures with a high yield and with no contamination by viable parent bacteria. To achieve this, differential centrifugation was employed to remove the bulk of the parent bacteria which were pelleted using a slow speed centrifugation. The minicell containing supernatant still had a large amount of parent bacteria. Next therefore, minicells were further purified using centrifugation coupled with a 5 - 25% discontinuous OptiPrep™ density gradient in 2.5% increments. To determine the optimal conditions for density gradient separation, samples were layered onto a gradient and centrifuged at various forces. The best separation of minicells from parent bacteria whilst maintaining a tight minicell band, was achieved at 1500 x *g* (Figure 31A). Minicells were still present in more dense gradient regions, however, parent bacteria became increasingly prevalent. Subsequent gradients were centrifuged at 1500 x *g*, with a 5 - 20% discontinuous gradient with 5% increments

between layers for ease of production, whilst maintaining visible band separation (Figure 31B).

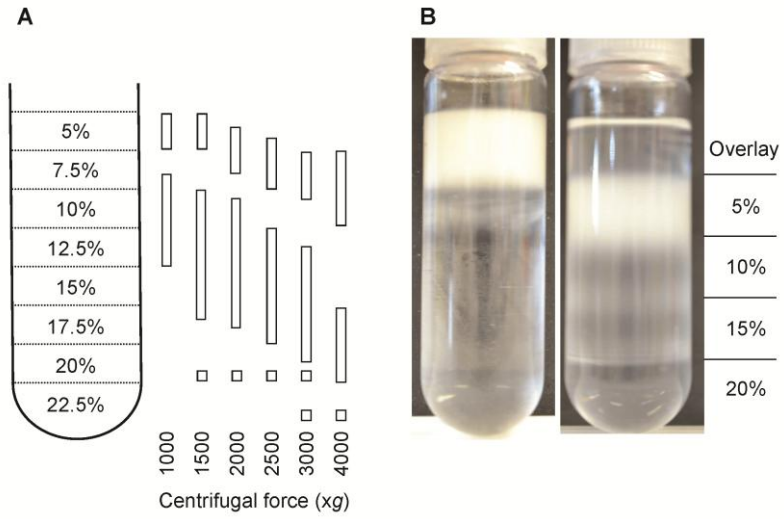

Figure 31: Minicell purification using a density gradient centrifugation. Following differential centrifugation the minicell enriched pellet was resuspended and layered onto a discontinuous OptiPrep density gradient. (A) Using a wide range of densities and various centrifugal forces, bands of minicells with varying degrees of parental bacterial contamination were separated. (B) Using the optimal centrifugal force (1500 x *g*) distinguishable zones were formed which were extracted to further enrich minicells.

Minicell enriched zones were extracted from density gradients and samples were viewed under the microscope which confirmed the presence of minicells with only minimal parental bacteria. At this stage very few elongated bacteria were detected, however, this did not exclude the possibility of freshly divided (hence small) viable bacteria. Culturing the harvested fractions allowed time for viable bacteria to elongate which was proposed to be enhanced with the increase of NaCl [0.8 M], although this effect was not observed using microscopic examination. After the subsequent density gradient centrifugation, some parental bacteria were detected in lower bands which were excluded.

Using pDual-GFP transformed DS410 in LB broth with overnight expression at 37°C, the minicell yield ranged from 0.73 x 10^{11} to 2.97 x 10^{11} and had a mean of 1.82 x 10^{11} minicells/L. The yields could be increased using alternative media, however, antigen protein yields were also affected by media changes. Purified minicells (Figure 32) devoid of contamination by viable parental bacteria were able to be

produced using this method for each of the bacterial strains in this study. The size of the minicells was determined using transmission electron microscopy and ranged between 435 nm to 562 nm.

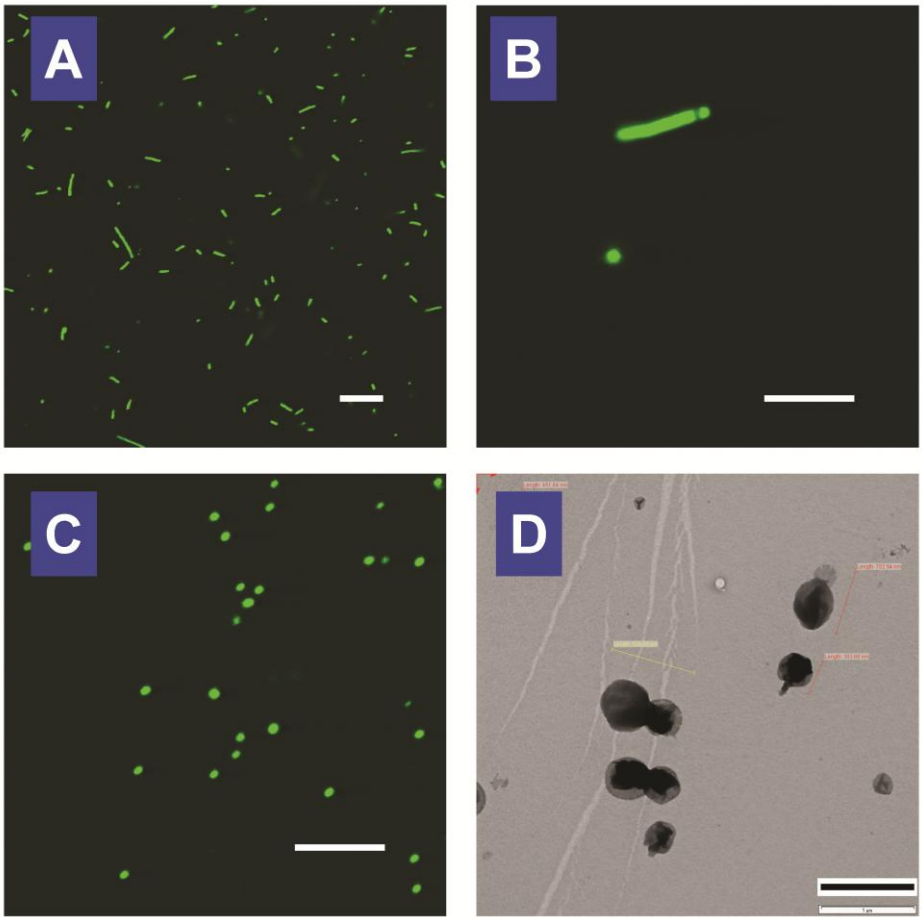

Figure 32: Microscope images of minicells. Minicell producing *E. coli* DS410 were transformed with pTrcHis2A-GFP cultured and induced with IPTG. (A)+(B) Prior to purification minicells can be seen in cultures. (B) Minicells bud off from the polar regions of bacteria and are released into the media. (C) The minicells are purified using differential and gradient centrifugation. (D) Purified minicells were visualised using transmission electron microscopy. Scale bars are (A) 20 µm, (B) + (C) 5 µm and (D) 1 µm.

4.3.2. Recombinant protein expression

4.3.2.1. Dual transformation causes reduced protein expression

A high level of GFP expression was detected when *E. coli* VIP 205 transformed with pBAD-GFP was induced with L-arabinose (Figure 33A). However, GFP expression was lost when the bacteria were dual-transformed with pBAD-GFP and pIASO-RFP

(Figure 33B). This loss was observed in repeated dual transformations. To confirm that this was not a short-term loss of expression due to transformation shock, several colonies were passaged over five days with no restoration of GFP expression detected. To examine if expression loss was strain-specific, DS410 and P678-54 strains were transformed with pTrc-GFP with and without pVRV5-RFP. In each strain there was a reduction in GFP expression in dual-transformants (Figure 33C). In single transformants DS410 strain expressed significantly more GFP than the P678-54 strain (p<0.0001). Subsequent experiments were done only with the DS410 strain based on these expression results. To remove the loss of expression following dual transformation, GFP and OVA proteins were cloned into the pDual GC vector which has both bacterial and mammalian promoters in a single plasmid. After 6 h or overnight induction with IPTG, similar GFP expression to single transformants (Figure 33D).

4.3.2.2. Effect of media on protein expression and minicell yield

In an effort to enhance both antigen-protein expression and minicell yields, a comparison was done using LB, TB, 2YT and BHI culture media. Single colony starter cultures were dispersed into the various media and when OD_{600} ~0.5, induced with 0.5 mM IPTG. Using flow cytometry to determine the GFP MFI and fluorescent microscopy to visualise expression, it was clear that LB cultures had superior GFP expression approximately double the other cultures (Figure 34). The minicell yield was however, greatly decreased with less than half that of the TB culture.

4.3.2.3. Effect of IPTG concentration and induction temperatures on protein expression

Protein expression was induced using various concentrations of IPTG in pDual-GFP transformed DS410 bacteria. Leaky expression was evident with GFP being expressed without IPTG, but expression was significantly increased at 0.2, 0.5 and 1 mM IPTG concentrations (Figure 33D). In another experiment using alternative media with various IPTG concentrations (Figure 34A), the same trend was observed. It was decided to induce later cultures with 0.5 mM IPTG.

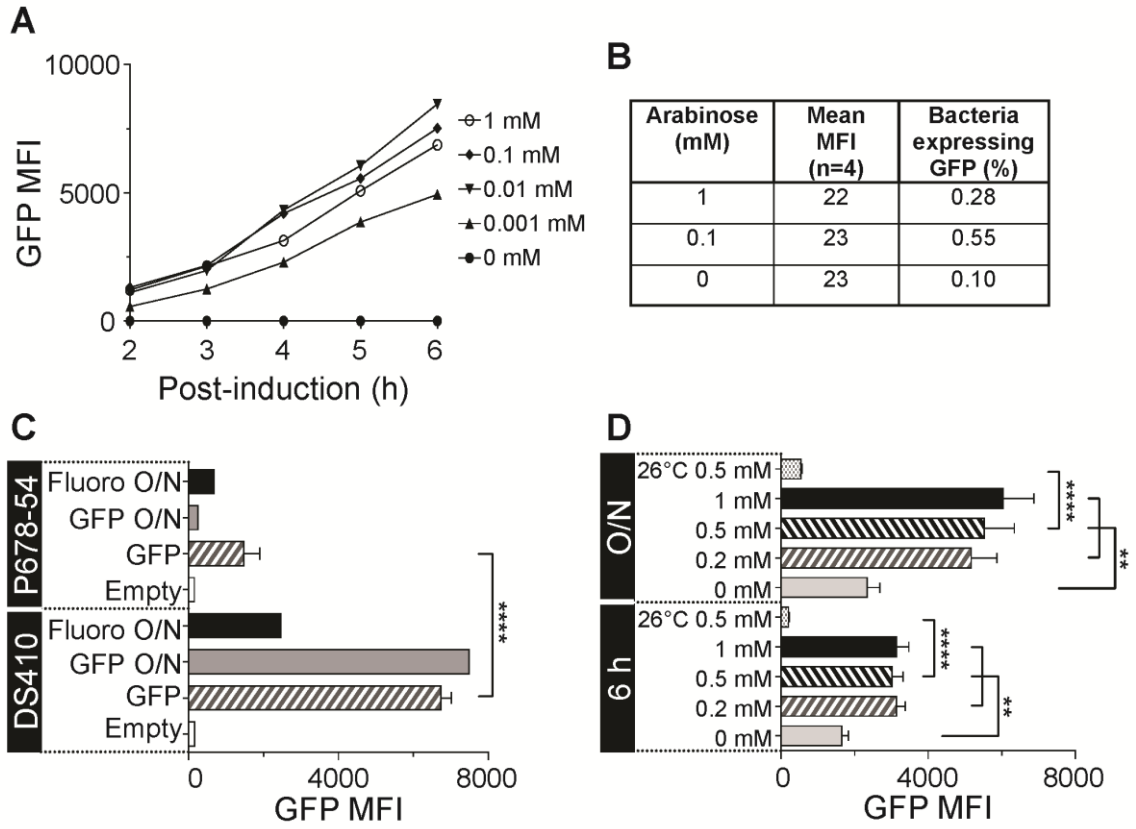

Arabinose (mM)	Mean MFI (n=4)	Bacteria expressing GFP (%)
1	22	0.28
0.1	23	0.55
0	23	0.10

Figure 33: GFP expression in single and double transformed minicell producing *E. coli* strains. (A) VIP205 transformed with pBAD-GFP were cultured and induced with a titration of L-arabinose. Samples taken over 6 h post-induction were analysed for GFP expression using flow cytometry to determine the median fluorescence intensity. (B) Dual transformation of VIP205 with pBAD-GFP and pIASO-RFP resulted in a reduction of GFP intensity and low frequency of GFP expressing cells with data showing overnight (O/N) cultures post-induction. (C) DS410 and P678-54 strains transformed with the empty vector pTrcHis2A or pTrcHis2A-GFP alone (n=4), or with both pTrcHis2A-GFP and pVRV5 (n=1) were induced with 0.5 mM IPTG and cultured for 6 h or O/N then GFP median fluorescence intensity was measured using flow cytometry. (D) DS410 transformed with pDual-GFP (n=5) were induced with 0.2, 0.5 and 1 mM IPTG then cultured at 37°C (or 26°C where stated). Samples taken after 6 h and O/N were analysed by flow cytometry for GFP expression. Data is presented as mean + SEM. Significance determined using log transformed data with one-way ANOVA followed by Bonferroni's post-test. $p<0.0001$ ****.

To assess if the induction temperature effects on protein yield, induced cultures were incubated at either 37°C or 26°C. After 4 h the effect on the frequency of bacteria expressing GFP and the GFP MFI was minimal in dual transformed pTrc-GFP and pVRV5-RFP DS410 and P678-54 strains (Figure 35A). In subsequent experiments using pDual-GFP transformed DS410 there was significant increases in GFP intensity at 37°C (Figure 33D). In larger scale cultures of DS410 transformed with

pDual-OVA, this temperature protein relationship was observed using a western blot with purified minicells (Figure 35B).

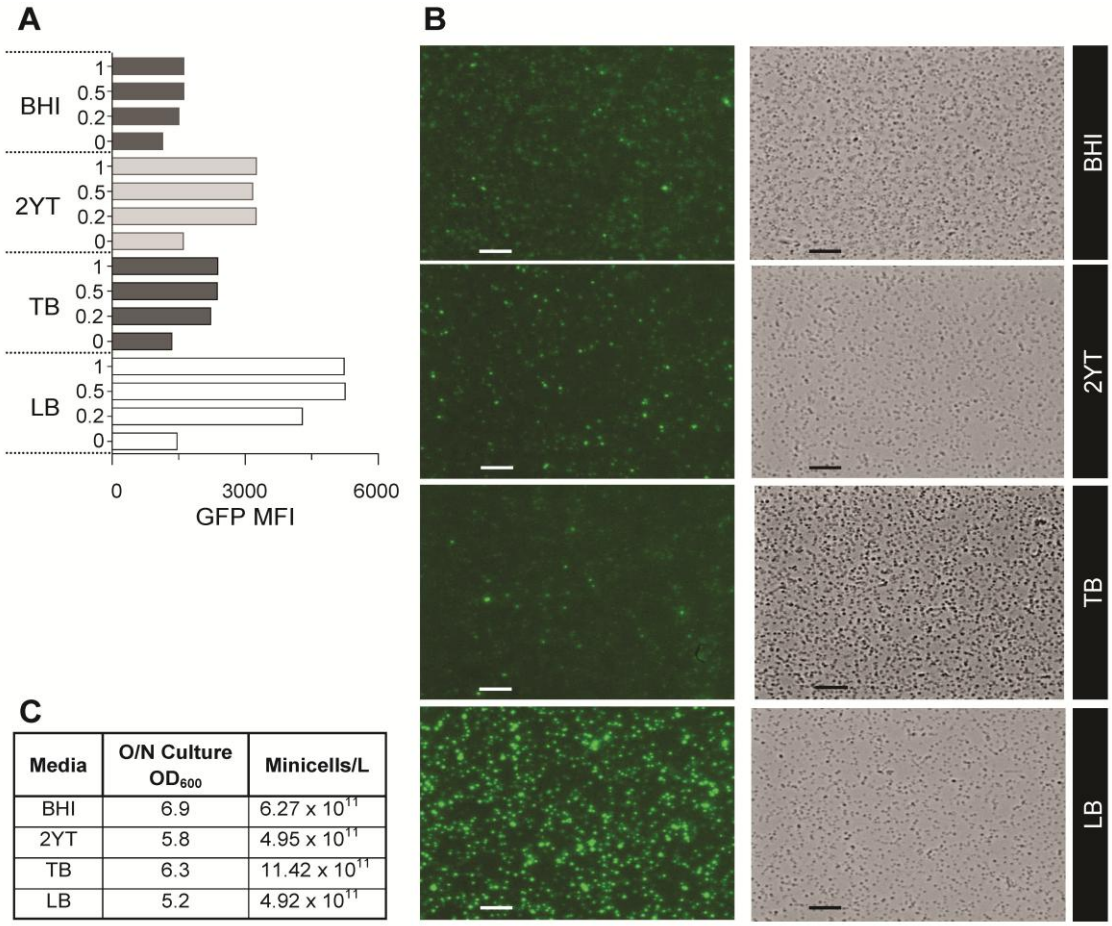

C

Media	O/N Culture OD_{600}	Minicells/L
BHI	6.9	6.27×10^{11}
2YT	5.8	4.95×10^{11}
TB	6.3	11.42×10^{11}
LB	5.2	4.92×10^{11}

Figure 34: The effect of culture media on GFP expression and minicell yield. *E. coli* DS410 was transformed with pDual-GFP then a single colony was used to inoculate BHI, 2YT, TB or LB media. Cultures were induced with various concentrations of IPTG then incubated overnight (O/N) at 37°C and 220 RPM. Minicells were then purified by differential and gradient centrifugation only. (A) Cultures either non-induced (0 mM) or induced with either 0.2 mM, 0.5 mM or 1 mM of IPTG were analysed by flow cytometry to determine the median fluorescence intensity of GFP. (B) Using samples from the 0.5 mM induced cultures, minicells were purified and GFP expression was confirmed by fluorescence microscopy (left), and brightfield microscopy shows a comparison of minicell yields for different media (right). (C) The culture OD_{600} and minicell yields are shown for the 0.5 mM IPTG induced cultures.

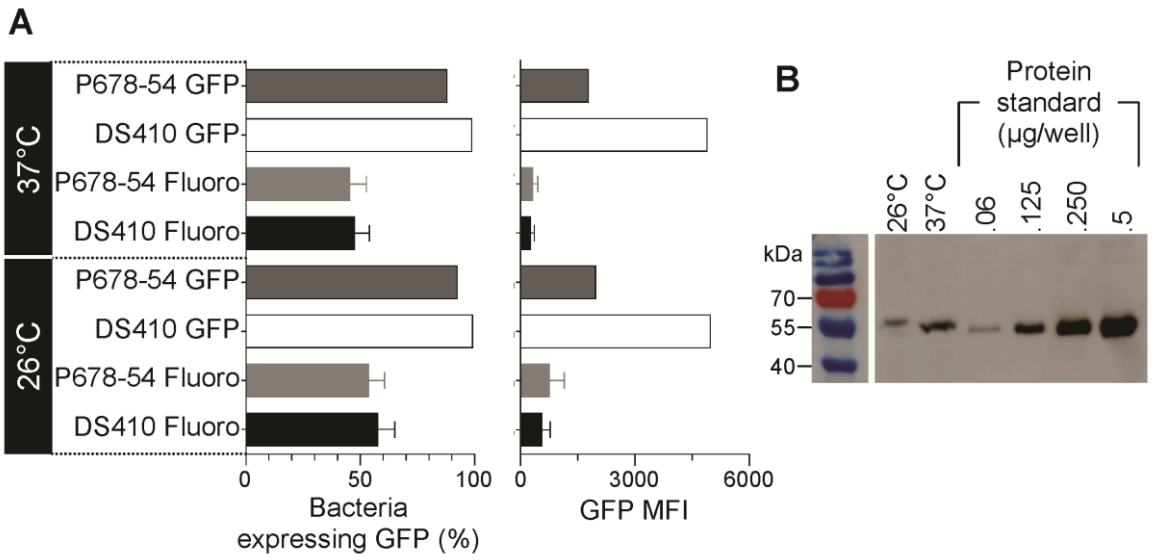

Figure 35: Effect of temperature on protein expression. (A) *E. coli* DS410 and p678-54 transformed with pTrcHis2A-GFP (n=1) or with both pTrcHis2A-GFP and pVRV5-RFP (n=5) were cultured in LB at 37°C until OD600 ~ 0.5, and then induced with 0.5 mM IPTG. Cultures continued for 4 h at either 26°C or 37°C, and then samples were analysed by flow cytometry to determine the frequency of bacteria expressing GFP, and the median fluorescence intensity of GFP. (B) Following the same protocol, *E. coli* DS410 transformed with pDual-OVA was cultured in LB, induced with 0.5 mM IPTG followed by overnight 26°C or 37°C incubations. Purified OVA minicells (10^{10}) were analysed by western blot with anti-his detection antibodies. A his-tagged serial-diluted protein standard (µg/well) was run to estimate OVA protein yield in each minicell dose.

4.3.3. Minicells contain both mammalian and bacterial expression vectors

This vaccine platform was designed to deliver both recombinant protein expressed by transformed bacteria, and plasmid DNA for mammalian expression of the homologous protein. Minicells should contain plasmids for both bacterial and mammalian protein expression. To confirm the presence of both plasmids, purified minicells were used as a PCR template to amplify insert regions. The expected DNA lengths were pDual-OVA (1667 bp) and pDual-Empty (1541 bp), pTrc-AMA1 (2072 bp) and pVRV5-AMA1 (1692 bp). Agarose gel electrophoresis of the PCR product confirmed the presence of respective plasmids (Figure 36). The presence of the band using pDual-empty is because an ampicillin resistance gene is located between the cloning restriction site.

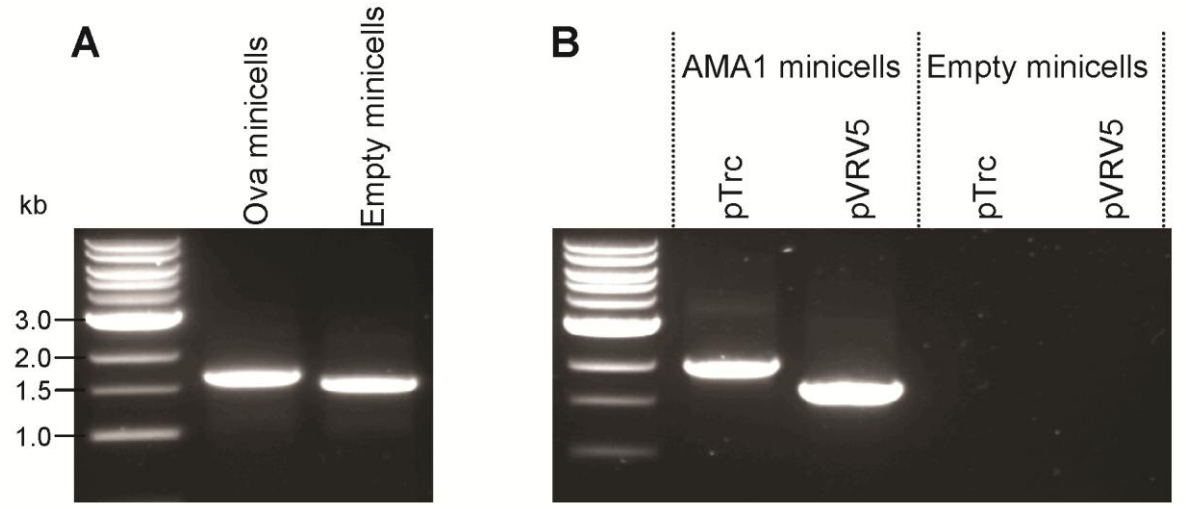

Figure 36: Confirmation of plasmid DNA in purified minicells. *E. coli* DS410 transformed with (A) pDual-OVA or pDual empty vector or with (B) pTrc-AMA1 and pVRV5-AMA1 or pTrcHis2A and pVRV5 empty vectors were used as a template for a PCR reaction. Amplifications used pDual and pTrc vector-specific, and pVRV5-AMA1 forward and reverse primers. Products were separated by electrophoresis on 0.8% agarose gels. A 1kb NEB DNA ladder was run in the left lane of each gel.

4.3.4. Confirmation of bi-specific antibody formation

Antibodies to the LPS endotoxin core purified from a hybridoma (8298-HB, ATCC) failed to show affinity to the surface of DS410 or P678-54 minicells (data not shown). Consequently, a hybridoma was generated producing antibodies to an unknown antigen on the minicell surface. Affinity was confirmed by flow cytometry using both strains as capture antigens.

For the targeting strategy of this platform, hybridoma produced monoclonal antibodies to the surface of the minicells are bound to antibodies to either DEC205 or Clec9a using protein A/G which binds to the Fc region of antibodies. The assessment of BsAb formation required primary antibodies to be biotinylated as secondary antibodies used for detection would bind non-specifically to protein A/G. Using GFP minicells as a capture target, a BsAb formed with anti-minicell antibodies and biotinylated anti-DEC205 successfully targeted minicells and was positive for biotinylation (Figure 37). This confirmed that the BsAb comprised both antibodies, and was able to retain its ability to bind to the minicell surface.

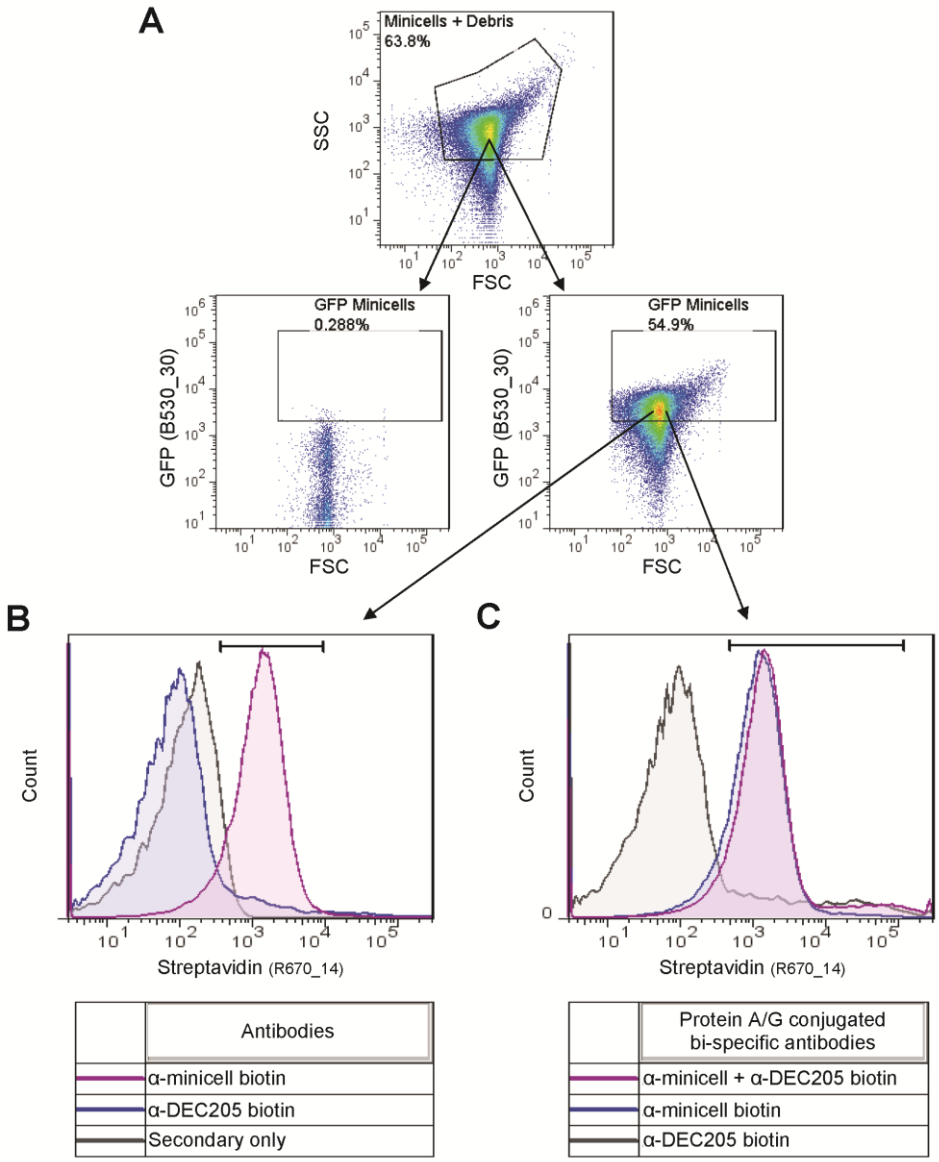

Figure 37: Confirmation of bi-specific antibody formation. Purified GFP expressing DS410 minicells were used as a capture antigen in a flow cytometry based assay. Minicells and debris was isolated by (A) forward and side scatter and GFP positive events gated using non-GFP minicells (left) to remove debris. GFP Minicells were incubated with (B) biotinylated primary antibodies against minicells or DEC205 then with streptavidin-Dylight 649 or (C) with antibodies conjugated using protein A/G. For BsAb structure confirmation, an anti-minicell conjugated to a biotinylated DEC205 was used with secondary streptavidin staining.

4.3.5. Minicell safety assessment

Since this novel delivery platform has a high content of LPS which could be associated with non-specific toxicity, it was necessary to evaluate health related effects on mice following a series of three immunisations. Weights, and serum

cytokines, were measured as well as physical examinations looking for signs of distress.

4.3.5.1. Body weight following minicell injections

Over the duration of the experiment, there was an increase in weight with each group including the PBS control groups, without significant inter-group variance (Figure 38A). To examine the short term effects, the weight variation of individual mice was calculated. The most rapid weight loss occurred on day 1 following the first dose with mean group losses in LPS i.p. (10.0%, $p<0.0001$), LPS s.c. (9.1%, $p<0.0001$) and 10^{10} minicells i.p (7.3%, $p<0.0001$) significant to respective starting weights. These losses lost significance after day 2, and by day 5 all groups were above their starting weight. After the second dose, losses were less extreme in the LPS i.p. (6.8%, $p<0.001$) and 10^{10} minicells i.p (4.4%, $p<0.01$) but weight recovery was prolonged. This persistent weight reduction was also detected after the third dose. Here weight reductions were detected in LPS i.p. (5.0%, $p<0.0001$) and 10^{10} minicells i.p (5.8%, $p<0.0001$), and for the first time also in s.c. injections of 10^{10} DS410 minicells (5.7%, $p<0.0001$) and P678-54 minicells (4.8%, $p<0.0001$).

To assess the prolonged weight difference, individual percentage variations were used to calculate the AUC of weight variance for individual mice (Figure 38B). Data indicates that for the first and second doses the administration route impacts on weight loss with mice receiving i.p. doses tending to lose more percentage of weight. There was also a non-significant trend of greater percentage weight reduction as the dose of minicells was increase. The strain of minicells did not appear to alter the outcome.

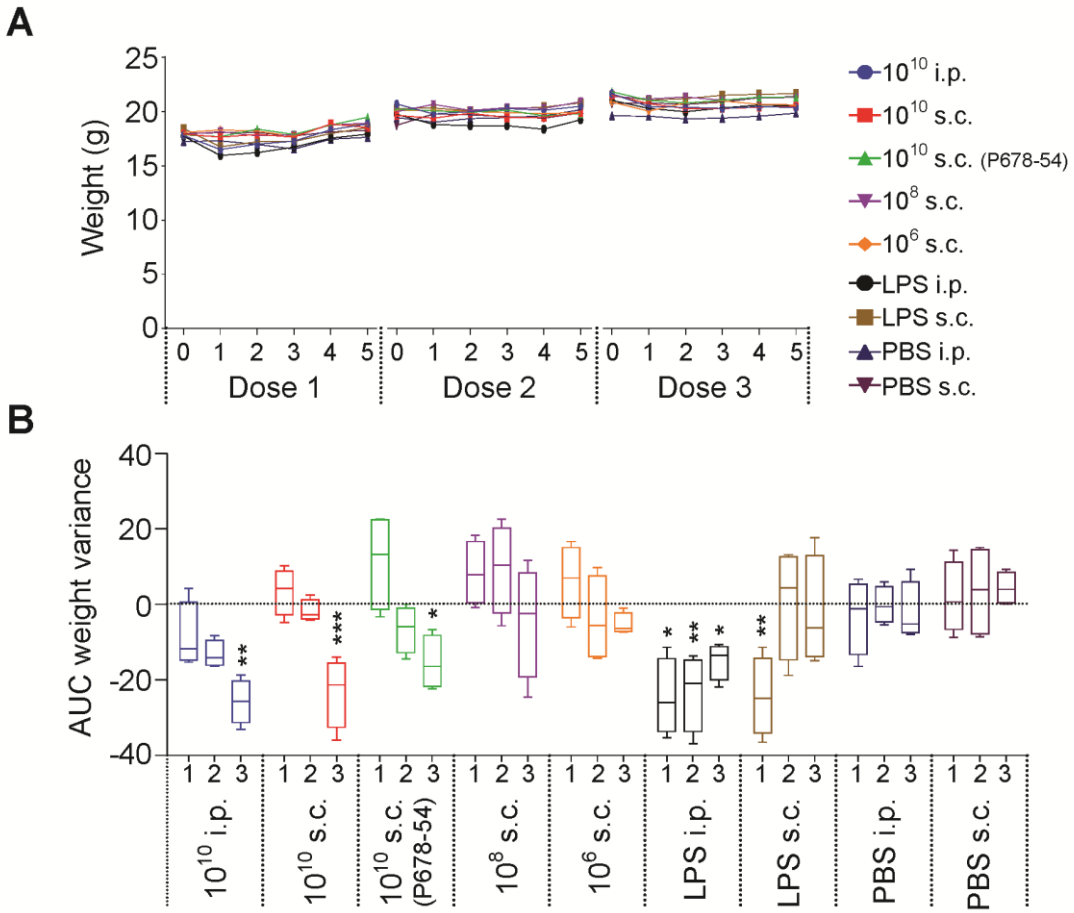

Figure 38: Weight variation following doses with minicells. BALB/c mice (n=4/group) received three doses of DS410 strain minicells at 10^{10}, 10^{8} or 10^{6} minicells per dose (or P678-54 were stated), or LPS (endotoxin equivalent of 10^{10} minicells), or PBS by s.c. or i.p. injections at 3 week intervals. (A) Mice were weighed before and then daily after each immunisation. Data shows the mean weight for each group. (B) Individual percentage weight variation calculated from start weight at each dose was used to calculate the AUC of weight variance. Data is shown as min to max whiskers plots. Statistical comparisons were made to the PBS control with the same route of administration, using one-way ANOVA followed by Bonferroni's post-test. $p<0.05$ *, $p<0.01$ ** and $p<0.001$ ***

4.3.5.2. Serum cytokines following minicell injections

To look at systemic cytokine responses to injections of minicell, serum was collected at various time-points and analysed by CBA. Pooled serum for doses 1 and 3 were assayed for multiple cytokines specifically: IL-1β, IL-2, IL-4, IL-5, IL-6, IL-10, IL-12p70, IL-13, IFN-γ and TNF (section 4.2.14.3). For all cytokines except IL-6, IL-10 and TNF, the detected responses were at or near detection levels, and only minor differences were observed between groups or time-points. IL-6, IL-10 and TNF

responses were quantified using pooled serum at individual time-points (Figure 39A) and that data used to generate AUC data to evaluate the breadth of response after each dose (Figure 39B). There was a large IL-6 response peaking after 6 h in the mice injected i.p. with either LPS or 10^{10} minicells and to a lesser extent LPS s.c. These groups also had rapid increases in both IL-10 and TNF with peaks at 1 h. The cytokine intensity was greatly decreased following the second and third doses.

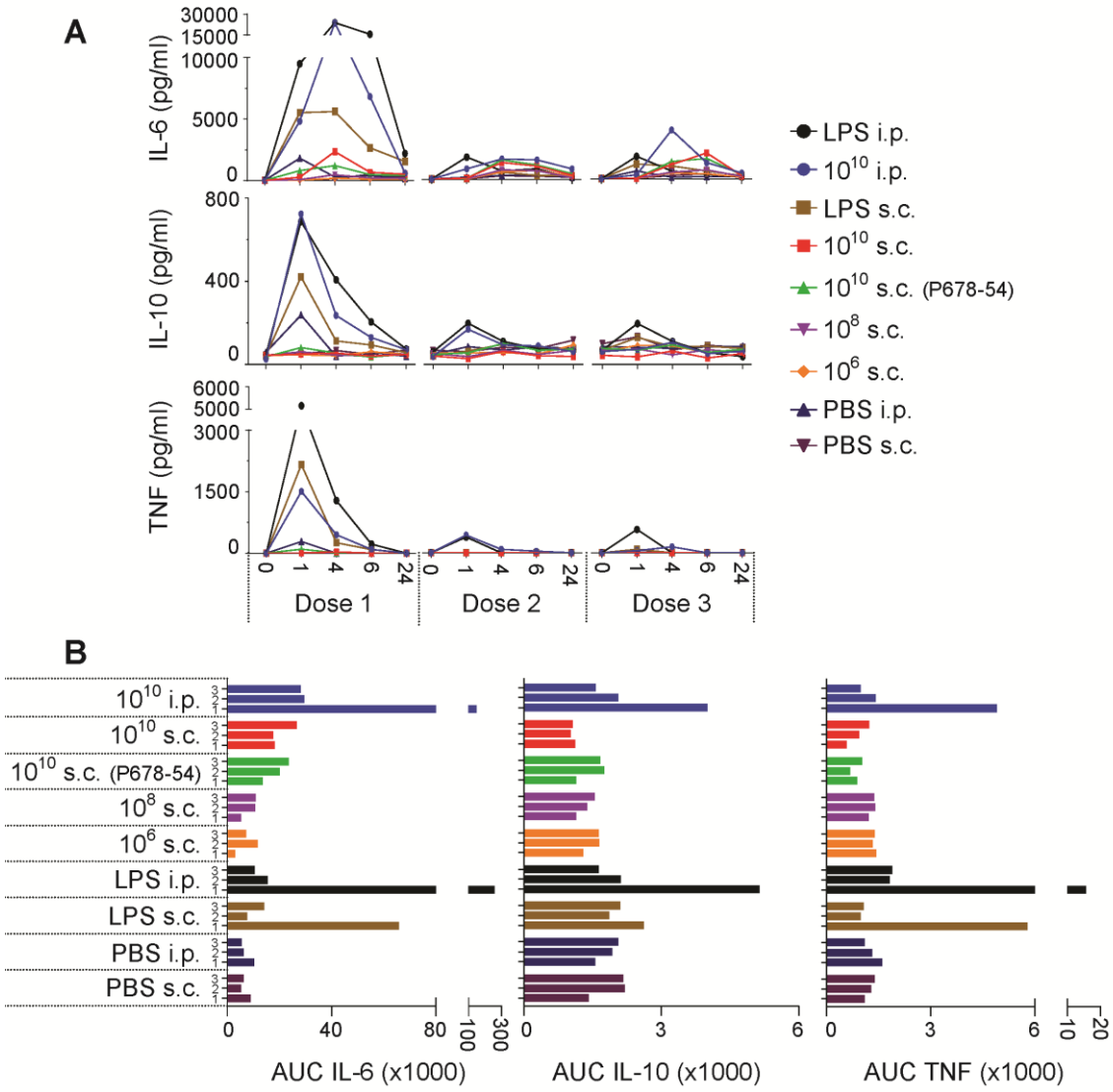

Figure 39: Serum cytokine analysis following minicell injections. BALB/c mice (n=4/group) received three doses of DS410 strain minicells at 10^{10}, 10^8 or 10^6 minicells per dose (or P678-54 were stated), or LPS (endotoxin equivalent of 10^{10} minicells), or PBS by s.c. or i.p. injections at 3 week intervals. (A) Serum samples were taken at 0, 1, 4, 6 and 24 h after each injection. Pooled samples were analysed using a cytometric bead array to quantify IL-6, IL-10 and TNF circulating cytokines. (B) The AUC for each cytokine is displayed for each dose (1, 2 and 3).

This data indicates that the administration route influences the intensity of cytokine responses in a similar way as seen with weight variations (Figure 38). The loss of cytokine intensity in the second and third doses is consistent with the loss of weight reductions. Only minor variations were detected between DS410 and P678-54 strains and minicell doses. A reduction in IL-6 cytokine responses was evident with lower minicell doses.

4.4. Discussion

The use of minicells as a delivery vehicle for vaccines incorporating both protein antigen and plasmid DNA has recently been evaluated showing the their ability to induce antibody and cellular immune responses, as well as protection against LCMV challenge[236,237]. Minicells as a delivery vehicle for chemotherapeutic drugs and siRNA has been effective against tumours when minicells are targeted to surface receptors of cancerous cells[227,238]. For several decades, researchers have adopted a minicell purification protocol described by Fraser and Curtiss[225], which was recently improved upon by the inclusion of antibiotics[236,237], or with antibiotic treatment, filtration and elongation for the complete elimination of viable parent bacteria[227,238]. The purification method developed for this study was based upon the protocol reported by MacDiarmid *et al*.[227], however, the filtration steps were removed and replaced with the additional gradient centrifugation post-elongation and antibiotic treatment for greater purification. At that stage, any parent bacteria should have elongated and then been killed. The increased size and density of the parent bacteria was sufficient for separation. A spread plate using antibiotic free media and 10^{10} minicells confirmed the sterility of purified minicells and fluorescent microscopy examination of GFP producing minicells showed an absence of elongated cells.

4.4.1. Factors effecting minicell and antigenic protein yield

In order to obtain a high minicell yield with a high antigen protein load, variations to bacteria strains, plasmid vectors, culture media and temperature conditions were trialled. The production of minicells occurs throughout the growth cycle, with highest levels of production in late-log phase and as long as 7 h into the stationary phase[225,343]. Whilst minicells are capable of forming in all media which support

growth of the parent bacteria[343], optimal yields are achieved using nutrient rich media which supports faster growth rates and vigorous aeration[343]. Experimental data supported these established findings, with TB and BHI cultures producing high minicell yields as opposed to LB and 2YT media (Figure 34). However, optimal GFP yields were achieved using LB media incubated at 26°C post-induction. The reduced temperature resulted in slight increases in protein yield but this also reduced the growth of the bacteria which would be expectedly reduced minicell yields[343]. The use of LB as media for recombinant protein expression in *E. coli* is supported by various studies[344-346], although modifications to broth formulations are capable of enhancing yields[347]. A review of the literature did not reveal a single media formulation which would be universally beneficial to increase recombinant protein yield, with media selection dependant on the protein of interest.

Codon optimisation for *E.coli* was considered as a possible cause of the low protein yield. It is well established that different organisms carry their own codon bias and that the lack of transfer RNA (tRNA) can result in difficulties in the expression of recombinant proteins[348,349]. An analysis of *Py*AMA-1 and ovalbumin genomic sequences, however, shows that low frequencies of rare *E. coli* K12 tRNA codons are present. It is possible that reducing the frequency of AGA (arginine) which was present in *Py*AMA-1 (1.8%) and ovalbumin (2.4%), but only makes up 2.1% of the endogenous tRNA population[348], could have enhanced protein expression as has been shown with other proteins including those from *P. falciparum*[350,351]. There are however, other possible explanations for the low protein yield including toxicity of the recombinant protein to the bacterium[349]. A study involving *E. coli* expression of 1000 *P. falciparum* genes established that only one-third of the proteins were capable of being expressed by the bacterium[352]. The cause of poor expression rates correlated directly with high molecular weight, protein disorder, and the lack of homology to E. coli proteins, rather than codon usage and the higher adenosines and thymidines[352]. Codon-optimisation of the target antigens was not performed during these experiments, however this option should be considered for future studies.

This platform was designed to deliver both a bacterial produced antigen protein, together with plasmid DNA with a mammalian promoter for expression of the homologous antigen post-immunisation. This required bacteria to be transformed

with both plasmids done either simultaneously or in stages. Using selective antibiotics it was evident that bacteria contained both plasmids, however, the dual transformation had an unexpected and large reduction in GFP expression (Figure 33 and Figure 35). It is possible that the plasmids were incompatible due to competition for replication factors[353]. Whilst it is possible to dual transform with incompatible plasmids as long as antibiotic pressure is maintained[354], competition pressures may result in fluctuations of plasmid copy numbers[355] resulting in reduced protein expression. To overcome competition factors, compatible plasmids with different origins of replication could be utilised[356]. Another alternative is to use a single plasmid which contains the same gene cassette but has within itself, both bacterial and mammalian promoters. One such vector was engineered by Giacalone *et al*. where expressed protein and plasmid DNA quantities were very similar in bacterial and dual expression vectors[236]. Using the same system but replacing GFP with the LCMV nucleoprotein a reduction in mean protein load from 6.8 µg to 1.2 µg was reported in 10^{10} minicells[237], suggesting that protein expression will vary depending on the protein itself. With the aim to reduce competing pressures, genes were inserted into multiple vectors including pDual GC (Stratagene, USA) which has a dual promoter system. In comparing vectors for GFP expression in dual transformants or single for pDual GC, variations were observed between vectors with pDualGC providing a higher median fluorescence intensity (Figure 33C and D, Figure 35A).

There were four antigen targets planned for assessment in the minicell model, however, only *Py*AMA-1 and ovalbumin minicells produced sufficient protein for progression into the mouse model for immunisation studies. In these constructs, the antigen load was approximately 1 µg and 0.1 µg per dose of 10^{10} minicells. Western blot analysis was unable to confirm the presence of *PyCSP*, and only very low amounts of the fusion Tfr-ovalbumin protein were detected.

4.4.2. Targeting dendritic cells using bi-specific antibodies

The novelty of the proposed minicell platform is the targeted delivery using BsAbs to the minicell surface and either DEC205 or Clec9a both of predominantly found on DCs and facilitate antigen uptake, processing and presentation[340,357,358]. The

formation of BsAbs required monoclonal antibodies to respective targets. The anti-minicell antibodies required the generation of a hybridoma as attempts to find a commercial antibody with the desired affinity were unsuccessful. The BsAb formation was confirmed by flow cytometry using minicells as capture antigens and a BsAb comprised of anti-minicell + protein A/G + biotinylated DEC205 with a subsequent streptavidin-fluorochrome stain.

It was anticipated that targeting minicells to DCs would enhance the low level of transfection efficiency observed in previous studies[236]. The bulk of purified *E. coli* minicells has a diameter of between 400 – 500 nm[359] similar to the sizes obtained for this study as determined by TEM (Figure 32). This size exceeds the DC optimal uptake particle size of between 40 – 50 nm as previously described[196] and it is this limitation which is anticipated to be overcome by inducing receptor-mediated endocytosis. This enhanced minicell uptake by targeting surface receptors of non-phagocytic cells has been reported[227,238], however, there are no publications where minicells have been targeted to DCs.

4.4.3. Minicell safety study

An important step to increasing the safety aspects of this platform was to remove all of the viable parent bacteria to limit the chances of the onset of toxic shock. The safety study of MacDiarmid *et al.* used pigs receiving a weekly i.v. dose of 5 x 10^9 minicells, and two dogs receiving weekly i.v. doses of 3 x 10^9 or 10^{10} minicells[227]. In the dogs, there was no increase in pro-inflammatory TNFα or IL-6 with serum samples taken 16 h post injection, and the only adverse effect was a temperature increase of 1°C which returned to normal within 4 h[227]. In pigs, spikes in TNFα and IL-6 were observed after the third dose, and returned to background levels within 24h, and pigs developed a minor fever from which they recovered within 2 h[227]. The dose evaluated herein was up to 10^{10} minicells delivered to mice with a much lower body weight, as such any adverse effects would be expected to be greater. Similar to the pig study, there was a rapid onset of the inflammatory cytokines IL-6 and TNF which was resolved within 24 h, however, there was a major increase in cytokine concentrations. Surprisingly, the induced cytokine responses were observed after

the first dose with greatly reduced responses from subsequent doses which is the reverse of data from the pig study.

As a measure of well-being, the weights of mice were recorded for 5 d post immunisation. Minicells administered i.p. resulted in mean weight losses of 7.4% within 24 h of injection following the initial dose. These losses were generally recovered within 5 d observation period. In subsequent doses the severity of weight reductions was lessened, however, as seen by the AUC values (Figure 38) the reductions were more sustained perhaps as a result in the decreased growth rate of the more mature mice. There was no difference between the DS410 and P678-54 strains, and the responses were influenced by both the dose and administration route.

4.5. Conclusion

During this study, minicells were purified using a novel technique derived from a combination of previous methods[225,227], which resulted in a high minicell yield and the complete removal of viable bacteria. The use of incompatible plasmid DNA in dual transformations was overcome by using a dual promoter vector, and culturing conditions were optimised. Whilst optimal minicell yields were achieved using high growth media, antigen expression is likely to require optimisation for different proteins. The combined weight and cytokine data supports the further evaluation of the platform using s.c. route with a 10^{10} minicell dose.

Chapter 5: Evaluation of antigen-specific immunogenicity and protective efficacy of ovalbumin and *Py*AMA-1 loaded minicells

5.1. Introduction

Minicells are small anucleate cells which can form when the mechanisms for septum formation at the mid-point of the bacterium have been disrupted[222,226,232]. Minicells form as a result of the premature formation of the septum at the polar regions of the bacterium[229,232]. The minicells bud off from the parent bacteria with cellular contents including cytoplasmic proteins and plasmid DNA, however, they are devoid of chromosomal DNA and as such are unable to replicate[223,224].

There has been very limited research done into the vaccine potential of bacterial minicells. The first report of the immunological potential of minicells was by Tankersley *et al*.[336] in 1974, when *Salmonella typhimurium* minicells were injected into rabbits resulting in antibodies with affinity to both minicells and parent bacteria. In 1979, the first study showing the potential for heterologous minicell antigen delivery was reported[360]. In that study, the immunisation of cows with minicells containing plasmid-induced K99 antigen proteins prevented fatal diarrhoea against challenge with an enterotoxigenic *E. coli*. However, in the pursuing 27 years almost no minicell vaccine related research was conducted.

In 2006, an *E. coli* minicell vaccine delivery platform was developed by Giacalone *et al.*[235] to deliver both recombinant antigenic protein and plasmid DNA. Their studies showed that minicells administered to mice could induce both antibody and cellular antigen-specific responses[235,237]. They also showed *in vitro* that macrophage cell lines J774A.1 and RAW 264.7, as well as BMDM and BMDDCs, were inefficiently transfected (between 0.02% to 0.2%)[236].

Whilst DCs are professional APCs and are efficient at the up-take and processing of particles up to 2 μm in diameter[197], they preferentially take up particles between 40

to 50 nm in diameter resulting in the induction of robust antibody and T cell-mediated responses[196]. Minicells produced in this study were between 435 nm and 562 nm in diameter (section 4.2.8) which is comparable with previously reported dimensions[235,360]. However, this size falls outside of the preferential range for DCs and is more likely to be phagocytised by macrophage cells[196], likely explaining the inefficient transfection rate in the Giacalone study[236].

In an attempt to overcome this inadequate minicell uptake by APCs, in particular DCs, studies in this chapter were designed to directly target minicells to DCs using BsAbs to the DEC205 and Clec9a receptors found on DCs. This targeting method derives from other minicell studies where chemotherapeutics where packaged in minicells and delivered to cancer cells via the epidermal growth factor receptor[227,238]. In those studies, the otherwise non-phagocytic cells took up the targeted minicells due to receptor mediated endocytosis. Furthermore, targeting is beneficial in that antigens are concentrated to the target cells, in this case professional APCs, reducing the required quantity of antigen and increasing vaccine efficacy[337].

Targeting DC receptors including DEC205 and Clec9a with proteins has been shown to enhance both cellular[358,361-363] and antibody[340,364,365] responses against target proteins in other models[363]. In each of those studies, the co-administration of an adjuvant with the targeted protein was required for the induction of cellular immune responses. Antibody responses could be induced by targeting each receptor, however, whilst DEC-205 targeting required an adjuvant[364,366], Clec9a induced antibody responses were equivalent with or without adjuvant[337,340]. In the minicell platform studied here, the bacterial components of the minicells, in particular the TLR4 agonist LPS[367], was intended to provide the adjuvant relied upon for DC maturation.

5.2. Experimental design

OVA minicells and PyAMA-1 minicells were produced in E. coli DS410 as previously described (Chapter 4:). The antigen load in these purified minicells was 0.1 µg and 1.0 µg respectively per 10^{10} minicell dose.

In the ovalbumin studies, PTP mice (n=4-5/group) received an i.v. transfer of 0.3 x 10^6 OTI $CD8^+$ and 0.3 x 10^6 OTII $CD4^+$ T cells. Mice were immunised by three s.c. injections at 2 week intervals at the base of the tail with either: ovalbumin loaded minicells (OVA minicells) with or without BsAbs to target DEC 205 or a non-specific isotype control (LTF_2); ovalbumin protein at 100 µg/dose alone, or with either empty minicells (10^{10}) or CT (1 µg); negative controls included PBS or empty minicells (10^{10}). Blood samples collected 12 days (doses 1 and 2) and 5 days (dose 3) after immunisations were analysed by flow cytometry to determine the frequency of transferred cells. Six days after the final immunisation, cells obtained from naive PTP mice were incubated with or without $OVA_{257-264}$ peptide (SIINFEKL) and differentially stained high and low respectively with VPD450. These cells were transferred i.v. into immunised mice (4.75 x 10^6 cells of each group) and then 24 h later mice were sacrificed to quantify frequency of donor OTI and OTII cells in the blood, draining lymph nodes (inguinal) and spleen, as well as to assess killing of SIINFEKL-coated cells. Sera were collected post-immunisations for detection of ovalbumin-specific antibodies via ELISA.

In the ovalbumin dose titration experiment (section 5.3.3), PTP mice (n=5/group) were immunised as described above, however, the original i.v. cell transfer was increased to 0.5 x 10^6 OTI $CD8^+$ and 0.5 x 10^6 OTII $CD4^+$ T cells, to increase the starting population making the transferred cells more detectable in non-proliferation immunisation groups. Mice were immunised with either 100 µg, 10 µg or 0.1 µg of ovalbumin protein alone or co-administered with CT, empty minicells (10^{10}) or the equivalent LPS content of 10^{10} minicells. Targeted minicell delivery was done using BsAbs to Clec9a instead of DEC205. The original project design was to evaluate targeting minicells to the DEC205 receptor, however, after the initial experiment we obtained an anti-clec9a antibody from the Shortman laboratory at the Walter and Elisa Hall Institute in Melbourne. We then wanted to evaluate both targets. One group had no adoptive transfer of cells to examine the endogenous killing capacity of ovalbumin + CT.

In the *Py*AMA-1 minicell experiment (section 5.3.4), BALB/c mice (n=5/group) were immunised with three s.c. doses at 3 week intervals with: *Py*AMA-1 protein and plasmid DNA loaded minicells (10^{10}) alone or coupled with BsAbs to either DEC205,

Clec9a or a non-specific isotype control (LTF_2); with empty minicells (10^{10}) with and without 1 µg of *Py*AMA-1 purified protein; or with PBS as a control. The positive control mice received two i.m. doses of 100 µg *Py*AMA-1 plasmid DNA (50 µg per tibialis anterior muscle/dose) at 3 week intervals followed by an i.p. boost with 10 µg *Py*AMA-1 protein mixed 1:1 with Alhydrogel[96]. Sera were collected nine days after each immunisation for antibody analysis. Ten days after the final immunisation, mice were challenged with 1000 *P. yoelii* 17XNL sporozoites delivered by i.v. injection. Blood taken pre and post-challenge was used to assess serum cytokines (section 2.10.1.7), antibodies (section 2.10.3.1), and parasitemia (section 2.10.3.1).

5.3. Results

The ability of minicells to generate antigen-specific T cell and antibody responses was assessed in both murine ovalbumin and malaria models. In the ovalbumin model, cellular responses were assessed by proliferation of OTI $CD8^+$ and OTII $CD4^+$ T cells in both *in vitro* and *in vivo* adoptively transferred models, the latter coupled with an *in vivo* antigen-specific cytolytic assay. Antibody responses specific for ovalbumin protein were detected by ELISA. In the malaria model, blood samples collected pre- and post-challenge with *P. yoelii* 17XNL sporozoites were assessed for cytokine responses, cell phenotypic activation markers and antibody responses by ELISA and a flow cytometry-based IFAT. To assess protection, parasitemia was evaluated using the flow cytometric assessment of blood (FCAB) assay.

5.3.1. *In vitro* proliferation of OTI or OTII cells by migrating dendritic cells

It was anticipated that following s.c. immunisation with minicells, DCs would migrate to lymphocyte rich lymph nodes and spleen, and present processed antigens. These migrating DCs would be expected to be high in expression of MHCII and CD11c surface receptors which could be quantified by surface staining and flow cytometry analysis. Accordingly, OVA minicells with or without BsAbs targeting DEC205 were injected into mice and DLNs harvested at 6 h intervals. Data (Figure 40) indicated that peak migration occurred at 24 h post-immunisation. The percentages of migrating DCs (mDCs) at 24 h were similar between all minicell immunisations with

no apparent impact of targeting DEC205. However, there was an increase in mDCs in the targeted minicell draining lymph nodes (DLNs) 42 h and 48 h. Only one mouse was immunised at each time-point so no statistical comparisons could be made to determine the significance of the increase.

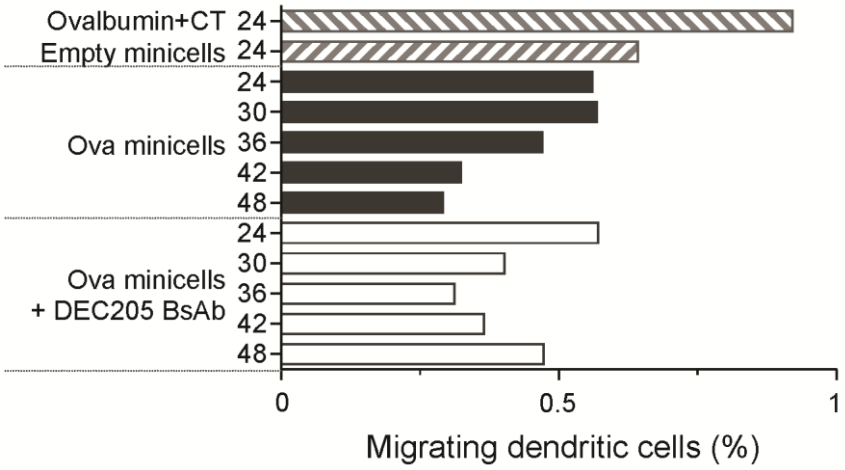

Figure 40: Frequency of migrating dendritic cells in draining lymph nodes following minicell immunisations. Mice (n=1/condition) were immunised s.c. with ovalbumin (100 µg) plus cholera toxin (CT; 1 µg), empty minicells (10^{10}), or ovalbumin minicells (10^{10}) with or without bi-specific antibodies targeting DEC205. At various time-points (24h to 48h) post-immunisation draining lymph nodes were harvested and stained for MHCII and CD11c receptors then analysed by flow cytometry. Migrating dendritic cells were classified based on high expression of both MHCII and CD11c high. Data shows the frequency of migrating dendritic cells.

To further assess whether these mDCs could take-up, process and display target antigen epitopes, an *in vitro* experiment examined epitope-specific $CD8^+$ or $CD4^+$ T cell proliferation using APCs from the DLN of immunised mice. OVA minicells were injected into mice (n=5/group), then based on the earlier results (Figure 40), mDCs were harvested at 24 h and incubated with CFSE stained OTI $CD8^+$ or OTII $CD4^+$ T cells. The number of $CD11c^+$ $MHCII^+$ CD103 high and low cells harvested form DLNs were too low for individual analysis, so the lymphocytes for each group were pooled for assay. After 72 h, proliferation could only be detected in the positive control mice immunised with ovalbumin (100 µg) with CT (Table 8). Proliferation could not be detected in any mice that had received ovalbumin minicells.

Table 8: MFI of CFSE stained OTI and OTII cells following in *vitro* stimulation with $CD11c^+$ $MHCII^+$ CD103 high and low cells.

Immunisation group	OTI		OTII	
	$CD103^{Low}$	$CD103^{High}$	$CD103^{Low}$	$CD103^{High}$
PBS + CT	3088	3087	2537	2535
Ovalbumin + CT	428	341	213	2255
Empty minicells	3089	3025	2554	2535
Empty+DEC205 BsAb	3146	3002	2554	2532
Empty+NS BsAb	3146	3034	2535	2566
Ova minicells	3168	3111	2526	2577
Ova minicells+DEC205 BsAb	3161	3108	2534	2587
Ova minicells+NS BsAb	3165	3155	2529	2567

To confirm that this lack of detectable proliferation was not a timing issue since all DLNs removed at 24 h post-immunisation, in a subsequent experiment mice (n=1/condition) were immunised with ovalbumin minicells at 6 hourly intervals between 24 h and 48 h before harvesting DLNs. DLN single cell suspensions were incubated with CFSE stained OTI or OTII cells and the MFI of CFSE was determined (Table 9). Consistent with the previous study, proliferation was only detected with ovalbumin (100 µg) co-administered with CT, with no detectable proliferation in any of the minicell immunised mice.

Table 9: MFI of CFSE stained OTI and OTII cells following *in vitro* stimulation with cells from DLNs

Immunisation group	OTI		OTII	
	Day 3	Day 5	Day 3	Day 5
PBS	19200	14100	18700	16800
Ovalbumin + CT	1827	398	3040	335
Empty minicells	18600	14000	20600	15700
Ova minicells 48h	18700	13700	18900	17100
Ova minicells 42h	19700	14200	19400	16900
Ova minicells 36h	19100	11600	19600	15800
Ova minicells 30h	19600	13200	20000	16700
Ova minicells 24h	19300	12600	19800	16800
Ova minicells+DEC205 BsAb 48h	19100	13600	18300	17200
Ova minicells+DEC205 BsAb 42h	19400	14800	19500	16600
Ova minicells+DEC205 BsAb 36h	19900	14600	19300	16600
Ova minicells+DEC205 BsAb 30h	19300	12800	19700	17900
Ova minicells+DEC205 BsAb 24h	20700	12100	19600	17800

5.3.2. Evaluation of ovalbumin minicells

5.3.2.1. Cell-mediated immune responses

To assess the ability of ovalbumin packaged minicells to be processed, presented and recognised by OTI $CD8^+$ T cells ($OVA_{257-264}$) and OTII $CD4^+$ T cells ($OVA_{232-339}$), an adoptive transfer experiment quantified the frequency of donor cells over three immunisations. The frequency of the transferred cells (Figure 41), distinguishable by the CD45.2 (Ly5.2) allele, was determined in peripheral blood samples collected post-immunisation.

Ovalbumin protein (100 µg/dose) co-administered with either CT or empty minicells resulted in significant increases in donor cell frequency after the 2^{nd} (OVA + CT $p<0.01$) or 3^{rd} dose (OVA + CT $p<0.0001$: OVA + Empty $p<0.05$) with increases detected after each dose. Whilst the data indicates similar proliferation mean values with both of these groups, there was a greater variance within the ovalbumin + empty minicell group (Figure 41).

The requirement for an adjuvant in this system was indicated by the failure of ovalbumin alone (100 µg) to generate significant increases in the frequency of donor cells (Figure 41). The minicell component of this platform has adjuvant properties as demonstrated by the ovalbumin + empty minicells. Despite this, OVA minicells administered with or without bi-specific antibodies to DEC205 failed to generate significant increases in frequency of transferred cells. A reasonable assumption was formed that this may be a result of the low ovalbumin dose within the minicells which was approximately 0.1 µg. This was evaluated in a subsequent ovalbumin dose titration experiment (section 5.3.3).

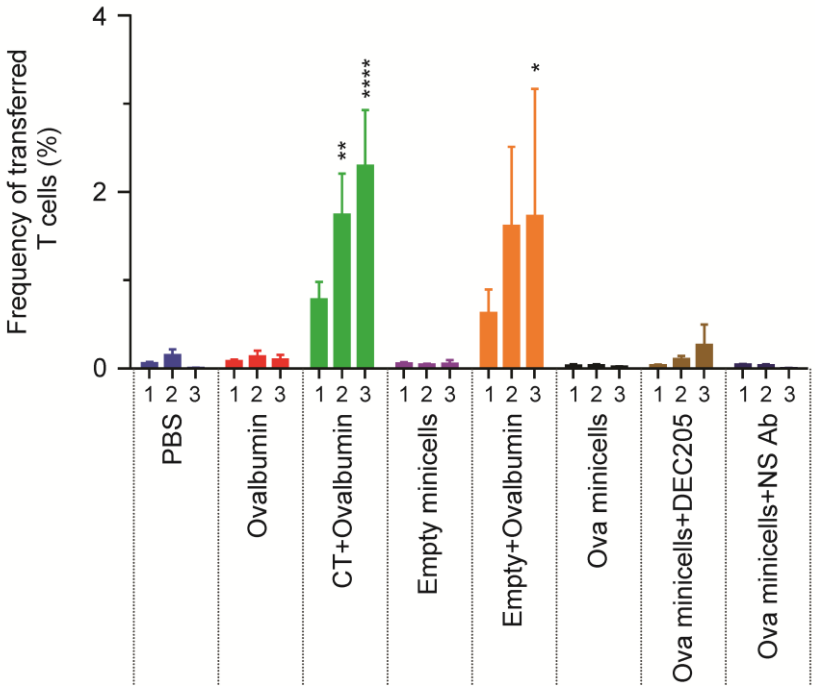

Figure 41: Frequency of adoptively transferred T cells in blood post-immunisation. Mice (n=4-5/group) received an i.v. transfer of OTI $CD8^+$ and OTII $CD4^+$ T cells (0.3 x 10^6 cells of each cell type) followed by three s.c. immunisations at 2 week intervals with either OVA minicells (10^{10}) with and without bi-specific antibodies to DEC205 or a non-specific target, empty minicells (10^{10}), or ovalbumin protein (100 µg) alone or co-administered with either CT (1 µg) or with empty minicells (10^{10}). Blood samples collected 12 days (dose 1 and 2) or 5 days (dose 3) post-immunisation were stained to detect adoptively transferred cells ($CD45.2^+V\alpha2^+$) and analysed by flow cytometry. Data is presented as mean and SEM of the frequency of transferred T cells post-immunisation (1, 2 or 3). Statistical significance was determined with log transformed data as compared to the PBS group using one-way ANOVA followed by Bonferroni's post-test $p<0.05$ *, $p<0.01$ **, $p<0.001$ *** and $p<0.0001$ ****.

To determine if the observed donor cell frequency in the blood was consistent with that within the DLN and spleen, site-specific samples were analysed 6 days after the final immunisation (Figure 42). The profile of donor cell frequency in the blood was consistent with the final dose samples taken 5 days after the final immunisation (Figure 41) with the exception of the adjuvanted ovalbumin groups. The donor cell frequency in those groups had increased approximately 2-fold in the day between taking the blood samples (Figure 42A). This suggests that either donor cell proliferation continued after 5 days or that cells were further stimulated by the presence of SIINFEKL peptide-coated cells administered for the *in vivo* CTL assay. There was significantly lower numbers of donor cells within the DLN of the empty minicells plus ovalbumin group compared with the CT adjuvanted group ($p<0.0001$),

and this did result in significantly different killing ability as determined by the CTL assay (Figure 42B). OVA minicells and ovalbumin (100 µg) without adjuvant did not induce significant CTL responses (Figure 42B).

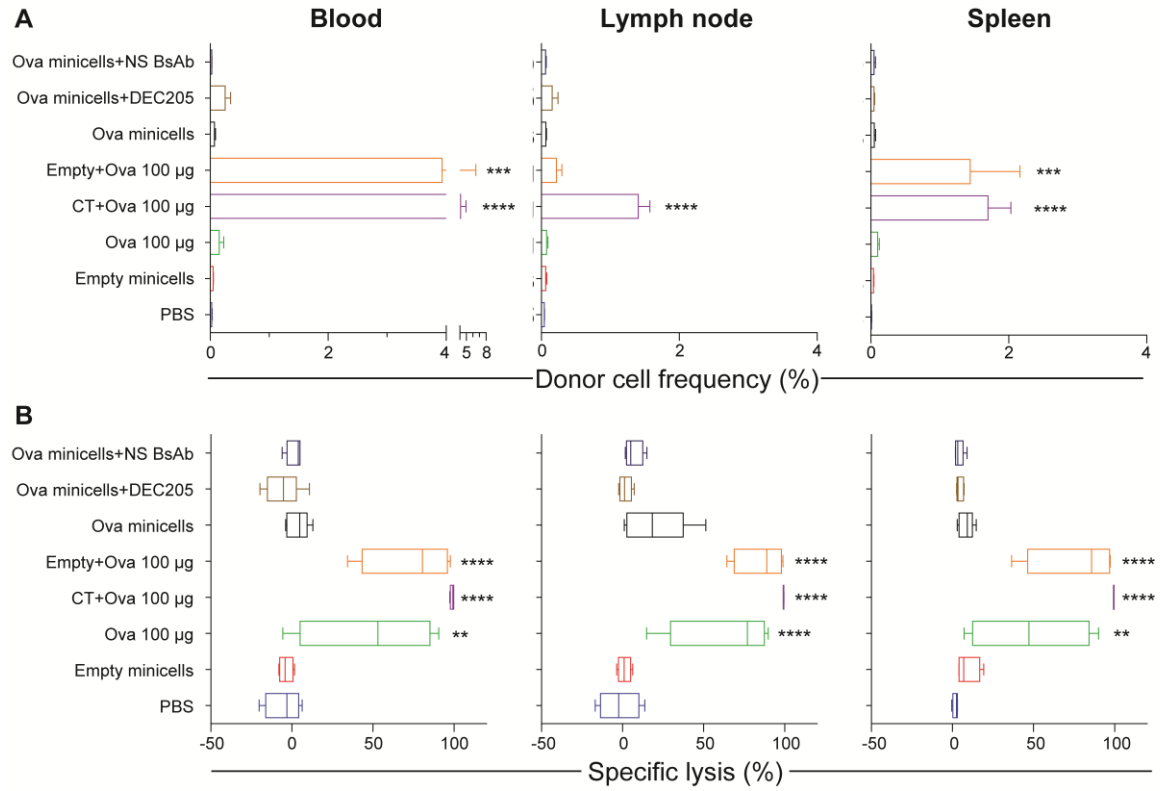

Figure 42: Frequency of adoptively transferred T cells and *in vivo* target cell lysis. Mice (n=4-5/group) received an i.v adoptive transfer of cells and immunisations as previously described (Figure 44). Six days after the final immunisation mice received an i.v. transfer of naive splenocytes with and without SIINFEKL peptide coating and differentially stained with VPD450 (4.75 x 10^6 of each high and low stained cells). After 24 h spleen, draining lymph nodes and blood were harvested and cells stained to detect adoptively transferred cells ($CD45.2^+V\alpha2^+$) and analysed by flow cytometry. (A) Site-specific frequency of donor cells is presented as mean and SEM. (B) SIINFEKL coated-specific cellular lysis is presented in box and whiskers plots. Statistical significance was determined with log transformed data as compared to the PBS group using one-way ANOVA with Bonferroni's post-hoc test $p<0.05$ *, $p<0.01$ **, $p<0.001$ *** and $p<0.0001$ ****.

Whilst OVA minicells did not induce proliferation of adoptively transferred cells (Figure 42A), it was possible that endogenous $CD8^+$ T cell populations may have been activated by the immunisations. To assess this, mice received an i.v. transfer of naive PTP mice splenocytes pre-incubated with or without SIINFEKL peptide and differentially stained with the VPD450 dye which is retained by viable cells. Cells harvested from the blood, draining lymph nodes and spleen were analysed for the

frequency of donor derived cells (Figure 42A) and the specific lysis of SIINFEKL coated cells (Figure 42B). Non-adjuvanted ovalbumin generated an antigen-specific cellular response despite its inefficiency in stimulating proliferation of the adoptively transferred T cells. In the non-adjuvanted ovalbumin group, significant antigen-specific lysis was evident in each sample site ($p<0.01$ – $p<0.001$) although there was high intra-group variability (Figure 42B). Immunisations with ovalbumin when co-administered with CT or empty minicells induced significant lysis of SIINFEKL target cells at each sample site ($p<0.0001$). Ovalbumin with CT was highly effective, inducing 98.8%, 99.2% and 99.4% of target cell lysis in the blood, DLN and spleen respectively. OVA minicells with or without BsAbs were ineffective at inducing either proliferation of donor cells or generating a cytolytic response.

5.3.2.2. Antibody responses

To evaluate the capacity of ovalbumin packaged minicells to induce ovalbumin-specific antibody responses, sera collected after the final immunisation was used in an ELISA with ovalbumin protein as the capture antigen (Figure 43). Data show that OVA minicells with or without BsAbs targeting DEC205 or a non-specific target were able to induce a significant anti-ovalbumin IgG responses. The distribution of endpoint titres within these groups had high variability with titres ranging from 400 to 409,600 (Ns BsAb), 12,800 to 204,800 (DEC205) and 12,800 to 819,200 (OVA minicells), with inter-group analysis not detecting significant differences.

Ovalbumin protein (100 µg) induced significant antibody responses compared to the PBS group ($p<0.0001$). These titres were significantly increased with the co-administration of CT ($p<0.0001$) or empty minicells ($p<0.05$) as an adjuvant, with CT clearly a potent adjuvant with each endpoint titre recorded at 3,276,800. Endpoint titre comparisons between ovalbumin with or without empty minicells, and the OVA minicell group were not significant despite the OVA minicells (10^{10}) having a 0.1 µg ovalbumin protein load.

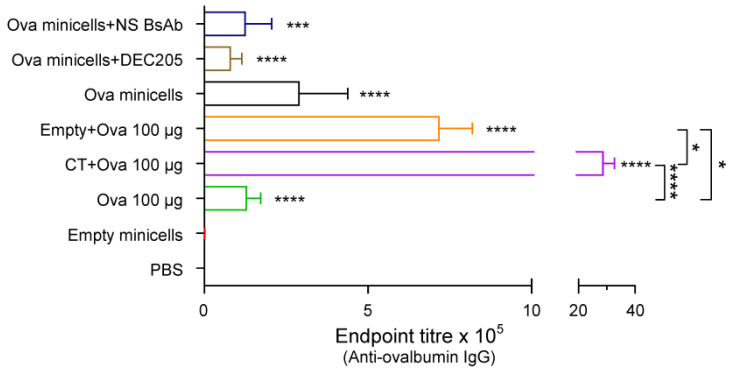

Figure 43: Ovalbumin-specific IgG responses following immunisations. Mice (n=4-5/group) received an i.v adoptive transfer of cells and immunisations as previously described (Figure 44). Sera collected 5 days after final immunisation was used to detect anti-ovalbumin IgG responses by ELISA with data presented as mean and SEM endpoint titres. Statistical significance was determined with log transformed data comparing groups to the PBS group and between adjuvanted groups using one-way ANOVA with Bonferroni's post-hoc test $p<0.05$ *, $p<0.01$ **, $p<0.001$ *** and $p<0.0001$ ****.

5.3.3. Evaluation of ovalbumin protein dose-related responses and minicell adjuvant effects

The low antigen load in OVA minicells may be the reason why there was a minimal induction of T cell responses to OVA minicell immunisations (section 5.3.2). To test the effect of dose on cellular and antibody responses, a dose titration of ovalbumin protein (0.1, 10 and 100 µg/dose) with or without empty minicells or CT was conducted. To evaluate whether factors other than LPS influenced the adjuvant effect of minicells, one group received ovalbumin (100 µg) with a 10^{10} minicell equivalent of LPS. OVA minicells were administered with or without BsAbs to the Clec9a receptor to evaluate the platform efficacy with an alternate target than DEC205 used in the previous study.

5.3.3.1. Cell-mediated immune responses

Ovalbumin dose related responses

To compare the effect of ovalbumin dose (antigen load) on antigen-specific cellular responses, the frequency of transferred cells was determined in blood samples collected after each immunisation (Figure 44). A dose related response was detected

with a step-wise increase in the frequency of transferred cells as ovalbumin doses were increased from 0.1 µg to 10 µg and again to 100 µg with or without adjuvant. An ovalbumin dose of 0.1 µg was insufficient to cause an increase in donor cells despite the inclusion of adjuvant.

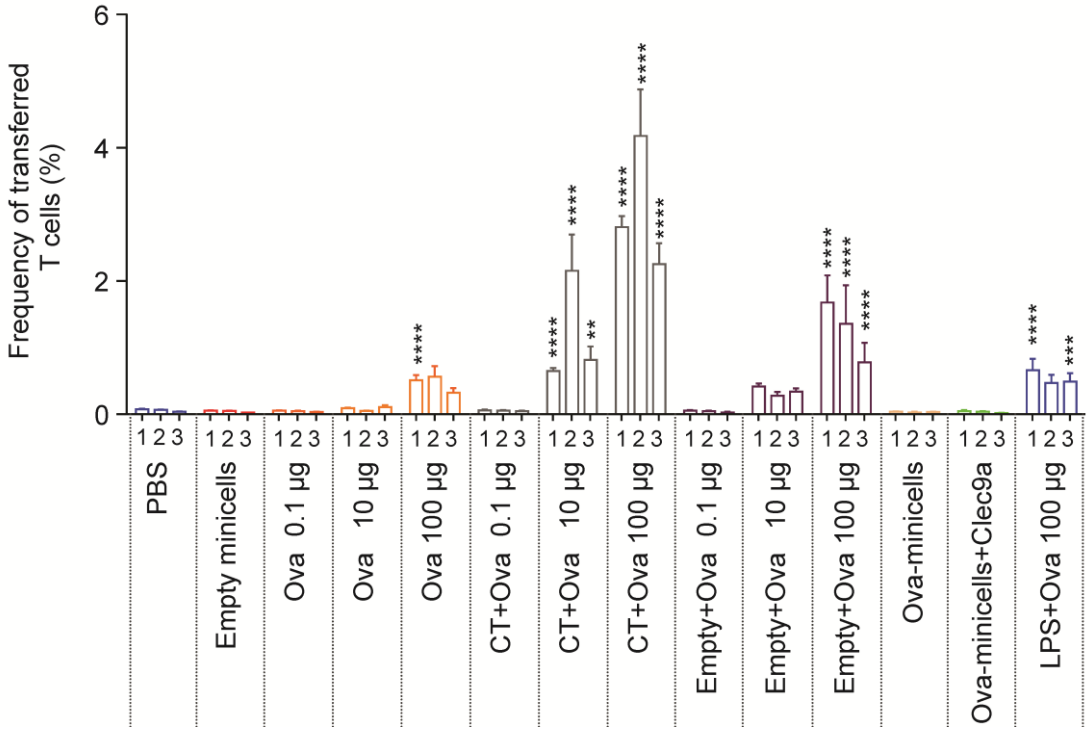

Figure 44: Frequency of adoptively transferred T cells in blood post-immunisation. Mice (n=5/group) received an i.v. transfer of OTI $CD8^+$ and OTII $CD4^+$ T cells (0.5 x 10^6 cells of each cell type) followed by three s.c. immunisations at 2 week intervals with either OVA minicells (10^{10}) with and without bi-specific antibodies to Clec9a or a non-specific target, empty minicells (10^{10}), or ovalbumin protein (100 µg, 10 µg or 0.1 µg/dose) alone or co-administered with either cholera toxin (CT; 1 µg),or with empty minicells (10^{10}) or ovalbumin protein (100 µg) with LPS (0.75 µg). Blood samples collected 12 days (dose 1 and 2) or 5 days (dose 3) post-immunisation were stained to detect adoptively transferred cells ($CD45.2^+V\alpha2^+$) and analysed by flow cytometry. Data is presented as mean and SEM of the frequency of transferred T cells post-immunisation (1, 2 or 3). Statistical significance was determined with log transformed data as compared to the PBS group using one-way ANOVA followed by Bonferroni's post-hoc test $p<0.05$ *, $p<0.01$ **, $p<0.001$ *** and $p<0.0001$ ****.

A dose dependant increase in donor cell frequency was also detected in the blood, DLN and spleen following the final immunisation (Figure 45A). In each sample site, an ovalbumin dose of 100 µg significantly increased donor cell frequencies as compared to a 10 µg dose when doses were co-administered with CT or empty minicells ($p<0.05$ to $p<0.0001$). A 10 µg ovalbumin dose was sufficient to induce

significant increases in adoptively transferred cell frequency when co-administered with empty minicells (in blood $p<0.01$and DLNs $p<0.05$), or with CT in all sample sites ($p<0.0001$). In contrast immunisations with 0.1 µg of ovalbumin with and without adjuvant did not induce significant increases in donor cell frequency in any sample site.

A trend of increased antigen-specific cellular lysis with dose was observed between the different ovalbumin dose groups whether administered with or without adjuvants (Figure 45B). With a 100 µg ovalbumin dose with or without adjuvant, target-specific lysis was very efficient with significance detected at each sample site ($p<0.0001$). When the ovalbumin was reduced to 10 µg per dose, target-specific lysis was still very efficient in all groups ($p<0.0001$), however, the non-adjuvanted group was significantly less effective than the 100 µg dose responses ($p<0.01$ in DLN and $p<0.0001$ in blood and spleen). At the lowest dose using 0.1 µg of ovalbumin, significant lysis was only detected in the DLN sample from mice when ovalbumin was co-administered with CT ($p<0.0001$).

Adjuvant capacity of minicells as compared to CT or LPS

To assess of adjuvant capacity of minicells and to compare this adjuvant effect to CT or an equivalent dose of LPS, mice were immunised with ovalbumin with or without each adjuvant. The frequency of transferred cells was quantified in blood following each immunisation (Figure 44). At a 100 µg dose of ovalbumin, the co-administration of empty minicells significantly increased the frequency of transferred cells ($p<0.0001$) compared to the PBS control and when compared to ovalbumin alone after the first dose only ($p<0.05$). At doses of 10 µg and 0.1 µg of ovalbumin, empty minicells were not sufficient to significantly increase responses.

CT is a highly potent adjuvant[368] and was the only adjuvant capable of significantly increasing donor cell frequency at 10 µg ovalbumin doses (Figure 44). When assessed at 100 µg ovalbumin dose, following the final immunisation, the CT induced donor cell frequency was not significantly different to the ovalbumin plus empty minicells. However, CT induced significant increases as compared to ovalbumin alone ($p<0.05$) or with LPS ($p<0.05$). Empty minicells and LPS adjuvanted responses were statistically similar.

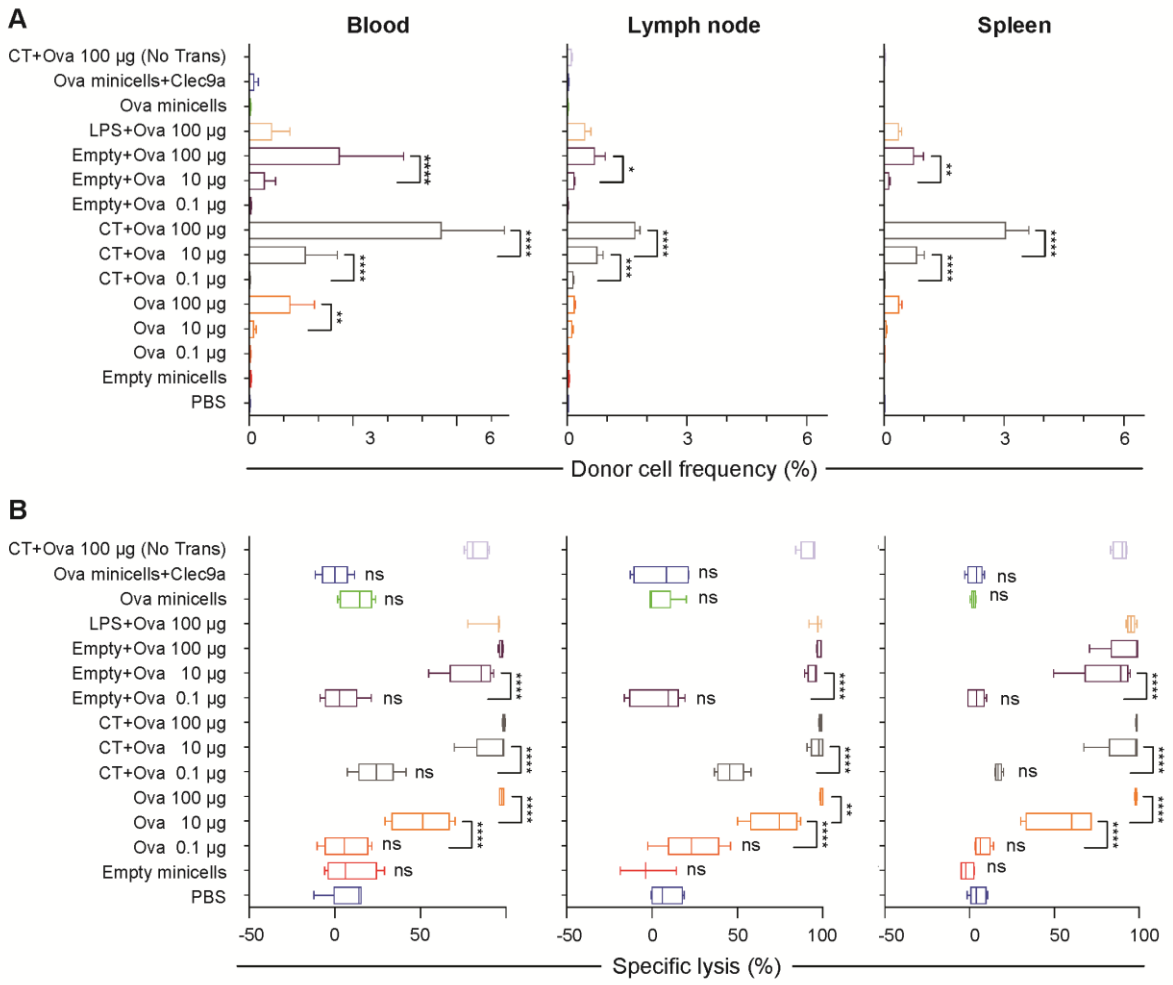

Figure 45: Frequency of adoptively transferred T cells and *in vivo* target cell lysis. Mice (n=5/group) received an i.v. adoptive transfer of cells and immunisations as previously described (Figure 44). Six days after the final immunisation mice received an i.v. transfer of naive cells with and without SIINFEKL peptide coating and differentially stained with VPD450 (4.5×10^6 of each). After 24 h spleen, draining lymph nodes and blood were harvested and cells stained to detect adoptively transferred cells ($CD45.2^+V\alpha2^+$) and analysed by flow cytometry. Site-specific frequency of donor cells is presented as mean and SEM (A). SIINFEKL coated-specific cellular lysis is presented in a min to max box and whiskers plot (B). Statistical significance was determined with (A) and without (B) log transformed data comparing successive ovalbumin doses within groups using one-way ANOVA with Bonferroni's post-hoc test $p<0.05$ *, $p<0.01$ **, $p<0.001$ *** and $p<0.0001$ ****.

Empty minicells were shown to significantly increase donor cell frequency in blood, DLNs and spleen following the final immunisation (Figure 45A) with 100 µg of ovalbumin ($p<0.0001$). However, when compared to ovalbumin alone, or ovalbumin with LPS, there were no significant differences. At a 100 µg ovalbumin dose, CT was significantly better at inducing increases in donor cell frequency than ovalbumin

alone or with empty minicells or LPS in each sample site (p<0.05 to p<0.0001), with the exception of ovalbumin with empty minicells in the blood.

Specific cell lysis (Figure 45B) was very efficient when a 100 µg ovalbumin dose was administered with and without adjuvant, with no significant differences detected between these groups. Empty minicells with 10 µg ovalbumin doses were able to induce significant target cell lysis as compared to the PBS control in each sample site (p<0.0001), however, increases were not significant when compare to the 10 µg ovalbumin only group. This indicates that the response was due to the ovalbumin component and not due to the effect of minicells. CT was an effective adjuvant at 100 µg and 10 µg ovalbumin doses (p<0.0001) and was the only group capable of significant lysis at the 0.1 µg ovalbumin dose, although this was only significant in the DLN samples (p<0.0001).

Ovalbumin minicells and targeting

OVA minicells alone or targeted to Clec9a failed to increase donor cell frequency in the blood during the course of immunisations (Figure 44) or in blood, DLNs or spleen after the final immunisation (Figure 45A). These immunisations were also ineffective at generating significant target-specific cell lysis (Figure 45B).

Endogenous versus exogenous specific lysis

To determine if the antigen-specific cell lysis was due endogenous or exogenous adoptively transferred T cells, one group of mice did not receive any OTI or OTII cells prior to immunisations. Groups with or without transferred cells were immunised with ovalbumin (100 µg/dose) with CT. Following three immunisations, the ability to lyse antigen-specific cell targets was evaluated (Figure 45B). Efficient target cell lysis was observed in the absence of adoptively transferred cells (no trans) in blood (82.7%), DLN (92.0%) and spleen (89.0%), however, lysis was lower than in those mice with transferred cells (98.9%, 98.8% and 98.7% respectively). Significance differences between these groups were detected in blood samples (p<0.05) but not DLN or spleen sites. These data suggest that it is not exogenous cells alone which are active in cell lysis, since target cell lysis could induced in mice without transferred

OTI $CD8^+$ T cells. The data does not, however, quantify the proportion of cells lysed by endogenous and exogenous cells.

5.3.3.2. Antibody responses

Minicell induced ovalbumin-specific antibody responses were assessed by ELISA using ovalbumin as a capture antigen, and sera collected after the 3rd immunisation (Figure 46). Whilst 100 µg of ovalbumin alone was able to induce significant anti-ovalbumin IgG responses (p<0.0001) as compared to the PBS control, significantly higher antibody titres were detected in mice where the same ovalbumin dose was co-administered with empty minicells (p<0.001), CT (p<0.0001) or LPS (p<0.0001). Ovalbumin alone or co-administered with empty minicells had a trend of decreased titres as the dose increased from 10 µg to 100 µg. This was reversed when CT was co-administered and significant increases were detected (p<0.0001). The highest antibody titres were recorded in mice which did not receive adoptively transferred T cells although this increase was not statistically significant relative to the comparative group which did receive OTI and OTII cells. Furthermore, antibody titres did not follow the same dose-related increases as observed in cellular responses.

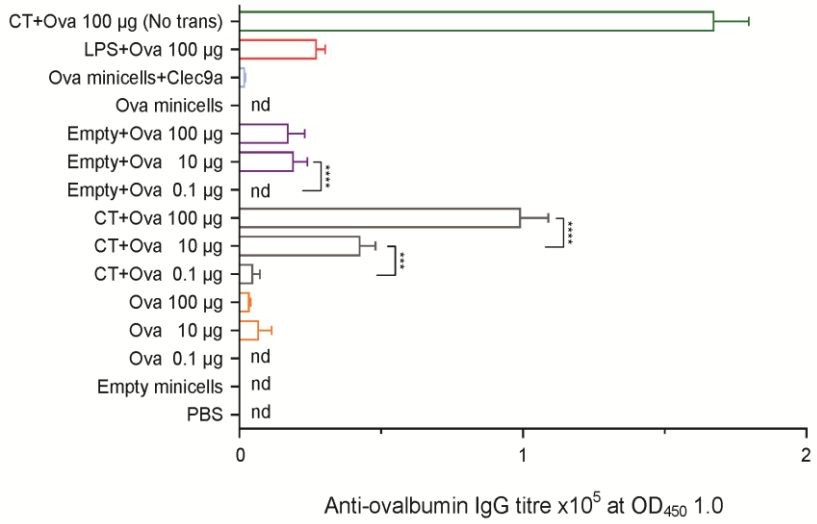

Figure 46: Ovalbumin-specific IgG responses following immunisations. Mice (n=5/group) received an i.v. adoptive transfer of cells immunisations as previously described (Figure 44). Sera collected 5 days after final immunisation was used to detect anti-ovalbumin IgG responses by ELISA with data presented as mean + SEM of the calculated titre where OD_{450} equalled 1.0. Statistical significance was determined with log transformed data comparing successive ovalbumin doses within groups using one-way ANOVA with Bonferroni's post-hoc test p<0.05 *, p<0.01 **, p<0.001 *** and p<0.0001 ****. (nd, nil detected)

All mice immunised with OVA minicells alone failed to reach an OD_{450} of 1.0, and when OVA minicells were targeted to Clec9, detected antibody titres were low. Whilst the OD_{450} value of 1.0 was arbitrarily picked as a reference point for this analysis, OVA minicell induced responses were near background in ELISA at a 1:200 serum dilution and would not have reached a level of positivity even if the threshold was reduced to an OD450 of 0.5. This contrasts with earlier data (Figure 43) where OVA minicells induced reasonable endpoint antibody titres. To compare antibody titres between experiments, the earlier data was used to calculate the titre at OD_{450} equal to 1.0 (Table 10). For each OVA minicell group, the ELISA was then repeated using the serum from both experiments simultaneously and confirmed both data sets. The reason for the discrepancy between the two experiments is not clear. The minicells used to immunise the mice had come from the same batch of purified minicells and no other logical explanation was apparent. In control groups which did not get ovalbumin, and groups immunised with 0.1 µg of ovalbumin (except with CT), an OD_{450} equal to 1.0 was not achievable and nil detected was recorded.

Table 10: Comparative immunisation group mean results of calculated titre at OD_{450} = 1.0

Immunisations	**Experiment 1 (3.4.3)**	**Experiment 2 (5.3.3)**
Ovalbumin (100 µg)	3300	3272
CT + ovalbumin (100 µg)	177107	99001
Empty + ovalbumin (100 µg)	132973	17061
OVA minicells	8441	●●●●●
OVA minicells + DEC205	2321	N/A
OVA minicells + Clec9a	N/A	1694 ●●
OVA minicells + NS BsAb	4978 ●	N/A

● = each represents a single mouse where no value could be calculated

5.3.4. Evaluation of *Plasmodium yoelii* Apical Membrane Antigen-1 packaged bacterial minicells

The ovalbumin model allowed for assessment of the capacity of minicells to induce cell-mediated immune and antibody responses, but it did not elicit information about their protective capacity. Using the malaria model, and the *Py*AMA-1 protein as the antigen, experiments were designed to determine cellular activation and cytokine expression post-sporozoite challenge, parasite-specific antibody responses post-immunisation and during infection, as well as protective capacity. An additional benefit of this model was that the *Py*AMA-1 protein antigen load was able to be increased to 1.0 μg/10^{10} minicells, a ten-fold increase to the antigen load in the OVA minicell studies. As noted above, the low ovalbumin antigen load could have been responsible for the lack of immune responses detected in those studies.

5.3.4.1. Cell-mediated immune responses

Cytokines

To quantify cytokine levels in circulation, pooled serum from mice collected pre-challenge (Day 0) and post-challenge (Days 2 to 10) was assayed using CBA for a range of Th1 and Th2 cytokines. A spike in IFN-γ was detected at days 7 and 8 in each group (Figure 47A). TNF and IL-6 responses rose during the course of infection, however, the profile of those cytokines were consistent between each immunisation group, so not antigen-specific. IL-1β, IL-2, IL-4, IL-5, IL-10, IL-12*p*70 and IL-13 were also assayed, however, cytokine levels remained close to the limit of detection for the assay.

Based on the IFN-γ peaks at days 7 and 8 with the pooled samples, individual samples from these days were assayed for IFN-γ, as well as TNF and IL-6 cytokines (Figure 47B). The CBA data indicates that in some of the AMA1 minicell immunised mice with or without BsAbs, there was increased IFN-γ responses although these differences did not reach significance in comparison to other groups. Mice which were not infected (Figure 51B) had very low IFN-γ responses which were at or near

detection levels (Figure 47B). No significant group differences were detected for TNF or IL-6 cytokines.

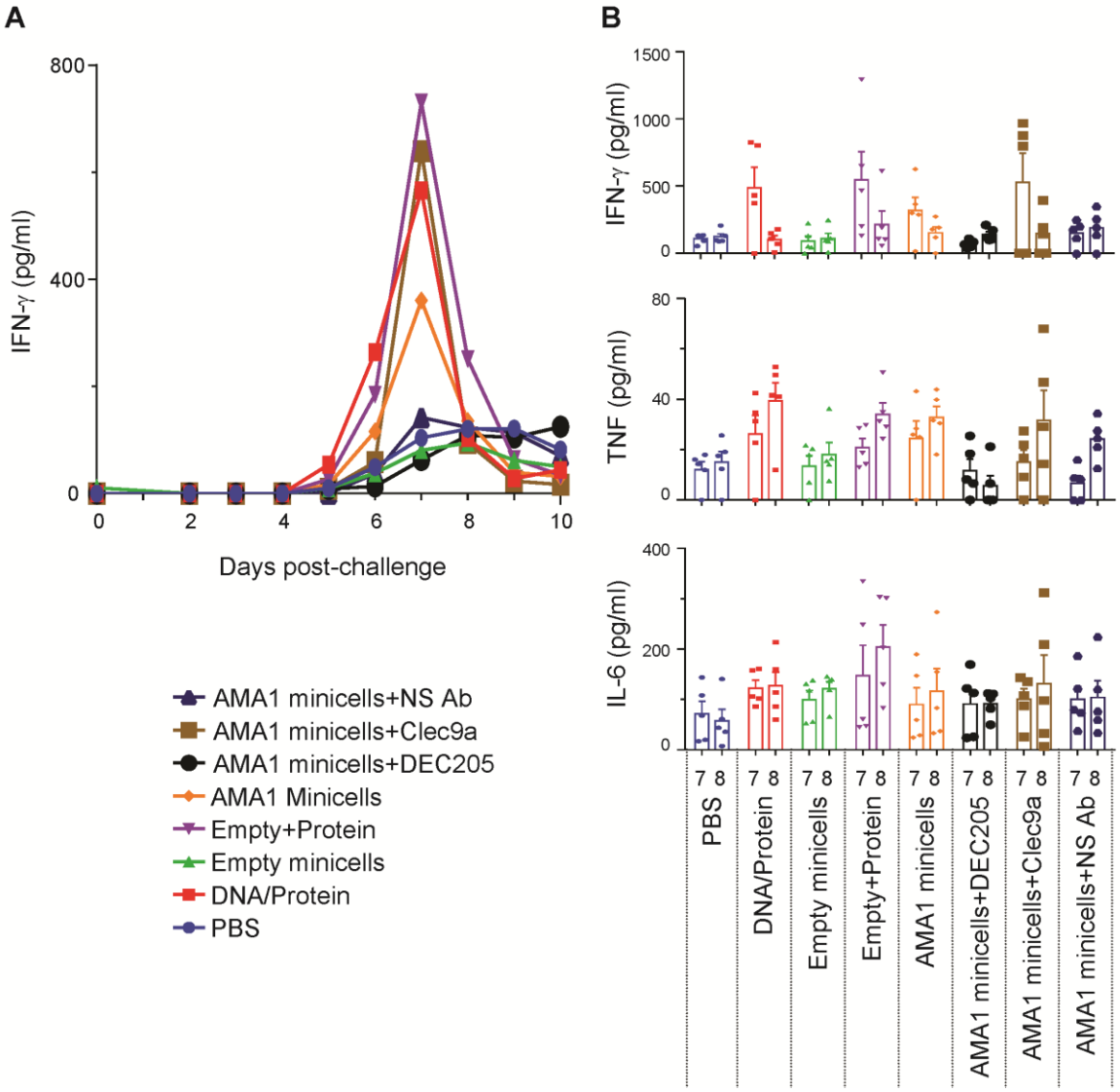

Figure 47: Circulating IFN-γ, TNF and IL-6 cytokine levels following immunisation and sporozoite challenge. Mice (n=5/group) received three s.c. immunisations at 3 week intervals with either AMA1 minicells (10^{10}) with and without bi-specific antibodies to DEC205, Clec9a or a non-specific target, empty minicells (10^{10}) with and without *Py*AMA-1 protein (1 µg), or a homologous DNA prime with *Py*AMA-1 protein boost regimen. Ten days after the final immunisation mice were challenged by i.v. injection with live *P. yoelii* 17XNL sporozoites (10^3). Post-challenge sera was analysed using CBA for cytokine responses. (A) Pooled samples from pre-challenge to day 10 is shown for IFN-γ, and (B) individual samples on days 7 and 8 were used to quantify IFN-γ, TNF and IL-6 responses. Statistical comparisons between groups (B) using log transformed data using two-way ANOVA followed by Bonferroni's post-hoc test detected no significant variation.

White blood cell counts and activation markers

To determine whether *Py*AMA-1 loaded minicells activated and/or increased cellular response during a *Plasmodium* infection, phenotypic activation markers were assessed using blood samples collected pre- and post- sporozoite challenge. During the first 10 days of infection, $CD8^+$ and $CD4^+$ T cells, B cells, monocytes and granulocytes were stained for various activation markers, specifically PD-L1, PD1, CD11a, CD49d, CD69, CD86 and GR-1 then analysed by flow cytometry.

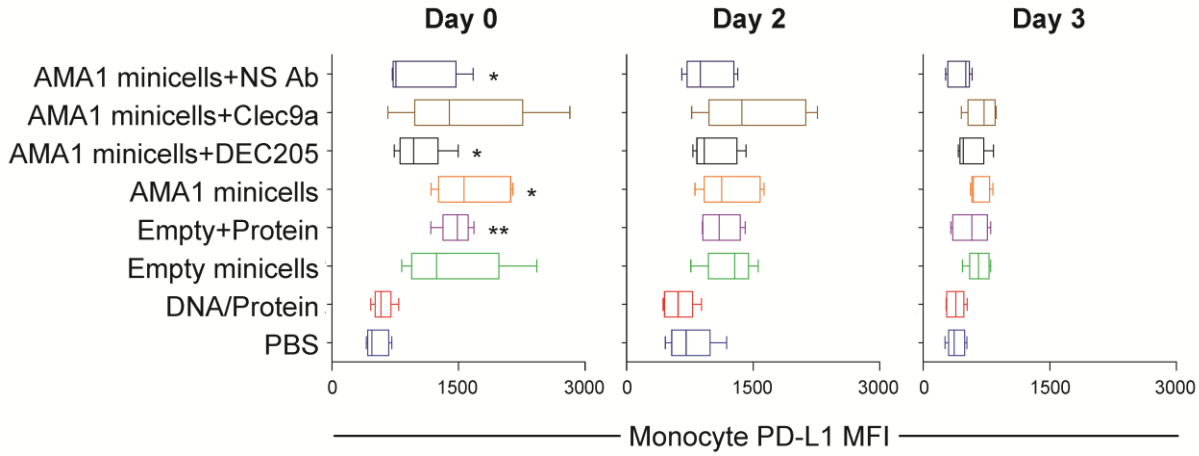

Figure 48: Monocyte PD-L1 expression following immunisation and sporozoite challenge. Mice (n=5/group) were immunised as previously described (Figure 47). Ten days after the final immunisation mice were challenged by i.v. injection with live *P. yoelii* 17XNL sporozoites (10^3). Blood collected pre- (day 0) and post-challenge (days 2 and 3) was analysed by flow cytometry with monocytes detected by FSC and SSC gating and Ly-6G (Gr-1) antibodies and programmed death-ligand 1 (PD-L1) expression levels detected by PD-L1 (CD274) antibodies. Data for days 0, 2 and 3 are shown as box and whiskers plots. Statistical comparisons to the PBS group used log transformed data using one-way ANOVA followed by Bonferroni's post-hoc test. $p<0.05$ *, $p<0.01$ **.

Monocyte PD-L1 expression was up-regulated in pre-challenge samples in all groups which received minicells (Figure 48), with significant increases detected in *Py*AMA-1 minicells alone ($p<0.05$) or targeted to DEC205 ($p<0.05$), or the non-specific antibody ($p<0.05$). This response did not appear to be antigen-specific since it was not restricted to *Py*AMA-1 minicells, with empty minicells with *Py*AMA-1 protein also having significant increased expression ($p<0.01$), and empty minicells alone had increased expression although it did not reach significance. Over the following 3 days, monocyte PD-L1 expression was reduced to levels similar to that in PBS and

DNA/protein immunised groups with no significant intergroup after Day 0. This suggests that the PD-L1 expression was not a result of any *Plasmodium*-specific antigen stimulation, but was due to the bacterial components of the minicells. This PD-L1 response was restricted to monocytes with expression on other cell types not significantly different to the PBS control group. No effect of minicells on activation markers PD1, CD11a, CD49d, CD69, CD86 and GR-1 was detected.

5.3.4.2. Antibody responses

Studies in the ovalbumin model showed that minicells could induce antigen-specific antibody responses even with a low antigen load (section 5.3.2.2). Furthermore, increases in ovalbumin from 0.1 µg to 10 µg increased titres so as to be detectible at OD_{450} = 1.0 (sections 5.3.3.2). The *Py*AMA-1 loaded minicells had an antigen load of 1 µg per 10^{10} minicell dose, and as a consequence of the higher antigen content, it was anticipated that antigen-specific antibody titres would be higher than those induced by the ovalbumin minicells. To assess antibody responses, an ELISA was conducted using *Py*AMA-1 recombinant protein produced in the RTS cell free transcription/translation reaction (section 4.2.6) as the capture antigen (Figure 49).

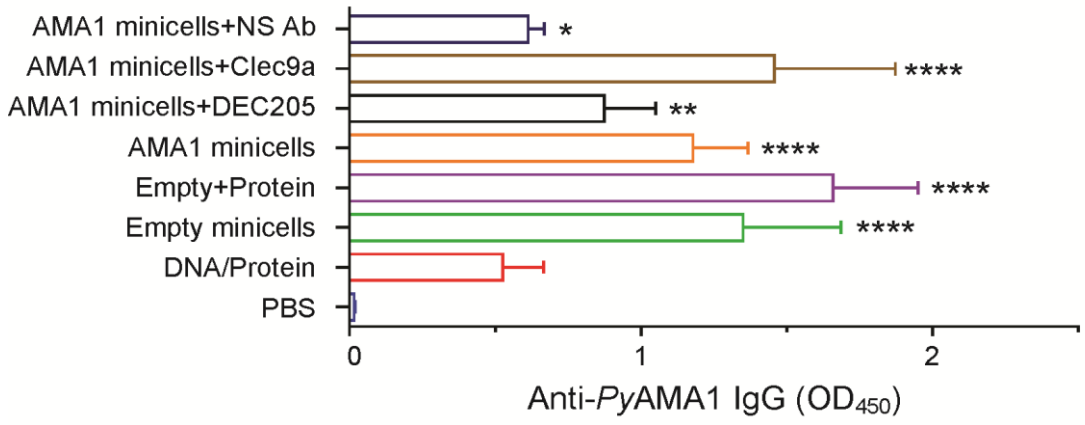

Figure 49: IgG antibodies against recombinant *Py*AMA-1 protein generated using RTS system and talon purification. Mice (n=5/group) were immunised as previously described (Figure 47). Sera collected nine days after final immunisation was diluted 1:200 then used in an ELISA against *Py*AMA-1 recombinant protein. Bars represent mean OD_{450} + SEM. Statistical comparisons to the PBS group used log transformed data using one-way ANOVA followed by Bonferroni's post-hoc test. $p<0.05$ *, $p<0.01$ ** and $p<0.0001$ ****.

All groups immunised with a minicell component had significant increases in antibody detected responses relative to the PBS control. There were no significant differences between empty minicells with or without *Py*AMA-1 protein, or any of the *Py*AMA-1 minicell immunised groups. Thus it is likely that the detected reactivity was not directed against the recombinant *Py*AMA-1, but instead a result of contamination of *E. coli* proteins from the RTS reaction kit, since significant responses (p<0.0001) from empty minicell immunisations alone were detected. Alternative sources for the *Py*AMA-1 protein were not available for further ELISA assessment.

To examine whether the *Py*AMA-1 minicell induced antibodies were parasite-specific, a flow-cytometry based IFAT was performed using *P. yoelii* blood-stage parasite extract (Figure 50). Pre-challenge sera in all minicell immunised groups had increased reactivity to the parasite extract as compared to the PBS and DNA/protein immunisation groups. The increased responses in these groups remained higher (non-significantly) than the PBS and DNA/protein immunisation groups until day 7, which coincided with the detection of parasitemia within the groups (section 5.3.4.3). To assess the antibody isotype responses IgG_1, IgG_{2a}, IgM, IgD and IgE were assayed using pre-challenge sera. Only IgG_1 isotype responses detected. IgG_1 data (Figure 50B) showed a similar response to the total IgG data at day 0 with positive responses in all minicell immunised groups. To compare IgG responses between groups over the first 22 days of infection, the AUC of IgG MFI (Figure 50C) was calculated. No significant differences between groups could be detected. Individual mouse data shows some mice with a low AUC but in each case these mice had no detectible parasitemia which accounts for the variation.

The antibody results indicate the minicells have induced a non-specific antibody response with a cross-reaction between minicells and both *Py*AMA-1 recombinant proteins and the parasite extract. Additional studies would be required to conclusively determine if *Py*AMA-1 specific antibodies have been induced by *Py*AMA-1 minicells. It is possible that a cross-reactive antigen in the minicells and either *Py*AMA-1 or other *P. yoelii* blood-stage antigens exists which has caused these results, although this has not been previously reported. An ELISA with purified recombinant *Py*AMA-1 protein may clarify the detected results, however, this protein was not available for study within the timeframe of this thesis.

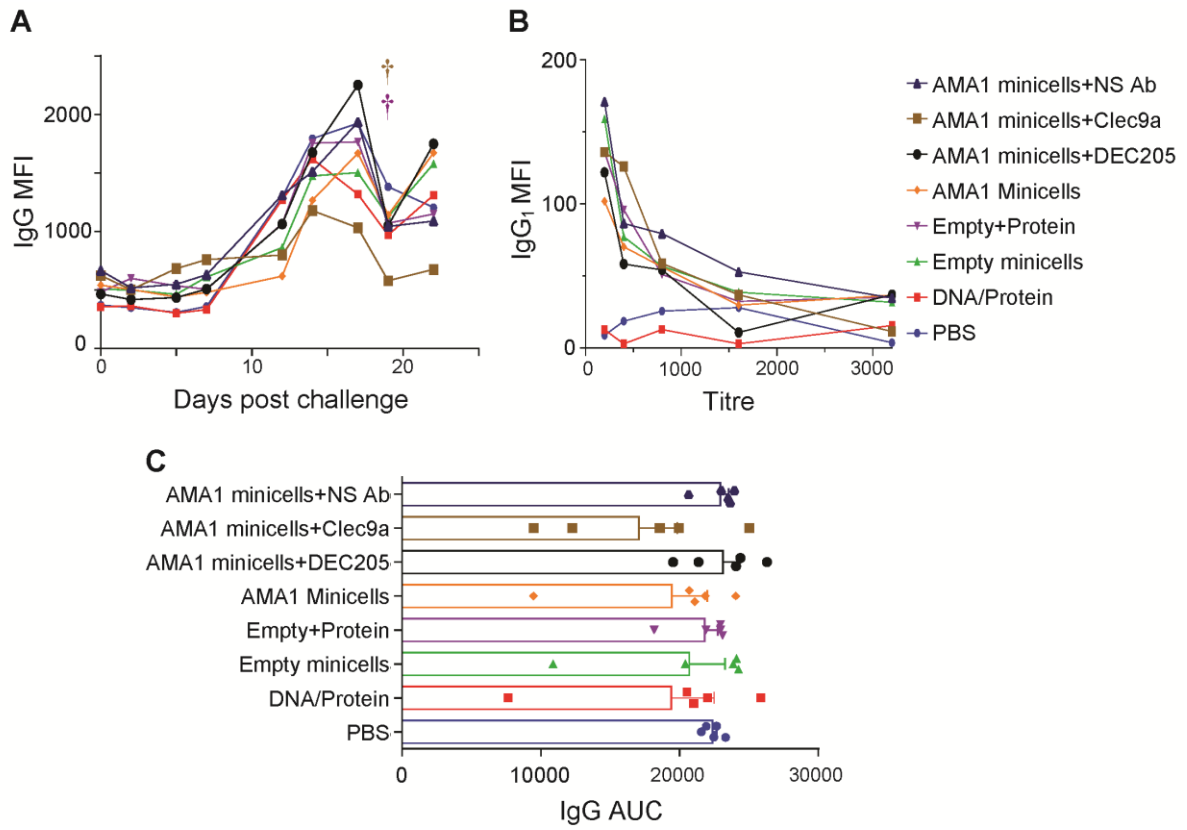

Figure 50: Serum antibodies against whole *P. yoelii* parasite extract. Mice (n=5/group) were immunised as previously described (Figure 47). Ten days after the final immunisation mice were challenged by i.v. injection with live *P. yoelii* 17XNL sporozoites (10^3). (A) Blood from individual mice diluted 1:300 was assessed for total IgG responses to *P. yoelii* blood-stage extract and the median fluorescence intensity (MFI) is presented as the group mean. (B)The MFI data of pooled pre-challenge sera in a 2-fold titration for IgG_1 responses is shown. (C) The area under the curve (AUC) of IgG MFI obtained from (A) is presented as individual mice data and mean + SEM. AUC statistical comparisons between groups used log transformed data then one-way ANOVA followed by Bonferroni's post-hoc test. No significant variation was detected. († dead mouse)

5.3.4.3. Protection

To assess the capacity of *Py*AMA-1 minicells to confer protection against sporozoite challenge, immunised mice were challenge with 1000 *P. yoelii* 17XNL sporozoites and parasitemia was measured during the course of infections using the FCAB assay. The mean parasitemia for each group (Figure 51A) shows a similar pattern for each group until day 18 post-challenge. However, four groups including AMA1 minicells targeted to DEC205 or the non-specific antibody control, empty minicells and PBS all had a one to two day delay in the onset of parasitemia. Furthermore, the

peak parasitemia detected within these groups was lower, but non-significantly less than each other group. No significant differences could be detected between immunisation groups based on the parasitemia AUC (Figure 51B).

The mean peak parasitemia in the non-immunised control (PBS) group was 13.0% which was lower than experimental challenges in other studies[283] where mean peak parasitemia was within the 30 to 40% range. Nonetheless, the parasitemia profile and the time-course of the infection appeared normal despite the lower peak.

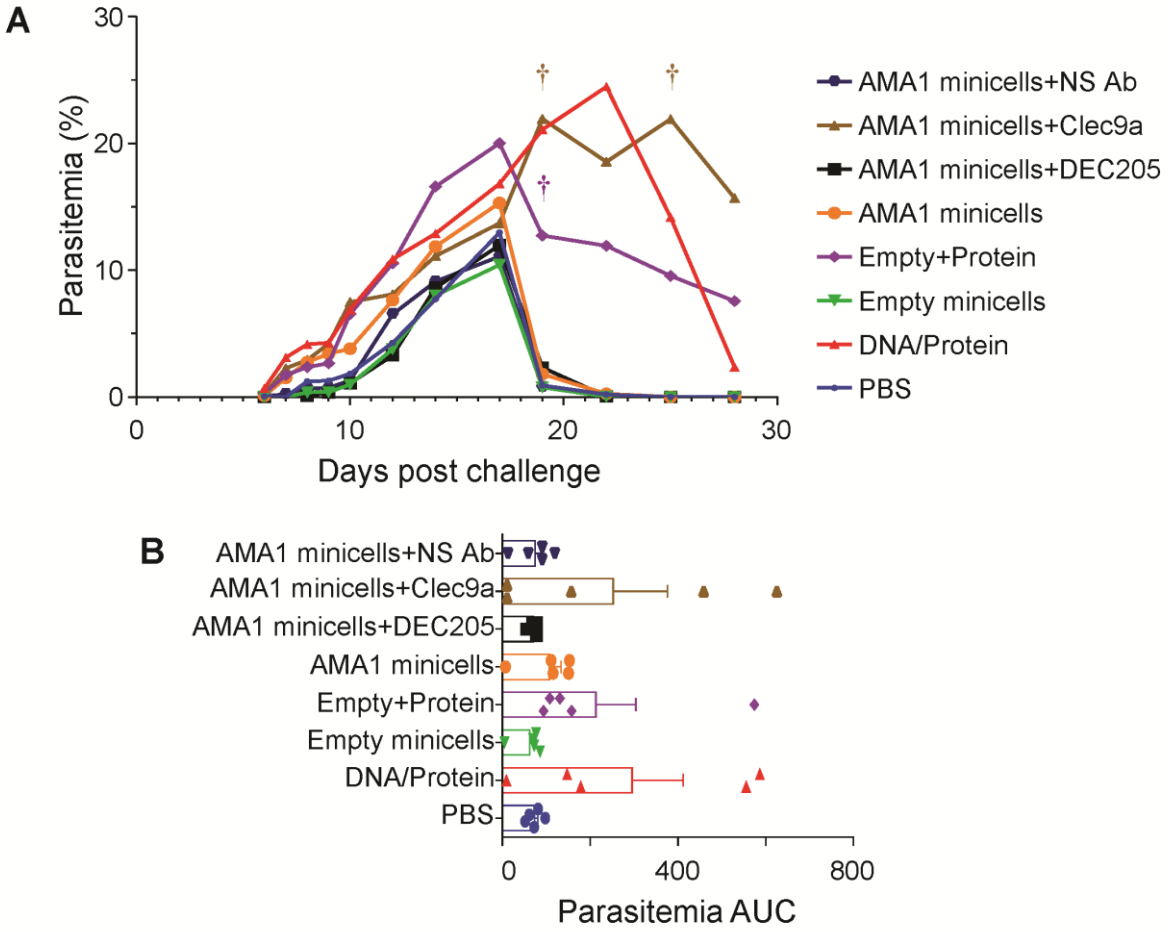

Figure 51: Parasitemia following immunisation and sporozoite challenge. Mice (n=5/group) were immunised as previously described (Figure 47). Ten days after the final immunisation mice were challenged by i.v. injection with live *P. yoelii* 17XNL sporozoites (10^3). (A) Kinetics of parasitemia and (B) area under the curve were assessed using the FCAB assay. Data is presented as group means (A) and mean and SEM with individual data points (B). AUC statistical comparisons between groups used log transformed data then one-way ANOVA followed by Bonferroni's post-hoc test. No significant variation was detected. († dead mouse).

There were six mice where parasites were not detected post-challenge. Four of these mice were in groups which received *Py*AMA-1 minicells either alone (1/5) of targeted to Clec9a (2/5) or the non-specific antibody (1/5); and another putatively protected mouse from the positive control DNA/protein (1/5), however, one mouse in the empty minicell group also had no detectable parasites (1/5). Unfortunately the absence of parasites in one mouse in the empty minicell group confounds whether protection in the other groups was actually: a result of the immunisations; due to technical reasons; or maybe it was a result of a cross-reactive antigen consistent with antibody data described above (Figure 49 and Figure 50).

5.4. Discussion

5.4.1. Targeting minicells to dendritic cells

The studies presented in this chapter were designed to evaluate the immunogenicity and protective capacity of antigen loaded minicells, and to see if responses could be enhanced by directly targeting DCs. We speculated, that by targeting DC surface receptors including DEC205 or Clec9a that receptor-mediated endocytosis would result in increased DC up-take of minicells, and subsequently a more robust immunological response. In order to test this, mice were immunised with minicells loaded with ovalbumin or *Py*AMA-1 proteins and plasmid DNA, with or without BsAbs to the DC targets.

Previous studies using phagocytic cell lines RAW264, J774 and DC2.4 have shown that these cells are inefficient in the uptake of minicells with a transfection efficiency of between 0.002% and 0.2%[236]. However, even non-phagocytic cells can be induced to take up minicells with the inclusion of targeting molecules[235] including BsAbs[227,238]. We were unable to assess the targeting strategy using RAW264, J774 or DC2.4 because neither cell has the DEC205 or Clec9a receptors. Instead, assessment of minicell uptake, migration and presentation was done by injecting naive mice with ovalbumin loaded minicells ± BsAbs and then harvesting their DLNs to determine if mDCs were capable of inducing the proliferation of transgenic OTI $CD8^+$ T cells or OTII $CD4^+$ T cells *in vitro*. At 24 h post-injection there was an increase in $CD11c^{high}$ $MHCII^{high}$ mDC population within the DLNs (Figure 40)

including the presence of $CD103^+$ dermal DCs (dDCs) (Table 8), which is consistent with previous studies[368]. These dDCs migrate from the skin regions to the DLNs and cross-present antigens making them a good target for vaccine delivery[369,370]. However, sorted mDCs with $CD103^+$ or $CD103^-$ phenotypes, from mice immunised with ovalbumin minicells ± BsAbs, failed to induce proliferation of OTI or OTII cells. Proliferation was achieved using lymphocytes from mice injected with ovalbumin protein and CT, confirming that the minicell non-response was not a technical problem. To assess whether the result was not due to a delay in DCs migrating to DLNs, or to minicell uptake by cell without high CD11c and MHCII expression, a subsequent time-course assay was conducted with unsorted cells harvested from DLNs. The same outcomes were found. Data from these experiments are indicative only, as they were obtained from single mice experiments, and pooled lymphocytes which prevent any statistical comparison. The limitation of mouse numbers was as result of financial feasibility and a cost-benefit determination.

To assess responses *in vivo*, the frequencies of adoptively transferred OTI or OT II cells were determined after three immunisations. There was no evidence of minicell induced proliferation of these cells when immunised with or without BsAbs. Furthermore, there was no detected cytolytic activity from minicell groups in the CTL assay, when OVA minicells were targeted to DEC205 or Clec9a. During this study, it was established that ovalbumin minicells were able to induce and antigen-specific IgG response, however, BsAb targeting did not significantly alter the titres.

5.4.2. Antigen dose requirements in minicells

In a LCMV minicell experimental model reported by Giacalone *et al.*[237], a dose titration of 10^{10}, 10^9, 10^8 and 10^7 minicells with an antigen protein component of 1.2 µg/dose down to 0.0012 µg/dose resulted in a protective efficacy with 89%, 40%, 20% and 0% respectively. In the *in vitro* and initial *in vivo* studies reported herein, ovalbumin minicells had an antigen load of 0.1 µg whereas the ovalbumin ± CT or empty minicell doses consisted of 100 µg of protein. It was hypothesised that the experimental outcomes may be directly related to the low ovalbumin component in minicells. We tested this using an *in vivo* proliferation and CTL experiment using an ovalbumin dose titration and showed the requirement for an increased antigen load

for the efficient killing of SIINFEKL labelled cells. When the ovalbumin dose was 0.1 µg, co-administration with empty minicells had no detectable effects. At this low ovalbumin dose, the only significant responses were with the co-administration of CT where antigen-specific target cell lysis was detected in the DLN (p<0.0001). Antibody responses were similarly dependant on a higher ovalbumin dose delivery. Experimental data suggests that whilst a higher 100 µg dose increased cellular responses, both cellular and antibody responses in the 10 µg per dose mice could be sufficiently efficacious for protection, with a frequency of antigen-specific $CD8^+$ T cells exceeding 2%[210]. The actual frequency of $CD8^+$ T cells would be higher than indicated in the presented data which represents only the exogenous $CD8^+$ T cells, and does not include the endogenous population. The presence of an endogenous population, whilst not quantified, was evident by significant CTL responses (p<0.0001) in mice which did not receive adoptively transferred cells (Figure 45B).

The ability to increase the antigen load in minicells is directly related to the ability of the bacteria to produce the protein. This was demonstrated in an earlier chapter (Chapter 4:). It may be possible to load exogenous proteins onto the minicells post-purification in a manner similar to the uptake of chemotherapeutic drugs[227,238], but this was not within the scope of this project. This type of loading would mean the inclusion of additional processing and related costs, however, it would render the platform usable for proteins which are unable to be produced in minicell producing strains. Minicells could be coated using a system of chemical linking in the same way that some VLP platforms have been developed[128,156,162] or the proteins could be fused with sequences directing them to the outer membrane as has been achieved with bacterial ghosts[274]. As an indicator of the antigen load requirements for an effective vaccine using bacteria-like particles against *Plasmodium*, a BG with derivative proteins from *Pb*CSP used 45 µg per dose[371].

5.4.3. Antigen loaded minicell induced immune responses

Cell-mediated immune responses

Whilst ovalbumin loaded minicells did not induced proliferation of OTI or OTII cells, nor induce cytolytic responses, empty minicells did act as an adjuvant when co-

administered with ovalbumin. The ovalbumin titration experiment suggested the poor result was likely to have been a consequence of the low 0.1 µg ovalbumin load. In the subsequent *Py*AMA-1 minicell experiment a higher antigen load of approximately 1 µg per dose was anticipated to be more immunogenic. In that experiment, cellular response data was limited to blood cytokine levels and WBC activation markers post-challenge. Minicells did not induce antigen-specific systemic cytokine responses in samples analysed during the challenge, with results similar to that of non-immunised controls.

When lymphocyte activation markers were assessed, an up-regulation of monocyte PD-L1 receptors was induced by minicell immunisations (Figure 48). This response was not antigen or target related, but was an up-regulation induced by minicells themselves. The PD-L1 response was only evident in monocytes and returned to PBS control levels by day 3 and did not rise during the course of the infection. Whilst PD-L1 can be expressed on various APCs, it is only expressed on monocytes that have been stimulated with up-regulation induced by exposure to IFN-γ[372] and macrophages can also be induced with LPS, and polyIC[373,374]. PD-L1 can have a stimulatory or inhibitory influence on T cells following interactions with PD-1 receptors under different experimental conditions[374]. Given the high LPS component of minicells, the observed up-regulation is likely to be related to LPS, but may also be a result of IFN-γ production following a Th1 response by T cells or NK cells[372].

Antibody responses

Initial ELISA results suggested that, despite the low antigen dose, OVA minicells were capable of inducing significant (p<0.0001) anti-ovalbumin IgG titres (Figure 43). The titre was similar to a 1000-fold higher protein only dose. However, in the subsequent dose titration experiment, ovalbumin loaded minicells did not induce any detectable IgG responses. This was not a minicell batch-related anomaly, as both experiments used minicells derived from the same purification. To investigate this discrepancy, a repeat ELISA was performed using sera from both experiments, which confirmed the different responses between experiments. Even at a serum dilution of 1:100, minicell induced IgG responses in the second experiment were close to background responses. This low antibody titre was consistent with the 0.1

µg ovalbumin immunised mice, where low but detectable IgG responses were only present in mice co-administered with CT. The low antibody responses are also consistent with previously reported studies of GFP minicells (7.6 µg/dose) and GFP+ GFP encoded plasmid DNA minicells (6.8 µg/dose) inducing IgG endpoint titres of $1:10^2$ and $1:10^5$ respectively[236].

Studies were unable to conclusively establish if minicells induced a specific antibody response against *Py*AMA-1 due to a potential cross-reactivity between the minicells and both the RTS purified recombinant *Py*AMA-1 protein and the parasite extract. Reactivity against the protein is likely a result of bacterial contaminants from the *E. coli* lysate components of the RTS reactions. Pre-challenge IgG_1 responses detected by a flow cytometry based IFAT showed that all minicell immunised mice had similar antibody responses against the parasite extract, regardless of the presence or absence of *Py*AMA-1. Other immunoglobulin subclasses including IgG_{2a}, IgM, IgD and IgE were tested by the IFAT, however, only IgG_1 responses were detected. There was no data to suggest that antigen loaded minicells had higher antibody responses. The IgG data obtained during the course of the infection was confounded by the potential effect of parasites in the challenge inducing antibody responses.

Protection from *P. yoelii* sporozoite challenge

The *Plasmodium* AMA-1 protein is expressed in both sporozoites and merozoites in liver and blood-stages of infection[82,328,375], and as such presents itself as a target for both cell-mediated and antibody responses. *Py*AMA-1 minicell immunisations with or without BsAbs had no apparent influence on parasitemia; and although four of these mice did not develop detectable parasitemia, one mouse in the empty minicell control group also had no detectable parasitemia, thus confounding the interpretation of the data.

5.5. Conclusion

The ability of minicell producing bacteria to yield sufficient quantities of recombinant protein for incorporation into minicells for presentation to the host immune system, appears to be the major limitation of this platform. Data from the ovalbumin dose titration immunisation experiment suggests that a protein dose of 10 µg is sufficient

when combined with minicells to induce significant cellular and antibody titres. In order to increase the antigen load within minicells, future studies could assess alternative proteins from *Plasmodium* or other disease models, *E. coli* codon optimisation, or a modified protein construct[371]. In this study, data did not show any increase in immunogenicity or protective efficacy as a result of targeting minicells to DCs. However, this strategy may have been similarly limited by the antigen load. Additional studies with high protein yielding minicells would be required to conclusively establish the immunological benefit of DC targeting with this platform.

Chapter 6: Discussion and conclusion

The *Plasmodium* species has co-evolved with humans and has developed a variety of immune evasion and immunomodulation strategies which enable it to persist in the host[376,377]. People living in malaria endemic regions are able to develop clinical immunity in that they are protected from disease rather than infection, however, protection quickly wanes when they leave the endemic location[378]. In light of this, the development of a vaccine against *Plasmodium* must improve upon nature.

Immunisations of mice[379] and man[380] with irradiated sporozoites have established the feasibility of developing a malaria vaccine. Recent work on whole-parasite vaccines includes radiation attenuated sporozoites[36,40,41], infectious sporozoites under chemoprophylaxis[42,43,381], genetically[44,45,382] or chemically[46] attenuated parasites. In a recent human trial, irradiated sporozoites induced sterile protection in 6/6 adults, however, this required five i.v. doses of 1.35 x 10^5 sporozoites[36]. Whilst clearly efficacious, the ability to deliver cryopreserved sporozoites to geographical-disperse communities in developing countries and to get subject compliance for the required five-dose regimen represents a serious hurdle.

Sub-unit vaccines are rationally designed at the molecular level to induce cell-mediated and/or antibody responses to specific pre-defined targets. Following the cloning of *P. falciparum* antigens in the 1980's, a study reported that immunisation with a recombinant protein incorporating the central repeat regions of the CSP induced high anti-CSP titres capable of inhibiting hepatoma cell invasion[383]. Subsequent sub-unit vaccine trials established that protective immunity could be conferred by immunisation with peptides representing defined epitopes from CSP, through the induction of cellular or antibody responses[63,72,75]. The most clinically advanced malaria vaccine candidate RTS,S/AS01, incorporating immunogenic regions of CSP into a VLP, has achieved only 30.1% vaccine efficacy in phase 3 clinical trials[37]. Other vaccine candidate antigens have been evaluated, however, approximately half of vaccine trials have focused on either CSP, AMA-1 or the merozoite surface antigen (reviewed in [384,385]).

A major hurdle for sub-unit vaccines is the fact that proteins and peptides are poorly immunogenic and require the co-administration of potent adjuvants[386]. There are only three adjuvants currently approved for human use- Alum, MF59 and monophosphoril lipid A[387]. Vaccines against intracellular pathogens such as *Plasmodium* require the induction of strong cell-mediated immunity and antibody responses which current vaccine platforms and adjuvant combinations are unable to achieve[388]. To address this issue, numerous novel adjuvants or adjuvant combinations are being evaluated and are in various stages of clinical development (reviewed in[388]).

Various sub-unit vaccine platforms have been evaluated as potential platforms for a malaria vaccine. Plasmid DNA showed potential to elicit antibody and cell-mediated responses in animal models with plasmid encoded *Py*CSP inducing a $CD8^+$ T cell dependant protection from sporozoite challenge[76]. Despite promising results in animal models, the efficacy of plasmid DNA as a homologous regimen in human clinical trials has been poor[77] (and reviewed in[389,390]). Viral vectors, including poxvectors and adenoviral vectors use host mechanisms to express target antigen within infected cells, and are particularly good at inducing robust T cell responses and to a lesser extent antibody responses, and can simultaneously deliver multiple antigens[124,390,391]. However, pre-exposure to these vectors may limit their ability to induce T cell responses[392] and antibody responses[391]. As a result of this limitation, and to enhance efficacy, vaccine regimens using multiple platforms have been investigated[324]. A recent clinical trial showed that a DNA prime with an adenovirus boost regimen incorporating both *Pf*CSP and *Pf*AMA-1 antigens, induced only low antibody titres, modest IFN-γ cellular responses and sterile protection in 27% of subjects[393]. It is likely that novel sub-unit vaccine platforms could overcome these limited immunological responses, and should to be investigated.

In pursuit of the requirement to develop novel delivery platforms, I have developed and evaluated in this thesis: chimeric VLPs and capsomeres, and bacterial minicells targeting DC receptors DEC205 or Clec9a. The chimeric VLP and capsomeres comprised of a modified MuPyV VP1 structural protein expressed in bacteria and incorporated defined $CD8^{+}$[73,75] and $CD4^{+}$[71,72,74] T cell and B cell[63] epitopes from *Py*CSP. These chimeric platforms have previously been evaluated for their ability to

induce robust epitope-specific antibody responses in other pathogen models[170,173,188], however, cell-mediated immune responses have not been evaluated. The bacterial minicells were purified from *E. coli* DS410 and contained recombinant ovalbumin or *Py*AMA-1 protein and plasmid DNA for mammalian expression of the same antigen. Previously, this platform has been shown to induce antibody[236] and cell-mediated responses, as well as a protective capacity in mice against an LCMV challenge[237]. However, in that study, APC uptake and expression of plasmid encoded antigens were low[236], hence the minicell platform in my study targeted DC surface receptors in an attempt to enhance uptake and immunogenicity. The ability of each platform to induce immunological responses and provide protection from challenge was evaluated using a murine model. The well studied and leading candidate vaccine antigens CSP and AMA1 were used since each has been shown to be protective in other platforms[37,97,390].

6.1. Chimeric virus like particles

The MuPyV VP1 structural protein chosen for study herein has been developed by the Middelberg laboratory to produce high yields of stable chimeric virus-like particles using a bacterial expression system[187,189,288,289], and displays antigenic epitopes on exposed surface loops using flexible linker sequences (MuPyV VP1-S4-G4S)[173,188]. The Middelberg laboratory has evaluated the ability of this platform to induce pathogen-specific antibodies, and to confer protection in mice in the influenza and group A streptococcus models[170,173,188]. The presented work is the first evaluation of the capacity of this platform to induce cellular immune responses as well as antibody responses and to confer protection against a complex pathogen using a murine malaria model.

Six chimeric MuPyV VP1-S4-G4S constructs were made by genetically inserting *P. yoelii* 17XNL CSP $CD8^+$ T cell epitopes$_{280-288}$[75],$_{58-67}$[73] or $CD4^+$ T cell epitopes$_{280-295}$[72],$_{57-70}$[74],$_{59-79}$[71], or a B cell epitope[63] individually into the S4 surface loop of the MuPyV VP1 protein with modified G4S flanking sequences[173]. Three of these constructs ($CD8_{280-288}$, $CD4_{59-79}$ and B cell) were expressed by *E. coli* with high levels of soluble protein and were able to form stable VLPs following purification. The other three constructs ($CD8_{58-67}$, $CD4_{280-295}$ and $_{57-70}$) were predominantly insoluble,

and aggregated when the GST tag was removed. This protein instability is documented in other VLP studies[156-158] and may be the result of a single amino acid within the insert[158], moreover there are currently no ways to predict chimeric protein stability. The epitopes could have been inserted into different regions of the VP1 protein which may have resolved the solubility and stability issues. The location of epitopes has been shown to impact on protein expression and VLP formation in HaPyV[176] and BVP[157] models. However, modifications to the insertion sites were not within the scope of this thesis.

To confirm that VLPs had formed without aggregation and to determine the size of the particles, both TEM imagery and AF4-MALS analysis was performed. TEM images showed that chimeric VLPs had the same appearance as wild-type VLPs. AF4-MALS separates particles based on their size and then uses light scattering to determine their size. The chimeric VLP diameters ranged from 41.5 to 42.3 nm which were slightly larger than the 40.0 nm wild-type VLP as expected due to the insertion of additional amino acids increasing the molecular weight of each protein, and the protrusion of inserted epitopes from the S4 surface loops.

A series of *in vitro* and *in vivo* experiments were conducted to assess the immunogenicity of each VLP construct. Initially, an *in vitro* assessment showed that the $CD8_{280\text{-}288}$ VLP was able to induce proliferation of transgenic CS-TCR $CD8^+$ T cells which specifically recognise the *Py*$CSP_{280\text{-}288}$ epitope. This confirmed that the chimeric $CD8_{280\text{-}288}$ VLP was able to be processed and presented by APCs, for recognition by $CD8^+$ T cells, as determined by the proliferation of the epitope-specific T cells.

Subsequently the capacity of the chimeric VLP platform to induce immune responses and confer protection was evaluated using VLPs as individual or pooled constructs. This enabled the evaluation of single constructs, and to determine if any synergistic effects would result from pooling constructs. In addition to evaluating a homologous VLP regimen, a plasmid DNA prime/VLP boost regimen was also included. Whilst plasmid DNA induces both antibody and cell-mediated immune responses (reviewed in[318]), the prime/boost delivery using heterologous platforms has been shown to both

arms of the adaptive immune response and enhances protective efficacy against challenge[93,318,394,395].

Consistent with the *in vitro* experiment, data from the murine studies confirmed that VLPs induced $CD8^+$ T cell responses *in vivo*. IFN-γ responses were detected when splenocytes were stimulated with either the $CD8_{280-288}$ peptide or *Py*CSP transfected cells expressing that $CD8_{280-288}$ epitope, indicative of a Th1 response. Notably the IFN-γ responses were consistently lower than the responses induced by plasmid DNA alone or the heterologous DNA prime/VLP boost regimen. Minimal differences were detected between the 10 µg and 30 µg per construct in pooled VLP doses, and the pooling VLPs offered no benefit.

The VLP immunisations induced a very weak response against the *Py*CSP $CD4^+_{59-79}$ T cell epitope. This was established by the limited cellular responses after restimulation with the $CD4_{59-79}$ peptide, which contrasted with the response of peptide-immunised mice which was consistently very high. Furthermore there was no apparent effect on antibody titres in mice immunised with B cell VLPs versus pooled VLPs containing both the B cell VLP and the $CD4_{59-79}$ VLP. Mice had been immunised with a dose of either 30 µg of peptide with polyIC or 10 µg to 30 µg of VLPs comparable to other HBV VLP studies with $CD4^+$ T cell epitopes[152,219]. In those studies, in contrast to my findings, enhanced antibody and cellular immune responses were reported[152,219]. No *in vivo* studies using the MuPyV VLP with $CD4^+$ T cell epitopes have been reported for a direct comparison, although the OVA $CD4^+$ T cell chimeric VLP has been shown to induce proliferation of OTII cells *in vitro*[202]. The comparative *Py*CSP_{59-79} epitope load in the 10 µg and 30 µg per construct in pooled VLP dose was only 0.52 µg and 1.56 µg respectively which may have contributed to the poor responses in my study.

As anticipated from previous VLP induced antibody analysis[170,173,188], the B cell chimeric VLP induced robust antibody responses. The antibody titres induced by a homologous VLP regimen were not significantly influenced by the dose of 10 µg or 30 µg in pooled VLP immunisations, nor did the pooling of VLPs significantly differ from B cell VLPs administered alone. Whilst there was no enhancement of antibody titres achieved by pooling VLPs, there were also no adverse effects. The ELISA

results from pooled sera show that a single VLP dose induced very low antibody titres, and that at least two doses of VLPs were required to generate robust titres in the homologous regimen. Antibody titres were further enhancement by a third immunisation, however, the significance was not determined as only pooled sera was available for analysis. In contrast to a previous study[173], there was a dominant IgG_3 response induced by the B cell VLP immunisations. This appears to have been influenced by the inserted epitope, since both VLPs were produced using the same MuPyV VP1-S4-G4S construct, using the same purification protocols and the same immunisation routes. The dose does not appear to be relevant with the published study using 23 µg per immunisation[173] whereas I used 10 µg in the pooled VLPs and 30 µg in the B cell VLP immunisations. IgG_3 antibodies against the same *Py*CSP B cell repeat has previously been protective in BALB/c mice[63], and as such the presence of this isotype is perhaps advantageous.

Importantly, the VLP induced antibodies were able to recognise conformational epitopes on recombinant protein, as well as on the surface of the sporozoite. Recognition of the CSP epitope on sporozoites is essential as antibodies to this target afford protection against challenge[63].

The prime/boost regimen, which only employed a single VLP boost with or without polyIC, induced significantly enhanced antibody responses when administered at 10 µg/construct as compared to homologous DNA immunisations (p<0.0001). When the dose of pooled VLPs was increased to 30 µg/construct significance was no longer detected. It is likely that a prime/boost regimen including at least two VLP boosts would further enhance antibody titres, as was detected in the homologous VLP regimen.

To assess whether the inclusion of an adjuvant would enhance the platforms performance, polyIC was co-administered with VLPs. PolyIC was selected as the adjuvant in this experiment because of its ability to enhance antibody as well as Th1 cellular responses in other platforms[294,295,297,312], in contrast to alum based adjuvants which are only efficient at inducing higher antibody titres[307]. In the literature there is contradictory evidence as to the requirement of adjuvants for VLPs[161,215,216,316,317]. VLPs with alum had a detrimental effect on CTL generation due to a prevention of

VLPs from entering into the MHC I processing pathway[307]. My results showed that whilst VLPs were self-adjuvanting in that they were able to induce cell-mediated and antibody responses without the requirement for adjuvants, the inclusion of polyIC resulted in an increased trend of both $CD8^+$ T cell and antibody responses.

6.2. Chimeric capsomeres

Following the expression of the MuPyV VP1 protein, five VP1 proteins link together forming a pentameric capsomere[168]. The removal of the first 28 amino acids from the N-terminus and the least 63 amino acids from the C-terminal regions of the VP1 protein prevents the formation of VLPs whilst maintaining the capsomere formation[168,170]. Genetic modifications to the MuPyV VP1 by Wibowo *et al.*[170] from the Middelberg laboratory resulted in a stable capsomere platform into which four epitope insertion sites were installed per VP1 protein. The advantage of the capsomere platform above VLPs is that it reduces the production costs by eliminating the need for the induction of VLP formation, and increases the antigen to vector ratio which has been shown to increase antigen-specific immunogenicity[174,175] and reduce anti-carrier titres[176]. However, studies by the Middelberg laboratory on the capsomere platform had previously focused only on antibody responses[170,173]. The studies reported in this thesis were the first to investigate the capacity of this capsomere platform to induce cell-mediated responses.

In contrast to VLPs, capsomeres need the inclusion of adjuvants for the induction of antibody responses[131,170,173]. This loss of self-adjuvant property is likely due to the loss of the highly repetitive array of VLPs which mimic the native virus[136], and/or their ability to cross-link B cell receptors[130]. Some self-adjuvanting effects can be recovered when the capsomeres are able to assemble into larger particles, the formation of which is dependent on genomic modifications, as shown with HPV capsomeres[178]. However, capsomeres in that study were capable of inducing cell-mediated responses without the particle size restrictions as seen with antibodies[178]. In another HPV study, capsomeres induced cell-mediated responses without adjuvant, however, responses were increased almost 10-fold with the inclusion of aluminium hydroxide, MPL and synthetic trehalose dicorynomycolate in squalene and Tween 80[179].

Homologous capsomere immunisations induced significant cellular responses as shown in ELISpot and CBA analysis after restimulation of splenocytes with *Py*CSP transfected A20 cells, or with the *Py*CSP $CD8_{280-288}$ peptide ($p<0.0001$). The ELISpot responses were robust in comparison to HPV capsomere responses with increases of approximately 5-fold in non-adjuvanted capsomeres[178] and 2-fold in adjuvanted capsomeres[179]. Whilst the data are not directly comparable, they do give some indication as to the performance of capsomeres within this study. Capsomeres in polyIC had a trend of increased cellular responses when compared to non-adjuvanted VLPs. This may be accounted for by the increased antigen load in capsomeres with three epitopes per protein resulting in triple the amount of epitopes, or by the location of the epitopes within the protein[155]. Capsomere induced cellular responses were very similar to VLPs co-administered with polyIC. Capsomeres preferentially induced responses against the *Py*CSP $CD8_{280-288}$ peptide, however, they also induced significant responses to the *Py*CSP $CD4_{59-79}$ peptide ($p<0.0001$) as detected in the ELISpot data.

Capsomeres induced significant IgG antibody responses against the B cell peptide ($p<0.0001$), and the antibodies recognised epitopes on recombinant protein and the surface of the sporozoites. The titres were however, significantly lower than those induced by VLPs regardless of whether capsomeres were administered with or without adjuvant ($p<0.05$). This may be related to highly repetitive structural array of VLPs[167,168,396], the size of the particles[178] or their ability to cross-link B cell receptors[130]. The dominant isotype induced by capsomeres was IgG1 which was the same as a previous study using the same capsomere construct but with incorporated GAS J8 epitopes[173]. Surprisingly, there was almost a complete absence in the IgG_3 isotype response in the capsomere immunised mice which was a dominant isotype induced by VLPs. The *Py*CSP B Cell repeat epitope which, as mentioned above, was suspected to have induced the IgG_3 response, was the same epitope inserted into the capsomeres. This suggests that an alternative processing pathway has occurred between the two platforms[397], or perhaps there was an inability of capsomeres to cross-link B cell receptors[130]. It would be interesting to further examine if there is a differential uptake of VLPs by APCs *in vivo* which may reveal

alternative processing pathways, however, this was not within the scope of this thesis.

VLPs administered without adjuvant induced robust IgG_1 and IgG_3 antibody responses indicative of a Th2 response[398,399] suggesting limited production of IFN-γ resulting from immunisations[398]. When VLPs were co-administered with polyIC, mice maintained similar IgG_1 and IgG_3 response, however, there was a more balanced Th1-Th2 response observed with the production of IgG_{2a} and IgG_{2b} isotypes (Figure 26b). This balance response was not observed following capsomere immunisations which were only co-administered with polyIC. These results were surprising, as polyIC is reported to be an effective inducer of Th1 responses[293], and further supports the suggestion of alternative processing pathways of VLPs and capsomeres.

The heterologous DNA prime/capsomere boost regimen significantly increased the cellular responses as detected by ELISpot ($p<0.01$) compared to the capsomere only immunisations. Whilst the reported data established that both VLP and capsomere platforms were capable of inducing $CD8^+$ T cell responses, both are considerable less efficient than plasmid DNA either alone or in a prime/boost regimen. These results are supported by other studies where using a dual platform including a plasmid DNA prime enhanced immune responses[93,320-324], including when used with a VLP boost[325].

In each of the VLP and capsomere experiments, immunological data showing robust cellular and antibody responses supported the potential to protect immunised mice from sporozoite challenge[63,299]. However, in my studies, protection was not induced by capsomeres, nor VLPs as homologous constructs. There was a significant reduction in the liver parasite burden in the group of mice immunised with the DNA/VLP regimen using 30 µg of each construct ($p<0.01$), and two out of five mice immunised with 10 µg of each construct had no parasite RNA detected. The probable cause of this low protective efficacy is that the magnitude of the responses did not surpass the threshold required for protection[63,73,210,301]. For example the passive transfer of monoclonal antibodies to the *Py*CSP B cell epitope protected mice at doses of 500 µg (100%), 250 µg (83%), 125 µg (67%) but was completely

ineffective at 62.5 µg (0%)[63]. Similarly, the adoptive transfer of *Py*CSP $CD8^{+}_{(280\text{-}289)}$T cell clones protected mice when each mouse received 20 x 10^6 (100%), and 10 x 10^6 (50%) but not 3 x 10^6 (0%)[73].

6.3. Bacterial minicells

Previous studies with bacterial minicells examining bacterial and protein functions[233,234], did not require the purification standards necessary for the immunisation of animals. Viable parental contamination of between one in 10^3 to 10^6 minicells was sufficient for the purposes of studying protein responses[222,335,336]. A protocol effective at removing all viable bacteria, described by MacDiarmid *et al*.[227] utilised differential and density gradient centrifugation, combined with various filtration, elongation and antibiotic treatment steps. The procedure was further refined in my doctoral studies. By adding an additional density gradient centrifugation all filtration steps were avoided. This novel procedure also produced high minicell yields and no contamination by viable parent bacteria. Additionally the purification costs and labour components were reduced.

Targeting minicells to non-phagocytic cells has previously been shown to enhance minicell uptake and minimise drug doses in cancer treatment[171,227]. This principle was the basis of my project where minicells loaded with recombinant protein and plasmid DNA were targeted to DCs using BsAbs directed against the DEC205 or Clec9a receptors. The rationale behind this strategy also came from reports indicating the DCs preferentially took up particles in the 40 to 50 nm diameter range whereas macrophages phagocytised larger particles[196,400]. It was hypothesised that targeting these receptors would overcome the poor minicell uptake as shown in previous studies[235], by initiating receptor mediated endocytosis[338,363,401].

Low protein yields were encountered with each antigen including GFP, *Py*CSP, *Py*AMA-1, Tfr-ovalbumin and ovalbumin. Different expression vectors including pBAD/Myc-HisA, pTrcHis2A and pDual GC, various culture conditions and media types were investigated to optimise protein expression. The greatest variability in protein expression and minicell yields were achieved by changing the media. LB was preferential for protein expression, whereas high growth media TB was better for

minicell yields. The low level protein expression observed in dual transformants were suspected to be a result of plasmid incompatibility[353]. This incompatibility is caused by plasmids with the same origin of replication, competing for replication factors[353] and can result in fluctuations in plasmid copy numbers[355]. It was anticipated that changing to the dual expression plasmid pDualGC would resolve these issues, because only a single transformation was required and therefore plasmid incompatibility issues are removed. This was investigated in the OVA model and with the GFP reporter but the protein yield was also very low. It appears that the low protein yield with a maximum dose of OVA (0.1 µg) and *Py*AMA-1 (1.0 µg) per 10^{10} minicells could limit the effectiveness of this platform. This is consistent with results in a dose related LCMV protection study where 1.2 µg, 0.12 µg and 0.012 antigen doses protected 8/9, 2/5, and 1/5 mice respectively[237].

The low antigen yield was suspected to be the cause of the lack of responsiveness of migrating DCs to stimulate the proliferation of transgenic OTI $CD8^+$ or OTII $CD4^+$ T cells in several *in vitro* experiments. To assess antigen requirements using this model, ovalbumin protein at 0.1, 10 and 100 µg was used to immunise mice with or without adjuvants. Although proteins were not encapsulated within minicells, this study did nonetheless give some indication of antigen requirements. Importantly it showed that a dose of 0.1 µg, which was the dose in the OVA minicell experiment, was insufficient to generate significant cellular or antibody responses. To get some perspective as to what a protein-only minicell platform may require to protect against a sporozoite challenge, bacterial ghosts required 45 µg of *Pb*CSP per dose[371]. That antigen dose would be difficult to achieve in minicells, however, minicells in my platform deliver both antigenic proteins as well as plasmid DNA. This combination of modalities enhances immunogenicity[236] and potentially reduces the protein load requirements.

There was a significant minicell-induced antibody response detected in the original ovalbumin minicell experiment when mice were immunised with OVA minicells alone (1:1.9 x 10^5) or targeted to DEC205 (1:0.8 x 10^5) (p<0.0001). Those endpoint titres exceeded those reported in a GFP DNA/protein minicell experiment where a mean titre of less than 1:1250 was induced by three doses of 10^{10} minicells with an antigen

load of 6.8 ± 1.7 μg[236]. The inclusion of targeting BsAbs did not significantly alter the magnitude of the responses.

Unexpectedly, the OVA minicell induced anti-ovalbumin antibody responses were not replicated in the subsequent experiment. Minicells used in both experiments were derived from the same batch of purified minicells, were given at the same administration route, dose and schedule of doses and sampling. To confirm that this was not a technical issue, the ELISA assay was repeated with minicell immunised sera analysed concurrently, with consistent results. Sera from the titration experiment were assayed at a dilution of 1:100 without detectable responses.

In the *Py*AMA-1 minicells antibody analysis there was a cross-reactive response with sera from mice immunised with *Py*AMA-1 or empty minicells, with the RTS generated recombinant protein, as well as the parasite extract. It is possible that the RTS generated protein had some *E. coli* contamination following purification which has then reacted with antibodies induced by the minicells themselves. Alternatively, it is possible that a minicell antigen (other than *Py*AMA-1) was cross-reactive with *Py*AMA-1, which was present in both assays. However, there was no conclusive data to suggest that there was any specific response against the antigen, with no increased titres detected in the *Py*AMA-1 minicell groups above that induced by empty minicells.

Experimental data did not present any evidence to suggest that either ovalbumin or *Py*AMA-1 loaded minicells were able to induce a cellular response. This contrasts with the one previous minicell study where approximately 5% of $CD8^+$ T cells expressed IFN-γ upon restimulation of splenocytes[237]. Immunogenicity assays such as ELISpot, CBA and ICS, were not performed in my *Py*AMA-1 minicell experiment due to funding constraints and time limitations. Nonetheless, there was no direct evidence of immunisation induced parasite-specific activation of cellular responses.

Likewise, there was no evidence to suggest that *Py*AMA-1 minicells induced protection from sporozoite challenge. This lack of protection is consistent with the poor immunogenicity of minicells as detected in the antibody and cellular assays. As

previously mentioned with the VLP and capsomere sections, there is a high level of immune responses required to protect against this complex pathogen[63,73,210,301].

6.4. Future directions

Experimental studies represented within this thesis have established that chimeric VLPs and capsomeres incorporating defined $CD8^+$ T cell epitopes are capable of inducing significant antigen-specific $CD8^+$ T cell responses. Having established this capability, and showing robust antibody inducing capabilities consistent with previous studies, further investigations are warranted into how these responses could be enhanced:

i. The location of the epitope within the chimeric MuPyV-VP1 protein is important for cross-linking B cell receptors in the VLP platform. For this reason epitopes were inserted into surface exposed regions of the VLP. This requirement is not essential for the insertion of epitopes specific for $CD8^+$ and $CD4^+$ T cell epitopes, and the immunogenicity may be enhanced by alternative epitope insertion sites. This may explain why capsomeres induced a moderate $CD4^+$ T cell response whereas the same responses induced by VLPs were very weak. Future studies should address this issue by evaluating alternative epitope insertion sites.
ii. All immunisations were administered s.c. at the base of the tail. This route of administration was utilised based on previous studies (REF) which indicated
iii. The heterologous plasmid DNA prime followed by a VLP or capsomere boost induced significantly higher $CD8^+$ T cell immune responses as compared to a homologous regimen. However, these responses were not significantly different to immunisations with plasmid DNA alone. The primary benefit of boosting with VLPs or capsomeres was in the induction of antibody responses, for which plasmid DNA alone was inefficient. The antibody titre subsequent to each dose of VLPs indicates that two or preferentially three VLP doses should be used to enhance antibody responses. Therefore, alternative dosing regimens should be investigated to optimise both cellular and antibody responses.

iv. It was apparent with the antibody titres and isotype responses, that VLP induced immunogenicity can be altered by the inclusion of adjuvants. PolyIC was included in this study due to its reported ability to induce a Th1 biased immune response[295,296,312], and it was this type of cellular immune response which we were interested in evaluating. Further studies should now be done to evaluate alternative adjuvants in order to optimise responses.

v. The different antibody isotype responses generated by immunisations with VLPs and capsomeres indicates that alternative processing pathways have been utilised. This may be the result of uptake of the particles by different antigen presenting cells, or by the ability of VLPs only to effectively cross-link B cell receptors and act in a T cell independent manner. The differential uptake could be investigated by evaluating the cells migrating to the DLNs following immunisation. This would be useful to better understand the mechanism of action of the platforms, which could result in a more rational approach to designing targeted immune responses.

The evaluation of the bacterial minicell platform was primarily hampered by the low antigen yield produced by the minicell-producing *E. coli* strains used in this study. Issues arose with plasmid incompatibility following dual-transformation, which was anticipated to be resolved using the pDualGC vector with dual promoters. When ovalbumin cDNA was inserted into this vector however, the protein yield remained very low. In order to increase the protein antigen yield the following studies could be done:

i. The *Plasmodium* CSP, and AMA-1 proteins were included in this study because they are leading antigens in vaccine candidate studies. They were however, difficult to express in minicell-producing *E.coli* strains. Other *Plasmodium* proteins, or alternatively proteins from different pathogens (such as LCMV[236,237]) should be evaluated firstly for antigen yield, and secondly for efficacy using the DC targeting minicell platform.

ii. The proteins used in this study were not altered in any way to enhance protein yields. It may be that by removing regions which are difficult to translate, codon-optimisation of the proteins, or a combination of both strategies may result in an increased antigen yield.

6.5. Conclusion

In my doctoral studies, I have evaluated chimeric VLPs and capsomeres as well as bacterial minicell sub-unit vaccine delivery platforms for their ability to induce cellular and antibody responses, and confer protection against sporozoite challenge.

A major advantage with the VLP platform is that it can be quickly adapted to newly identified target antigens with relatively simple cloning, expression, purification and VLP formation protocols. My research has shown that chimeric VLPs induced robust antibody titres, and a moderate $CD8^+$ T cell response, but only a very small $CD4^+$ T cell response. Chimeric capsomeres similarly induced $CD8^+$ T cell responses, and in contrast to VLPs induced moderate $CD4^+$ T cell responses and reduced antibody responses. The data further suggest that a DNA prime/VLP boost regimen is more immunogenic with regards to T cell responses than a homologous regimen, but nonetheless responses were insufficient to protect mice from sporozoite challenge. Since DNA priming induced high cell-mediated responses, and antibody titres increased markedly after the second VLP immunisation, it would appear that a prime/boost regimen with at least two VLP immunisations should be evaluated in future studies.

Minicells and other bacterial-derived platforms including outer-membrane vesicles and bacterial ghosts have the potential to be protective and licensed as shown with the recent approval of the meningococcal B OMV vaccine[253]. Furthermore, the ability to target minicells to professional APCs has the potential to increase uptake by receptor-mediated endocytosis, enhancing immune responses and reducing dose load requirements. During my studies, I investigated the potential of bacterial minicells as a vaccine platform, in both malaria parasite and ovalbumin models. In each model, minicells were packaged with antigens in the form of recombinant protein, and plasmid DNA for mammalian expression of the same protein. I developed a novel purification protocol which resulted in a high minicell yield and was efficient at removing all contaminating viable parent bacteria. This minicell package contains not only the antigen-specific material but surrounded by LPS it will activate DCs through TLR and pattern recognition receptors associated with bacterial PAMP recognition. The presented work establishes that the major limitation

of this platform is antigen load, which compromises the capacity of this platform to induce robust immune responses and confer protection. This may be overcome with high levels of protein expression by the bacteria perhaps using alternative proteins, or fragments of proteins which enable a high level of expression. Increasing the antigen load would be essential to conclusively determine if the strategy of targeting minicells to DCs would improve the efficacy of the platform.

Chapter 7: List of references

1. WHO. World Malaria Report 2013. Geneva: World Health Organization; 2013.

2. Breman JG. The ears of the hippopotamus: Manifestations, determinants, and estimates of the malaria burden. American Journal of Tropical Medicine and Hygiene 2001;64:1-11.

3. WHO. World malaria report 2005. Geneva: World Health Organization; 2005.

4. Sachs J, Malaney P. The economic and social burden of malaria. Nature 2002;415:680-5.

5. Korenromp EL, Miller J, Cibulskis RE, Cham MK, Alnwick D, Dye C. Monitoring mosquito net coverage for malaria control in Africa: possession vs. use by children under 5 years. Tropical Medicine & International Health 2003;8:693-703.

6. Hyde JE. Mechanisms of resistance of *Plasmodium falciparum* to antimalarial drugs. Microbes and Infection 2002;4:165-74.

7. Mu J, Myers RA, Jiang H, et al. *Plasmodium falciparum* genome-wide scans for positive selection, recombination hot spots and resistance to antimalarial drugs. Nature Genetics 2010;42:268-72.

8. White NJ, Pongtavornpinyo W. The de novo selection of drug-resistant malaria parasites. Proceedings of the Royal Society of London Series B-Biological Sciences 2003;270:545-54.

9. Noedl H, Socheat D, Satimai W. Artemisinin-resistant malaria in Asia. New England Journal of Medicine 2009;361:540-1.

10. Dondorp AM, Nosten F, Yi P, et al. Artemisinin resistance in *Plasmodium falciparum* malaria. New England Journal of Medicine 2009;361:455-67.

11. Price RN, Douglas NM, Anstey NM. New developments in *Plasmodium vivax* malaria: severe disease and the rise of chloroquine resistance. Current Opinion in Infectious Diseases 2009;22:430-5.

12. Cox-Singh J, Davis TME, Lee KS, et al. *Plasmodium knowlesi* malaria in humans is widely distributed and potentially life threatening. Clinical Infectious Diseases 2008;46:165-71.

13. Miller LH, Ackerman HC, Su X-z, Wellems TE. Malaria biology and disease pathogenesis: insights for new treatments. Nature Medicine 2013;19:156-67.

14. Medica DL, Sinnis P. Quantitative dynamics of *Plasmodium yoelii* sporozoite transmission by infected anopheline mosquitoes. Infection and Immunity 2005;73:4363-9.

15. Yamauchi LM, Coppi A, Snounou G, Sinnis P. *Plasmodium* sporozoites trickle out of the injection site. Cellular Microbiology 2007;9:1215-22.

16. Doolan DL, Dobano C, Baird JK. Acquired Immunity to Malaria. Clinical Microbiology Reviews 2009;22:13-36.

17. Scherf A, Lopez-Rubio JJ, Riviere L. Antigenic variation in *Plasmodium falciparum*. Annual Review of Microbiology 2008;62:445-70.

18. Mackintosh CL, Beeson JG, Marsh K. Clinical features and pathogenesis of severe malaria. Trends in Parasitology 2004;20:597-603.

19. Baird JK, Masbar S, Basri H, Tirtokusumo S, Subianto B, Hoffman SL. Age-dependent susceptibility to severe disease with primary exposure to *Plasmodium falciparum*. Journal of Infectious Diseases 1998;178:592-5.

20. Freund J, Thomson KJ, Sommer HE, Walter AW, Schenkein EL. Immunization of rhesus monkeys against malarial infection (*P-knowlesi*) with killed parasites and adjuvants. Science 1945;102:202-4.

21. Freund J, Thomson KJ, Sommer HE, Walter AW, Pisani TM. Immunization of monkeys against malaria by means of killed parasites with adjuvants. American Journal of Tropical Medicine 1948;28:1-22.

22. Clyde DF, Most H, McCarthy VC, Vanderbe.Jp. Immunization of man against sporozite-induced *falciparum* malaria. American Journal of the Medical Sciences 1973;266:169-77.

23. Moorthy VS, Newman RD, Okwo-Bele JM. Malaria vaccine technology roadmap. Lancet 2013;382:1700-1.

24. Fenner F, Henderson DA, Arita I, Jezek Z, Ladnyi ID. Smallpox and its eradication. Geneva: World Health Organization; 1988.

25. Levine MM, Lagos R, Esparza J. Vaccines and vaccination in historical perspective. In: Levine MM, ed. New Generation Vaccines. 4 ed. New York: Informa Healthcare; 2010.

26. WHO. The 10 leading causes of death in the world, 2000 and 2011: World Health Organization; 2013.

27. De Gregorio E, Rappuoli R. Vaccines for the future: learning from human immunology. Microbial Biotechnology 2012;5:149-55.

28. Germain RN. Vaccines and the future of human immunology. Immunity 2010;33:441-50.

29. WHO. Immunization, vaccines and biologicals, IVB document centre: WHO vaccine-preventable diseases: monitoring system–2010 global summary: World Health Organization; 2010.

30. Rhee JH. Towards Vaccine 3.0: new era opened in vaccine research and industry. Clinical and experimental vaccine research 2014;3:1-4.

31. Zeltins A. Construction and characterization of virus-like particles: A review. Molecular Biotechnology 2013;53:92-107.

32. Levitz SM, Golenbock DT. Beyond empiricism: Informing vaccine development through innate immunity research. Cell 2012;148:1284-92.

33. Doolan DL, Hoffman SL. Multi-gene vaccination against malaria: A multistage, multi-immune response approach. Parasitology Today 1997;13:171-8.

34. Overstreet MG, Cockburn IA, Chen YC, Zavala F. Protective CD8+ T cells against *Plasmodium* liver stages: immunobiology of an 'unnatural' immune response. Immunological Reviews 2008;225:272-83.

35. Nussenzweig RS, Long CA. Malaria vaccines - Multiple targets. Science 1994;265:1381-3.

36. Seder RA, Chang L-J, Enama ME, et al. Protection against malaria by intravenous immunization with a nonreplicating sporozoite vaccine. Science 2013;341:1359-65.

37. Mian-McCarthy S, Agnandji ST, Lell B, et al. A phase 3 trial of RTS,S/AS01 malaria vaccine in African infants. New England Journal of Medicine 2012;367:2284-95.

38. Epstein JE, Richie TL. The whole parasite, pre-erythrocytic stage approach to malaria vaccine development: a review. Current Opinion in Infectious Diseases 2013;26:420-8.

39. Vaughan AM, Kappe SHI. Vaccination using radiation- or genetically attenuated live sporozoites. Methods in molecular biology (Clifton, NJ) 2013;923:549-66.

40. Hoffman SL, Goh LML, Luke TC, et al. Protection of humans against malaria by immunization with radiation-attenuated *Plasmodium falciparum* sporozoites. Journal of Infectious Diseases 2002;185:1155-64.

41. Hoffman SL, Billingsley PF, James E, et al. Development of a metabolically active, non-replicating sporozoite vaccine to prevent *Plasmodium falciparum* malaria. Hum Vaccines 2010;6:97-106.

42. Roestenberg M, Teirlinck AC, McCall MBB, et al. Long-term protection against malaria after experimental sporozoite inoculation: an open-label follow-up study. Lancet 2011;377:1770-6.

43. Bijker EM, Bastiaens GJH, Teirlinck AC, et al. Protection against malaria after immunization by chloroquine prophylaxis and sporozoites is mediated by preerythrocytic

immunity. Proceedings of the National Academy of Sciences of the United States of America 2013;110:7862-7.

44. Mueller A-K, Labaied M, Kappe SH, Matuschewski K. Genetically modified *Plasmodium* parasites as a protective experimental malaria vaccine. Nature 2004;433:164-7.

45. Spring M, Murphy J, Nielse R, et al. First-in-human evaluation of genetically attenuated *Plasmodium falciparum* sporozoites administered by bite of *Anopheles* mosquitoes to adult volunteers. Vaccine 2013;31:4975-83.

46. Good MF, Reiman JM, Rodriguez IB, et al. Cross-species malaria immunity induced by chemically attenuated parasites. Journal of Clinical Investigation 2013;123:3353-62.

47. Silvie O, Semblat JP, Franetich JF, Hannoun L, Eling W, Mazier D. Effects of irradiation on *Plasmodium falciparum* sporozoite hepatic development: implications for the design of pre-erythrocytic malaria vaccines. Parasite Immunology 2002;24:221-3.

48. Luke TC, Hoffman SL. Rationale and plans for developing a non-replicating, metabolically active, radiation-attenuated *Plasmodium falciparum* sporozoite vaccine. Journal of Experimental Biology 2003;206:3803-8.

49. Epstein JE, Tewari K, Lyke KE, et al. Live attenuated Malaria vaccine designed to protect through hepatic CD8(+) T cell immunity. Science 2011;334:475-80.

50. Schofield L, Villaquiran J, Ferreira A, Schellekens H, Nussenzweig R, Nussenzweig V. Gamma-interferon, CD8+ T-cells and antibodies required for immunity to malaria sporozoites. Nature 1987;330:664-6.

51. Conteh S, Chattopadhyay R, Anderson C, Hoffman SL. *Plasmodium yoelii*-infected *A. stephensi* inefficiently transmit malaria compared to intravenous route. PLoS One 2010;5:e8947.

52. Coppi A, Natarajan R, Pradel G, et al. The malaria circumsporozoite protein has two functional domains, each with distinct roles as sporozoites journey from mosquito to mammalian host. Journal of Experimental Medicine 2011;208:341-56.

53. Gardner MJ, Hall N, Fung E, et al. Genome sequence of the human malaria parasite *Plasmodium falciparum*. Nature 2002;419:498-511.

54. Florens L, Liu X, Wang YF, et al. Proteomics approach reveals novel proteins on the surface of malaria-infected erythrocytes. Molecular and Biochemical Parasitology 2004;135:1-11.

55. Bozdech Z, Llinas M, Pulliam BL, Wong ED, Zhu JC, DeRisi JL. The transcriptome of the intraerythrocytic developmental cycle of *Plasmodium falciparum*. PLoS Biology 2003;1:85-100.

56. Llinas M, Bozdech Z, Wong ED, Adai AT, DeRisi JL. Comparative whole genome transcriptome analysis of three *Plasmodium falciparum* strains. Nucleic Acids Research 2006;34:1166-73.

57. Doolan DL, Southwood S, Freilich DA, et al. Identification of *Plasmodium falciparum* antigens by antigenic analysis of genomic and proteomic data. Proceedings of the National Academy of Sciences of the United States of America 2003;100:9952-7.

58. Doolan DL. Plasmodium immunomics. International Journal for Parasitology 2011;41:3-20.

59. Dame JB, Williams JL, McCutchan TF, et al. Structure of the gene encoding the immunodominant surface-antigen on the sporozoite of the human malaria parasite *Plasmodium-falciparum*. Science 1984;225:593-9.

60. Enea V, Ellis J, Zavala F, et al. DNAcloning of *Plasmodium-falciparum* circumsporozoite gene - amino-acid-sequence of repetitive epitope. Science 1984;225:628-30.

61. Stewart MJ, Vanderberg JP. Malaria sporozoites leave behind trails of circumsporozoite protein during gliding motility. Journal of Protozoology 1988;35:389-93.

62. Frevert U, Sinnis P, Cerami C, Shreffler W, Takacs B, Nussenzweig V. Malaria circumsporozoite protein binds to heparan-sulfate proteoglycans associated with the surface-membrane of hepatocytes. Journal of Experimental Medicine 1993;177:1287-98.

63. Charoenvit Y, Mellouk S, Cole C, et al. Monoclonal, but not polyclonal, antibodies protect against *Plasmodium-yoelii* sporozoites Journal of Immunology 1991;146:1020-5.

64. Mishra S, Nussenzweig RS, Nussenzweig V. Antibodies to *Plasmodium* circumsporozoite protein (CSP) inhibit sporozoite's cell traversal activity. Journal of Immunological Methods 2012;377:47-52.

65. Nussenzweig V, Nussenzweig RS. Rationale for the development of an engineered sporozoite malaria vaccine. Advances in Immunology 1989;45:283-334.

66. Greenwood B. Immunological correlates of protection for the RTS,S candidate malaria vaccine. Lancet Infectious Diseases 2011;11:75-6.

67. Romero P, Maryanski JL, Corradin G, Nussenzweig RS, Nussenzweig V, Zavala F. Cloned cyto-toxic T-cells recognize an epitope in the circumsporozoite protein and protect against malaria. Nature 1989;341:323-6.

68. Rodrigues MM, Cordey AS, Arreaza G, et al. CD8+ cytolytic T-cell clones derived against the *Plasmodium-yoelii* circumsporozoite protein protect against malaria. International Immunology 1991;3:579-85.

69. Kumar KA, Sano G, Boscardin S, et al. The circumsporozoite protein is an immunodominant protective antigen in irradiated sporozoites. Nature 2006;444:937-40.

70. Cohen J, Nussenzweig V, Nussenzweig R, Vekemans J, Leach A. From the circumsporozoite protein to the RTS, S/AS candidate vaccine. Hum Vaccines 2010;6:90-6.

71. Grillot D, Michel M, Muller I, et al. Immune-responses to defined epitopes of the circumsporozoite protein of the murine malaria parasite, *Plasmodium*-yoelii. European Journal of Immunology 1990;20:1215-22.

72. Weiss WR, Mellouk S, Houghten RA, et al. Cytotoxic T-cells recognize a peptide from the circumsporozoite protein on malaria-infected hepatocytes. Journal of Experimental Medicine 1990;171:763-73.

73. Weiss WR, Berzofsky JA, Houghten RA, Sedegah M, Hollindale M, Hoffman SL. A T-cell clone directed at the circumsporozoite protein which protects mice against both *Plasmodium-yoelii* and *Plasmodium-berghei* Journal of Immunology 1992;149:2103-9.

74. Franke ED, Corradin G, Hoffman SL. Induction of protective CTL responses against the *Plasmodium yoelii* circumsporozoite protein by immunization with peptides. Journal of Immunology 1997;159:3424-33.

75. Franke ED, Sette A, Sacci J, Southwood S, Corradin G, Hoffman SL. A subdominant CD8(+) cytotoxic T lymphocyte (CTL) epitope from the *Plasmodium yoelii* circumsporozoite protein induces CTLs that eliminate infected hepatocytes from culture. Infection and Immunity 2000;68:3403-11.

76. Sedegah M, Hedstrom R, Hobart P, Hoffman SL. Protection against malaria by immunization with plasmid DNA encoding circumsporozoite protein. Proceedings of the National Academy of Sciences of the United States of America 1994;91:9866-70.

77. Wang RB, Doolan DL, Le TP, et al. Induction of antigen-specific cytotoxic T lymphocytes in humans by a malaria DNA vaccine. Science 1998;282:476-80.

78. Valenzuela P, Medina A, Rutter WJ. Synthesis and assembly of hepatitis-b virus surface-antigen particles in yeast. Nature 1982;298:347-50.

79. Casares S, Brumeanu TD, Richie TL. The RTS,S malaria vaccine. Vaccine 2010;28:4880-94.

80. Polhemus ME, Remich SA, Ogutu BR, et al. Evaluation of RTS,S/AS02A and RTS,S/AS01B in adults in a high malaria transmission area. PLoS One 2009;4:e6465.

81. Agnandji ST, Lell B, Soulanoudjingar SS, et al. First results of phase 3 trial of RTS,S/AS01 malaria vaccine in African children. New England Journal of Medicine 2011;365:1863-75.

82. Silvie O, Franetich JF, Charrin S, et al. A role for apical membrane antigen 1 during invasion of hepatocytes by *Plasmodium falciparum* sporozoites. Journal of Biological Chemistry 2004;279:9490-6.

83. Triglia T, Healer J, Caruana SR, et al. Apical membrane antigen 1 plays a central role in erythrocyte invasion by *Plasmodium* species. Molecular Microbiology 2000;38:706-18.

84. Healer J, Triglia T, Hodder AN, Gemmill AW, Cowman AF. Functional analysis of *Plasmodium falciparum* apical membrane antigen 1 utilizing interspecies domains. Infection and Immunity 2005;73:2444-51.

85. Treeck M, Zacherl S, Herrmann S, et al. Functional analysis of the leading malaria vaccine candidate AMA-1 reveals an essential role for the cytoplasmic domain in the invasion process. PLoS Pathogens 2009;5:e1000322.

86. Crewther PE, Culvenor JG, Silva A, Cooper JA, Anders RF. *Plasmodium falciparum* - 2 antigens of similar size are located in different compartments of the rhoptry. Experimental Parasitology 1990;70:193-206.

87. Anders RF, Adda CG, Foley M, Norton RS. Recombinant protein vaccines against the asexual blood stages of *Plasmodium falciparum*. Hum Vaccines 2010;6:39-53.

88. Chelimo K, Ofulla AV, Narum DL, Kazura JW, Lanar DE, John CC. Antibodies to *Plasmodium falciparum* antigens vary by age and antigen in children in a malaria-holoendemic area of Kenya. Pediatric Infectious Disease Journal 2005;24:680-4.

89. Narum DL, Ogun SA, Thomas AW, Holder AA. Immunization with parasite-derived apical membrane antigen 1 or passive immunization with a specific monoclonal antibody protects BALB/c mice against lethal *Plasmodium yoelii yoelii* YM blood-stage infection. Infection and Immunity 2000;68:2899-906.

90. Burns JM, Flaherty PR, Romero MM, Weidanz WP. Immunization against *Plasmodium chabaudi* malaria using combined formulations of apical membrane antigen-1 and merozoite surface protein-1. Vaccine 2003;21:1843-52.

91. Stowers AW, Kennedy MC, Keegan BP, Saul A, Long CA, Miller LH. Vaccination of monkeys with recombinant *Plasmodium falciparum* apical membrane antigen 1 confers protection against blood-stage malaria. Infection and Immunity 2002;70:6961-7.

92. Kocken CHM, Withers-Martinez C, Dubbeld MA, et al. High-level expression of the malaria blood-stage vaccine candidate *Plasmodium falciparum* apical membrane antigen 1 and induction of antibodies that inhibit erythrocyte invasion. Infection and Immunity 2002;70:4471-6.

93. Miao J, Li X, Liu ZX, Xue CF, Bujard H, Cui LW. Immune responses in mice induced by prime-boost schemes of the *Plasmodium falciparum* apical membrane antigen 1 (*Pf*AMA1)-based DNA, protein and recombinant modified vaccinia Ankara vaccines. Vaccine 2006;24:6187-98.

94. Amante FH, Crewther PE, Anders RF, Good MF. A cryptic T cell epitope on the apical membrane antigen 1 of *Plasmodium chabaudi adami* can prime for an anamnestic antibody response - Implications for malaria vaccine design. Journal of Immunology 1997;159:5535-44.

95. Xu HJ, Hodder AN, Yan HR, Crewther PE, Anders RF, Good MF. CD4(+) T cells acting independently of antibody contribute to protective immunity to *Plasmodium chabaudi* infection after apical membrane antigen 1 immunization. Journal of Immunology 2000;165:389-96.

96. Schussek S, Trieu A, Apte SH, Sidney J, Sette A, Doolan DL. Immunization with Apical Membrane Antigen 1 confers sterile infection-blocking immunity against *Plasmodium* sporozoite challenge in a rodent model. Infection and Immunity 2013;81:3586-99.

97. Remarque EJ, Faber BW, Kocken CHM, Thomas AW. Apical membrane antigen 1: a malaria vaccine candidate in review. Trends in Parasitology 2008;24:74-84.

98. Malkin EM, Diemert DJ, McArthur JH, et al. Phase 1 clinical trial of apical membrane antigen 1: an asexual blood-stage vaccine for *Plasmodium falciparum* malaria. Infection and Immunity 2005;73:3677-85.

99. Polhemus ME, Magill AJ, Cummings JF, et al. Phase I dose escalation safety and immunogenicity trial of *Plasmodium falciparum* apical membrane protein (AMA-1) FMP2.1, adjuvanted with AS02A, in malariu-naive adults at the Walter Reed Army Institute of Research. Vaccine 2007;25:4203-12.

100. Chesne-Seck ML, Pizarro JC, Vulliez-Le Normand B, et al. Structural comparison of apical membrane antigen 1 orthologues and paralogues in *apicomplexan* parasites. Molecular and Biochemical Parasitology 2005;144:55-67.

101. Hollingdale MR, Nardin EH, Tharavanij S, Schwartz AL, Nussenzweig RS. Inhibition of entry of *Plasmodium-falciparum* and *Plasmodium-vivax* sporozoites into cultured-cells - an *invitro* assay of protective antibodies. Journal of Immunology 1984;132:909-13.

102. Potocnjak P, Yoshida N, Nussenzweig RS, Nussenzweig V. Mono-valent fragments (fab) of monoclonal-antibodies to a sporozoite surface-antigen (PB44) protect mice against malarial infection. Journal of Experimental Medicine 1980;151:1504-13.

103. Yoshida N, Nussenzweig RS, Potocnjak P, Nussenzweig V, Aikawa M. Hybridoma produces protective antibodies directed against the sporozoite stage of malaria parasite. Science 1980;207:71-3.

104. Rosenberg R, Wirtz RA, Schneider I, Burge R. An estimation of the number of malaria sporozoites ejected by a feeding mosquito. Transactions of the Royal Society of Tropical Medicine and Hygiene 1990;84:209-12.

105. Beier JC, Onyango FK, Koros JK, et al. Quantitation of malaria sporozoites transmitted invitro during salivation by wild afrotropical anopheles. Medical and Veterinary Entomology 1991;5:71-9.

106. Shin SCJ, Vanderberg JP, Terzakis JA. Direct infection of hepatocytes by sporozoites of *Plasmodium-berghei*. Journal of Protozoology 1982;29:448-54.

107. Doolan DL, Hoffman SL. The complexity of protective immunity against liver-stage malaria. Journal of Immunology 2000;165:1453-62.

108. Todryk SM, Hill AVS. Malaria vaccines: the stage we are at. Nature Reviews Microbiology 2007;5:487-90.

109. Sturm A, Amino R, van de Sand C, et al. Manipulation of host hepatocytes by the malaria parasite for delivery into liver sinusoids. Science 2006;313:1287-90.

110. Barry AE, Leliwa-Sytek A, Tavul L, et al. Population Genomics of the immune evasion (var) genes of *Plasmodium falciparum*. PLoS Pathogens 2007;3:e70.

111. Osier FHA, Fegan G, Polley SD, et al. Breadth and magnitude of antibody responses to multiple *Plasmodium falciparum* merozoite antigens are associated with protection from clinical malaria. Infection and Immunity 2008;76:2240-8.

112. Murungi LM, Kamuyu G, Lowe B, et al. A threshold concentration of anti-merozoite antibodies is required for protection from clinical episodes of malaria. Vaccine 2013;31:3936-42.

113. Richie TL, Saul A. Progress and challenges for malaria vaccines. Nature 2002;415:694-701.

114. Goodman AL, Draper SJ. Blood-stage malaria vaccines - recent progress and future challenges. Annals of Tropical Medicine and Parasitology 2010;104:189-211.

115. Wang QA, Brown S, Roos DS, Nussenzweig V, Bhanot P. Transcriptome of axenic liver stages of *Plasmodium yoelii*. Molecular and Biochemical Parasitology 2004;137:161-8.

116. Lyon JA, Thomas AW, Hall T, Chulay JD. Specificities of antibodies that inhibit merozoite dispersal from malaria-infected erythrocytes. Molecular and Biochemical Parasitology 1989;36:77-85.

117. O'Donnell RA, de Koning-Ward TF, Burt RA, et al. Antibodies against merozoite surface protein (MSP)-1(19) are a major component of the invasion-inhibitory response in individuals immune to malaria. Journal of Experimental Medicine 2001;193:1403-12.

118. Richards JS, Beeson JG. The future for blood-stage vaccines against malaria. Immunology and Cell Biology 2009;87:377-90.

119. Elliott SR, Kuns RD, Good MF. Heterologous immunity in the absence of variant-specific antibodies after exposure to subpatent infection with blood-stage malaria. Infection and Immunity 2005;73:2478-85.

120. Pombo DJ, Lawrence G, Hirunpetcharat C, et al. Immunity to malaria after administration of ultra-low doses of red cells infected with *Plasmodium falciparum*. Lancet 2002;360:610-7.

121. Doolan DL, Sedegah M, Hedstrom RC, Hobart P, Charoenvit Y, Hoffman SL. Circumventing genetic restriction of protection against malaria with multigene DNA immunization: CD8(+) T cell-, interferon gamma-, and nitric oxide-dependent immunity. Journal of Experimental Medicine 1996;183:1739-46.

122. Tine JA, Lanar DE, Smith DM, et al. NYVAC-Pf7: A poxvirus-vectored, multiantigen, multistage vaccine candidate for *Plasmodium falciparum* malaria. Infection and Immunity 1996;64:3833-44.

123. Rogers WO, Baird JK, Kumar A, et al. Multistage multiantigen heterologous prime boost vaccine for *Plasmodium knowlesi* malaria provides partial protection in rhesus macaques. Infection and Immunity 2001;69:5565-72.

124. Ockenhouse CF, Sun PF, Lanar DE, et al. Phase I/IIa safety, immunogenicity, and efficacy trial of NYVAC-*Pf*7, a pox-vectored, multiantigen, multistage vaccine candidate for *Plasmodium falciparum* malaria. Journal of Infectious Diseases 1998;177:1664-73.

125. Kushnir N, Streatfield SJ, Yusibov V. Virus-like particles as a highly efficient vaccine platform: Diversity of targets and production systems and advances in clinical development. Vaccine 2012;31:58-83.

126. Stanley MA. Human papillomavirus vaccines. Reviews in Medical Virology 2006;16:139-49.

127. Chackerian B. Virus-like particles-flexible platforms for vaccine development. Expert Review of Vaccines 2007;6:381-90.

128. Chackerian B, Lenz P, Lowy DR, Schiller JT. Determinants of autoantibody induction by conjugated papillomavirus virus-like particles. Journal of Immunology 2002;169:6120-6.

129. Bachmann MF, Rohrer UH, Kundig TM, Burki K, Hengartner H, Zinkernagel RM. The influence of antigen organization on B-cell responsiveness. Science 1993;262:1448-51.

130. Grgacic EVL, Anderson DA. Virus-like particles: Passport to immune recognition. Methods 2006;40:60-5.

131. Thones N, Herreiner A, Schadlich L, Piuko K, Muller M. A direct comparison of human papillomavirus type 16 L1 particles reveals a lower immunogenicity of capsomeres than viruslike particles with respect to the induced antibody response. Journal of Virology 2008;82:5472-85.

132. Akira S, Takeda K, Kaisho T. Toll-like receptors: critical proteins linking innate and acquired immunity. Nature Immunology 2001;2:675-80.

133. Kawai T, Akira S. The role of pattern-recognition receptors in innate immunity: update on Toll-like receptors. Nature Immunology 2010;11:373-84.

134. Barton GM, Medzhitov R. Toll-like receptors and their ligands. Toll-Like Receptor Family Members and Their Ligands 2002;270:81-92.

135. Plummer EM, Manchester M. Viral nanoparticles and virus-like particles: platforms for contemporary vaccine design. Wiley Interdisciplinary Reviews-Nanomedicine and Nanobiotechnology 2011;3:174-96.

136. Lechmann M, Murata K, Satoi J, Vergalla J, Baumert TF, Liang TJ. Hepatitis C virus-like particles induce virus-specific humoral and cellular immune responses in mice. Hepatology 2001;34:417-23.

137. Zhu F-C, Zhang J, Zhang X-F, et al. Efficacy and safety of a recombinant hepatitis E vaccine in healthy adults: a large-scale, randomised, double-blind placebo-controlled, phase 3 trial. Lancet 2010;376:895-902.

138. Maupas P, Goudeau A, Coursaget P, Drucker J, Bagros P. Immunization against hepatitis-B in man. Lancet 1976;1:1367-70.

139. Michel ML, Tiollais P. Hepatitis B vaccines: Protective efficacy and therapeutic potential. Pathologie Biologie 2010;58:288-95.

140. Galibert F, Mandart E, Fitoussi F, Tiollais P, Charnay P. Nucleotide-sequence of the hepatitis-b virus genome (subtype ayw) cloned in *Escherichia-coli*. Nature 1979;281:646-50.

141. Valenzuela P, Gray P, Quiroga M, Zaldivar J, Goodman HM, Rutter WJ. Nucleotide-sequence of the gene coding for the major protein of hepatitis-b virus surface-antigen. Nature 1979;280:815-9.

142. RECOMBIVAX HB® product monograph. 2012. (Accessed 05.06.2014, at http://www.merck.ca/assets/en/pdf/products/RECOMBIVAX_HB-PM_E.pdf.)

143. ENGERIX®-B product monograph. 2013. (Accessed 5.06.2014, at http://www.gsk.com.au/resources.ashx/vaccineproductschilddataproinfo/505/FileName/01B298A55325FABF7209FC53FAA8ED5C/Engerix-B_PI_006_approved.pdf.)

144. CERVARIX® product monograph. 2014. (Accessed 5.06.2014, at http://www.gsk.com.au/resources.ashx/vaccineproductschilddataproinfo/496/FileName/3E81056AE2FE8CAE629CF2AEB25C5463/Cervarix_PI_010_Approved.pdf.)

145. GARDASIL® product monograph. 2013. (Accessed 05.06.2014, at http://www.merck.ca/assets/en/pdf/products/GARDASIL-PM_E.pdf.)

146. Harper DM. Currently approved prophylactic HPV vaccines. Expert Review of Vaccines 2009;8:1663-79.

147. Smolen KK, Gelinas L, Franzen L, et al. Age of recipient and number of doses differentially impact human B and T cell immune memory responses to HPV vaccination. Vaccine 2012;30:3572-9.

148. Zhang LF, Zhou J, Chen S, et al. HPV6b virus like particles are potent immunogens without adjuvant in man. Vaccine 2000;18:1051-8.

149. Roldao A, Mellado MCM, Castilho LR, Carrondo MJT, Alves PM. Virus-like particles in vaccine development. Expert Review of Vaccines 2010;9:1149-76.

150. Trieu A, Kayala MA, Burk C, et al. Sterile protective immunity to malaria is associated with a panel of novel *P. falciparum* antigens. Molecular & Cellular Proteomics 2011;10:M111.007948-1-16.

151. Schussek S, Trieu A, Doolan DL. Genome- and proteome-wide screening strategies for antigen discovery and immunogen design. Biotechnology Advances 2014;32:403-14.

152. Schodel F, Moriarty AM, Peterson DL, et al. The position of heterologous epitopes inserted in Hepatitis-b virus core particles determines their immunogenicity. Journal of Virology 1992;66:106-14.

153. Gedvilaite A, Frommel C, Sasnauskas K, et al. Formation of immunogenic virus-like particles by inserting epitopes into surface-exposed regions of hamster polyomavirus major capsid protein. Virology 2000;273:21-35.

154. Dorn DC, Lawatscheck R, Zvirbliene A, et al. Cellular and humoral immunogenicity of hamster polyomavirus-derived virus-like particles harboring a mucin 1 cytotoxic T-cell epitope. Viral Immunology 2008;21:12-26.

155. Crisci E, Almanza H, Mena I, et al. Chimeric calicivirus-like particles elicit protective anti-viral cytotoxic responses without adjuvant. Virology 2009;387:303-12.

156. Jegerlehner A, Tissot A, Lechner F, et al. A molecular assembly system that renders antigens of choice highly repetitive for induction of protective B cell responses. Vaccine 2002;20:3104-12.

157. Pejawar-Gaddy S, Rajawat Y, Hilioti Z, et al. Generation of a tumor vaccine candidate based on conjugation of a MUC1 peptide to polyionic papillomavirus virus-like particles. Cancer Immunology Immunotherapy 2010;59:1685-96.

158. Rueda P, Moron G, Sarraseca J, Leclerc C, Casal JI. Influence of flanking sequences on presentation efficiency of a CD8(+) cytotoxic T-cell epitope delivered by parvovirus-like particles. Journal of General Virology 2004;85:563-72.

159. Lawatscheck R, Aleksaite E, Schenk JA, et al. Chimeric polyomavirus-derived virus-like particles: The immunogenicity of an inserted peptide applied without adjuvant to mice depends on its insertion site and its flanking linker sequence. Viral Immunology 2007;20:453-60.

160. Anggraeni MR, Connors NK, Wu Y, Chuan YP, Lua LHL, Middelberg APJ. Sensitivity of immune response quality to influenza helix 190 antigen structure displayed on a modular virus-like particle. Vaccine 2013;31:4428-35.

161. Kawano M, Morikawa K, Suda T, et al. Chimeric SV40 virus-like particles induce specific cytotoxicity and protective immunity against influenza A virus without the need of adjuvants. Virology 2014;448:159-67.

162. Peacey M, Wilson S, Baird MA, Ward VK. Versatile RHDV virus-like particles: Incorporation of antigens by genetic modification and chemical conjugation. Biotechnology and Bioengineering 2007;98:968-77.

163. Roehn TA, Jennings GT, Hernandez M, et al. Vaccination against IL-17 suppresses autoimmune arthritis and encephalomyelitis. European Journal of Immunology 2006;36:2857-67.

164. Jegerlehner A, Wiesel M, Dietmeier K, et al. Carrier induced epitopic suppression of antibody responses induced by virus-like particles is a dynamic phenomenon caused by carrier-specific antibodies. Vaccine 2010;28:5503-12.

165. Rayment I, Baker TS, Caspar DLD, Murakami WT. Polyoma-virus capsid structure at 22.5-A resolution. Nature 1982;295:110-5.

166. Salunke DM, Caspar DLD, Garcea RL. Self-assembly of purified polyomavirus capsid protein-VP1. Cell 1986;46:895-904.

167. Liddington RC, Yan Y, Moulai J, Sahli R, Benjamin TL, Harrison SC. Structure of simian virus-40 at 3.8-A resolution. Nature 1991;354:278-84.

168. Garcea RL, Salunke DM, Caspar DLD. Site-directed mutation affecting polyomavirus capsid self-assembly *invitro*. Nature 1987;329:86-8.

169. Ohlschlager P, Osen W, Dell K, et al. Human papillomavirus type 16 L1 capsomeres induce L1-specific cytotoxic T lymphocytes and tumor regression in C57BL/6 mice. Journal of Virology 2003;77:4635-45.

170. Wibowo N, Chuan YP, Lua LHL, Middelberg APJ. Modular engineering of a microbially-produced viral capsomere vaccine for influenza. Chemical Engineering Science 2012.

171. Mach H, Volkin DB, Troutman RD, et al. Disassembly and reassembly of yeast-derived recombinant human papillomavirus virus-like particles (HPV VLPs). Journal of Pharmaceutical Sciences 2006;95:2195-206.

172. McCarthy MP, White WI, PalmerHill F, Koenig S, Suzich JA. Quantitative disassembly and reassembly of human papillomavirus type 11 virus-like particles *in vitro*. Journal of Virology 1998;72:32-41.

173. Middelberg APJ, Rivera-Hernandez T, Wibowo N, et al. A microbial platform for rapid and low-cost virus-like particle and capsomere vaccines. Vaccine 2011;29:7154-62.

174. Liu WL, Zou P, Liu ZQ, Yun L, Jian D, Chen YH. High epitope density in a single recombinant protein molecule of the extracellular domain of influenza A virus M2 protein significantly enhances protective immunity. Vaccine 2004;23:366-71.

175. De Filette M, Jou WM, Birkett A, et al. Universal influenza A vaccine: Optimization of M2-based constructs. Virology 2005;337:149-61.

176. Gedvilaite A, Zvirbliene A, Staniulis Z, Sasnauskas K, Kruger DH, Ulrich R. Segments of Puumala hantavirus nucleocapsid protein inserted into chimeric polyomavirus-derived virus-like particles induce a strong immune response in mice. Viral Immunology 2004;17:51-68.

177. Rose RC, White WI, Li ML, Suzich JA, Lane C, Garcea RL. Human papillomavirus type 11 recombinant L1 capsomeres induce virus-neutralizing antibodies. Journal of Virology 1998;72:6151-4.

178. Schaedlich L, Senger T, Gerlach B, et al. Analysis of modified human papillomavirus type 16 L1 capsomeres: the ability to assemble into larger particles correlates with higher immunogenicity. Journal of Virology 2009;83:7690-705.

179. Senger T, Schadlich L, Textor S, et al. Virus-like particles and capsomeres are potent vaccines against cutaneous alpha HPVs. Vaccine 2010;28:1583-93.

180. Fligge C, Giroglou T, Streeck RE, Sapp M. Induction of type-specific neutralizing antibodies by capsomeres of human papillomavirus type 33. Virology 2001;283:353-7.

181. Benjamin TL. Polyoma Virus: Old Findings and New Challenges. Virology 2001;289:167-73.

182. Gross L. A filterable agent, recovered from Ak leukemic extracts, causing salivary gland carcinomas in C3H mice. Proc Soc Exp Biol Med 1953;83:414-21.

183. Teunissen EA, de Raad M, Mastrobattista E. Production and biomedical applications of virus-like particles derived from polyomaviruses. Journal of Controlled Release 2013;172:305-21.

184. Schmidt U, Rudolph R, Bohm G. Mechanism of assembly of recombinant murine polyomavirus-like particles. Journal of Virology 2000;74:1658-62.

185. Eckhart W. *Polyomavirinae* and their replication. Fields, B N And D M Knipe1991:727-42.

186. Franzen AV, Tegerstedt K, Hollanderova D, Forstova J, Ramqvist T, Dalianis T. Murine polyomavirus-VP1 virus-like particles immunize against some polyomavirus-induced tumours. In Vivo 2005;19:323-6.

187. Liew MWO, Rajendran A, Middelberg APJ. Microbial production of virus-like particle vaccine protein at gram-per-litre levels. Journal of Biotechnology 2010;150:224-31.

188. Rivera-Hernandez T, Hartas J, Wu Y, et al. Self-adjuvanting modular virus-like particles for mucosal vaccination against group A streptococcus (GAS). Vaccine 2013;31:1950-5.

189. Chuan YP, Lua LHL, Middelberg APJ. High-level expression of soluble viral structural protein in *Escherichia coli*. Journal of Biotechnology 2008;134:64-71.

190. Rivera Hernandez T. Bioengineering virus-like particles for vaccine development: The University of Queensland; 2012.

191. Pattenden LK, Middelberg APJ, Niebert M, Lipin DI. Towards the preparative and large-scale precision manufacture of virus-like particles. Trends in Biotechnology 2005;23:523-9.

192. Figdor CG, van Kooyk Y, Adema GJ. C-type lectin receptors on dendritic cells and Langerhans cells. Nature Reviews Immunology 2002;2:77-84.

193. Gamvrellis A, Leong D, Hanley JC, Xiang SD, Mottram P, Plebanski M. Vaccines that facilitate antigen entry into dendritic cells. Immunology and Cell Biology 2004;82:506-16.

194. Paustian C, Caspell R, Johnson T, et al. Effect of multiple activation stimuli on the generation of Th1-polarizing dendritic cells. Human Immunology 2011;72:24-31.

195. Heath WR, Belz GT, Behrens GMN, et al. Cross-presentation, dendritic cell subsets, and the generation of immunity to cellular antigens. Immunological Reviews 2004;199:9-26.

196. Fifis T, Gamvrellis A, Crimeen-Irwin B, et al. Size-dependent immunogenicity: Therapeutic and protective properties of nano-vaccines against tumors. Journal of Immunology 2004;173:3148-54.

197. Manolova V, Flace A, Bauer M, Schwarz K, Saudan P, Bachmann MF. Nanoparticles target distinct dendritic cell populations according to their size. European Journal of Immunology 2008;38:1404-13.

198. Smith CM, Belz GT, Wilson NS, et al. Cutting edge: Conventional CD8 alpha(+) dendritic cells are preferentially involved in CTL priming after footpad infection with herpes simplex virus-1. Journal of Immunology 2003;170:4437-40.

199. Belz GT, Smith CM, Eichner D, et al. Cutting edge: Conventional CD8 alpha(+) dendritic cells are generally involved in priming CTL immunity to viruses. Journal of Immunology 2004;172:1996-2000.

200. Keller SA, Bauer M, Manolova V, Muntwiler S, Saudan P, Bachmann MF. Cutting edge: limited specialization of dendritic cell subsets for MHC class II-associated presentation of viral particles. Journal of Immunology 2010;184:26-9.

201. Pushko P, Kort T, Nathan M, Pearce MB, Smith G, Tumpey TM. Recombinant H1N1 virus-like particle vaccine elicits protective immunity in ferrets against the 2009 pandemic H1N1 influenza virus. Vaccine 2010;28:4771-6.

202. Bickert T, Wohlleben G, Brinkman M, et al. Murine polyomavirus-like particles induce maturation of bone marrow-derived dendritic cells and proliferation of T cells. Medical Microbiology and Immunology 2007;196:31-9.

203. Gedvilaite A, Dorn DC, Sasnauskas K, et al. Virus-like particles derived from major capsid protein VP1 of different polyomaviruses differ in their ability to induce maturation in human dendritic cells. Virology 2006;354:252-60.

204. Zhu J, Paul WE. CD4 T cells: fates, functions, and faults. Blood 2008;112:1557-69.

205. Williams MA, Tyznik AJ, Bevan MJ. Interleukin-2 signals during priming are required for secondary expansion of CD8(+) memory T cells. Nature 2006;441:890-3.

206. Murphy KM, Reiner SL. The lineage decisions of helper T cells. Nature Reviews Immunology 2002;2:933-44.

207. Lenz P, Day PM, Pang YYS, et al. Papillomavirus-like particles induce acute activation of dendritic cells. Journal of Immunology 2001;166:5346-55.

208. Goldmann C, Petry H, Frye S, et al. Molecular cloning and expression of major structural protein VP1 of the human polyomavirus JC virus: Formation of virus-like particles useful for immunological and therapeutic studies. Journal of Virology 1999;73:4465-9.

209. Chuan YP, Wibowo N, Connors NK, et al. Microbially synthesized modular virus-like particles and capsomeres displaying group A streptococcus hypervariable antigenic determinants. Biotechnology and Bioengineering 2014;111:1062-70.

210. Schmidt NW, Podyminogin RL, Butler NS, et al. Memory CD8 T cell responses exceeding a large but definable threshold provide long-term immunity to malaria. Proceedings of the National Academy of Sciences of the United States of America 2008;105:14017-22.

211. Peacey M, Wilson S, Perret R, et al. Virus-like particles from rabbit hemorrhagic disease virus can induce an anti-tumor response. Vaccine 2008;26:5334-7.

212. Brinkman M, Walter J, Grein S, et al. Beneficial therapeutic effects with different particulate structures of murine polyomavirus VP1-coat protein carrying self or non-self CD8 T cell epitopes against murine melanoma. Cancer Immunology Immunotherapy 2005;54:611-22.

213. Moffat JM, Cheong W-S, Villadangos JA, Mintern JD, Netter HJ. Hepatitis B virus-like particles access major histocompatibility class I and II antigen presentation pathways in primary dendritic cells. Vaccine 2013;31:2310-6.

214. Sedlik C, Saron MF, Sarraseca J, Casal I, Leclerc C. Recombinant parvovirus-like particles as an antigen carrier: A novel nonreplicative exogenous antigen to elicit protective antiviral cytotoxic T cells. Proceedings of the National Academy of Sciences of the United States of America 1997;94:7503-8.

215. Mazeike E, Gedvilaite A, Blohm U. Induction of insert-specific immune response in mice by hamster polyomavirus VP1 derived virus-like particles carrying LCMV GP33 CTL epitope. Virus Research 2012;163:2-10.

216. Storni T, Lechner F, Erdmann I, et al. Critical role for activation of antigen-presenting cells in priming of cytotoxic T cell responses after vaccination with virus-like particles. Journal of Immunology 2002;168:2880-6.

217. Caparros-Wanderley W, Clark B, Griffin BE. Effect of dose and long-term storage on the immunogenicity of murine polyomavirus VP1 virus-like particles. Vaccine 2004;22:352-61.

218. Schwarz K, Meijerink E, Speiser DE, et al. Efficient homologous prime-boost strategies for T cell vaccination based on virus-like particles. European Journal of Immunology 2005;35:816-21.

219. Birkett A, Lyons K, Schmidt A, et al. A modified hepatitis B virus core particle containing multiple epitopes of the *Plasmodium falciparum* circumsporozoite protein provides a highly immunogenic malaria vaccine in preclinical analyses in rodent and primate hosts. Infection and Immunity 2002;70:6860-70.

220. Barth H, Ulsenheimer A, Pape GR, et al. Uptake and presentation of hepatitis C virus-like particles by human dendritic cells. Blood 2005;105:3605-14.

221. Visciano ML, Tagliamonte M, Tornesello ML, Buonaguro FM, Buonaguro L. Effects of adjuvants on IgG subclasses elicited by virus-like particles. Journal of Translational Medicine 2012;10.

222. Adler HI, Fisher WD, Cohen A, Hardigre AA. Miniature *Escherichia coli* cells deficient in DNA. Proceedings of the National Academy of Sciences of the United States of America 1967;57:321-6.

223. Roozen KJ, Fenwick RG, Curtiss R. Synthesis of ribonucleic acid and protein in plasmid-containing minicells of *Escherichia-coli* K-12. Journal of Bacteriology 1971;107:21-33.

224. Meagher RB, Tait RC, Betlach M, Boyer HW. Protein expression in *Escherichia-coli* minicells by recombinant plasmids. Cell 1977;10:521-36.

225. Frazer AC, Curtiss R, 3rd. Production, properties and utility of bacterial minicells. Current Topics in Microbiology and Immunology 1975;69:1-84.

226. Adler HI, Fisher WD, Stapleto.Ge. Genetic control of cell division in bacteria. Science 1966;154:417-30.

227. MacDiarmid JA, Mugridge NB, Weiss JC, et al. Bacterially derived 400 nm particles for encapsulation and cancer cell targeting of chemotherapeutics. Cancer Cell 2007;11:431-45.

228. Khachatourians GG. Minicells as specialized vaccine and vaccine carriers. Recombinant DNA vaccines: rationale and strategies New York: Marcel Dekker, Inc 1992:323-33.

229. Vicente M, Rico AI, Martinez-Arteaga R, Mingorance J. Septum enlightenment: Assembly of bacterial division proteins. Journal of Bacteriology 2006;188:19-27.

230. Deboer PAJ, Crossley RE, Rothfield LI. A division inhibitor and a topological specificity factor coded for by the minicell locus determine proper placement of the division septum in *Escherichia-coli*. Cell 1989;56:641-9.

231. Ward JE, Lutkenhaus J. Overproduction of *FtsZ* induces minicell formation in *Escherichia coli* Cell 1985;42:941-9.

232. Garrido T, Sanchez M, Palacios P, Aldea M, Vicente M. Transcription of ftsZ oscillates during the cell-cycle of *Escherichia coli*. EMBO Journal 1993;12:3957-65.

233. Crooks JH, Ullman M, Zoller M, Levy SB. Transcription of plasmid DNA in *Escherichia-coli* minicells. Plasmid 1983;10:66-72.

234. Clarkcurtiss JE, Curtiss R. Analysis of recombinant DNA using *Escherichia-coli* minicells. Methods in Enzymology 1983;101:347-62.

235. Giacalone MJ, Gentile AM, Lovitt BT, Xu T, Surber MW, Sabbadini RA. The use of bacterial minicells to transfer plasmid DNA to eukaryotic cells. Cellular Microbiology 2006;8:1624-33.

236. Giacalone MJ, Sabbadini RA, Chambers AL, Pillai S, McGuire KL. Immune responses elicited by bacterial minicells capable of simultaneous DNA and protein antigen delivery. Vaccine 2006;24:6009-17.

237. Giacalone MJ, Zapata JC, Berkley NL, et al. Immunization with non-replicating *E-coli* minicells delivering both protein antigen and DNA protects mice from lethal challenge with lymphocytic choriomeningitis virus. Vaccine 2007;25:2279-87.

238. MacDiarmid JA, Amaro-Mugridge NB, Madrid-Weiss J, et al. Sequential treatment of drug-resistant tumors with targeted minicells containing siRNA or a cytotoxic drug. Nature Biotechnology 2009;27:643-51.

239. MacDiarmid JA, Brahmbhatt H. Minicells: Versatile vectors for targeted drug or si/shRNA cancer therapy. Current Opinion in Biotechnology 2011;22:909-16.

240. Nestorovich EM, Danelon C, Winterhalter M, Bezrukov SM. Designed to penetrate: Time-resolved interaction of single antibiotic molecules with bacterial pores. Proceedings of the National Academy of Sciences of the United States of America 2002;99:9789-94.

241. Nicholson RI, Gee JMW, Harper ME. EGFR and cancer prognosis. European Journal of Cancer 2001;37:S9-S15.

242. Heidel JD, Liu JY-C, Yen Y, et al. Potent siRNA inhibitors of ribonucleotide reductase subunit RRM2 reduce cell proliferation *in vitro* and *in vivo*. Clinical Cancer Research 2007;13:2207-15.

243. Inselbur.J. Replication of colicin E1 plasmid DNA in minicells from a unique replication initiation site. Proceedings of the National Academy of Sciences of the United States of America 1974;71:2256-9.

244. Reeve JN. Selective expression of transduced or cloned DNA in minicells containing plasmid pkb280. Nature 1978;276:728-9.

245. Carleton HA, Lara-Tejero M, Liu X, Galan JE. Engineering the type III secretion system in non-replicating bacterial minicells for antigen delivery. Nature Communications 2013;4:1590.

246. Grillot-Courvalin C, Goussard S, Huetz F, Ojcius DM, Courvalin P. Functional gene transfer from intracellular bacteria to mammalian cells. Nature Biotechnology 1998;16:862-6.

247. Dersch P, Isberg RR. An immunoglobulin superfamily-like domain unique to the *Yersinia pseudotuberculosis* invasin protein is required for stimulation of bacterial uptake via integrin receptors. Infection and Immunity 2000;68:2930-8.

248. Arnold R, Jehl A, Rattei T. Targeting effectors: the molecular recognition of Type III secreted proteins. Microbes and Infection 2010;12:346-58.

249. Galan JE, Wolf-Watz H. Protein delivery into eukaryotic cells by type III secretion machines. Nature 2006;444:567-73.

250. Kulp A, Kuehn MJ. Biological functions and biogenesis of secreted bacterial outer membrane vesicles. In: Gottesman S, Harwood CS, eds. Annual Review of Microbiology, Vol 64, 2010. Palo Alto: Annual Reviews; 2010:163-84.

251. Ellis TN, Kuehn MJ. Virulence and immunomodulatory roles of bacterial outer membrane vesicles. Microbiology and Molecular Biology Reviews 2010;74:81-+.

252. Berleman J, Auer M. The role of bacterial outer membrane vesicles for intra- and interspecies delivery. Environmental Microbiology 2013;15:347-54.

253. Novartis Vaccines and Diagnostics I. Bexsero®- product monograph. 2013.

254. Bjune G, Hoiby EA, Gronnesby JK, et al. Effect of outer-membrane vesicle vaccine against group-B meningococcal disease in Norway. Lancet 1991;338:1093-6.

255. Sierra GVG, Campa HC, Varcacel NM, et al. Vaccine against group B neisseria-meningitidis protection trial and mass vaccination results in Cuba. NIPH (National Institute of Public Health) Annals (Oslo) 1991;14:195-210.

256. Demoraes JC, Perkins BA, Camargo MCC, et al. Protective efficacy of a serogroup-B meningococcal vaccine in Sao-Paulo, Brazil. Lancet 1992;340:1074-8.

257. Boslego J, Garcia J, Cruz C, et al. Efficacy, safety, and immunogenicity of a meningococcal group-B (15-p1.3) outer-membrane protein vaccine in Iquique, Chile. Vaccine 1995;13:821-9.

258. Tappero JW, Lagos R, Ballesteros AM, et al. Immunogenicity of 2 serogroup B outer-membrane protein meningococcal vaccines - A randomized controlled trial in Chile. Jama-Journal of the American Medical Association 1999;281:1520-7.

259. O'Hallahan J, McNicholas A, Galloway Y, O'Leary E, Roseveare C. Delivering a safe and effective strain-specific vaccine to control an epidemic of group B meningococcal disease. The New Zealand Medical Journal 2009;122:48-59.

260. Kadurugamuwa JL, Beveridge TJ. Virulence factors are released from pseudomonas-aeruginosa in association with membrane-vesicles during normal growth and exposure to gentamicin - a novel mechanism of enzyme-secretion. Journal of Bacteriology 1995;177:3998-4008.

261. Kolling GL, Matthews KR. Export of virulence genes and shiga toxin by membrane vesicles of *Escherichia coli* O157 : H7. Applied and Environmental Microbiology 1999;65:1843-8.

262. Moe GR, Zuno-Mitchell P, Hammond SN, Granoff DM. Sequential immunization with vesicles prepared from heterologous *Neisseria meningitidis* strains elicits broadly protective serum antibodies to group B strains. Infection and Immunity 2002;70:6021-31.

263. Alaniz RC, Deatherage BL, Lara JC, Cookson BT. Membrane vesicles are immunogenic facsimiles of *Salmonella typhimurium* that potently activate dendritic cells, prime B and T cell responses, and stimulate protective immunity *in vivo*. Journal of Immunology 2007;179:7692-701.

264. Tani C, Stella M, Donnarumma D, et al. Quantification by LC-MSE of outer membrane vesicle proteins of the Bexsero((R)) vaccine. Vaccine 2014;32:1273-9.

265. Ferrari G, Garaguso I, Adu-Bobie J, et al. Outer membrane vesicles from group B *Neisseria meningitidis* Delta gna33 mutant: Proteomic and immunological comparison with detergent-derived outer membrane vesicles. Proteomics 2006;6:1856-66.

266. Kesty NC, Kuehn MJ. Incorporation of heterologous outer membrane and periplasmic proteins into *Escherichia coli* outer membrane vesicles. Journal of Biological Chemistry 2004;279:2069-76.

267. Chen DJ, Osterrieder N, Metzger SM, et al. Delivery of foreign antigens by engineered outer membrane vesicle vaccines. Proceedings of the National Academy of Sciences of the United States of America 2010;107:3099-104.

268. Mayr UB, Walcher P, Azimpour C, Riedmann E, Haller C, Lubitz W. Bacterial ghosts as antigen delivery vehicles. Advanced Drug Delivery Reviews 2005;57:1381-91.

269. Muhammad A, Champeimont J, Mayr UB, Lubitz W, Kudela P. Bacterial ghosts as carriers of protein subunit and DNA-encoded antigens for vaccine applications. Expert Review of Vaccines 2012;11:97-116.

270. Witte A, Wanner G, Sulzner M, Lubitz W. Dynamics of PhiX174 protein e-mediated lysis of *Escherichia-coli*. Archives of Microbiology 1992;157:381-8.

271. Ebensen T, Paukner S, Link C, et al. Bacterial ghosts are an efficient delivery system for DNA vaccines. Journal of Immunology 2004;172:6858-65.

272. Paukner S, Kohl G, Lubitz W. Bacterial ghosts as novel advanced drug delivery systems: antiproliferative activity of loaded doxorubicin in human Caco-2 cells. Journal of Controlled Release 2004;94:63-74.

273. Paukner S, Kohl G, Jalava K, Lubitz W. Sealed bacterial ghosts - Novel targeting vehicles for advanced drug delivery of water-soluble substances. Journal of Drug Targeting 2003;11:151-61.

274. Jechlinger W, Haller C, Resch S, Hofmann A, Szostak MP, Lubitz W. Comparative immunogenicity of the Hepatitis B virus core 149 antigen displayed on the inner and outer membrane of bacterial ghosts. Vaccine 2005;23:3609-17.

275. Paukner S, Kudela P, Kohl G, Schlapp T, Friedrichs S, Lubitz W. DNA-loaded bacterial ghosts efficiently mediate reporter gene transfer and expression in macrophages. Molecular Therapy 2005;11:215-23.

276. Kudela P, Koller VJ, Lubitz W. Bacterial ghosts (BGs)-Advanced antigen and drug delivery system. Vaccine 2010;28:5760-7.

277. Haslberger AG, Kohl G, Felnerova D, Mayr UB, Furst-Ladani S, Lubitz W. Activation, stimulation and uptake of bacterial ghosts in antigen presenting cells. Journal of Biotechnology 2000;83:57-66.

278. Dougan G, Sherratt D. The transposon Tn*1* as a probe for studying ColE1 structure and function. Molecular & General Genetics 1977;151:151-60.

279. Cardoso FC, Roddick JS, Groves P, Doolan DL. Evaluation of approaches to identify the targets of cellular immunity on a proteome-wide scale. PLoS One 2011;6:e27666.

280. Teasdale RD, Dagostaro G, Gleeson PA. The signal for golgi retention of bovine-beta-1,4-galactosyltransferase is in the transmembrane domain. Journal of Biological Chemistry 1992;267:4084-96.

281. Kumada Y, Kuroki D, Yasui H, Ohse T, Kishimoto M. Characterization of polystyrene-binding peptides (PS-tags) for site-specific immobilization of proteins. Journal of Bioscience and Bioengineering 2010;109:583-7.

282. Kogot JM, Sarkes DA, Val-Addo I, Pellegrino PM, Stratis-Cullum DN. Increased affinity and solubility of peptides used for direct peptide ELISA on polystyrene surfaces through fusion with a polystyrene-binding peptide tag. Biotechniques 2012;52:95-102.

283. Apte SH, Groves PL, Skwarczynski M, et al. Vaccination with lipid core peptides fails to induce epitope-specific T cell responses but confers non-specific protective immunity in a malaria model. PLoS One 2012;7:e40928.

284. Charoenvit Y, Leef MF, Yuan LF, Sedegah M, Beaudoin RL. Characterization of *Plasmodium-yoelii* monoclonal-antibodies directed against stage-specific sporozoite antigens. Infection and Immunity 1987;55:604-8.

285. Apte SH, Groves PL, Roddick JS, da Hora VP, Doolan DL. High-throughput multi-parameter flow-cytometric analysis from micro-quantities of *Plasmodium*-infected blood. International Journal for Parasitology 2011;41:1285-94.

286. Schussek S, Groves PL, Apte SH, Doolan DL. Highly sensitive quantitative real-time PCR for the detection of *Plasmodium* liver-stage parasite burden following low-dose sporozoite challenge. PLoS One 2013;8:e77811.

287. Witney AA, Doolan DL, Anthony RM, Weiss WR, Hoffman SL, Carucci DJ. Determining liver stage parasite burden by real time quantitative PCR as a method for evaluating pre-erythrocytic malaria vaccine efficacy. Molecular and Biochemical Parasitology 2001;118:233-45.

288. Chuan YP, Fan YY, Lua LHL, Middelberg APJ. Virus assembly occurs following a pH- or Ca(2+)-triggered switch in the thermodynamic attraction between structural protein capsomeres. Journal of the Royal Society Interface 2010;7:409-21.

289. Liew MWO, Chuan YP, Middelberg APJ. High-yield and scalable cell-free assembly of virus-like particles by dilution. Biochemical Engineering Journal 2012;67:88-96.

290. Stanley M, Lowy DR, Frazer I. Prophylactic HPV vaccines: Underlying mechanisms. Vaccine 2006;24:106-13.

291. Alexopoulou L, Holt AC, Medzhitov R, Flavell RA. Recognition of double-stranded RNA and activation of NF-kappa B by Toll-like receptor 3. Nature 2001;413:732-8.

292. Matsumoto M, Seya T. TLR3: Interferon induction by double-stranded RNA including poly(I : C). Advanced Drug Delivery Reviews 2008;60:805-12.

293. Coffman RL, Sher A, Seder RA. Vaccine adjuvants: Putting innate immunity to work. Immunity 2010;33:492-503.

294. Tewari K, Flynn BJ, Boscardin SB, et al. Poly(I:C) is an effective adjuvant for antibody and multi-functional CD4+ T cell responses to *Plasmodium falciparum* circumsporozoite protein (CSP) and alpha DEC-CSP in non human primates. Vaccine 2010;28:7256-66.

295. Kastenmueller K, Espinosa DA, Trager L, et al. Full-length *Plasmodium falciparum* circumsporozoite protein administered with long-chain poly(IC) or the toll-like receptor 4 agonist glucopyranosyl lipid adjuvant-stable emulsion elicits potent antibody and CD4(+) T cell immunity and protection in mice. Infection and Immunity 2013;81:789-800.

296. Salem ML, Kadima AN, Cole DJ, Gillanders WE. Defining the antigen-specific T-Cell response to vaccination and poly(I : C)/TLR3 signaling - Evidence of enhanced primary and memory CD8 T-Cell responses and antitumor immunity. Journal of Immunotherapy 2005;28:220-8.

297. Cui Z, Qiu F. CD4(+) T helper cell response is required for memory in CD8(+) T lymphocytes induced by a poly(I : C)-adjuvanted MHC I-restricted peptide epitope. Journal of Immunotherapy 2007;30:180-9.

298. Schneider-Ohrum K, Giles BM, Weirback HK, Williams BL, DeAlmeida DR, Ross TM. Adjuvants that stimulate TLR3 or NLPR3 pathways enhance the efficiency of influenza virus-like particle vaccines in aged mice. Vaccine 2011;29:9081-92.

299. Weiss WR, Sedegah M, Beaudoin RL, Miller LH, Good MF. CD8+ T-cells (cytotoxic/suppressors) are required for protection in mice immunized with malaria sporozoites. Proceedings of the National Academy of Sciences of the United States of America 1988;85:573-6.

300. Majarian WR, Daly TM, Weidanz WP, Long CA. Passive-immunization against murine malaria with an IgG3 monoclonal-antibody. Journal of Immunology 1984;132:3131-7.

301. Schmidt NW, Butler NS, Badovinac VP, Harty JT. Extreme CD8 T cell requirements for anti-malarial liver-stage immunity following immunization with radiation attenuated sporozoites. PLoS Pathogens 2010;6:e10000998.

302. Valmori D, Romero JF, Men Y, Maryanski JL, Romero P, Corradin G. Induction of a cytotoxic T-cell response by coinjection of a T-helper peptide and a cytotoxic T-lymphocyte peptide in incomplete freunds-adjuvant (IFA) - further enhancement by pre-injection of IFA alone. European Journal of Immunology 1994;24:1458-62.

303. Chen XJS, Casini G, Harrison SC, Garcea RL. Papillomavirus capsid protein expression in *Escherichia coli*: Purification and assembly of HPV11 and HPV16 L1. Journal of Molecular Biology 2001;307:173-82.

304. Gleiter S, Lilie H. Coupling of antibodies via protein Z on modified polyoma virus-like particles. Protein Science 2001;10:434-44.

305. Gasteiger E, Hoogland C, Gattiker A, et al. Protein identification and analysis tools on the ExPASy server. In: Walker JM, ed. The Proteomics Protocols Handbook: Humana Press; 2005.

306. Stehle T, Harrison SC. Crystal structures of murine polyomavirus in complex with straight-chain and branched-chain sialyloligosaccharide receptor fragments. Structure 1996;4:183-94.

307. Harris SJ, Woodrow SA, Gearing AJH, Adams SE, Kingsman AJ, Layton GT. The effects of adjuvants on CTL induction by V3:Ty-virus-like particles (V3-VLPs) in mice. Vaccine 1996;14:971-6.

308. Thoenes N, Herreiner A, Schaedlich L, Piuko K, Mueller M. A direct comparison of human papillomavirus type 16 L1 particles reveals a lower immunogenicity of capsomeres than viruslike particles with respect to the induced antibody response. Journal of Virology 2008;82:5472-85.

309. Snapper CM, Mond JJ. Towards a comprehensive view of immunoglobulin class switching. Immunology Today 1993;14:15-7.

310. Szomolanyi-Tsuda E, Welsh RM. T-cell-independent antiviral antibody responses. Current Opinion in Immunology 1998;10:431-5.

311. Ochsenbein AF, Pinschewer DD, Sierro S, Horvath E, Hengartner H, Zinkernagel RM. Protective long-term antibody memory by antigen-driven and T help-dependent differentiation of long-lived memory B cells to short-lived plasma cells independent of secondary lymphoid organs. Proceedings of the National Academy of Sciences of the United States of America 2000;97:13263-8.

312. Longhi MP, Trumpfheller C, Idoyaga J, et al. Dendritic cells require a systemic type I interferon response to mature and induce CD4(+) Th1 immunity with poly IC as adjuvant. Journal of Experimental Medicine 2009;206:1589-602.

313. Trumpfheller C, Caskey M, Nchinda G, et al. The microbial mimic poly IC induces durable and protective CD4(+) T cell immunity together with a dendritic cell targeted vaccine. Proceedings of the National Academy of Sciences of the United States of America 2008;105:2574-9.

314. Hovenden M, Hubbard MA, AuCoin DP, et al. IgG subclass and heavy chain domains contribute to binding and protection by mAbs to the poly gamma-D-glutamic acid capsular antigen of *Bacillus anthracis*. PLoS Pathogens 2013;9:e1003306.

315. Briles DE, Claflin JL, Schroer K, Forman C. Mouse IgG3 antibodies are highly protective against infection with *streptococcus-pneumoniae*. Nature 1981;294:88-90.

316. Freyschmidt EJ, Alonso A, Hartmann G, Gissmann L. Activation of dendritic cells and induction of T cell responses by HPV 16 L1/E7 chimeric virus-like particles are enhanced by CpG ODN or sorbitol. Antiviral Therapy 2004;9:479-89.

317. Ding F-X, Wang F, Lu Y-M, et al. Multiepitope peptide-loaded virus-like particles as a vaccine against Hepatitis B virus-related hepatocellular carcinoma. Hepatology 2009;49:1492-502.

318. Moore AC, Hill AVS. Progress in DNA-based heterologous prime-boost immunization strategies for malaria. Immunological Reviews 2004;199:126-43.

319. Leitner WW, Seguin MC, Ballou WR, et al. Immune responses induced by intramuscular or gene gun injection of protective deoxyribonucleic acid vaccines that express the circumsporozoite protein from *Plasmodium berghei* malaria parasites. Journal of Immunology 1997;159:6112-9.

320. Vuola JM, Keating S, Webster DP, et al. Differential immunogenicity of various heterologous prime-boost vaccine regimens using DNA and viral vectors in healthy volunteers. Journal of Immunology 2005;174:449-55.

321. Kent SJ, Zhao A, Best SJ, Chandler JD, Boyle DB, Ramshaw IA. Enhanced T-cell immunogenicity and protective efficacy of a human immunodeficiency virus type 1 vaccine regimen consisting of consecutive priming with DNA and boosting with recombinant fowlpox virus. Journal of Virology 1998;72:10180-8.

322. Hanke T, Samuel RV, Blanchard TJ, et al. Effective induction of simian immunodeficiency virus-specific cytotoxic T lymphocytes in macaques by using a multiepitope gene and DNA prime-modified vaccinia virus Ankara boost vaccination regimen. Journal of Virology 1999;73:7524-32.

323. Doolan DL, Hoffman SL. DNA-based vaccines against malaria: status and promise of the multi-stage malaria DNA vaccine operation. International Journal for Parasitology 2001;31:753-62.

324. Hill AVS, Reyes-Sandoval A, O'Hara G, et al. Prime-boost vectored malaria vaccines: Progress and prospects. Hum Vaccines 2010;6:78-83.

325. Ding H, Tsai C, Gutierrez RA, et al. Superior neutralizing antibody response and protection in mice vaccinated with heterologous DNA prime and virus like particle boost against HPAI H5N1 virus. PLoS One 2011;6:e16563.

326. Baer K, Klotz C, Kappe SHI, Schnieder T, Frevert U. Release of hepatic *Plasmodium yoelii* merozoites into the pulmonary microvasculature. Plos Pathogens 2007;3:1651-68.

327. John CC, Moormann AM, Pregibon DC, et al. Correlation of high levels of antibodies to multiple pre-erythrocytic *Plasmodium falciparum* antigens and protection from infection. American Journal of Tropical Medicine and Hygiene 2005;73:222-8.

328. Tarun AS, Peng X, Dumpit RF, et al. A combined transcriptome and proteome survey of malaria parasite liver stages. Proceedings of the National Academy of Sciences of the United States of America 2008;105:305-10.

329. Cubas R, Zhang S, Kwon S, et al. Virus-like particle (VLP) lymphatic trafficking and immune response generation after immunization by different routes. Journal of Immunotherapy 2009;32:118-28.

330. Schneider J, Gilbert SC, Blanchard TJ, et al. Enhanced immunogenicity for CD8+ T cell induction and complete protective efficacy of malaria DNA vaccination by boosting with modified vaccinia virus Ankara. Nature Medicine 1998;4:397-402.

331. Levy SB. Resistance of minicells to penicillin lysis - a method of obtaining large quantities purified minicells. Journal of Bacteriology 1970;103:836-9.

332. Barker GR, Cordery CS, Jackson D, Legrice SFJ. Isolation by differential and zonal centrifugation of minicells segregated by *Escherichia-coli*. Journal of General Microbiology 1979;111:387-97.

333. Christen AA, Pall ML, Manzara T, Lurquin PF. Rapid isolation of *Escherichia-coli* minicells by glass-fiber filtration - study of plasmid-coded polypeptides. Gene 1983;23:195-8.

334. Park S-Y, Lee J-Y, Chang W-S, Choy HE, Kim G-J. A coupling process for improving purity of bacterial minicells by holin/lysin. Journal of Microbiological Methods 2011;86:108-10.

335. Kool AJ, Vanzeben MS, Nijkamp HJJ. Identification of messenger ribonucleic-acids and proteins synthesized by bacteriocinogenic factor clo-df13 in purified minicells of *Escherichia-coli*. Journal of Bacteriology 1974;118:213-24.

336. Tankersley WG, Woodward JM. Induction and isolation of a minicell-producing strain of *Salmonella-typhimurium*. Proc Soc Exp Biol Med 1974;145:802-5.

337. Shortman K, Lahoud MH, Caminschi I. Improving vaccines by targeting antigens to dendritic cells. Experimental and Molecular Medicine 2009;41:61-6.

338. Trumpfheller C, Longhi MP, Caskey M, et al. Dendritic cell-targeted protein vaccines: a novel approach to induce T-cell immunity. Journal of Internal Medicine 2012;271:183-92.

339. Lahoud MH, Ahmet F, Kitsoulis S, et al. Targeting antigen to mouse dendritic cells via clec9a induces potent CD4 T cell responses biased toward a follicular helper phenotype. Journal of Immunology 2011;187:842-50.

340. Caminschi I, Proietto AI, Ahmet F, et al. The dendritic cell subtype-restricted C-type lectin Clec9A is a target for vaccine enhancement. Blood 2008;112:3264-73.

341. Hoshino K, Takeuchi O, Kawai T, et al. Cutting edge: Toll-like receptor 4 (TLR4)-deficient mice are hyporesponsive to lipopolysaccharide: Evidence for TLR4 as the Lps gene product. Journal of Immunology 1999;162:3749-52.

342. Harlow E, Lane D. Antibodies: A laboratory manual. New York, USA

Cold Spring Harbor Laboratory Press; 1988.

343. Dougan G, Kehoe M. The minicell system as a method for studying expression from plasmid DNA. Methods in Microbiology 1984;17:233-58.

344. Bahreini E, Aghaiypour K, Abbasalipourkabir R, Goodarzi MT, Saidijam M, Safavieh SS. An optimized protocol for overproduction of recombinant protein expression in *Escherichia coli*. Preparative Biochemistry & Biotechnology 2014;44:510-28.

345. Mazumdar S, Sachdeva S, Chauhan VS, Yazdani SS. Identification of cultivation condition to produce correctly folded form of a malaria vaccine based on *Plasmodium falciparum* merozoite surface protein-1 in *Escherichia coli*. Bioprocess and Biosystems Engineering 2010;33:719-30.

346. McKinstry WJ, Hijnen M, Tanwar HS, et al. Expression and purification of soluble recombinant full length HIV-1 pr55(Gag) protein in *Escherichia coli*. Protein Expression and Purification 2014;100:10-8.

347. Sheikh IH, Kaushal DC, Singh V, Kumar N, Chandra D, Kaushal NA. Cloning, overexpression and characterization of soluble 42 kDa fragment of merozoite surface protein-1 of *Plasmodium vivax*. Protein Expression and Purification 2014;103:64-74.

348. Terpe K. Overview of bacterial expression systems for heterologous protein production: from molecular and biochemical fundamentals to commercial systems. Applied Microbiology and Biotechnology 2006;72:211-22.

349. Rosano GL, Ceccarelli EA. Recombinant protein expression in *Escherichia coli:* advances and challenges. Frontiers in Microbiology 2014;5.

350. Tang L, Jiang R, Zheng K, Zhu X. Enhancing the recombinant protein expression of halohydrin dehalogenase HheA in *Escherichia coli* by applying a codon optimization strategy. Enzyme and Microbial Technology 2011;49:395-401.

351. Zhou ZY, Schnake P, Xiao LH, Lal AA. Enhanced expression of a recombinant malaria candidate vaccine in *Escherichia coli* by codon optimization. Protein Expression and Purification 2004;34:87-94.

352. Mehlin C, Boni E, Buckner FS, et al. Heterologous expression of proteins from *Plasmodium falciparum*: Results from 1000 genes. Molecular and Biochemical Parasitology 2006;148:144-60.

353. Uhlin BE, Nordstrom K. Plasmid incompatibility and control of replication - copy mutants of R-factor R1 in *Escherichia-coli* K-12. Journal of Bacteriology 1975;124:641-9.

354. Yang W, Zhang L, Lu ZG, Tao W, Zhao ZH. A new method for protein coexpression in *Escherichia coli* using two incompatible plasmids. Protein Expression and Purification 2001;22:472-8.

355. Novick RP. Plasmid incompatibility. Microbiological Reviews 1987;51:381-95.

356. Zeng JM, Zhang L, Li YQ, et al. Over-producing soluble protein complex and validating protein-protein interaction through a new bacterial co-expression system. Protein Expression and Purification 2010;69:47-53.

357. Jiang WP, Swiggard WJ, Heufler C, et al. The receptor DEC-205 expressed by dendritic cells and thymic epithelial-cells is involved in antigen-processing. Nature 1995;375:151-5.

358. Sancho D, Joffre OP, Keller AM, et al. Identification of a dendritic cell receptor that couples sensing of necrosis to immunity. Nature 2009;458:899-903.

359. Jaffe A, Dari R, Hiraga S. Minicell-forming mutants of *Escherichia-coli* - production of minicells and anucleate rods. Journal of Bacteriology 1988;170:3094-101.

360. Acres SD, Isaacson RE, Khachatourians G, Babiuk L, Kapitany RA. Vaccination of cows with purified K99 antigen, K99+ anucleated live *E. coli*, and whole cell bacterins containing enterotoxigenic *E. coli* for prevention of enterotoxigenic colibacillosis of calves. Proceedings, Second International Symposium on Neonatal Diarrhea 1979:443-55.

361. Bonifaz L, Bonnyay D, Mahnke K, Rivera M, Nussenzweig MC, Steinman RM. Efficient targeting of protein antigen to the dendritic cell receptor DEC-205 in the steady state leads to antigen presentation on major histocompatibility complex class I products and peripheral CD8(+) T cell tolerance. Journal of Experimental Medicine 2002;196:1627-38.

362. Hawiger D, Inaba K, Dorsett Y, et al. Dendritic cells induce peripheral T cell unresponsiveness under steady state conditions *in vivo*. Journal of Experimental Medicine 2001;194:769-79.

363. Bonifaz LC, Bonnyay DP, Charalambous A, et al. *In vivo* targeting of antigens to maturing dendritic cells via the DEC-205 receptor improves T cell vaccination. Journal of Experimental Medicine 2004;199:815-24.

364. Boscardin SB, Hafalla JCR, Masilamani RF, et al. Antigen targeting to dendritic cells elicits long-lived T cell help for antibody responses. Journal of Experimental Medicine 2006;203:599-606.

365. Soares H, Waechter H, Glaichenhaus N, et al. A subset of dendritic cells induces CD4(+) T cells to produce IFN-gamma by an IL-12 independent but CD70-dependent mechanism *in vivo*. Journal of Experimental Medicine 2007;204:1095-106.

366. Corbett AJ, Caminschi I, McKenzie BS, et al. Antigen delivery via two molecules on the CD8(-) dendritic cell subset induces humoral immunity in the absence of conventional "danger". European Journal of Immunology 2005;35:2815-25.

367. Takeuchi O, Hoshino K, Kawai T, et al. Differential roles of TLR2 and TLR4 in recognition of gram-negative and gram-positive bacterial cell wall components. Immunity 1999;11:443-51.

368. Apte SH, Redmond AM, Groves PL, Schussek S, Pattinson DJ, Doolan DL. Subcutaneous cholera toxin exposure induces potent CD103(+) dermal dendritic cell activation and migration. European Journal of Immunology 2013;43:2707-17.

369. Bursch LS, Wang L, Igyarto B, et al. Identification of a novel population of Langerin(+) dendritic cells. Journal of Experimental Medicine 2007;204:3147-56.

370. Bedoui S, Whitney PG, Waithman J, et al. Cross-presentation of viral and self antigens by skin-derived CD103(+) dendritic cells. Nature Immunology 2009;10:488-95.

371. Nganou-Makamdop K, van Roosmalen ML, Audouy SAL, et al. Bacterium-like particles as multi-epitope delivery platform for *Plasmodium berghei* circumsporozoite protein induce complete protection against malaria in mice. Malaria Journal 2012;11:50.

372. Freeman GJ, Long AJ, Iwai Y, et al. Engagement of the PD-1 immunoinhibitory receptor by a novel B7 family member leads to negative regulation of lymphocyte activation. Journal of Experimental Medicine 2000;192:1027-34.

373. Yamazaki T, Akiba H, Iwai H, et al. Expression of programmed death 1 ligands by murine T cells and APC. Journal of Immunology 2002;169:5538-45.

374. Loke P, Allison JP. PD-L1 and PD-L2 are differentially regulated by Th1 and Th2 cells. Proceedings of the National Academy of Sciences of the United States of America 2003;100:5336-41.

375. Zhou Y, Ramachandran V, Kumar KA, et al. Evidence-based annotation of the malaria parasite's genome using comparative expression profiling. PLoS One 2008;3:e1570.

376. Good MF, Doolan DL. Malaria vaccine design: Immunological considerations. Immunity 2010;33:555-66.

377. Stanisic DI, Barry AE, Good MF. Escaping the immune system: How the malaria parasite makes vaccine development a challenge. Trends in Parasitology 2013;29:612-22.

378. Langhorne J, Ndungu FM, Sponaas A, Marsh K. Immunity to malaria: more questions than answers. Nature Immunology 2008;9:725-32.

379. Nussenzweig R, Vanderbe J, Most H, Orton C. Protective immunity produced by injection of x-irradiated sporozoites of *Plasmodium berghei*. Nature 1967;216:160-2.

380. Rieckman.Kh, Carson PE, Beaudoin RL, Cassells JS, Sell KW. Sporozoite induced immunity in man against an Ethiopian strain of *Plasmodium-falciparum*. Transactions of the Royal Society of Tropical Medicine and Hygiene 1974;68:258-9.

381. Roestenberg M, McCall M, Hopman J, et al. Protection against a malaria challenge by sporozoite inoculation. New England Journal of Medicine 2009;361:468-77.

382. Mikolajczak SA, Lakshmanan V, Fishbaugher M, et al. A next-generation genetically attenuated *Plasmodium falciparum* parasite created by triple gene deletion. Molecular Therapy 2014:2014.85. [Epub ahead of print].

383. Ballou WR, Sherwood JA, Neva FA, et al. Safety and efficacy of a recombinant-DNA *Plasmodium-falciparum* sporozoite vaccine. Lancet 1987;1:1277-81.

384. Girard MP, Reed ZH, Friede M, Kieny MP. A review of human vaccine research and development: Malaria. Vaccine 2007;25:1567-80.

385. Schwartz L, Brown GV, Genton B, Moorthy VS. A review of malaria vaccine clinical projects based on the WHO rainbow table. Malaria Journal 2012;11:11.

386. Moser M, Leo O. Key concepts in immunology. Vaccine 2010;28:C2-C13.

387. Montomoli E, Piccirella S, Khadang B, Mennitto E, Camerini R, De Rosa A. Current adjuvants and new perspectives in vaccine formulation. Expert Review of Vaccines 2011;10:1053-61.

388. Reed SG, Bertholet S, Coler RN, Friede M. New horizons in adjuvants for vaccine development. Trends in Immunology 2009;30:23-32.

389. Kutzler MA, Weiner DB. DNA vaccines: ready for prime time? Nature Reviews Genetics 2008;9:776-88.

390. Bruder JT, Angov E, Limbach KJ, Richie TL. Molecular vaccines for malaria. Hum Vaccines 2010;6:54-77.

391. Tamminga C, Sedegah M, Regis D, et al. Adenovirus-5-vectored *P. falciparum* vaccine expressing CSP and AMA1. Part B: Safety, immunogenicity and protective efficacy of the CSP component. PLoS One 2011;6:e24586.

392. Catanzaro AT, Koup RA, Roederer M, et al. Phase 1 safety and immunogenicity evaluation of a multiclade HIV-1 candidate vaccine delivered by a replication-defective recombinant adenovirus vector. Journal of Infectious Diseases 2006;194:1638-49.

393. Chuang I, Sedegah M, Cicatelli S, et al. DNA prime/adenovirus boost malaria vaccine encoding *P-falciparum* CSP and AMA1 induces sterile protection associated with cell-mediated immunity. Plos One 2013;8:e55571.

394. Jones TR, Narum DL, Gozalo AS, et al. Protection of Aotus monkeys by *Plasmodium falciparum* EBA-175 region II DNA prime-protein boost immunization regimen. 2000 Jun 05; Annecy Le Vieux, France. p. 303-12.

395. Walsh DS, Gettayacamin M, Leitner WW, et al. Heterologous prime-boost immunization in rhesus macaques by two, optimally spaced particle-mediated epidermal deliveries of *Plasmodium falciparum* circumsporozoite protein-encoding DNA, followed by intramuscular RTS,S/AS02A. Vaccine 2006;24:4167-78.

396. Griffith JP, Griffith DL, Rayment I, Murakami WT, Caspar DLD. Inside polyomavirus at 25-A resolution. Nature 1992;355:652-4.

397. Kamphorst AO, Guermonprez P, Dudziak D, Nussenzweig MC. Route of antigen uptake differentially impacts presentation by dendritic cells and activated monocytes. Journal of Immunology 2010;185:3426-35.

398. Snapper CM, Paul WE. Interferon-gamma and B-cell stimulatory factor-I reciprocally regulate Ig isotype production. Science 1987;236:944-7.

399. Sin JI, Bagarazzi M, Pachuk C, Weiner DB. DNA priming-protein boosting enhances both antigen-specific antibody and Th1-type cellular immune responses in a murine herpes simplex virus-2 gD vaccine model. DNA and Cell Biology 1999;18:771-9.

400. Xiang SD, Scholzen A, Minigo G, et al. Pathogen recognition and development of particulate vaccines: Does size matter? Methods 2006;40:1-9.

401. Mahnke K, Guo M, Lee S, et al. The dendritic cell receptor for endocytosis, DEC-205, can recycle and enhance antigen presentation via major histocompatibility complex class II-positive lysosomal compartments. Journal of Cell Biology 2000;151:673-83.

Chapter 8: Appendices

Appendix A: Buffers and media

Buffer	Composition
Annealing buffer	10 mM Tris (pH 7.5-8.0) + 50 mM NaCl + 1 mM EDTA in milliQ water
Antibody purification binding buffer	5.8 mM Na_2HPO_4 + 4.2 mM NaH_2PO_4 + 150 mM NaCl + 10 mM EDTA in MilliQ water
Dulbecco's balanced salt solution	Obtained from QIMR media store
ELISA carbonate buffer	18 mM Na_2CO_3 + 45 mM $NaHCO_3$ in deionised water adjusted to pH 9.6
FCAB buffer	PBS + 2 mM EDTA + 0.5% FCS
FCAB fix/lyse buffer	PBS + 4% w/v paraformaldehyde + 0.0067% w/v saponin
GST column elution buffer	40 mM Tris-base + 200 mM NaCl + 1 mM EDTA + 5% (v/v) glycerol + 5 mM DTT + 10 mM reduced glutathione in milliQ water adjusted to pH 8.0
Hybridoma culture media	RPMI media (Life Technologies) supplemented with penicillin (60 mg/L) and streptomycin (100 mg/L), 1.5 mM L-glutamine, 5 nM β-2-Mercaptoethanol and 5% FCS
KD-MEM media	Dulbecco's Modified Eagle's Medium (SAFC Global, St. Louis, USA) supplemented with 136 nM folic acid + 32 mM L-asparagine + 67 mM L-arginine + 24 mM sodium bicarbonate + 10 mM HEPES + 5 nM β-2-mercaptoethanol + 1.5 mM L-glutamine + 100 units/L penicillin + 100 mg/L streptomycin
Luria-Bertani broth (LB)	10 g/L peptone + 5 g/L yeast extract + 10 g/L NaCl in milliQ water
Lysis buffer	40 mM Tris-base + 200 mM NaCl + 1 mM EDTA + 5% (v/v) glycerol + 5 mM DTT in milliQ water adjusted to pH 8.0
MACS buffer	PBS + 2 mM EDTA + 0.5% FCS
Red blood cell lysis buffer	0.168 M NH_4Cl in deionised water
SDS-Page running	25mM Tris + 200 mM Glycine + 0.1% SDS in deionised water
Super optimal broth with catabolite repression (SOC)	20 g/L peptone + 5 g/L yeast extract + 0.5 g/L NaCl + 20 mM glucose in milliQ water

Talon wash buffer	20 mM sodium phosphate, 500 mM sodium chloride, and 10 mM Imidazole in milliQ water adjusted to pH8.0
Terrific broth (TB)	12 g/L peptone + 24 g/L yeast extract + 4 ml/L glycerol + 2.31 g/L KH_2PO_4 + 12.54 g/L K_2HPO_4 in milliQ water
Tris-borate buffer (TBE)	90 mM Tris + 90 mM boric acid + 2 mM EDTA in deionised water
VLP Assembly buffer	500 mM $(NH_4)_2SO_4$ + 20 mM Tris-base + 1 mM $CaCl_2$ + 5% (v/v) glycerol in milliQ water adjusted to pH 7.4
Western blot transfer	25mM Tris + 200 mM Glycine + 0.1% SDS in deionised water + 20 % methanol

Appendix B: Oligonucleotides used for chimeric VLP and capsomere constructs

Oligonucleotide name	Oligonucleotide sequence 5’ to 3’	T_M (°C)
CD8 Dom Forward	AGCTATGTGCCGAGCGCGGAACAGATT	63
CD8 Dom Reverse	AATCTGTTCCGCGCTCGGCACATAGTC	63
CD8 SubDom Forward	ATTTATAACCGTAACATCGTGAACCGTCTG	59
CD8 SubDom Reverse	CAGACGGTTCACGATGTTACGGTTATAAAT	59
CD4 Dom 1 Forward	AGCTATGTGCCGAGCGCGGAACAGATTCTGGAATTTGTGAAACAGATC	70
CD4 Dom 1 Reverse	GATCTGTTTCACAAATTCCAGAATCTGTTCCGCGCTCGGCACATAGCT	70
CD4 Dom 2 Forward	AAAATTTATAACCGTAAAATCGTGAACCGTCTGCTGGGCGAT	66
CD4 Dom 2 Reverse	ATCGCCCAGCAGACGGTTCACGATGTTACGGTTATAAATTTT	66
CD4 SubDom Forward	TATAACCGTAACATCGTGAACCGTCTGCTGGGCGATGCGCTGAACGG CAAACCGGAAGAAAAA	75
CD4 SubDom Reverse	TTTTTCTTCCGGTTTGCCGTTCAGCGCATCGCCCAGCAGACGGTTCAC GATGTTACGGTTATA	75
B Cell Forward	CAGGGCCCGGGTGCGCCGCAAGGTCCAGGGGCCCCG	79
B Cell Reverse	CGGGGCCCCTGGACCTTGCGGCGCACCCGGGCCCTG	79

Appendix C: Flow cytometry antibodies

Target	Assay	Fluorochrome	Clone	Isotype	Supplier
CD4	ICS, OVA minicell CTL, AMA1 minicell	BV510	RM4-5	R IgG_{2a}	Biolegend
	OVA minicell adoptive transfer	PerCP/Cy5.5	GK 1.5	R IgG_{2a}	Biolegend
CD8	ICS	PE-Cy7	53-6.7	R IgG_{2a}	Biolegend
	OVA and AMA1 minicell	APC-Cy7	53-6.7	R IgG_{2a}	Biolegend
CD11a	AMA1 minicell	AF647	M17/4	R IgG_{2a}	Biolegend
CD11c	OVA migrating DCs sorting	PE	N418	AH IgG	Biolegend
CD19	AMA1 minicell	PE Cy5	6D5	R IgG_{2a}	Biolegend
CD 45.1	OVA minicell	FITC	A20	M IgG_{2a}	Biolegend
CD 45.2	OVA minicell	PE	104	M IgG_{2a}	Biolegend
CD 49d	AMA1 minicell	PE	9C10	R IgG_{2a}	Biolegend
CD 69	AMA1 minicell	FITC	H1.2F3	AH IgG	Biolegend
CD 71	FCAB	PE	R172.7	R IgG_{2a}	Biolegend
CD 86	AMA minicell	AF700	P03	R IgG_{2b}	Biolegend
CD90.1 (Thy1.1)	CS-TCR	PE	OX-7	M IgG_1	BD
CD103	OVA migrating DCs sorting	P.Blue	2E7	AH IgG	Biolegend
PD-L1 (CD274)	AMA1 minicell	BV421	10F.9G2	R IgG_{2b}	Biolegend
PD-1 (CD279)	AMA1 minicell	BV605	29F.1A12	R IgG_{2a}	Biolegend
Gr-1 (Ly-6G/C)	AMA1 minicell	PE Cy7	RB6-8C5	R IgG_{2b}	BD
Vα2 TCR	OVA minicell	APC	B20.1	R IgG_{2a}	E.Bioscience
	OVA minicell	PE	B20.1	R IgG_{2a}	Biolegend
MHC II	OVA migrating DCs sorting	FITC	M5/114.15.2	R IgG_{2b}	Biolegend
Goat α-mouse Ig	IFAT (flow)	FITC	Polyclonal	G Ig	BD
IFN-γ	ICS	APC	XMG 1.2	R IgG_1	Biolegend
IL-2	ICS	PE	JES6-5H4	R IgG_{2b}	Biolegend
TNF	ICS	FITC	MP6-XT22	R IgG_1	E.Bioscience
α-mouse IgG_1	AMA1 minicell-Isotype	APC	RMG1	R IgG	Biolegend
α-mouse IgG_{2a}	AMA1 minicell-Isotype	FITC	R19-15	R IgG_1	BD
α-mouse IgD	AMA1 minicell-Isotype	P.Blue	11-26c.2a	R IgG_{2a}	Biolegend
α-mouse IgM	AMA1 minicell-Isotype	PE Cy7	R6-60.2	R IgG_{2a}	BD
α-mouse IgE	AMA1 minicell-Isotype	PE	RME-1	R IgG_1	Biolegend

Appendix D: Oligonucleotides for vector and plasmid DNA constructs used in the bacterial minicell studies

Project	Name	Direction	RE site	Oligonucleotide sequence 5' to 3' – (underlined sequences represent restriction enzyme sites)
pIASO and pVRV5 construction	RegionA	F	*Bgl*II	ATATagatctGCTGTGCCTTCTAGTTG
	RegionA (+*Mfe*I)	R	*Mfe*I	CGGGcaattgTCAGAATTGGTTAAT
	RegionB (+*Mfe*I)	F	*Mfe*I	GAAAcaattgTTACGCCCCGCCCTGCCACTC
	RegionB (+*Apa*I)	R	*Apa*I	CAAAgggcccATGGAGAAAAAAATCACTGGAT
	RegionC (+*Apa*I)	F	*Apa*I	ATATgggcccAACACCCCTTGTATTACT
	RegionC	R	*Spe*I	GGGGTAactagtCAATAATCAATGTCAACAT
	V5	F	*Not*I	GGCCGC*a*GGTAAGCCTATCCCTAACCCTCTCCTCGG TCTCGATTCTACG
	V5	R	*Bgl*II	GATCTCGTAGAATCGAGACCGAGGAGAGGGTTAGG GATAGGCTTACC*t*GC
Fluorescent genes	RFP-pVRV5	F	*BamH*I	GAGAggatccATGGTGAGCAAGGGCGAGGAGG
	RFP-pVRV5	R	*Not*I	ACCTgcggccgcCTTGTACAGCTCGTCCATGC
	GFP-pTrcHis2A	F	*Sac*I	ATCCgagctcAATGAGTAAAGGAGAAGAACTT
	GFP-pTrcHis2A	R	*Kpn*I	GATAggtaccTTTTTGTATAGTTCATCCATGC
	GFP-pDualGC	F	*Ear*I	CCctcttcAATGAGTAAAGGAGAAGAACTTTTC
	GFP-pDualGC	R	*Ear*I	CGctcttcCAAGTTTGTATAGTTCATCCATGC
***Plasmodium yoelii* genes**	*Py*AMA1-pVRV5	F	*BamH*I	CCGGGCggatccATGAAAGAAATATATTATATATTTATT TT
	*Py*AMA1-pVRV5	R	*Not*I	TTAAgcggccgcATAATATGGTTTTTCCATCAAAACG
	*Py*AMA1-pTrcHis2A	F	*Sac*I	GCCCgagctcAATGAAAGAAATATATTATATATTTATTTT ATGC
	*Py*AMA1-pTrcHis2A	R	*Kpn*I	TACAggtaccGTATAATATGGTTTTTCCATCAAAACG
	*Py*AMA1-pIVEX	F	*Not*I	GAAGTTTgcggccgcATGAAAGAAATATATTATATATTTA TTTT
	*Py*AMA1-pIVEX	R	*Sac*I	GTTTTTTgagctcCATAATATGGTTTTTCCATCAAAACG
	*Py*CSP-pVRV5	F	*BamH*I	TACCggatccATGAAGAAGTGTACCATTTTAGTTGTAG
	*Py*CSP-pVRV5	R	*Not*I	ACCTgcggccgcATTAAAGAATACTAATACTAATAATATT AC
	*Py*CSP-pTrcHis2A	F	*Sac*I	ATTTgagctcAATGAAGAAGTGTACCATTTTAGTTGTA
	*Py*CSP-pTrcHis2A	R	*Kpn*I	GGGATggtaccTTATTAAAGAATACTAATACTAATAATA TTAC
	*Py*CSP-pIVEX	F	*Not*I	CTTAgcggccgcATGAAGAAGTGTACCATTTTAG
	*Py*CSP-pIVEX	R	*Sac*I	GGCCGCAgagctcCATTAAAGAATACTAATACTAATAAT ATTACAAATCC
Ovalbumin genes	Ova-pDualGC	F	*Ear*I	ATctcttcAATGGGCTCCATCGGCGCA
	TransOva-pDualGC	F	*Ear*I	CGctcttcAATGATGGATCAAGCTAGATCA
	Ova and TfrOva-pDualGC	R	*Ear*I	CGctcttcAAAGAGGGGAAACACATCTGCCA
Sequencing	pIASO	F		GAGAGGGCTCTGCTGTGTGCTGC
	pIASO	R		CCCCAGAATAGAATGACACC
	pBAD	F		ATGCCATAGCATTTTTATCC
	pBAD	R		CTGAATTAATCTGTATCAGG
	*Py*AMA1 (int500)	F		GTCATTGTGTGCAAAACATACC
	PyCSP (int200)	F		GCTCTCAACGGAAAACCAGAAG
	pTrcHis2	F		GCGAAGCGGCACTGCT
	pTrcHis2	R		TCTGAGTTCGGCATGGGGT
	pDUAL GC	F		GCGAAGCGGCACTGC
	pDual GC SV40	R		CACTGCATTCTAGTTGTGG
	Ova and TfrOva (int)	R		TTGTCTGACTTTCTACCCAGGA

Appendix E: Amino acid sequences

Plasmodium yoelii 17XNL circumsporozoite protein

MKKCTILVVASLLLVDSLLPGYGQNKSVQAQRNLNELCYNEENDNKLYHVLNSKNGKIYNRNIVNRLL
GDALNGKPEEKKDDPPKDGNKDDLPKEEKKDDLPKEEKKDDPPKDPKKDDPPKEAQNKLNQPVVAD
ENVDQGPGAPQGPGAPQGPGAPQGPGAPQGPGAPQGPGAPQGPGAPQGPGAPQGPGAPQGPGAPQGPG
APQGPGAPQGPGAPQGPGAPQGPGAPQGPGAPQGPGAPQGPGAPQGPGAPQGPGAPQGPGAPQEPPQQ
PPQQPPQQPPQQPPQQPPQQPPQQPPQQPRPQPDGNNNNNNNNGNNNEDSYVPSAEQILEFVKQISSQL
TEEWSQCSVTCGSGVRVRKRKNVNKQPENLTLEDIDTEICKMDKCSSIFNIVSNSLGFVILLVLVFFN-

Plasmodium yoelii 17XNL apical membrane antigen-1

MKEIYYIFILCSIYLINLSYCSEGPNQVISEDGNINYESIPKENTERSIKLINPWDKYMEKYDIEKVHGSGI
RVDLGEDARVENRDYRIPSGKCPVIGKGITIQNSEVSFLKPVATGDKPVRSGGLAFPETDVHISPITITN
LKTMYKDHQDIVNLNDMSLCAKHTSLYVPGKDATSAYRHPVVYDKSNSTCYMLYVAAQENMGPRYC
SNDANNENQPFCFTPEKIENYKDLSYLTKNLRDDWETSCPNKSIKNAKFGIWVDGYCTDYQKHVVHD
SDSLLKCNQIIFNESASDQPKQYERHLEDATKIRQGIVERNGKLIGEALLPIGSYKSGQIKSHGKGYNW
GNYDSKNNKCYIFETKPTCLINDKNFIATTALSSTEEFEENFPCEIYKNKIAEEIKVLNLNQNTSNGNNSI
KFPRIFISTDKNSLNCPCDPTKLTESTCEFYVCSCVEQRQYIAENNDVIIKEEFIGDYENPKQKLLIIIVLI
GVGIIIVILLVAYYFKSGKKGENYDRMGQADDYGKSKSRKDEMLDPEVSFWGEDKRASHTTPVLMEK
PYY-

MuPyV VP1-S4-G4S^{173} with flanking G4S sequence underlined

GGMAPKRKSGVSKCETKCTKACPRPAPVPKLLIKGGMEVLDLVTGPDSVTEIEAFLNPRMGQPPTPE
SLTEGGQYYGWSRGINLATSDTEDSPGNNTLPTWSMAKLQLPMLNEDLTCDTLQMWEAVSVKTEVV
GSGSLLDVHGFNKPTDTVNTKGISTPVEGSQYHVFAVGGEPLDLQGLVTDARTKYKEEGVVTIKTITK
KDMVNKDQVLNPISKAKLDKDGMYPVEIWHPDPAKNENTRYFGNYTGGTTTPPVLQFTNTLTTVLLD
ENGVGPLCKGEGLYLSCVDIMGWRVTRGGGGSSAGGGGSYDVHHWRGLPRYFKITLRKRWVKNP
YPMASLISSLFNNMLPQVQGQPMEGENTQVEEVRVYDGTEPVPGDPDMTRYVDRFGKTKTVFPGN

VP1ΔNΔC^{170} with epitope insertion sites underlined

GSHVLIKGGMEVLDLVTGPDSVTEIEAFLNPRMGQPPTPESLTEGGQYYGWSRGINLATSAGTEDSP
GNNTLPTWSMAKLQLPMLNEDLTCDTLQMWEAVSVKTEVVGSGSLLDVHGFNKPTDTVNTKGISTP
VEGSQYHVFAVGGEPLDLQGLVTDARTKYKEEGVVTIKTITKKDMVNKDQVLNPISKAKLDKDGMYP
VEIWHPDPAKNENTRYFGNYTGGTTTPPVLQFTNTLTTVLLDENGVGPLCKGEGLYLSCVDIMGWRV
TRSAYDVHHWRGLPRYFKITLRKRWVKNPYV

Appendix F: VLP and capsomere estimated weights and Pi values

	Construct	Weight + GST (kDa)	Pi + GST	Weight – GST (kDa)	Pi -GST
VLP	Wild	69.59	6.08	43.29	6.06
	CD8 Dom	70.56	5.98	44.27	5.87
	CD8 Sub-Dom	70.84	6.32	44.55	6.62
	CD4 Dom 1	71.42	5.98	45.13	5.88
	CD4 Dom 2	71.26	6.32	44.96	6.62
	CD4 Sub-Dom	71.98	6.20	45.69	6.30
	B Cell	70.60	6.08	44.31	6.06
Capsomere	Wild	58.99	5.91	32.85	5.73
	CD8 Dom	61.92	5.66	35.77	5.34
	CD8 Sub-Dom	62.77	6.66	36.62	7.83
	CD4 Dom 1	64.50	5.67	38.35	5.38
	CD4 Dom 2	64.01	6.66	37.86	7.82
	CD4 Sub-Dom	66.18	6.23	40.03	6.38
	B Cell	62.04	5.91	35.89	5.73